



Provided by the author(s) and University of Galway in accordance with publisher policies. Please cite the published version when available.

Title	Analysis of the behaviour of hybrid concrete lattice girder slabs during construction using laboratory and field testing
Author(s)	Shane, Newell
Publication Date	2020-01-31
Publisher	NUI Galway
Item record	http://hdl.handle.net/10379/15759

Downloaded 2024-04-24T11:14:18Z

Some rights reserved. For more information, please see the item record link above.



**Analysis of the behaviour of hybrid concrete
lattice girder slabs during construction using
laboratory and field testing**

Shane Newell

Supervisor: Dr. Jamie Goggins



A thesis submitted to the National University of Ireland as fulfilment of the requirements for the Degree of Doctor of Philosophy.

Civil Engineering,
National University of Ireland, Galway.

November 2019

Abstract

One of the emerging technologies in construction is the development of ‘smart structures’ which have sensors which will allow more efficient, resilient and sustainable structures to be designed and constructed. This research focusses on the use of embedded sensors and testing to better understand the behaviour of hybrid concrete lattice girder flat slabs, which is classified as a Modern Method of Construction (MMC). Despite the popularity of concrete flat slabs in structures and the increasing adoption of hybrid concrete lattice girder slabs to construct flat slabs, there is a dearth of information on how they perform during construction and in use. A programme of insitu field monitoring and laboratory testing was conducted to investigate the actual behaviour of hybrid concrete lattice girder flat slabs.

In the literature, there are very few case studies in relation to monitoring of concrete floors using field data. The methodology and implementation of a real-time structural health monitoring strategy for hybrid concrete lattice girder flat slabs are described. Vibrating-wire strain gauges and electrical resistance strain gauges were embedded in both the precast plank and insitu concrete topping of the floor system, which were used to monitor various aspects of the behaviour of the floor during the manufacturing, construction and operational phases. Environmental conditions were also monitored so that a holistic analysis of the factors which influence the behaviour of the concrete floor could be undertaken.

The rich field data from the monitoring was used to examine early-age behaviour of the hybrid concrete slab. Predicted values for peak temperature and temperature differentials in the concrete were found to be conservative and greater than values measured in the field. The field data was also used to determine restraint factors in the insitu topping at various locations in the hybrid concrete slab and it was found that the restraint factor varied between 0.16 to 0.37 (zero indicating no restraint and unity being fully restrained). There was good correlation between predicted flexural behaviour of the hybrid concrete slab using the finite element models and the actual behaviour measured in the field. The actual degree of rotational restraint provided by supporting walls to the slab was noticeably different to that assumed and this confirms the rationale in some design codes for additional torsional reinforcement

to be provided at slab edges. In addition, the load transfer mechanism through the hybrid concrete floor during the construction of a multi-storey concrete frame construction in which concrete floors are temporarily supported by floors below is analysed. It indicates that the slab behaves linearly elastic and is uncracked during the construction phase.

In addition, a one-dimensional finite difference model was developed which took account of heat of hydration, heat transfer mechanisms and environmental conditions and was compared with measured concrete temperatures in the hybrid slab. Accurate predictions of thermal behaviour of concrete slabs is critical for the development of passive design strategies in buildings and the utilisation of the thermal mass properties of concrete floors. The 1-D model was shown to have good correlation with the measured concrete temperatures. The significant influence of ambient temperature and solar radiation on the thermal behaviour of the hybrid concrete floor are analysed during the construction phase using the field data.

To investigate the interaction between the various components of the lattice girder plank (i.e. top chord, bottom chord and diagonals of the lattice girder; concrete; reinforcement) during the construction stage in more detail under controlled conditions, a series of experimental laboratory tests were conducted. The testing is a significant addition to the literature on experimental testing of lattice girder precast planks during construction as it analyses all the components of the precast floor. The dominant design parameters for controlling stiffness and the deflection of the plank during construction stage are the diameter of the top chord of the lattice girder and the spacing of the lattice girders. The experimental data was used to produce design tables for erection spans which take account of the multi-span nature of lattice girder planks when temporarily propped. The experimental results reported conclude that there is potential improvement of the arrangement of temporary propping possible for lattice girder planks during construction that could reduce costs, labour and congestion on site, which will improve the construction process for flat slabs.

Table of Contents

Abstract	i
Table of Contents	iii
Table of Figures	viii
Table of Tables	xiii
Acknowledgements	xiv
Declarations	xv
List of Publications	xvi
1 Introduction	1
1.1 Introduction.....	1
1.2 Research motivation and objectives.....	6
1.3 Outline of the thesis	7
1.4 References.....	10
2 Background	13
2.1 Chapter Summary	13
2.2 Precast concrete	14
2.2.1 Sustainability.....	18
2.2.2 Hybrid concrete construction	21
2.2.3 The future trends in precast concrete	23
2.3 Precast concrete lattice girder planks.....	26
2.3.1 Production	32
2.3.2 Codes of practice.....	36
2.3.3 Design	37
2.3.4 Lattice girder floors at construction stage	41
2.4 Experimental testing of precast lattice girder planks	48
2.4.1 Codes of practice.....	48
2.4.2 Löfgren <i>et al.</i>	51
2.4.3 Filigran.....	58

2.4.4	Torre <i>et al.</i>	70
2.4.5	Cheng <i>et al.</i>	73
2.4.6	Miscellaneous	76
2.5	Structural health monitoring	78
2.5.1	SHM components.....	79
2.5.2	Benefits of SHM	81
2.5.3	SHM of concrete floors.....	84
2.5.4	Future of SHM	88
2.6	Conclusions.....	92
2.7	References	94
3	Real-time Monitoring to Investigate Structural Performance of Hybrid Precast Concrete Educational Buildings	106
	Article Overview	106
	Abstract	107
3.1	Introduction.....	107
3.2	SHM Strategy.....	108
3.2.1	Methodology	108
3.2.2	Demonstrator buildings.....	111
3.2.3	Sensors	112
3.2.4	Material Testing.....	113
3.3	Engineering building.....	113
3.3.1	Void form flat slab (VFFS).....	113
3.3.2	Evaluating structural capacity	115
3.4	Institute for lifecourse and society building.....	116
3.4.1	Hybrid concrete lattice girder floor.....	117
3.5	Human biology building	119
3.5.1	Early-age thermal effects	121
3.5.2	Construction stage behaviour.....	127
3.6	Conclusions.....	129

Acknowledgements.....	130
3.7 References.....	131
4 Real-time Monitoring of Concrete–Lattice-girder Slabs during Construction	134
Article Overview.....	134
Abstract.....	135
4.1 Introduction.....	135
4.2 Human Biology Building.....	137
4.2.1 Hybrid concrete lattice girder flat slab.....	138
4.3 Instrumentation.....	139
4.3.1 Material testing.....	141
4.3.2 Environmental conditions.....	142
4.4 Results.....	143
4.4.1 Temperature rise and temperature differentials.....	143
4.4.2 Early-age thermal cracking.....	146
4.4.3 Deriving restraint factors.....	148
4.4.4 Construction stage behaviour of hybrid concrete flat slab.....	151
4.4.5 Strain profile.....	153
4.4.6 Time dependent effects.....	157
4.5 Practical applications.....	159
4.6 Conclusions.....	160
Acknowledgements.....	161
4.7 References.....	162
5 Investigation of Thermal Behaviour of a Hybrid Precasted Concrete Floor using	165
Embedded Sensors.....	165
Article Overview.....	165
Abstract.....	166
5.1 Introduction.....	167
5.2 Methodology.....	170
5.2.1 Case study building.....	170

5.2.2	Embedded sensors and data acquisition	171
5.2.3	Material testing	174
5.2.4	Environmental conditions	174
5.2.5	Data post-processing	174
5.2.6	Numerical model.....	177
5.3	Results.....	179
5.3.1	Early-age thermal effects	179
5.3.2	Thermal gradients	185
5.3.3	Horizontal spatial temperature distribution.....	188
5.3.4	Coefficient of thermal expansion.....	190
5.3.5	Solar irradiance	194
5.3.6	Thermal loadings.....	197
5.4	Conclusions.....	198
	Acknowledgements	201
5.5	References	202
6	Experimental Study of Hybrid Precast Concrete Lattice Girder Floor at Construction Stage.....	206
	Article Overview	206
	Abstract	207
6.1	Introduction.....	208
6.1.1	Precast concrete lattice girder floor.....	208
6.2	Experimental set-up	212
6.2.1	Instrumentation	215
6.2.2	Concrete properties	218
6.2.3	Steel properties.....	219
6.3	Test results	220
6.3.1	Moment-deflection behaviour	220
6.3.2	Initial cracking	223
6.3.3	Initial Stiffness	225

6.3.4	Deflection at construction stage	228
6.3.5	Strain distribution.....	231
6.3.6	Ultimate limit state.....	240
6.4	Conclusions.....	247
6.4.1	Recommendations for future research	249
	Acknowledgements	250
6.5	References	251
7	Conclusions	254
7.1	Chapter Summary	254
7.2	Thesis conclusions	254
7.2.1	Reflection.....	263
7.2.2	Original work and contributions to knowledge.....	266
7.3	Recommendations for future work	267
	Appendix A. Photographs of SHM implementation in HBB	269
	Appendix B. Photographs of experimental testing.....	276
	Appendix C. One-dimensional numerical thermal model for hybrid concrete slab.....	284
	Appendix D. SHM as a teaching tool.....	296
	Appendix E. Data sheets for instrumentation used in research.....	304
	Appendix F. SHM strategy for HBB	317

Table of Figures

Figure 1-1 Top 10 disruptive technologies in construction (World Economic Forum) [14].....	3
Figure 1-2 Concrete flat slab [15].....	4
Figure 1-3 Precast concrete lattice girder plank (Keegan Precast)	5
Figure 1-4 Typical section of hybrid concrete lattice girder flat slab [16]	5
Figure 2-1 Comparison of past and present use of precast concrete (London).....	15
Figure 2-2 Venn diagram of sustainable development [8].....	18
Figure 2-3 British Precast sustainability charter [16]	20
Figure 2-4 The four industrial revolutions [26]	25
Figure 2-5 Lattice girder plank [28].....	27
Figure 2-6 Flat slab [30].....	28
Figure 2-7 Flat slab using hybrid concrete lattice girder floor system (Oran Precast)	28
Figure 2-8 Steel lattice girder.....	30
Figure 2-9 Lattice girder configurations [3].....	31
Figure 2-10 Alternative lattice girder planks	32
Figure 2-11 Pallet carousel system for manufacture of lattice girder planks.....	34
Figure 2-12 Pallet carousel for lattice girder planks	35
Figure 2-13 Lattice girder plank with reinforcement and lattice girders	36
Figure 2-14 Limiting design criteria for resistance of flooring units [3].....	38
Figure 2-15 Typical section of a hybrid concrete lattice girder floor at a joint between planks	40
Figure 2-16 Flow of forces across joint between planks [40].....	40
Figure 2-17 Proprietary temporary propping prior to erection of lattice girder planks	42
Figure 2-18 Lattice girder planks supported by temporary props during construction [41]	42
Figure 2-19 Montaquick precast floor.....	46
Figure 2-20 Construction loads for checking deflection during construction in accordance with EN 13747 (Annex J)	49
Figure 2-21 Construction loads during casting of concrete in accordance with EN 1996-1-6 [48]	50

Figure 2-22 Possible loading arrangements for testing in accordance with EN 13747 [38].....	51
Figure 2-23 Test plank used by Löfgren (2001) [49].....	53
Figure 2-24 Test configuration used by Löfgren (2001) [49].....	54
Figure 2-25 Comparison of experimental result and analytical model [49]	55
Figure 2-26 Test set-up used by Verdugo [52]	57
Figure 2-27 Typical load-deflection curve for lattice girder plank [52]	57
Figure 2-28 Approved bending moments and shear force of one type of lattice girder from DIBt Technical Approval [61]	59
Figure 2-29 Test configuration for tests conducted by Bertram et al. [63].....	61
Figure 2-30 Test set-up for 4-point bending [63]	61
Figure 2-31 Moment-deflection diagram for lattice girder plank [63]	62
Figure 2-32 Buckling of top chord in bending tests [63].....	62
Figure 2-33 Ultimate moment per lattice girder in tests [42].....	63
Figure 2-34 Ultimate shear force per lattice girder in tests [42].....	64
Figure 2-35 Shear failure modes at supports [63].....	64
Figure 2-36 Technical approval for Filigran lattice girder [64].....	65
Figure 2-37 Lattice girder slab tested by Torre et al. [65]	71
Figure 2-38 Buckling of top chord in bending test [65].....	72
Figure 2-39 Buckling of diagonal in shear test [65]	72
Figure 2-40 Lattice girder plank tested by Cheng & Fan [67].....	74
Figure 2-41 Comparison of test and numerical model by Cheng & Fan. [67].....	75
Figure 2-42 Precast plank with folded wire fabric mesh [69].....	76
Figure 2-43 Load-deflection and strain data from tests conducted by Park and Yoon [69].....	76
Figure 2-44 Basic components of a SHM system [83]	79
Figure 2-45 Optimum design solution based on life-cycle minimisation with and without monitoring [89]	83
Figure 2-46 Concrete frame in Cardington (ECBP)	87
Figure 2-47 Pyramid model of decreasing data volume and increasing data value [111].....	89
Figure 2-48 Smart Infrastructure [110].....	91
Figure 3-1 Visual schematic of the SHM methodology	111
Figure 3-2 Sensors embedded in the buildings' structure.....	112

Figure 3-3 Cobiax VFFS system being installed in the EB (left) and with gauges installed (right).....	114
Figure 3-4 Strain profile at one of the instrumented sections in the Engineering Building [5]	115
Figure 3-5 Graph showing comparative unit cost of materials for retrofitting of void form flat slab [10].....	116
Figure 3-6 Comparison of predicted strain (EC2) and measured strain in ILAS building (ecs = shrinkage strain, ecc = creep strain, eci = flexural strain).....	118
Figure 3-7 Precast Concrete Lattice Girder Plank (with embedded sensors)	120
Figure 3-8 Typical section showing locations of vibrating wire gauge installed in the flat slab system.	121
Figure 3-9 Concrete temperatures in the 65mm thick precast plank (7 days after manufacture)	122
Figure 3-10 Concrete temperature in 335mm insitu structural topping (7 days after pour)	124
Figure 3-11 Strain and temperature profile in insitu topping (7 days).....	126
Figure 3-12 Strain profile through second floor	128
Figure 3-13 Bending moment in second floor along GL H	129
Figure 4-1 Human Biology Building (under construction).....	138
Figure 4-2 Precast Concrete Lattice Girder Plank (with embedded sensors)	139
Figure 4-3 Sensors embedded in the building's structure: (a) thermistors; (b) VW gauges; (c) ER gauges.....	140
Figure 4-4 Typical section showing locations of vibrating wire gauge installed in the flat slab system (dimensions in mm).....	141
Figure 4-5 Part of second floor slab of HBB with insitu instrumentation	142
Figure 4-6 Concrete temperature in a 65mm thick precast plank (7d after manufacture)	144
Figure 4-7 Concrete temperature in the 335mm insitu precast plank (7d after pour)	145
Figure 4-8 Comparison of measured strain and theoretical strain capacity (7d)	148
Figure 4-9 Insitu strain-temperature curve for insitu topping in hybrid concrete slab	150
Figure 4-10 Measured change in strain in the second floor when (i) when the third floor was poured and (ii) striking of props.....	152

Figure 4-11 Measured change in strain in the second floor when (i) when the third floor was poured and (ii) striking of props.....	153
Figure 4-12 Predicted and measured bending moments in second floor of HBB; (a) Along GL H, (b) Along GL 22	156
Figure 4-13 Comparison of predicted and measured strains in second floor of HBB	158
Figure 5-1 Visual schematic of the SHM methodology [10].....	169
Figure 5-2 Human Biology Building	170
Figure 5-3 Precast Concrete Lattice Girder Plank	171
Figure 5-4 Sensors embedded in the building's structure: (a) thermistors; (b) VW gauges; (c) ER gauges.....	172
Figure 5-5 Embedded sensors in one zone of the second floor of HBB [13]	173
Figure 5-6 Typical section showing locations of vibrating wire gauge installed in the flat slab system [13]	173
Figure 5-7 Comparison of apparent and corrected strains from VW strain gauges	176
Figure 5-8 Determination of Time Zero from measured temperature in the concrete	177
Figure 5-9 Concrete temperature in the 335mm insitu structural topping (14 days after pour).....	182
Figure 5-10 Temperature profile in concrete slab for first 24 hours.....	184
Figure 5-11 Temperature profile in concrete slab for (a) negative temperature differential on 30th Dec 20 15, and (b) positive temperature differential on 19th July 2016.....	187
Figure 5-12 Temperature distribution in concrete slab along GL H at approximately peak temperature during hydration phase (20.00, 20th June 2015).....	189
Figure 5-13 Temperature distribution in concrete slab at 18.00, 19th July 2016 along GL 22	190
Figure 5-14 Insitu strain-temperature curve for the insitu topping at one location in the slab	191
Figure 5-15 Variation of insitu restrained coefficient of thermal expansion in slab	192
Figure 5-16 Comparison of concrete temperature and solar irradiance in the precast plank.....	195

Figure 5-17 Comparison of concrete temperature and solar irradiance in the insitu topping	197
Figure 6-1 Precast concrete lattice girder plank.....	209
Figure 6-2 Typical dimensions of lattice girders	210
Figure 6-3 Temporary props prior to erection of lattice girder planks	211
Figure 6-4 Configuration of precast lattice girder plank tested	213
Figure 6-5 Four point bending of precast plank.....	215
Figure 6-6 Experimental test set-up in laboratory.....	215
Figure 6-7 ER strain gauges bonded to (a) longitudinal reinforcement, (b) bottom chord, (c) diagonal, (d) top chord and (e) concrete surface	216
Figure 6-8 Schematic of instrumentation.....	217
Figure 6-9 Moment-deflection behaviour of lattice girder planks.....	221
Figure 6-10 Cracking on concrete plank.....	222
Figure 6-11 Vertical displacement of lattice girder planks at different load levels	223
Figure 6-12 Measured strain profile in concrete plank (S22.5_08/05/05).....	225
Figure 6-13 Measured strains of specimen S29-14/07/06-2018	236
Figure 6-14 Measured strains of specimen S10-14/07/06-2018	237
Figure 6-15 Strains in longitudinal reinforcement of concrete planks (a) S29-14/07/06 and (b) S10-14/07/06	238
Figure 6-16 Strains profile along longitudinal reinforcement of plank (S10-14/07/06).....	239
Figure 6-17 Crack pattern on plank soffit (S10-14/07/06)	239
Figure 6-18 Strain profile for lattice girder plank.....	240
Figure 6-19 Failure mode of planks	241
Figure 6-20 Transverse cracking on middle third of plank soffit	246
Figure 6-21 Cracking on surface of plank.....	246

Table of Tables

Table 2-1 Permissible spans and minimum tensile reinforcement for specific lattice girder plank at construction stage [42].....	44
Table 2-2 Test programme conducted by Bertram et al. [63].....	61
Table 2-3 Permissible bending moment and shear forces for a Filigran lattice girder to determine erection spans (based on testing) [64].....	65
Table 2-4 Permitted spans during erection for girder [63].....	68
Table 6-1 Details of test planks.....	214
Table 6-2 Table of Instrumentation.....	218
Table 6-3 Concrete mix design for precast concrete planks (1m ³).....	219
Table 6-4 Stiffness of lattice girder planks	227
Table 6-5 Deflection characteristics of lattice girder planks during construction	231
Table 6-6 Failure mode of planks	242
Table 6-7 Predicted failure of planks	244

Acknowledgements

I would like to express my sincere gratitude and appreciation to my supervisor, Dr. Jamie Goggins for his expertise, time, advice and support during the duration of this research project. His guidance and feedback throughout the project were invaluable. I would like to acknowledge the financial support of the European Commission through the Horizon 2020 project Built2Spec (637221). Without this financial support, this project could not have happened.

Throughout this project, many people have assisted me. I would like to thank the many staff at NUI Galway who have helped me and in particular, Colm Walsh for his assistance with the instrumentation and laboratory testing, Peter Fahy for his support with the material testing, Dr. Magda Hajdukiewicz, Gerry Hynes and Dr. Oscar de la Torre. In Oran-Precast, I would like to thank Dave Holleran, Marcin Rybczynski and Sean Burke for their support during the project. I would also like to thank all the construction personnel, building professionals and students that facilitated and helped with installing the structural health monitoring systems. A special thanks to Guilherme Wenceloski and Marília Dantas for their assistance during the installation phase in the Human Biology Building. I would also like to acknowledge Prof. Padraic O'Donoghue and Dr. Annette Harte for their contribution as members of my Graduate Research Committee.

Finally, and most importantly, I would like to thank my wife Clíona and children (Seán, Cillian, Dónal and Dara) for their love and support. Without their sacrifices and encouragement throughout this project, it would not have been possible for me to undertake this work. This thesis is dedicated to my family.

Declarations

This thesis or any part thereof, has not been, or is not currently being submitted for any degree at any other university.

Shane Newell

Shane Newell

The work reported herein is as a result of my own investigation, except where acknowledged and referenced.

Shane Newell

Shane Newell

List of Publications

The work contained in this thesis consists of the following publications in international peer-reviewed journals:

Chapter 3: Newell S, Goggins J, Hajdukiewicz M (2016) Real-time monitoring to investigate structural performance of hybrid precast concrete educational buildings. *Journal of Structural Integrity and Maintenance* Vol. 1, Issue 4, pp. 147-155.
(<http://dx.doi.org/10.1080/24705314.2016.1240525>)

Chapter 4: Newell S, Goggins J (2017) Real-time monitoring of concrete–lattice-girder slabs during construction. *Proceedings of the Institution of Civil Engineers - Structures and Buildings* Vol. 170, Issue 12, pp. 885-900.
(<https://doi.org/10.1680/jstbu.16.00198>)

Chapter 5: Newell S, Goggins J (2018) Investigation of thermal behaviour of a hybrid concrete floor using embedded sensors. *International Journal of Concrete Structures and Materials* 12:66
(<https://doi.org/10.1186/s40069-018-0287-y>)

Chapter 6: Newell S, Goggins J (2019) Experimental study of hybrid precast concrete lattice girder floor at construction stage. *Structures* Vol. 20, pp. 866-885.
(<https://doi.org/10.1016/j.istruc.2019.06.022>)

Note: Shane Newell is the primary author for each journal paper.

1 Introduction

1.1 Introduction

Offsite construction and prefabrication have existed in various forms in the construction industry for many years; however, offsite construction methods have become increasingly popular in the construction industry over the last decade. Offsite construction, also referred to as Modern Methods of Construction (MMC), offers many advantages in terms of quality of construction, cost control, speed of project delivery, health and safety, and environmental credentials (reduced waste, reduced materials etc.). There is no agreed definition for MMC, but according to Nawi *et al.* [1], the term MMC in the UK is used to collectively describe both offsite-based construction technologies and innovative onsite technologies.

As far back as the Egan report '*Rethinking Construction*' [2] in the UK in 1998, the adoption of MMC such as off-site prefabrication to deliver efficiencies, improve quality and reduce waste has been promoted in the construction industry. Warszawski [3] noted that the industrialisation of the construction process is an investment in equipment, facilities and technology with the objective of maximising production output, minimising labour resources, and improving quality. The next stage in the advancement of the construction industry is the adoption of Design for Manufacture and Assembly (DfMA) principles and harnessing the power of Building Information Modelling (BIM) technology. DfMA refers to a set of principles for enabling a design process that facilitates the optimisation of all manufacture and assembly functions, contributing to the minimisation of cost and delivery time, whilst also maximising quality and customer satisfaction ([4], [5]). The primary advantages of DfMA, according to Buildoffsite (UK based membership organisation with members from a wide range of client, supply, professional services and academic organisations) are [6]:

- Health and safety: factory condition is 80% safer than site conditions.

Chapter 1. Introduction

- Cost: site labour is approximately 2.2 times more expensive than factory-based labour.
- Productivity: factory productivity reaches 80% compared with 40% for a typical site.
- Sustainability: waste is reduced to just 2-3% in efficient factories and almost all can be recycled.

Beyond the need to improve the manner in which the construction industry delivers projects, another factor for the change to MMC is the capacity of the construction industry in highly developed industrialised nations to meet the future requirements of society. Farmer in his 2016 report '*Modernise or Die*' [7], which looked at the UK construction labour model identified a skills crisis in mainstream construction. He highlighted a decrease of 20-25% in the workforce in the next decade and that the rate of new entrants is lagging behind those leaving the industry. This scenario is not unique to the UK and will be a major challenge for the construction sector in the future.

Sustainability is the other key driver for change in the construction industry presently and will be in the future. Consideration of environmental pollution, natural resource depletion and accompanying social problems, sustainable development and sustainable construction have become a growing concern throughout the world [8]. Buildings are one of the heaviest consumers of natural resources and account for a significant portion of greenhouse gas emissions. According to the European Directive on Energy Efficiency in Buildings, buildings in the European Union consume 40% of the energy and create 36% of the greenhouse gases (GHG) [9]. In Ireland, buildings accounted for 35% of total final energy consumption and 59% of electricity consumption in 2014, making it the second largest energy end-use behind transport [10]. In the last twenty years, there has been a successful focus on reducing operational energy of buildings. As a consequence, the embodied energy component has increased as a percentage of the life cycle energy use of buildings [11]. Utilising prefabrication technologies has the potential to optimise materials by reducing construction waste, energy use, water consumption, and environmental emissions and, therefore, deliver more sustainable building projects. One of the current challenges for the construction sector is that

Chapter 1. Introduction

there are several assessment tools for sustainability, but they are not consistent in their approach, and therefore, it can be challenging for decision makers (clients, designers, architects, engineers, contractors) to determine the most sustainable option for a specific project.

Side by side with the drive for more sustainable development will be the increased use of sensors in structures to monitor energy performance, structural behaviour and condition of structural components. Many commentators [12] have suggested that we are experiencing a fourth industrial revolution (also known as Industry 4.0) due to rapid advances in digital technology and the revolutionary merging of the digital and physical realms [13]. A 2018 report by the World Economic Forum [14] into the future of the construction industry cited ten emerging technologies (Figure 1-1) which will dramatically change the way in which the construction industry operates in the future. The development of ‘smart structures’ or ‘intelligent structures’ which have sensors will allow more efficient and resilient structures to be designed and constructed but will also ensure better understanding of how our structures perform during use in real conditions (normal and extreme). The information from ‘smart structures’ will, therefore, also contribute to improved design of future structures in terms of efficiency and sustainability, which will provide better whole-life value.



Figure 1-1 Top 10 disruptive technologies in construction (World Economic Forum) [14]

Chapter 1. Introduction

Flat slabs (Figure 1-2) are one of the most widely used forms of floor construction providing minimum structural depths, fast construction and uninterrupted service zones. Flat slabs are a quick method of floor construction as quick turnaround is possible because of the simple formwork requirements. It is also possible to use prefabricated services in conjunction with flat slabs because of the uninterrupted service zones beneath the floor. Flat slabs offer flexibility and adaptability to the client/occupier, as there are no restrictions on positioning of services or partitions and, therefore, there is potential to change internal layout in the future, if required.

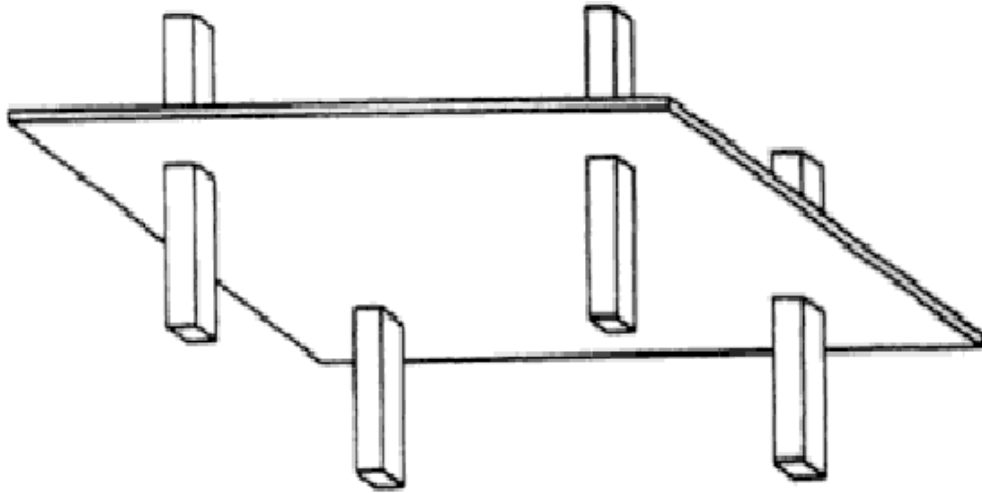


Figure 1-2 Concrete flat slab [15]

The focus of this research is hybrid concrete lattice girder slabs (Figure 1-3 and Figure 1-4) which can be used as an alternative to insitu concrete flat slab construction. Hybrid concrete construction (HCC) which is classified as a MMC, combines insitu and precast concrete to maximise the benefits of both forms of construction. Lattice girder precast soffit slabs consist of a precast plank, with a lattice girder truss which protrudes from the plank to provide stiffness in the temporary state and to ensure composite action with the insitu structural concrete topping. The precast planks are temporarily propped until the structural concrete topping has reached the required compressive strength. The precast planks may be designed and detailed for both one-way and two-way spanning action. The quality of the factory produced soffits provides the opportunity to take advantage of the thermal mass properties of the concrete slab by exposing them.

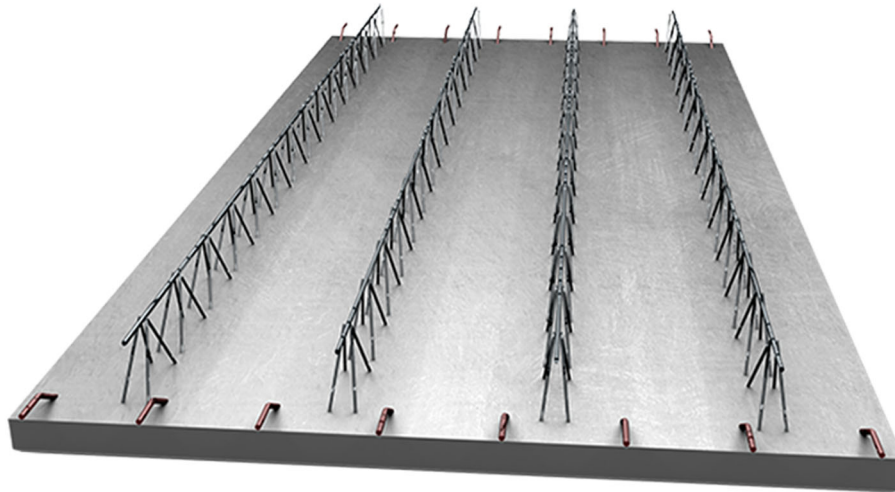


Figure 1-3 Precast concrete lattice girder plank (Keegan Precast)

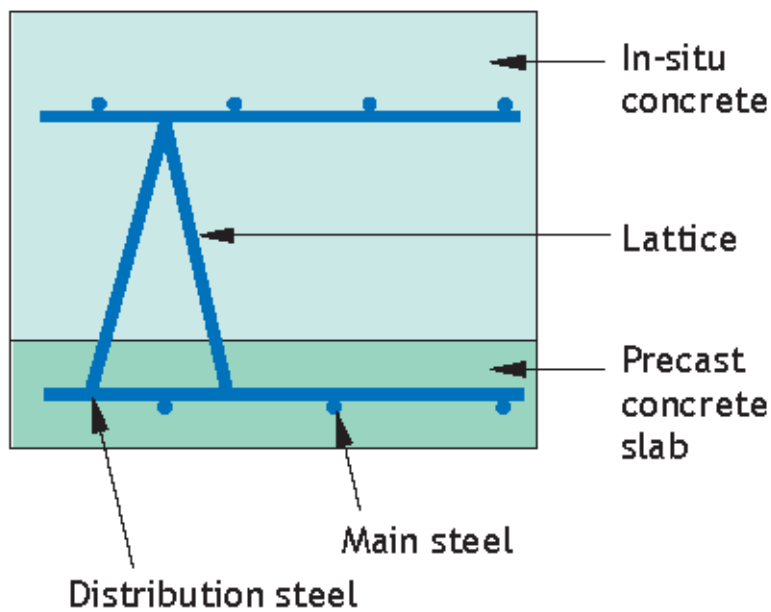


Figure 1-4 Typical section of hybrid concrete lattice girder flat slab [16]

Flat slabs are one of the most popular forms of floor construction in the world. Hybrid concrete lattice girder slabs which is a MMC offers a sustainable and economical option for the provision of flat slab floors in structures. However, in order for the potential of this floor product to be maximised in the future, it is critical that the behaviour of the floor structure is fully understood and that the design and construction of the floor are optimised. The development of ‘smart’ hybrid concrete lattice girder flat slabs (possibly with embedded sensors) should lead to a more

economical and faster form of construction, but could also produce floors which use less resources, minimise waste, have high levels of quality control and make the construction process safer. The research described in this thesis shall contribute to the current knowledge of this floor product, review current design practices and ascertain areas where further research might improve the performance of this floor product.

1.2 Research motivation and objectives

Despite the popularity of concrete flat slabs in structures and the increasing adoption of hybrid concrete lattice girder slabs to construct flat slabs, there is little information on how they perform during construction and in use. Although, structural health monitoring is not a new concept and the technology to monitor concrete floors has been available for many years, there is a scarcity of data on the actual behaviour of the hybrid concrete floor. In order to remain competitive, the precast concrete industry must be able to provide robust data for designers which demonstrates how their products perform in real structures. One of the key design decisions, if utilising lattice girder precast slabs, is the provision of temporary propping during the construction stage until the insitu concrete topping has cured sufficiently. The behaviour of lattice girder planks during construction is complex because of the interaction between the steel lattice girder, concrete and steel reinforcement and currently there is no available generic model which accurately predicts the behaviour of the floor product during construction. A number of researchers ([17]–[20]) have noted that the current procedure for determining the erection spans (distance between temporary props on site) of lattice girder planks was conservative and was based solely on tests. The lack of published experimental data on lattice girder planks during construction limits the understanding of how the floor product behaves and the development of numerical models which can be used to predict its behaviour accurately. The primary motivations of the research described in this thesis are to gain a better understanding of the hybrid concrete lattice girder floor and highlight areas where further optimisation could be possible. This would ultimately improve the potential uptake of the floor product as there would be robust information for all stakeholders (clients, designers, contractors) which could inform their decision-making process.

Chapter 1. Introduction

The main objectives of this research are summarised as follows:

1. A review of previous relevant studies on hybrid concrete lattice girder floors, experimental testing of lattice girder planks at construction stage and structural health monitoring (SHM);
2. Develop and implement a SHM methodology in a real building to study hybrid concrete lattice girder floors during the manufacture and construction phases;
3. Analyse the rich data from the SHM of the hybrid concrete lattice girder floor to investigate actual behaviour of the floor. Compare actual and predicted behaviour of the floor and explore the primary factors which impact its structural and thermal behaviour;
4. Experimental testing to study the behaviour of lattice girder planks at construction stage. Analyse the interaction between the various components of the floor (lattice girder, concrete, reinforcement) during a four-point bending load test and investigate the prediction of deflection and initial stiffness of the plank;
5. Identify primary design parameters which affect the behaviour of the lattice girder plank at construction stage and potential for optimisation. Determine further research that may be required to develop a generic model for predicting accurately the behaviour of the floor product at construction stage.

This project received funding through the Horizon 2020 project Built2Spec [21]. The Built2Spec project (“Tools for the 21st Century Construction Site”) involving twenty organisations (collaboration between academics and industry partners) throughout Europe looked at emerging technologies and how they could improve the construction processes and reduce the gap between a building’s designed and as-built performance.

1.3 Outline of the thesis

The thesis is presented as a series of journal papers (Chapters 3-6). The four journal papers in this thesis have been peer-reviewed and published in international journals in the area of civil and structural engineering.

Chapter 1. Introduction

Chapter 1 of the thesis introduces the research topic, outlining the background to the key aspects of the research and the overall motivation and aims. **Chapter 2** presents a review of the literature relevant to this research. A brief introduction of the precast concrete industry and the development of the lattice girder plank are detailed. Experimental studies on the behaviour of lattice girder planks at construction stage are reviewed and the topic of structural health monitoring is discussed.

Chapter 3 focuses on the implementation of a structural health monitoring (SHM) strategy on three educational buildings recently constructed in Ireland (2010-2016). The motivation and methodology for the SHM are presented and the type of sensors used in the buildings are outlined. The application of real-time monitoring data to analyse the behaviour of concrete structures is presented for a variety of structural aspects such as evaluating structural capacity, early-age thermal effects and predicted strains.

Chapter 4 focuses on the application of real-time monitoring of a hybrid concrete lattice girder flat slab during the manufacture and construction phase for the Human Biology Building (HBB) which commenced construction in Galway (Ireland) in 2015. The data from the SHM system are used to compare measured and predicted behaviour of the concrete floor with respect to early-age thermal cracking, restraint factors and the flexural moments. In addition, the measured strain profile of the concrete floor during the construction of the building is analysed.

Furthermore, **Chapter 5** reports on the application of the SHM data from the HBB to study the thermal response of the hybrid concrete lattice girder flat slab during the manufacture, construction and operational stages. The development of a one-dimensional numerical model is described and compared with the real-time data from the SHM system.

Chapter 6 presents the results of an experimental testing programme to investigate the behaviour of lattice girder planks at construction stage. The development of strain in the lattice girder, concrete surface and longitudinal reinforcement during four-point bending load tests are discussed. The prediction of deflection, initial stiffness and failure mode of the plank are also examined.

Chapter 1. Introduction

Chapter 7 provides a summary of the research and the main conclusions based on the research reported in this thesis. Recommendations for future work to build on the work presented herein are subsequently presented.

Six appendices are included which provide some additional details in relation to the research undertaken. These include (i) photographs of the SHM implementation for the HBB, (ii) photographs of the experimental testing of lattice girder planks, (iii) 1-D numerical model of temperature profile in hybrid concrete slab, (iv) some published articles which demonstrates the potential for using SHM as a teaching tool in engineering education, (v) data sheets for instrumentation used for the SHM and laboratory testing and (vi) description of SHM system implemented in Human Biology Building with accompanying drawings.

1.4 References

- [1] M. N. M. Nawi, F. A. A. Hanifa, K. A. M. Kamar, A. Lee, and M. A. N. Azman, “Modern Method of Construction: An Experience from UK Construction Industry,” *Aust. J. Basic Appl. Sci.*, vol. 8, no. 5, pp. 527–532, 2014.
- [2] J. S. Egan, “Rethinking Construction: the Report of the Construction Task Force,” HMSO, London, UK, 1998.
- [3] A. Warszawski, *Industrialized and Automated Building Systems: A Managerial Approach*, 2nd Ed. E & FN Spon, 1999.
- [4] O. Molloy, E. A. Warman, and S. Tilley, *Design for Manufacturing and Assembly: Concepts, architectures and implementation*. Springer, 1998.
- [5] S. Martínez, A. Jardón, J. Gonzalez Victores, and C. Balaguer, “Flexible field factory for construction industry,” *Assem. Autom.*, vol. 33, no. 2, pp. 175–183, 2013.
- [6] Buildoffsite, “BIM and DFMA,” 2019. [Online]. Available: <https://www.buildoffsite.com/trainingaccreditation/bim-dfma/>. [Accessed: 16-Jul-2019].
- [7] M. Farmer, “Modernise or Die: The Farmer Review of the UK Construction Labour Market,” Construction Leadership Council, London, UK, 2016.
- [8] Y. Chen, G. E. Okudan, and D. R. Riley, “Sustainable performance criteria for construction method selection in concrete buildings,” *Autom. Constr.*, vol. 19, no. 2, pp. 235–244, 2010.
- [9] European Commission, “Energy performance of buildings,” 2019. [Online]. Available: <https://ec.europa.eu/energy/en/topics/energy-efficiency/energy-performance-of-buildings>. [Accessed: 16-Jul-2019].
- [10] D. Dineen and M. Howley, “Energy Efficiency in Ireland 2016 Report,” Sustainable Energy Authority of Ireland (SEAI), 2016.

Chapter 1. Introduction

- [11] R. Azari and N. Abbasabadi, “Embodied energy of buildings : A review of data, methods, challenges, and research trends,” *Energy Build.*, vol. 168, pp. 225–235, 2018.
- [12] K. Schwab, *The fourth industrial revolution*, 1st Ed. Penguin, 2017.
- [13] Arup, “The Fourth industrial revolution: meet the technologies reshaping the built environment,” 2019. [Online]. Available: <https://www.arup.com/perspectives/the-fourth-industrial-revolution-meet-the-technologies-reshaping-the-built-environment>. [Accessed: 17-Jul-2019].
- [14] M. Buehler, P. P. Buffet, and S. Castagnino, “The Fourth Industrial Revolution is about to hit the construction industry. Here’s how it can thrive,” *World Economic Forum*, 2018. [Online]. Available: <https://www.weforum.org/agenda/2018/06/construction-industry-future-scenarios-labour-technology/>. [Accessed: 17-Jul-2019].
- [15] C. H. Goodchild, R. M. Webster, and K. S. Elliott, “Economic Concrete Frame Elements to Eurocode 2 (CCIP-025),” Cement and Concrete Industry Publication (UK), Surrey, UK, 2009.
- [16] R. Whittle and H. Taylor, “Design of Hybrid Concrete Buildings: A guide to the design of buildings combining in-situ and precast concrete,” Concrete Centre (UK), 2007.
- [17] Y. M. Cheng and Y. Fan, “Laboratory and numerical test on concrete plank composite with reinforcement truss,” *J. Struct. Eng.*, vol. 20, no. 4, pp. 207–216, 1994.
- [18] I. Löfgren, “Lattice Girder Elements in Four Point Bending – Pilot Experiment (Report No. 01:7),” Chalmers University, Sweden, Göteborg, 2001.
- [19] G. Bertram, J. Furche, J. Hegger, and U. Bauermeister, “Permissible Span of Semi-precast Slabs in Case of Erection (Zulässige Montagestützweiten von Elementdecken mit verstärkten Gitterträgern),” *Beton- und Stahlbetonbau*, vol. 106, no. 8, pp. 540–550, 2011.

Chapter 1. Introduction

- [20] J. Furche and Bauermeister U, “Load tests: Long erection spans with strengthened lattice girders,” *Betonwerk+ Fert.*, vol. 77, no. 8, pp. 4–17, 2011.
- [21] Built2Spec, “Built2Spec,” *Tools for the 21st century construction worksite*, 2019. [Online]. Available: <https://built2spec-project.eu/>. [Accessed: 17-Jul-2019].

2 Background

2.1 Chapter Summary

This research is focused on investigating the behaviour of precast concrete lattice girder slabs during construction. A brief overview of the precast concrete industry in general terms is presented in Section 2.2 and the topics of sustainability (Section 2.2.1) and hybrid concrete construction (Section 2.2.2) with respect to precast concrete are also discussed. The future trends and challenges for the precast concrete industry in construction are reviewed in Section 2.2.3.

This chapter provides a summary of the existing literature on lattice girder planks (Section 2.3), experimental testing of the lattice girder planks (Section 2.4) and structural health monitoring (Section 2.5). In this study, experimental testing and structural health monitoring systems are used to investigate the behaviour of the lattice girder plank during construction stage when the precast plank must support its self-weight, construction loading and the weight of the insitu concrete topping.

The history and development of the lattice girder plank as a precast concrete floor product are presented in Section 2.3. Section 2.3.1 describes the production process for the floor product and the codes of practice which underpin its application in structures are reviewed in Section 2.3.2. The overall design of the hybrid concrete floor is discussed in Section 2.3.3 and the specific behaviour and design of the lattice girder plank at construction stage is examined in Section 2.3.4. The most significant literature published on experimental testing of lattice girder planks is reviewed in Section 2.4.

The general topic of structural health monitoring (SHM) and its origins are presented in Section 2.5 and the primary components of a typical SHM system are summarised in Section 2.5.1. The potential benefits of utilising a SHM system in a structure are detailed in Section 2.5.2 and the future direction of SHM systems and

what it will possibly mean for construction are presented in Section 2.5.4. The current application of SHM to concrete floors is reviewed in Section 2.5.3.

2.2 Precast concrete

Although precast concrete is not a new idea, it was not until after the Second World War (1945-1960) that precast concrete was used extensively in the construction industry. The main driver for this breakthrough was the extraordinary demand for housing and the introduction of semi-automation in the production process. Elliott and Hamid [1] refer to this period after 1945 as the ‘mass production and standardisation period’.

Nowadays, the use of precast concrete in construction is well established. In the 1960’s, precast concrete was exploited for use in modularised developments in which ‘production-orientated’ design led to some oppressive architecture most evident in Eastern Europe [2]. However, the precast industry has evolved from an industry which mass-produced modular units which offered little flexibility to standardisation in which pre-determined components were used and connected [3]. The difference in the use of precast concrete can be illustrated in Figure 2-1 by observing the two precast structures (Camelford house on left, 1960s and SIS building on right, 1994) beside the Vauxhall Bridge in London. Today, although a precast manufacturer may produce a family of standardised components, there is variation permitted within a family of components to meet specific project requirements. Bespoke designs can be achieved using standard precast components, which need not imply a modular appearance [4]. As the construction industry moves towards off-site pre-fabrication, the precast concrete industry is well placed to meet demand for sustainable and efficient structural components which can be manufactured in a controlled environment and delivered to site as required.

In Ireland, the popularity of concrete as a construction material can be largely attributed to fact that the country has large deposits of the raw materials required to produce cement and high-quality aggregates. Relative to its size, Ireland has a sizeable number of companies involved in the manufacture of precast products for sale in the domestic Irish market and for export to the UK. For some precast manufacturers in Ireland, the majority of their products are exported to the UK. This

Chapter 2. Background

export market for precast products to the UK has grown significantly in the last decade and has grown to €130 million in 2017 from a non-existent market in 2006 [5].



Figure 2-1 Comparison of past and present use of precast concrete (London)

Precast concrete offers many possibilities for most construction projects. Where previously, the design approach may have been to try to use precast concrete for the entire project, most designers now consider a variety of construction materials and methods to achieve specific performance criteria related to the project. This means that a mix of materials and construction methods ('mixed construction') may be the most suitable and economical solution for a project.

The primary advantages for choosing precast concrete are [6]:

(i) Cost

Using precast elements reduces requirements for formwork and scaffolding and this will reduce cost of both labour and resources. In addition to construction costs, operational costs for projects should also be considered.

Chapter 2. Background

Structures with significant precast concrete components offer benefits in terms of fire resistance, sound insulation and fabric energy storage (thermal mass) which can result in lower operating and maintenance costs.

(ii) Programme

Speed of construction is typically one of the key considerations in most building projects. As mentioned previously, the reduction in resources required for formwork and scaffolding will also result in savings in the construction programme. To take advantage of using precast products to reduce the programme, the layout of the building should be designed to maximise repetition of precast elements and the use of standardised components.

(iii) Performance

Concrete products have inherent durability and fire resistance properties without additional treatments when designed and detailed correctly. For most structures, concrete products meet vibration criteria without any change to the original design. For some specific uses (laboratories and hospitals), additional measures may be required, but they are generally less than for other materials. Due to its high density and damping qualities, concrete has advantages over many lightweight construction materials for sound insulation.

(iv) Quality control

Precast products are manufactured in a controlled environment so that tight tolerances can be achieved and quality control systems can be employed to ensure that the product arrives on site without defects or blemishes. High quality concrete finishes can be achieved for precast products as the formwork used is typically bespoke steel moulds and dedicated concrete mix designs are used for manufacture. As production takes place in an enclosed space, the manufacturing process is not dependent on the weather. Most precast manufacturers have dedicated concrete supplies and this ensures consistency of the colour and texture of precast products, which is particularly important when the concrete is left exposed.

Chapter 2. Background

(v) Design

Precast concrete can deliver economical design solutions for many projects because of the efficient production process which minimises waste, maximises material efficiency and produces a range of concrete finishes. In particular, prestressed precast concrete products offers the opportunity to deliver longer spans or shallower construction depths. The design of most precast concrete products are typically the responsibility of the manufacturer and the design are based on proven technologies and methodologies which have been developed over many years. Precast concrete can also make complex shapes affordable if there is sufficient repetition of elements.

(vi) Off-site construction

Precast concrete products can be stored at the factory and delivered just-in-time to site so that the components can be installed directly from the lorry. This minimises the space requirements on site; which can be critical for urban projects. Off-site manufacturing of precast concrete shifts the balance of work from the site to a factory-controlled environment. This reduces the level of activity on site and this can enhance the safety environment for the workforce. Once precast floors are installed, they provide a safe working platform for site operatives and in many projects precast stairs are installed with rising elements so that there is safe and easy access between floors (once handrails are installed). Precast products are typically delivered to site without packaging and there are no site offcuts which considerably reduces waste.

Precast concrete flooring accounts for approximately 50-60% of precast concrete components produced by the industry (based on volume of concrete). In the context of floor components, there are five main types of products which are used in the industry [3]:

- prestressed hollowcore floor
- reinforced and prestressed double-tee floor
- beam and block floors
- composite prestressed beam plank floor

- composite beam and plank (used with a structural topping)

2.2.1 Sustainability

There are many definitions for sustainable development, but one of the most common is from Brundtland Report for the World Commission on Environment and Development in 1987 [7]:

“Sustainable development is development that meets the needs of the present without compromising the ability of future generations to meet their own needs.” The three pillars of sustainable development are economy, society and environment; if any one of the pillars is weak then the development as a whole is unsustainable. Sustainable development must balance economic, social and environmental objectives in equal harmony.

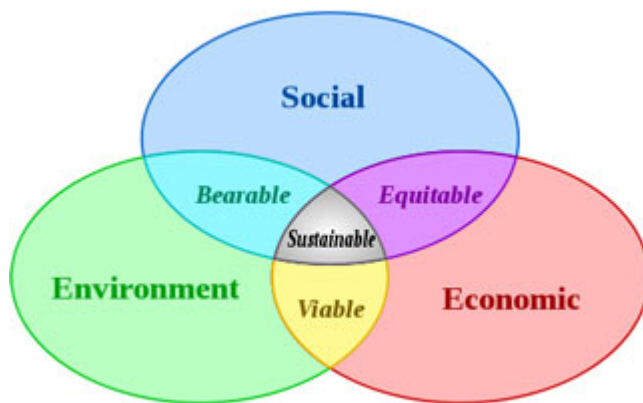


Figure 2-2 Venn diagram of sustainable development [8]

Many governments have developed strategies in the form of legislation and/or programmes to promote sustainable development ([9], [10]). Sustainable construction has a key role in achieving progress in sustainable development because of its impact on environment and society. There is a growing consensus [11] that a sustainable approach to construction can also lead to competitive advantages such as more innovative practices, reduced costs and more efficient processes which in turn can reduce the impact on the environment and deliver better buildings and structures to customers and users. The issue of sustainability of projects and consideration of the environmental, social and economic impacts are

Chapter 2. Background

increasingly to the forefront during the design phase of projects. Precast concrete offers opportunities for designers to influence the sustainability credentials of the project.

The durability characteristics of concrete allow specification of components with a long service life which require no additional finishes and are maintenance free. This allows for the reuse of buildings rather than replacement if the buildings are designed for flexibility and multiple uses. Concrete is resistant to fire, extreme weather and is also adaptable to changing uses. Long-term durability and the resilience of concrete are increasingly important when designing projects on a whole-life basis for environmental, economic and social impacts.

The energy used for space heating accounts for 20-50% of a building's energy consumption depending on the type, and around a third of the carbon emissions from all UK buildings [12]. The high thermal mass or fabric energy storage (FES) properties of concrete can be exploited, if designed appropriately, to reduce both heating and cooling loads in buildings and therefore operational costs. The exposed concrete can absorb unwanted heat, helping to regulate internal temperature and reduce CO₂ emissions associated with mechanical cooling. Precast concrete is ideally suited to utilising the thermal mass of concrete because of the high-quality finish that can be achieved for exposed surfaces. In order to take advantage of the thermal mass of concrete, the building form, orientation, fabric and finishes must be considered at the design stage. Using concrete floors to provide thermal mass whilst also fulfilling structural and aesthetic roles offer the best opportunity to make significant savings in capital and operating costs over the lifetime of the building. Reductions in heating energy consumption of 2-15% are possible [13] by utilising the energy storage properties of concrete.

The use of precast products reduces noise and waste from the construction site to the factory where it can be managed and controlled. The precast concrete sector uses more waste than it produces [14]. In the UK, the Waste and Resources Action Programme (WRAP) estimated that the use of precast flooring could reduce waste by approximately 30-40% in comparison with traditional building methods [15].

Chapter 2. Background

A whole-life approach to projects must be considered for sustainable construction so that products are seen as a resource at the end of life (circular economy). Therefore, the potential for reuse and recycling of precast concrete components at the end of life must be considered at design stage so that components can be diverted from landfill. The development of environmental product declarations (EPDs) for precast concrete products will provide designers with information on the whole-life sustainability of products. The use of electronic tagging of precast products is increasingly popular in the industry and this increases the opportunity for reuse of the product in the future. The major challenge for the precast industry is to develop connections and joints which allow the reuse of concrete products rather than recycling of the precast concrete products as aggregate at the end of life.

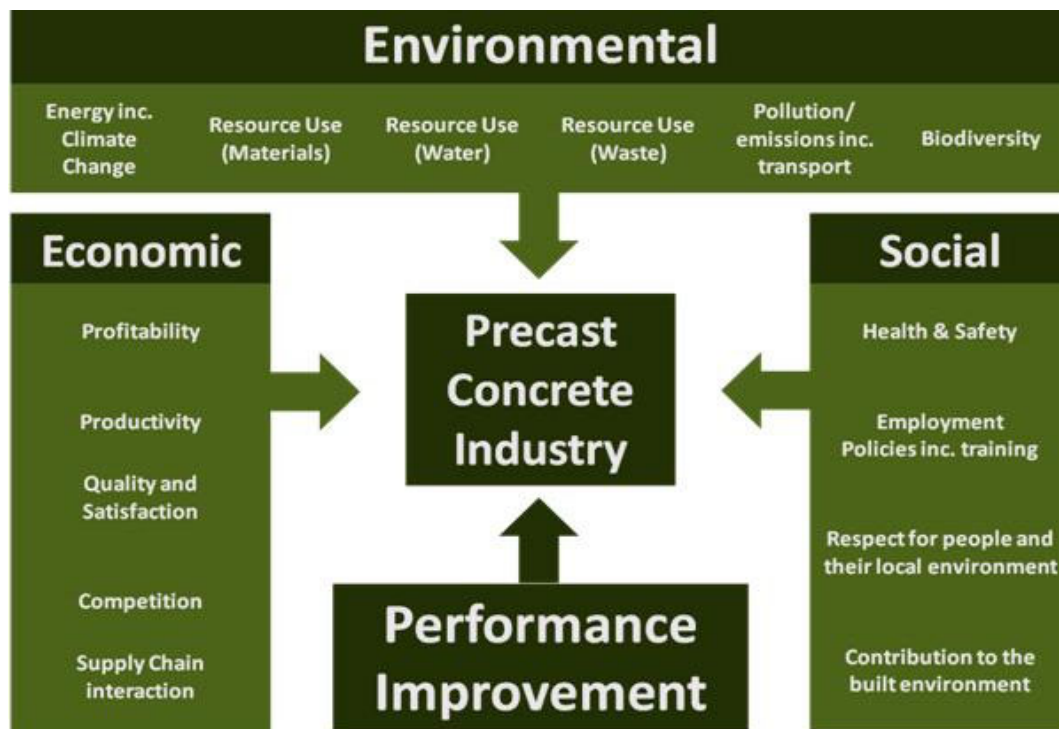


Figure 2-3 British Precast sustainability charter [16]

In addition to the inherent sustainability characteristics of concrete, the precast concrete industry has changed its production processes to improve the sustainability of their products. In the last ten years (2008-2018), the UK precast industry has reduced manufacturing carbon emissions by 28%, mains water consumption by 30% and factory waste to landfill by over 96% [17]. The industry has also increased the use of recycled materials and by-products from other industries (aggregates,

steel reinforcement and cementitious materials) in their products which reduces their embodied carbon. In the UK, British Precast (trade association of precast concrete manufacturers) developed a ‘Sustainability Charter’ which outlines a set of sustainability principles to make their products and operations more sustainable (Figure 2-3).

2.2.2 Hybrid concrete construction

The term ‘hybrid’ is used to describe construction where precast concrete is used in combination with cast insitu concrete. Hybrid construction is different to ‘mixed’ construction which is used to define the use of two or more materials in the same project. Hybrid concrete construction (HCC) takes advantage of the excellent combination offered by concrete of durable strength, stiffness, thermal mass, fire resistance and sound insulation, with the added construction speed and convenience achieved by precasting [3]. HCC produces simple, buildable and economic structures which result in faster, safer construction and reduced costs.

HCC was developed and promoted by the precast industry to meet industry requirements for increased prefabrication, increased off-site activity, safer and faster construction, and consistent performance [18]. In the UK, the use of HCC was promoted by the Egan report [19] (1998) by encouraging the construction industry to deliver efficiency improvements, using a similar approach to that which occurred in other industries (such as manufacturing). The Egan report stated that ‘The industry must design projects for ease of construction making maximum use of standard components and processes’.

Hybrid concrete technology is used primarily to achieve fast and cost effective construction by removing labour-intensive operations on-site and replacing them with mechanised production in precasting yards and factories [18]. The primary advantages of HCC are:

(i) Cost

Cost is typically one of the most influential factors when determine the type of frame material. The structure of a building typically represents only 10% of the construction costs [18]. However, the choice of structural frame material can also

Chapter 2. Background

have a significant effect on other elements of the construction such as programme, services and cladding. HCC can reduce frame costs by using precast elements for repetitive elements and/or to act as permanent formwork. Traditional formwork typically accounts for up to 40% of in-situ frame costs [20].

(ii) Speed

One the major benefits of HCC is speed. HCC transfers work away from site into the factory and therefore reduces the duration of the overall programme on site. Some contractors have reduced construction time on site for a typical concrete framed building by 50% [21]. In order to maximise the benefits of HCC, there must be sufficient coordination and pre-design between the project team before the project commences on site.

(iii) Buildability

Buildability is the extent to which design simplifies construction and eradicates unnecessary cost, subject to the requirements of the completed building [18]. The use of HCC encourages design and construction issues to be resolved early in the design process prior to manufacture of elements. This means that precast components can be stored in the factory and delivered 'just-in-time' to site. This eliminates the need for site storage and can reduce crane time.

(iv) Construction

The trend in the industry towards off-site construction with more prefabrication and reduced site activity are suited to HCC as a high percentage of the work is transferred from the site to the factory and therefore, there is less requirement for skilled labour on site in comparison to traditional construction methods.

(v) Safety

A site-specific safety plan and method statement are prepared for erection of precast components on site. HCC reduces the number of site tasks and personnel on site. Where precast slabs are used, it reduces potential for accidents by providing successive working platforms.

To maximise the benefits of HCC, a more collaborative approach between the various stakeholders is required. It is recommended that there is early involvement of specialist contractors, such as precast manufacturers and frame contractors. Ideally, they should be appointed during the conceptual design phase whilst various structural options are being considered. This allows the specialist knowledge of precast manufacturer to liaise with other members of the design team and ensure that the design intent and practicalities of manufacturing and erection on site are compatible.

2.2.3 The future trends in precast concrete

The ultimate goal of the precast concrete industry is to produce a product which is better and/or cheaper and/or faster than the competition [22]. The optimal product would, of course, be one which is better and cheaper and faster and produced by considering the three pillars of sustainable development (social, economic and environment). The precast industry is well placed to meet the future needs of the construction industry as it moves towards increased prefabrication (off-site construction), reduced on-site processes and high-quality workmanship. Clients, engineers, architects and contractors are now more aware of the advantages which precast products can deliver in terms of quality, speed, finish and economy. One of the key challenges for the precast industry is being able to provide robust data which demonstrates how their products behave in real structures and how their performance can enhance the overall project during the construction and operational phase.

The trend in the construction industry towards moving work from site to the controlled environment of factory production has gathered pace in the last ten years. It has impacted all site operations as contractors strive to reduce potential risks to programme, health and safety, and quality control. The proportion of prefabrication in the super structure, including steel and precast concrete elements, prefabricated formwork and rebar cages has increased from about 25% in 1990 to between 40-60% today [1].

The implementation of Building Information Modelling (BIM) to the construction sector will be one of the defining challenges for the construction industry in the future. BIM is an intelligent model-based design process that adds value across the

Chapter 2. Background

entire lifecycle of building and infrastructure projects. The use of digital design models has been common practice in manufacturing industry (Boeing, Toyota) for decades, but up to recently have been rarely used in the architecture, engineering and construction (AEC) sectors. The implementation of BIM for the precast industry offers opportunities for the sector to improve the manufacture, design, pricing, logistics and quality management processes related to their products. It is important that the precast concrete industry is a key stakeholder in the implementation of BIM, so that it can maximise the potential for increasing the market share of precast products. This will require manufacturers to develop product data sheets (PDS) for their products for use by other stakeholders in the BIM process.

The requirements for sustainability will continue to dominate the construction industry in the future. As outlined previously (Section 2.2.1), precast concrete with continued innovation is well positioned to be part of the solution as the drive for sustainable development continues across the construction industry. One of the key challenges for the industry will be development of a ‘circular economy’ for precast concrete products such that products will be designed for re-use and material recovery. The use of BIM technologies will have a significant role in this “closed loop” approach so that the information which will allow products to be tracked, documented and re-used will be provided to the client at the end of the construction phase. The advent of Environmental Product Declarations (EPDs) in accordance with EN 15804 (‘Sustainability of construction works - Environmental product declarations. Core rules for the product category of construction products’) [23] will allow designers to consider the whole life carbon assessment of a product so that a building’s embodied, operational and end-life carbon emissions can be assessed.

In the future, it is envisaged that construction products will become increasingly complex. This will entail precast concrete products manufactured with integrated building services and embedded sensors in precast concrete components so that performance of the products can be optimised during manufacture, construction and in service. The age of “Internet of Things” (IoT) with respect to construction products could involve devices embedded in objects and connected via the Internet, enabling them to send and receive data. The rapid pace of change in the IoT era has

Chapter 2. Background

led to introduction of smart wireless sensors, mobile applications and cloud-based technologies in society, including the precast concrete sector. It is likely that the next wave of technological advances (including BIM) in conjunction with the IoT will allow real-time data to be available to all stakeholders (precast manufacturers, designers, contractors, clients) so that the efficiency and performance of precast products can be optimised.

The term ‘*Industry 4.0*’ also known as the Fourth Industrial Revolution is used to describe the current digital transformation of industry. The first three industrial revolutions came about because of mechanisation, electricity and automation. The term ‘*Industry 4.0*’ originated in Germany in 2011 [24] and has become a strategic initiative of the German government [25] to ensure that the German industrial sector is competitive in the future. Building on the previous digital revolution, the fourth industrial revolution is the combination of advanced manufacturing techniques with the Internet of Things (IoT) and Building Information Modelling (BIM). In the context of the precast concrete industry, the development of cyber-physical systems will mean more efficient and less wasteful production of components and the use of real-time data during the manufacture and operational phase of precast components to optimise ‘smart’ precast concrete products using sensors and devices embedded in the components. ‘*Industry 4.0*’ will involve the integration of all physical and virtual processes so that there is real-time communication between automated machines, plant, personnel and the internet (i.e. development of ‘smart’ factories).

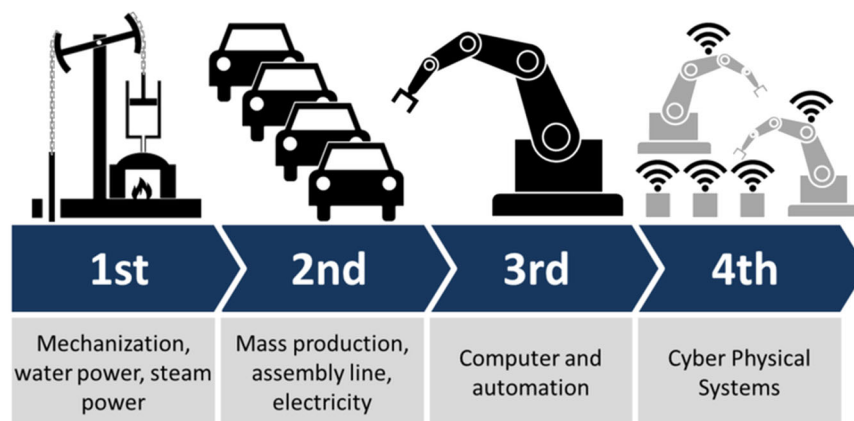


Figure 2-4 The four industrial revolutions [26]

Chapter 2. Background

This research is focussed on one of the most popular forms of HCC used to construct floors (hybrid concrete lattice girder slabs). In order for any precast product to be competitive in the future, it is critical that the economical and sustainability credentials of the product are disseminated to the relevant stakeholders in the construction industry. Using field and laboratory testing, this research provides robust data and information on the actual behaviour of hybrid concrete lattice girder slabs which can be used to understand how this floor product behaves in real structures. Without this information, it is possible that other MMC may become more common for construction of floors. With the current digital revolution in the construction industry (*'Industry 4.0'* and/or Internet of Things), and the development of 'smart' structures, one of the challenges of this new era will be how data are managed so that the information has value and informs the decision-making process during the manufacture, construction and operational phase of structures. The utilisation of rich field data to investigate various behavioural characteristics of hybrid concrete lattice girder slabs is a key objective of this research.

2.3 Precast concrete lattice girder planks

Precast concrete lattice girder planks (Figure 2-5) are a very popular product used to construct concrete floors. In Germany, it was estimated that 70% of all floors in high-rise building structures are constructed using the lattice girder floor system [27]. The lattice girder floor system is also known as the Omnia slab, Filigree slab or Half-slab. The use of steel lattice girders in the manufacture of precast products was first developed in the 1950s. The lattice girder plank comprises of a thin layer of concrete with a projecting lattice girder which is later cast with an insitu concrete topping to create a monolithic slab.

The precast concrete plank is used in conjunction with a structural topping and, therefore, relies on composite action to resist flexural and shear stresses. The rectangular planks are laid between supports and act as a permanent formwork for the insitu concrete topping (hybrid concrete construction). The lattice girder plank can be manufactured using conventional steel reinforcement or prestressing strands. For total slab depths up to 200mm, the prestressed plank has a greater load capacity (5-20%) than the reinforced plank, but as the thickness of the structural topping

Chapter 2. Background

increases, the efficiency of the prestressed plank reduces and the reinforced plank becomes more economical. The load capacity of the reinforced concrete slab is almost linearly proportional to the total depth. The focus of this project is on the lattice girder plank with steel reinforcement, which is the most popular form of the product.

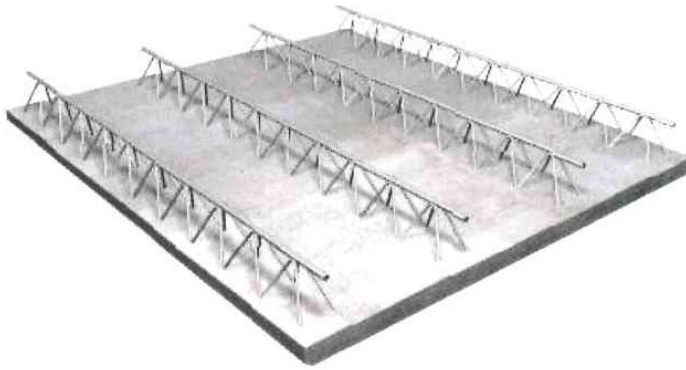


Figure 2-5 Lattice girder plank [28]

Concrete flat slabs floors are directly supported by columns without the use of intermediary beams (Figure 2-6 and Figure 2-7). The hybrid concrete lattice girder floor is a form of flat slab which is one of the most widely used forms of floor construction because of the advantages it offers in terms of speed, simplicity, flexibility in layout, minimum structural depths and a flat soffit for service distribution. Flush soffits allow prefabrication of services resulting in up to 15% cost saving through reduced waste [29]. Flat slabs can be constructed with exposed soffits so that the thermal mass properties of the concrete can be exploited. The advantages of using hybrid concrete construction to construct flat slabs rather than traditional insitu concrete are the elimination of formwork, reduction in labour, reduction in steel fixing, quality of finish and improved health and safety on site (Section 2.2.2). The hybrid concrete lattice girder floor can be used in conjunction with precast or insitu rising elements (columns and walls).

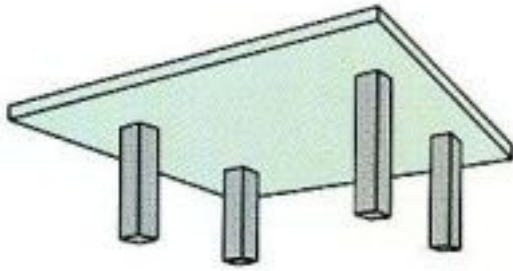


Figure 2-6 Flat slab [30]



Figure 2-7 Flat slab using hybrid concrete lattice girder floor system (Oran Precast)

Although, it is difficult to obtain accurate data in relation to the proportion of floors that are constructed using a flat slab structure, the use of flat slabs for commercial and public buildings is very common throughout the world. For spans between 5 and 9 m, flat slabs are the preferred option for construction of concrete frame buildings where a regular grid is used. With respect to the use of hybrid concrete (precast and insitu) to construct flat slabs, their popularity has increased as the industry has moved towards off-site construction, where possible. The Concrete Centre in the UK estimated in 2012 that 80% of concrete framed buildings are flat

Chapter 2. Background

slabs and this equated to approximately 4 million m² of flooring per year [31]. Cost model studies were commissioned by the Concrete Centre in the UK in 2013 [32] to compare costs of constructing different types of buildings with different structural solutions. The independent cost model study indicated that for a three storey office (out-of-town business park) and a six storey office (city centre), the concrete flat slab option was the most economical solution (£/m²) and offers a significant advantage in lead times in comparison to steel framed options. Using data collected from an actual construction project, Cho [33] conducted a comparison of a hybrid concrete floor and a traditional cast insitu slab floor and determined that the construction productivity of the hybrid concrete floor was 1.7 times that of a traditional concrete slab system. Construction productivity was measured in terms of time taken to complete a floor. The research also showed that the hybrid concrete floor was more economical than the traditional concrete slab system for a variety of simulated scenarios based on different resources.

There are a number of proprietary types of lattice girder planks such as ‘Omnia’, ‘Filigree’ and ‘Katzenburger’. The depth of the precast plank varies between 50-100mm. The planks can be manufactured up to 3.4m wide and 12m long, but the sizes can be dictated by transportation and site restrictions. The top surface of the plank is roughened to ensure bond between the precast plank and insitu structural topping. Most lattice girder planks are manufactured using conventional high strength reinforcement rather than prestressing. The cover to the reinforcement in the bottom of the plank is typically 25mm for internal environments and one hour fire resistance. The triangulated lattice girders are manufactured using drawn wire spot-welded in a semi-automatic production process. The height of the lattice girder can vary between 70 and 400mm and is dictated by the overall depth of the composite slab. The lattice girder consists of:

- diagonals - pairs of small diameter bars (5-9mm diameter) are bent into a zigzag pattern where the inclination of the bars is between 40° and 70° to the longitudinal direction;
- top chord - single bar (5-16mm diameter), depending on the span of the floor and propping methods used;
- bottom chord - two bars of similar size (5-14mm diameter).

Chapter 2. Background

The diagonals are typically smooth and the top and bottom chord can be manufactured using ribbed or smooth reinforcement. In Europe, the steel used for the lattice girder is typically grade B500A (yield strength = 500N/mm^2) in accordance with EN 10080 [34]. The lattice girder provides a number of important functions:

- (i) the girders provide stiffness to the plank during the temporary condition until the structural topping has reached sufficient strength.
- (ii) the lattice girder increases the mechanical bond between the precast plank and insitu topping.
- (iii) the girders acts as a support (spacer) for the top layer of reinforcement in the structural insitu topping.
- (iv) the bottom chord of the girder contributes to the flexural reinforcement in the precast plank.
- (v) the girders are convenient lifting points for unloading and placing planks on site.



Figure 2-8 Steel lattice girder

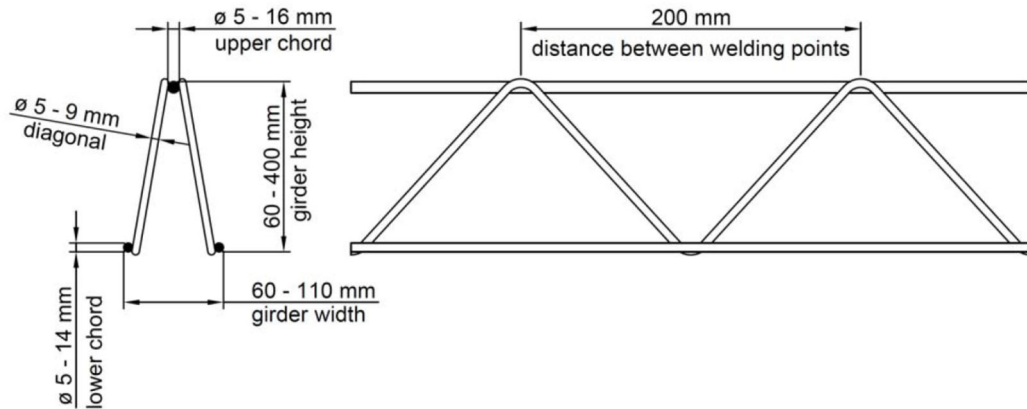


Figure 2-9 Lattice girder configurations [3]

In addition to the standard lattice girder plank, void formers may be incorporated into the manufacturing process using expanded polystyrene blocks or hollow recycled plastic spheres (Figure 2-10). The principle of voided flat slabs is to reduce the self-weight of the slab by eliminating concrete which provides little structural benefit. The voids in the slab reduce the volume of concrete required by displacing nonworking dead load. The key requirement during the manufacturing process is to ensure that the void formers are sufficiently adhered or tied to the precast plank so that they will not move during the pouring of the structural topping. The lattice girder plank can also be manufactured with an edge shutter (typically galvanised steel plate) to minimise formwork requirements on site and service openings may be pre-formed in the plank to allow for integration of services (mechanical and electrical) in the floor slab. In recent years, lattice girder planks have been manufactured with pipework embedded in the precast plank so that the exposed concrete soffit can act as a heating or cooling medium (fabric energy storage).



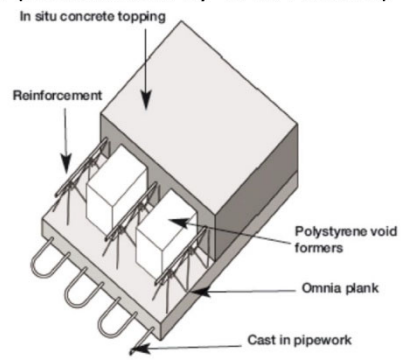
(a) Polystyrene blocks with lattice girder plank (*Nordimpianti*)



(b) Spherical voids with lattice girder plank (*Cobiax deck* by Oran Precast)



(c) Edge shutter cast with lattice girder plank (Oran Precast)



(d) Integrated pipework in lattice girder plank (*Coolslab*® by Hanson)

Figure 2-10 Alternative lattice girder planks

2.3.1 Production

Precast concrete lattice girder planks are manufactured using concrete varying between C28/35 to C40/50 and this largely depends on the requirements for early-strength in the concrete so that the planks may be stripped from their moulds the next day after manufacture. The planks can be manufactured using normal and lightweight aggregate, but the use of lightweight aggregates is rare. Manufacturers use either self-compacting concrete (SCC) or vibrating tables to compact the concrete. Admixtures are typically used to control water-cement ratio of the concrete mix and to achieve specific workability (or consistence) characteristics in the wet concrete.

The concrete required for production of precast elements will often have to satisfy different requirements to those of insitu concrete. The strength of the concrete at demoulding is typically the critical parameter for precast manufacturers rather than characteristic compressive strength at 28 days. The high early strength required so

Chapter 2. Background

that lattice girder planks can be demoulded the day after manufacture ensures that the necessary strength for construction and structural requirements are typically guaranteed. Manufacturers can also use rapid-hardening cements and/or thermal curing to ensure that the concrete strength is sufficient to allow lifting of the planks the day after manufacture.

Lattice girder planks are typically manufactured using a pallet carousel system rather than stationary production systems (see, for example Figure 2-11). Pallet carousel production systems were developed in Germany and Austria in the 1970s due to increasing labour costs and higher quality requirements and are the most efficient production method for walls and floor products. This production method which is similar to that employed in the automobile industry is characterised by moving production tables (pallets) and fixed work stations for plant personnel. In this system, the work pallet moves to the worker. Tools and any necessary resources are located at the workstation where they are needed. During the production process, automation is used where possible to improve the precision, quality and efficiency of the finished product. The pallet carousel has two main advantages [22]:

- Better organisation of entire production procedure. The materials required can be made available without internal transportation and individual workers carry out the same work at the same place at the same time.
- Lower plant costs because the individual operations are carried out at workstations specially designed for those operations.



Figure 2-11 Pallet carousel system for manufacture of lattice girder planks

Most modern precast concrete plants use CAD-CAM (Computer Aided Design-Computer Aided Manufacturing) systems to automate many tasks during the production process. Each pallet is made of steel material with a smooth surface which is resistant to vibrations, easy to clean and ensures a high-quality concrete finish on the plank soffit. A robot reads the CAD data for the plank and marks the contours of the plank (using water soluble paint) and any openings on the pallet (See, for example, Figure 2-12a). Magnetic shutters are used to define the edge of the concrete plank (See, for example, Figure 2-12b). The degree of automation varies between plants, but typically the reinforcement and lattice girders are selected by a robot which automatically cuts the reinforcement and lattice girders required for the plank and places them on the pallet (See, for example, Figure 2-12c). The lattice girders are placed after the reinforcement in the plank are positioned on the pallet. The reinforcement and lattice girders are then tied and checked by plant operatives to ensure it complies with the CAD drawing for the plank prior to casting of the concrete plank (Figure 2-13). The concrete can be placed using a variety of devices which will ensure that the concrete complies with the mix design specification and that there is minimal waste.



(a) Robot plotter



(b) Magnetic shutters



(c) Automatic placement of reinforcement

Figure 2-12 Pallet carousel for lattice girder planks

Compaction of the concrete is achieved using a horizontal shaking system using low or high frequency vibration unless SCC is used for the manufacture of the planks. After casting and compaction, the pallets are typically stored in a curing

chamber, which is usually closed and heated to increase the early strength of the concrete. Curing chambers are usually manufactured to allow vertical storage of pallets to minimise the space required on the factory floor and the chambers are usually filled and emptied automatically or semi-automatically. The curing chambers ensure that the concrete has the minimum strength for lifting the plank without cracking of the concrete. The pallets are typically removed the day after casting for demoulding, then the pallets and magnetic shutters are cleaned for the next production cycle. The production schedule and storage of precast planks are controlled to ensure delivery of planks in specific order and to minimise storage and lifting of products. It is anticipated that the integration of BIM technologies (Industry 4.0) will further enhance the production process of precast concrete components and make them more efficient and sustainable in the future.

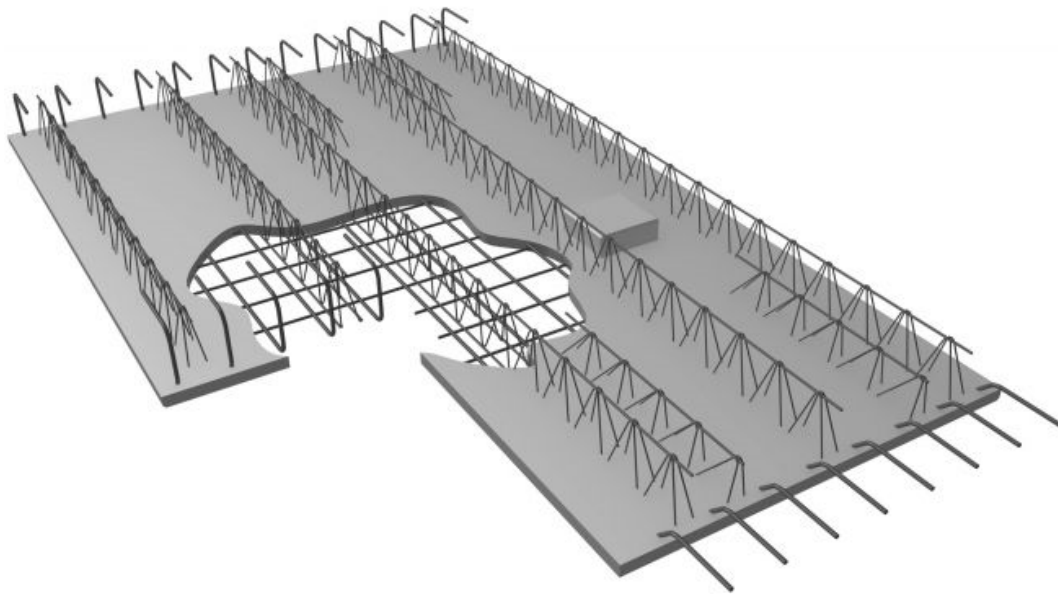


Figure 2-13 Lattice girder plank with reinforcement and lattice girders

2.3.2 Codes of practice

The overarching standard in relation to precast concrete products is EN 13369 ‘Common rules for precast concrete products’ [35]. EN 13369 specifies the requirements, basic performance criteria and evaluation of conformance for unreinforced, reinforced and prestressed precast concrete products manufactured using normal- and heavyweight concrete according to EN 206 ‘Concrete:

Specification, Performance, Production and Conformity’ [36]. All specific products standards related to precast concrete are structured in the same way as EN 13369 and written ‘by exception’ to EN 13369; they either accept what is in EN 13369 or have mirror clauses that elucidate or supersede those in EN 13369 [37]. This approach was adopted so that all product standards are all based on a uniform approach and that conflicting statements were avoided [37]. EN 13747 ‘Precast concrete products – products for floor systems’ [38] is the relevant standard for precast concrete lattice girder planks. This standard relates to all precast floor plates manufactured using reinforced or prestressed normal weight concrete used in conjunction with cast-insitu concrete (topping) for the construction of composite floor slabs. The code contains an Annex which gives examples of different types of composite slabs made with floor plates. The standard does not cover reinforced plates less than 40mm thick nor prestressed plates less than 50mm thick.

Annex F of EN 13747 states providing the shear forces can be transferred through the interface between precast plank and insitu concrete topping, the design of composite slabs is identical to the design of a monolithic slab offering the same configuration. Therefore, the design of a hybrid concrete lattice girder floor shall be in accordance with EN 1992 Part 1-1 ‘Design of concrete structures’ [39]. The properties and strength of the concrete in the precast plank at 28 days (as stated by the manufacturer) should be taken into account when considering the design of the floor system in permanent situations.

2.3.3 Design

The five different limiting design criteria for the capacity of flooring units, as illustrated in Figure 2-14 are [3]:

- bearing capacity
- shear capacity
- flexural capacity
- deflection limits
- handling restrictions

Precast manufacturers will typically try to have a set of standardised cross sections and reinforcement patterns for a given flooring product which will cover the widest

possible combination of floor loading and spans. Many manufacturers can produce load-span tables for common configurations to allow designers to determine structural floor depths at preliminary design stage.

As noted previously, the design approach for a hybrid concrete lattice girder floor is the same as an insitu flat slab provided the shear forces can be transferred through the joint between the precast plank and insitu topping. If there are differences in the grade of concrete used for the precast plank and insitu topping, the lower grade of concrete is used for the design of the hybrid concrete floor.

The design of hybrid concrete lattice girder floors must take account of:

- (i) the construction stage prior to and during placement of the insitu topping,
- (ii) the permanent stage (composite phase) when the insitu topping has reached sufficient strength and the precast lattice girder plank and insitu topping act compositely (e.g. hybrid concrete).

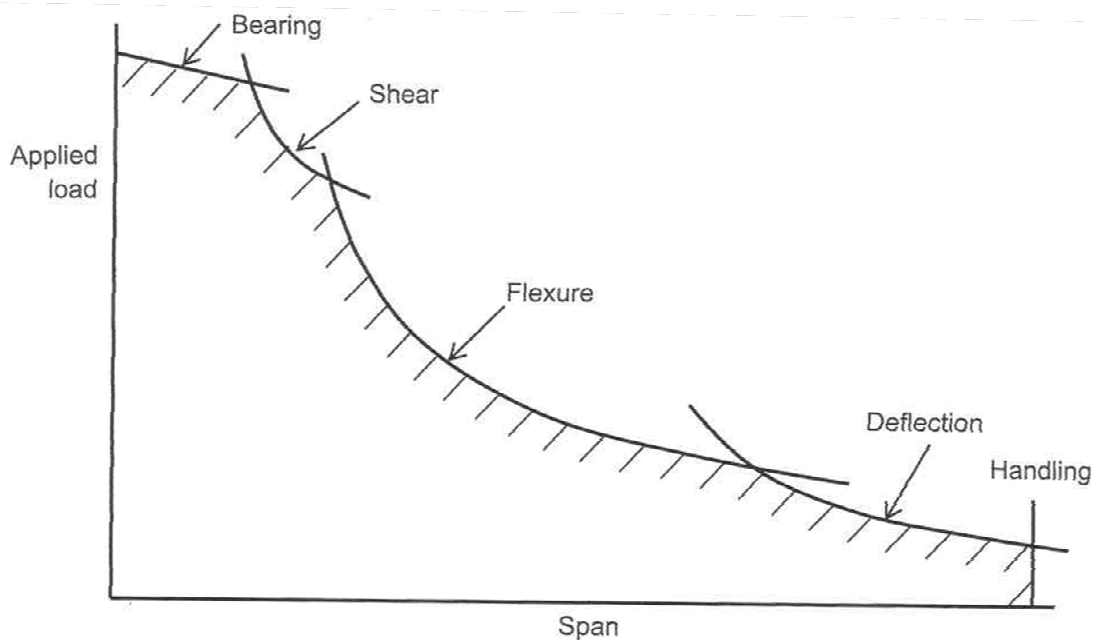


Figure 2-14 Limiting design criteria for resistance of flooring units [3]

The main focus of this research is the construction stage, but the configuration of the lattice girder plank will directly influence the behaviour of the floor at both construction and permanent stages. Similar to the design of an insitu flat slab, the

Chapter 2. Background

designer must consider both ultimate limit states (bending, shear, punching shear) and serviceability limit states (deflection, durability, fire resistance, cracking) when hybrid concrete floor is functioning as a composite floor. Initially, when the lattice girder planks were manufactured, they were only used for one-way spanning systems. However, in the last decade, the utilisation of two-way spanning action has increased significantly in Ireland and the UK. To achieve two-way section, the key consideration is the transfer of bending moments across the joints between adjacent planks. EN 13747 (Annex F) details a number of reinforcement options for ensuring continuity across the joints between adjacent planks.

The bottom layer of reinforcement is contained within the precast plank and reinforcement used are typically no greater than 12-14mm diameter (H12/H14). The top layer of reinforcement is positioned on site and the lattice girder is used as a reinforcement chair to support the reinforcement. A layer of 'stitching' bars (or lap bar) are placed perpendicular across the joint between adjacent planks and its function is to transfer the moment across the joints. A typical cross-section of a hybrid concrete lattice girder floor at a joint between planks is shown in Figure 2-15. For a positive bending moment (typically between supports), the top section of the floor is subject to compression, which is resisted primarily by the insitu concrete topping. The tensile stresses in the bottom of the section are resisted by the reinforcement in the precast plank. At the joints between planks, the stitching bars ensure continuity of the tensile stresses from the reinforcement in one plank to the adjacent plank (Figure 2-16a). For a negative bending moment (typically at columns or cantilevers), the tensile stresses are resisted by the reinforcement in the insitu topping and the compressive stresses are resisted primarily by the concrete in the precast plank and the insitu topping (Figure 2-16b). Allowance must be made in design for the reduced depth of the slab at the location of the joints between adjacent planks. In 2011, Stehle *et al.* [40] conducted a series of experimental tests to investigate the performance of joints in hybrid concrete lattice girder floors in two-way spanning slabs. They concluded that if adequate bond conditions are provided, joints in hybrid concrete lattice girder floors can satisfactorily transfer bending forces and achieve two-way spanning action.

Chapter 2. Background

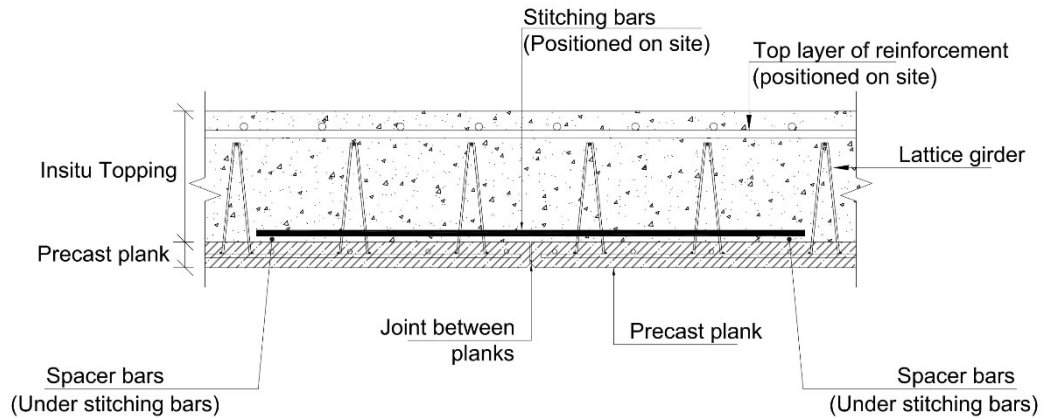


Figure 2-15 Typical section of a hybrid concrete lattice girder floor at a joint between planks

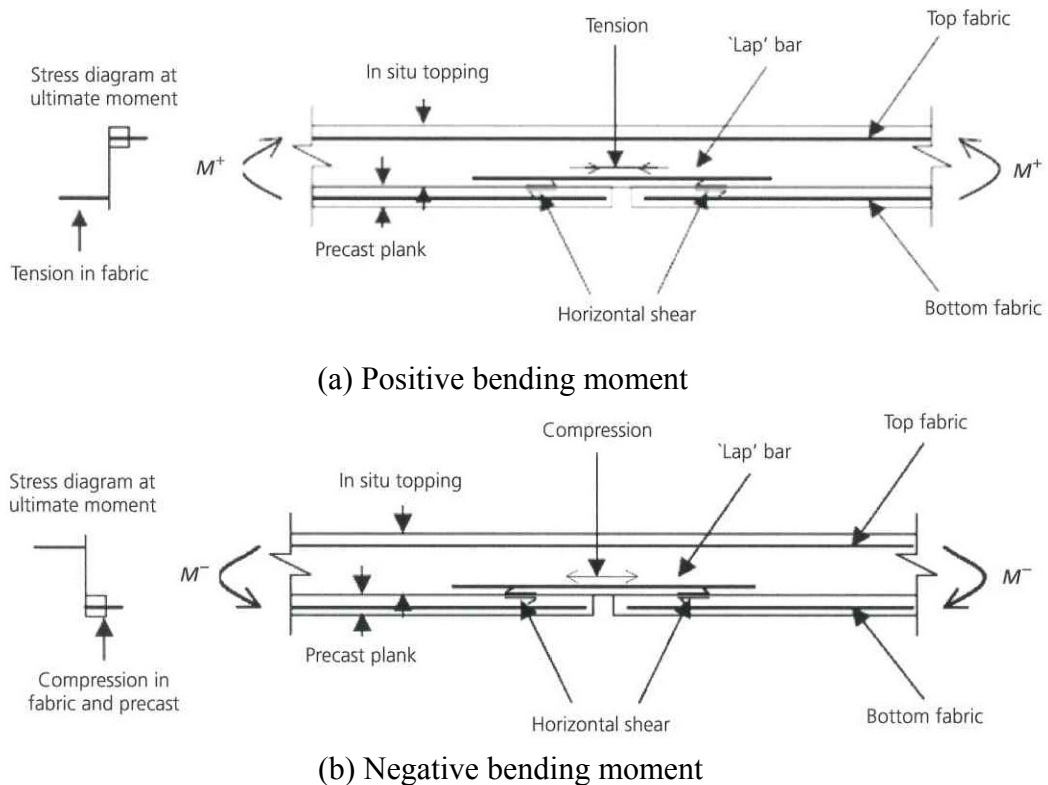


Figure 2-16 Flow of forces across joint between planks [40]

Vertical shear resistance is typically not an issue for hybrid concrete lattice girder floors unless there are large concentrated loads or large openings. Punching shear resistance at the columns or bending resistance are generally the critical design checks for the floor system. However, deflection can also be critical for long spans particularly if there are significant façade loadings. In the majority of cases, the

required shear resistance at the interface between the precast plank and insitu topping is provided by the diagonals of the lattice girders.

2.3.4 Lattice girder floors at construction stage

Delivery of lattice girder planks is usually coordinated between the precast manufacturer and the contractor so that deliveries can be just-in-time (JIT) and the number of precast planks required to be stored on site is minimised. The planks are loaded onto the delivery trucks in accordance with an agreed placement sequence to reduce the necessity of double handling and to minimise craneage.

At construction stage, the lattice girder plank must support its own self-weight, the weight of the wet insitu concrete topping and any construction loading that may arise. The lattice girders embedded in the precast plank must provide the necessary stiffness to the plank until the insitu concrete topping has achieved a specified compressive strength such that the floor system behaves as a composite floor. The stiffness of the precast plank during construction is related to the moment of inertia created by the lattice girders. The girder height, diameter of the top and bottom chord in the girders and the spacing of the girders will determine the stiffness of the precast plank.

Depending on the configuration of lattice girders in the precast plank, the planks may be positioned on site with or without the requirement for temporary propping. When there are relatively short spans and/or the lattice girder has sufficient stiffness, the planks may be positioned on site without temporary supports. Planks can be designed such that they can be erected with spans of over 5m without the requirement for temporary propping. However, the more common scenario requires the precast plank to be supported by temporary propping which are typically in place on site prior to erection of the lattice girder planks (see, for example, Figure 2-17 and Figure 2-18). The spacing of the temporary propping is specified by the designer of the hybrid concrete lattice girder floor and typically takes account of the proprietary propping system employed by many contractors. The advantage of using temporary propping is to reduce the flexural stresses on the lattice girder plank when the plank has to support the wet concrete of the insitu topping. On any project, a value engineering exercise must be undertaken to evaluate the advantages of specifying heavier lattice girders such that the planks can be erected without the

Chapter 2. Background

requirement of temporary propping versus the cost and disruption of temporary propping on site but lighter lattice girders.



Figure 2-17 Proprietary temporary propping prior to erection of lattice girder planks



Figure 2-18 Lattice girder planks supported by temporary props during construction [41]

Chapter 2. Background

The characteristics of the lattice girders in the precast plank (top chord diameter, bottom chord diameter, height and spacing) will dictate the behaviour of the precast plank during construction. In the middle of the span (between supports and temporary props), the top chord of the girder is typically subjected to compressive stresses and the tensile stresses are resisted by a combination of the bottom chord of the girders, the reinforcement in the precast plank and the concrete in the plank. Conversely, at the location of temporary props and supports, the top chord of the girder is typically subjected to tensile stresses and the compressive stresses are resisted by a combination of the bottom chord of the girders, the reinforcement in the precast plank and the concrete in the plank. The interaction between the steel lattice girders and the concrete plank is relatively complex and is dependent on the location in the plank and the characteristics of the lattice girders and concrete.

At construction stage, the designer of the lattice girder plank must check the following:

- (1) The compression resistance of the top chord is not exceeded
- (2) The compression resistance of the diagonal is not exceeded
- (3) The deflection of the lattice girder plank is less than the permitted value
- (4) The maximum crack width of the concrete is less than the permitted value

The most critical design checks are typically the compression resistance of the top chord and the deflection of the plank. However, for deep slabs, and hence, tall lattice girders, the compression resistance of the diagonal of the girder can be critical. The maximum crack width is typically 0.1-0.3mm and is checked in accordance with EN 1992 Part 1-1 [39]. However, smaller values may be specified particularly if the soffit of the slab will be left exposed after construction. The design of the lattice girder plank during construction is not covered by any code of practice. There is currently no design model used in the industry to predict the behaviour of the lattice girder planks during construction and the behaviour of the precast product is largely based on tests conducted. An example of tabular data provided by a German lattice girder manufacturer (Filigran Trägersysteme GmbH) in relation to the allowable span of a specific lattice girder plank during construction is shown in Table 2-1.

Chapter 2. Background

Table 2-1 Permissible spans and minimum tensile reinforcement for specific lattice girder plank at construction stage [42]

Girder Spacing (cm)	Girder Height (cm)	Permissible spans (m) during construction for Lattice Girder with 16mm ϕ Top Chord and 9mm ϕ Diagonal for an overall slab thickness (cm) of											
		22	24	26	28	30	32	34	36	38	40	42	44
50	18	4.05	3.91	3.79	3.62	3.42	3.24	3.08	2.93	2.80	2.68	2.57	2.46
	20		4.07	3.85	3.62	3.42	3.24	3.08	2.93	2.80	2.68	2.57	2.46
	22			3.85	3.62	3.42	3.24	3.08	2.93	2.80	2.68	2.57	2.46
	24				3.62	3.42	3.24	3.08	2.93	2.80	2.68	2.57	2.46
	26					3.42	3.24	3.08	2.93	2.80	2.68	2.57	2.46
	28						3.24	3.08	2.93	2.80	2.68	2.57	2.46
	30							3.08	2.93	2.80	2.68	2.57	2.46

Girder Spacing (cm)	Girder Height (cm)	Required reinforcement ¹ (cm ² /m) for an overall slab thickness (cm) of											
		22	24	26	28	30	32	34	36	38	40	42	44
50	18	3.06	3.06	3.06	2.98	2.81	2.66	2.53	2.41	2.30	2.20	2.11	2.02
	20		2.96	2.83	2.66	2.51	2.38	2.26	2.15	2.06	1.97	1.89	1.81
	22			2.57	2.41	2.28	2.16	2.05	1.95	1.87	1.78	1.71	1.64
	24				2.20	2.07	1.96	1.87	1.78	1.70	1.62	1.56	1.49
	26					1.93	1.83	1.73	1.65	1.58	1.51	1.45	1.39
	28						1.70	1.61	1.54	1.47	1.40	1.34	1.29
	30							1.50	1.43	1.36	1.30	1.25	1.20

1) including bottom chord of lattice girder

The table is based on tests conducted by the company and can be used by designers to determine the required spacing of temporary props on site for a specific lattice girder configuration. The table also specifies the minimum reinforcement (cm²/m) required in the precast plank to resist the tensile stresses in the concrete plank during construction. In Germany, the use of lattice girder planks are regulated by technical

Chapter 2. Background

approvals and a global factor of safety of 1.75 and 2.1 was applied to the test results for ductile steel failure and brittle steel failure respectively to determine the permissible spans of the planks at construction stage [42].

Annex J of EN 13747 ‘Precast concrete products – products for floor systems’ [38] describes the testing to determine the allowable span of the lattice girder planks at construction stage. The standard states that the allowable spans must satisfy both ultimate limit state (i.e. failure) and serviceability limit states (i.e. deflection). The failure modes which must be checked are bending failure due to buckling of the top chord of the lattice girder and shear failure due to buckling of the diagonal of the lattice girder. At ultimate limit state, the lattice girder plank must support the self-weight of the plank (and void formers if present), the self-weight of the wet insitu concrete topping and temporary loads during floor construction. The standard states that until such time that there are European regulations in relation to temporary construction loads, the value should be based on site safety regulations applicable to the country in which precast products are used (minimum of 1kN/m^2). EN 13747 specifies that the deflection of the plank between temporary props and/or supports should not exceed 10mm for spans less than 4m and ‘span/400’ mm for spans greater than 4m. The deflection limits are based on the plank supporting the self-weight of the plank (and void formers if present) and the self-weight of the wet insitu concrete topping.

The compression buckling resistance of the top chord and diagonals must be determined to check the resistance of the lattice girder plank at ultimate limit state. The compression buckling resistance is checked in accordance with EN 1993 Part 1-1 ‘Design of steel structures’ [43]. One of the key parameters for determining the buckling resistance of an element is the buckling length (L_{cr}); however, Eurocode 3 does not provide guidance in relation to buckling lengths because there was no consensus between the contributing countries when the Eurocodes were drafted [44]. Therefore, designers have used conservative assumptions for the buckling length of the diagonal and top chord in the lattice girder. In addition, designers in Ireland and the UK have continued to use the guidance on buckling lengths provided in BS 5950 [45], which was the code of practice for design of steel structures and was superseded by Eurocode 3 in 2010.

Chapter 2. Background

In order to increase the flexural stiffness of the lattice girder floor products, a number of products have been developed (primarily in Germany) which increase the stiffness of lattice girder planks so that the minimum span of the plank without the requirement for temporary propping is increased. 'Montaquick' is a proprietary precast floor product in which the top chord of the lattice girder is replaced by a channel shaped sheet steel which is filled with concrete at the same time as casting the precast plank (Figure 2-19). The increased compression buckling resistance of the concrete top chord (in comparison to the conventional reinforcement in top chord of lattice girder) permits increased spans for the plank during construction. The 'Montaquick' floor product may be considered for projects in which the extra cost of the concrete top chord is lower than the cost of providing temporary propping.

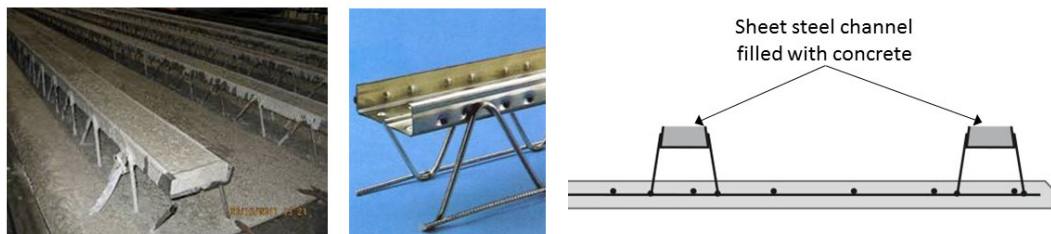


Figure 2-19 Montaquick precast floor

At construction stage, forces from back-propping of the floor(s) above may also have to be evaluated. Typically, props for supporting floors above, should be vertically aligned so that the self-weight of the floors and wet insitu concrete is transferred to the floors below such that it does not negatively impact the long-term performance of the slab.

The cost of erecting lattice girder planks on site will be a function of labour costs, cost of propping and craneage. Craneage costs may be reduced by maximising the size of the precast planks that can be transported to site and lifted on site. The cost of labour and propping are directly related as site operatives are required to erect temporary propping prior to positioning of precast planks and remove props after the hybrid concrete floor can support its own self-weight. From a contractor's perspective, there is a desire to maximise the spacing of temporary propping so that it would reduce congestion on site, site operations (and hence labour costs) and the

Chapter 2. Background

cost of temporary props. Where labour costs are high, it might be more economical to change the configuration of the lattice girders to minimise the quantity of temporary propping required for a given project.

The cost of temporary propping for supporting lattice girder planks during construction is difficult to determine as there are several factors which influence the overall cost. In addition to the cost of labour required to erect and dismantle temporary propping on site, the height of the props, spacing of props and the loads on the props (related to thickness of supporting slab and spacing) will impact the cost of the props. Most contractors rent the temporary propping for each project and many use proprietary propping systems which speed up the erection process of the props on site. Based on discussions with contractors, precast manufacturers and quantity surveyors in Ireland, indicative costs for temporary propping of precast planks appears to be in the range of €20-50/m². The higher figure would apply to projects with very high floor to ceiling heights and hence the requirement for longer props. In comparison to the cost for the supply and erection of precast lattice girder planks, the cost of the temporary propping would be at least 20% of the total cost of erecting precast lattice girder precast planks on site (excluding the cost of the top layer of reinforcement and the insitu topping).

Although precast concrete lattice girder planks were first developed almost fifty years ago, the design of the floor product during the construction stage (prior to composite action between the precast plank and the insitu topping) is largely based on testing of simply supported planks which is not the typical support condition for lattice girder planks during construction. There is no specific code of practice or generic design model which can be used by designers to predict the allowable span of lattice girder planks and consequently the required spacing of temporary propping to meet serviceability and ultimate limit state requirement (i.e. deflection, cracking and failure). This research uses a combination of embedded sensors and experimental testing to study the behaviour of the lattice girder plank during the construction stage so that key parameters which control its behaviour can be analysed. In order for any floor product to be competitive, it is important that there is robust data available to designers which demonstrate the actual performance of the product in real structures.

2.4 Experimental testing of precast lattice girder planks

Notwithstanding the popularity of hybrid concrete lattice girder floors, there is relatively little published literature on experimental testing of the lattice girder planks to investigate their behaviour at construction stage. Lack of comprehensive experimental data on the product and how the various elements (lattice girder, reinforcement, concrete) act together limits the development of numerical modelling to better predict their behaviour in real projects and possible optimisation of the floor product.

Publication of test data by manufacturers is very limited and in many cases is not published due to commercial considerations. Typically, design tables provided by manufacturers and/or conservative analysis tools are used to determine the allowable span of the precast planks at construction stage.

2.4.1 Codes of practice

Annex J of EN 13747 ‘Precast concrete products – products for floor systems’ [38] relates to experimental testing to determine erection spans of precast floor products (including lattice girder floor planks). This Annex can be used by manufacturers of lattice girder planks to establish the allowable spans for their precast plank during construction. The Annex states that the properties of the floor plate should be specified by the manufacturer and that the allowable erection spans should be based on satisfying both ultimate limit state (failure) and serviceability limit state (deflection) criteria subject to combinations of permanent and variable loading (actions) which will generate the most unfavourable stresses in the plank at the supports and in the spans. The permanent loading will be the self-weight of the precast plank (G_{pl}) and any void formers (G_b) if used in the hybrid concrete floor. The variable loading acting on the plank during construction will be weight of the insitu concrete topping (Q_{co}) and temporary loading during floor construction (Q_s). The minimum loading which should be adopted for temporary loading during floor construction is specified as 1kN/m^2 unless the site safety regulations valid in the country in which the product is used specify a higher value.

When checking deflection, the standard states that the mid-span deflection between props or between temporary supports shall not be greater than 10mm if the erection

Chapter 2. Background

span (l_{er}) is less than 4m and ($l_{er}/400$) mm if the erection span exceeds 4m. The deflection should be checked when the plank is subject to the combination of actions of the self-weight of the precast plank, self-weight of void formers and the weight of the wet insitu concrete topping (Figure 2-20). Interestingly, it does not require the consideration of the temporary construction loading (Q_s) when checking deflection. This guidance in relation to construction loading during casting of concrete is slightly different to EN 1991 Part 1-6 ‘General Actions – Actions during execution’ [46]. The code states that “Operations during execution which can cause excessive cracking and/or early deflections and which may adversely affect the durability, fitness for use and/or aesthetic appearance in the final stage shall be avoided”. Clause 4.11.2 of EN 1991-1-6 states that the simultaneous action of the weight of the wet insitu concrete topping and working personnel with small site equipment should be considered to cause the maximum effect as shown in Figure 2-21. The code requires 3m square ‘working area’ subject to a load equivalent to 10% of the self-weight of the wet concrete (but not less than 0.75kN/m^2) and a construction load of 0.75kN/m^2 outside the working area for the remainder of the span. For verification of service ability limit states, (for loads during construction), EN 1991-1-6 states that the combination of actions to be taken into account should be characteristic and quasi-permanent combinations as defined in EN 1990 [47].

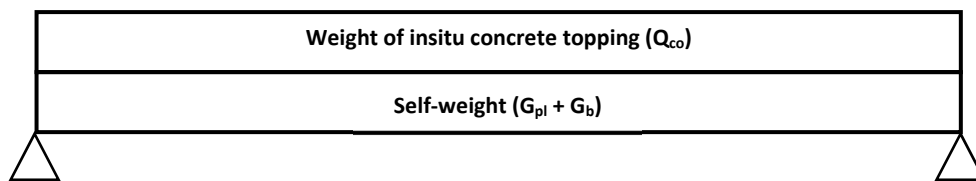


Figure 2-20 Construction loads for checking deflection during construction in accordance with EN 13747 (Annex J)

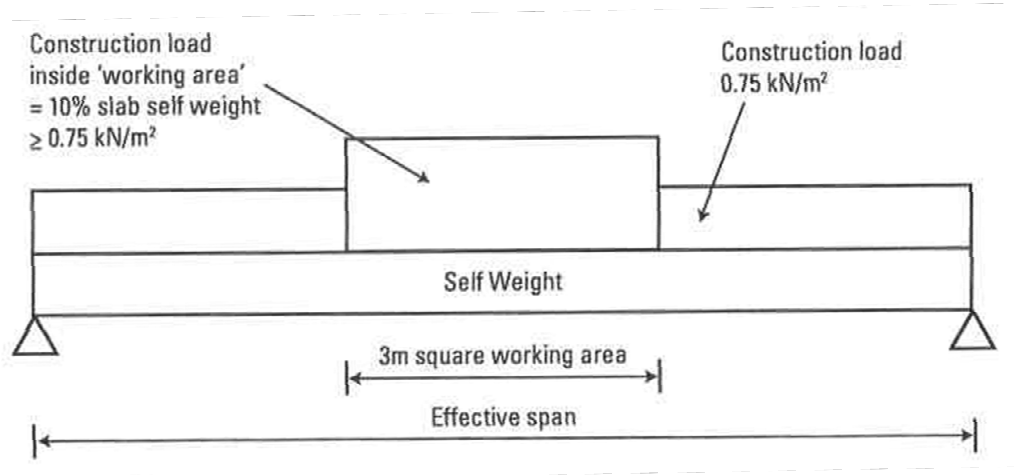


Figure 2-21 Construction loads during casting of concrete in accordance with EN 1996-1-6 [48]

Some authors, such as the Steel Construction Institute (SCI) in the UK, have suggested that there should also be an allowance at ultimate and serviceability limit state for heaping of wet concrete during casting of concrete for a composite slab [48]. SCI recommends that a construction loading of 0.75 kN/m^2 should be allowed for the full span of the slab and an additional loading of 10% of the self-weight of the wet concrete (but not less than 0.75 kN/m^2) should be allowed over a $3 \text{ m} \times 3 \text{ m}$ 'working area' to cause maximum effect. SCI suggests that the deflections should only be verified for the fully concreted state (i.e. with no patterned loading).

It would be preferable in the future if there was consistency in the codes of practice in relation to what loads should be considered acting on the plank for the purposes of checking for deflection (serviceability limit state). Otherwise, there is potential for manufacturers to use different criteria for assessing deflection and this may lead to confusion and misunderstanding for designers when selecting precast concrete lattice girder planks and temporary propping arrangements.

EN 13747 permits the plank to be tested in single span or double span configuration and it permits a variety of loading arrangements to determine the erection spans, as shown in Figure 2-22. Annex J provides specific guidelines in relation to the testing equipment, test configuration and loading of the precast plank to determine the erection span. It states that two tests should be carried out for each type of precast floor. If the difference between two results is greater than 15% of the mean value,

Chapter 2. Background

a third test is necessary and the mean value is the calculated on the basis of the three tests. The erection span (l_{er}) stated on any manufacturers test report is based on the plank meeting ultimate limit state (moment and shear resistance) and serviceability limit state (deflection) criteria and these are determined from the tests conducted. The code recommends that a test coefficient (γ_E) of 1.2 should be applied to the failure moment and failure shear force determined from the tests.

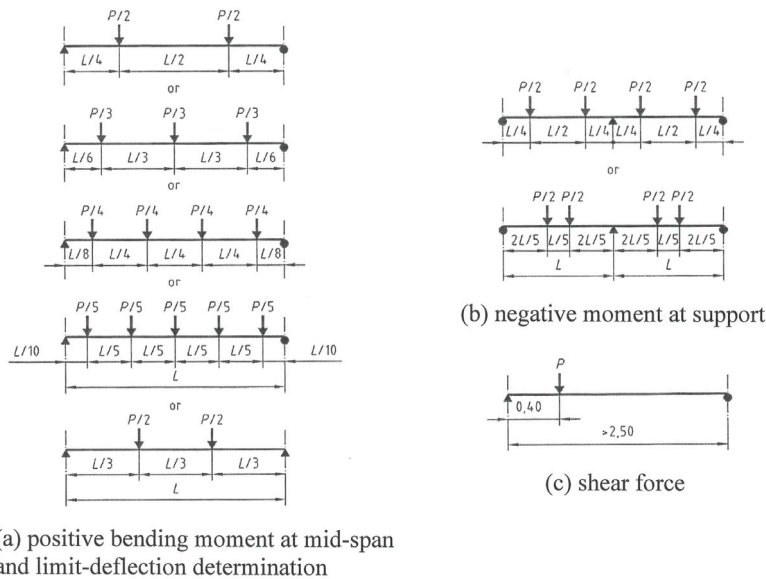


Figure 2-22 Possible loading arrangements for testing in accordance with EN 13747 [38]

2.4.2 Löfgren *et al.*

In 2001, Löfgren at Chalmers University in Sweden published a report [49] which described experimental testing of two lattice girder planks in order to evaluate the behaviour of the floor product in bending. In the report, the author stated that the current design method for lattice girder floors was based on empirical expressions based on full scale tests performed in the 1970s and was overly conservative and not sufficient to describe the mechanical behaviour of the floor product. It was envisaged that this research would provide information for a larger test series so that a mechanical model could be developed that describes the behaviour of the lattice girder floor and the mechanisms of failure. The report was commissioned by a concrete manufacturer in Sweden in response to the demand for improved construction methods for concrete structures. This experimental study was part of

Chapter 2. Background

an ongoing research project in Chalmers University which focused on developing industrialised construction methods for concrete construction [50] so that the process could be more efficient. At that time, it was noted that the cost of labour (erecting and dismantling formwork, tying reinforcement and casting and finishing concrete) for insitu concrete construction was almost equal to the cost of the material (labour represents approximately 40% of construction cost and formwork accounts for almost half of the expenditure).

Tests were conducted on two identical lattice girder planks, simply supported and loaded by four-point bending. The planks were 1.2m wide x 2.01m long and 50mm thick with two lattice girders 0.8m apart (Figure 2-23). The concrete grade for the plank was C26/35 and the planks were tested 34 and 35 days respectively after manufacture. The two lattice girders were type 10-6-5, H = 200mm (top chord $\phi = 10$ mm, diagonal $\phi = 6$ mm, bottom chord $\phi = 5$ mm and height 200mm) and all the steel in the girder was cold-worked. The longitudinal reinforcement consisted of nine 10mm diameter bars.

The load tests were conducted by means of displacement control and the load was applied by a hydraulic jack (refer to Figure 2-23 and Figure 2-24). Displacement was measured using displacement transducers at midspan and the two load points. Ten electric resistance strain gauges were bonded to the top chord, bottom chord, diagonals and reinforcement in the first test and twelve in the second test. Material testing was conducted on the concrete used in the planks to determine the compressive strength and modulus of elasticity in accordance with Swedish standards. The material properties of the top chord of the lattice girder and the longitudinal reinforcement was also determined using tensile tests.

During the tests, cracking was visually observed but the authors found it difficult to observe because of the small crack widths. The tests were stopped when the midspan deflection reached 50mm. The load-displacement curves for the two tests showed good agreement. It was found in both tests that failure was due to buckling of the top chord in the lattice girder. Cracking of the concrete was observed at low load, typically at 20% of the peak load. However, crack widths were small even at peak load. The authors proposed that the behaviour of the lattice girder plank can be divided into three phases:

Chapter 2. Background

- 1) Initial response, for which section is uncracked and load-deformation curve is nearly linear.
- 2) Second phase is initiated by cracking of the concrete in tension and the response becomes non-linear and the flexural stiffness of the plank reduced.
- 3) The last phase is reached when the top chord starts to buckle. These were found to occur at relatively low stresses (260-300MPa), which primarily depends on the slenderness of the top chord.

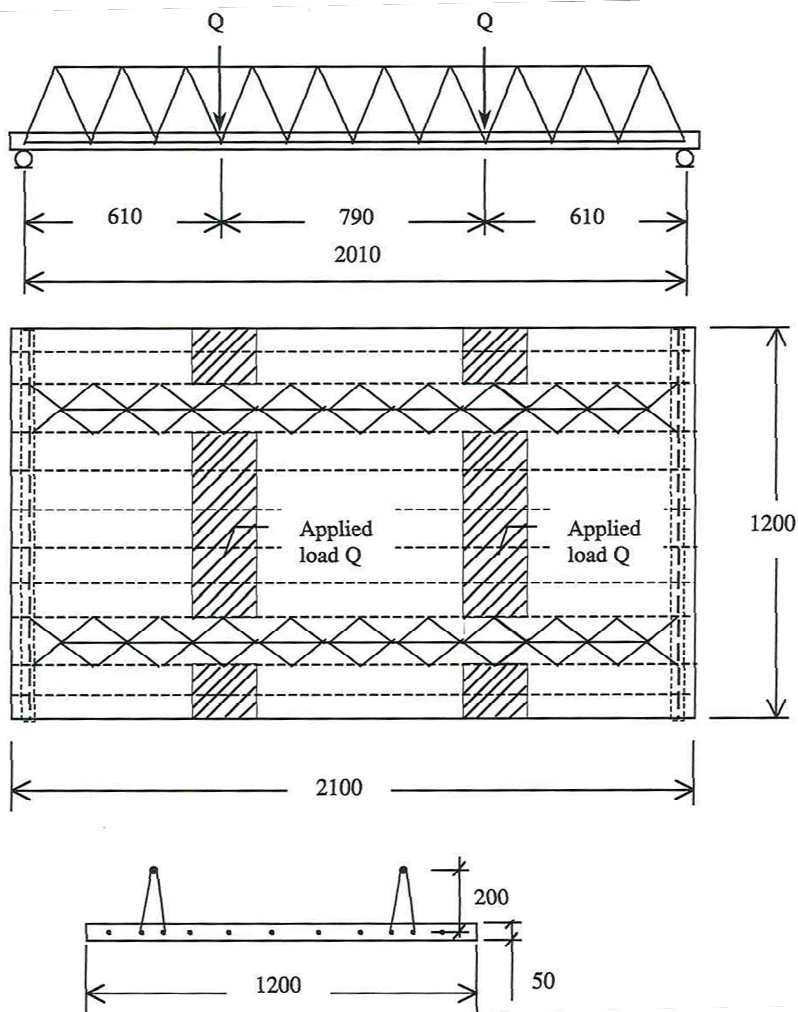


Figure 2-23 Test plank used by Löfgren (2001) [49]

An analytical model was developed using the transformed area method to analyse the flexural behaviour of the plank. An effective flange width for the concrete was assumed rather than the full width of the plank as for slender and wide flanges, plane sections do not remain plane. For the uncracked section (phase 1), the calculated stiffness was calculated using the transformed section. After the concrete

Chapter 2. Background

cracks (phase 2), it was assumed that the concrete does not contribute to the stiffness of the lattice girder plank. It was reported that the analytical model was sensitive to the choice of concrete tensile strength. The tensile strength was not measured directly but was determined in accordance with CEB-FIB Model Code 1990 [51] which provides a relationship between the characteristic compressive strength (f_{ck}) and the tensile strength (f_{ctm}). It was also noted that shrinkage of the concrete would produce stresses in the section even before the load is applied and that the concrete could have tensile stresses due to shrinkage which account for up to 30% of the tensile resistance of the concrete.

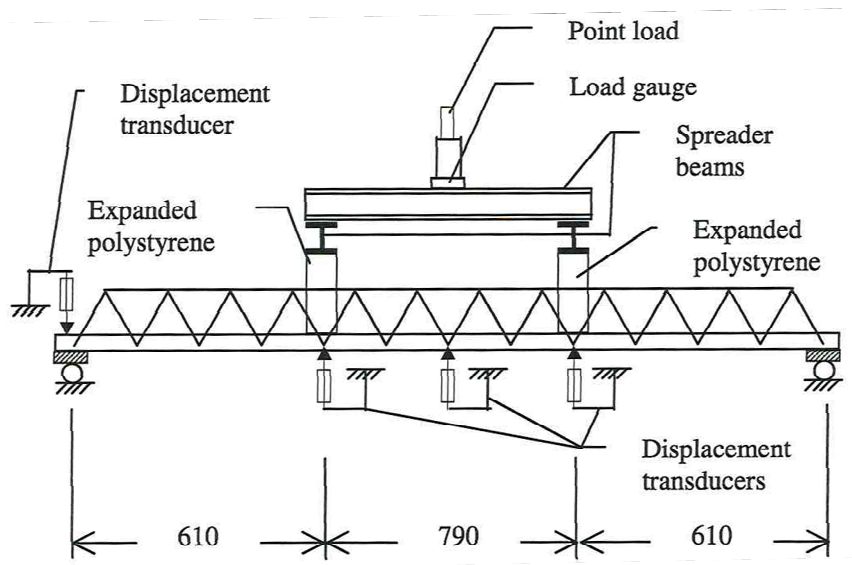


Figure 2-24 Test configuration used by Löfgren (2001) [49]

Chapter 2. Background

To investigate the sensitivity of the model, a simple parameter variation was undertaken in which the tensile strength concrete, elastic modulus of the concrete, effective width of the concrete and the elastic modulus of the reinforcement were changed in the model. The parameter variation indicated that the most critical parameter was the tensile strength of the concrete and that a relatively small variation of the tensile strength in the model can have a significant difference in the predicted deflection of the lattice girder plank. The next most important parameter was the elastic modulus of the concrete.

The conclusions of the 2001 study undertaken by Löfgren were that the analytical model was relatively accurate (Figure 2-25) in predicting the flexural behaviour of the lattice girder plank, but that further investigation was required to investigate its suitability for different loading conditions, material properties and geometry. One of the major limitations of this study was that the testing was based on two tests of one type of lattice girder plank only.

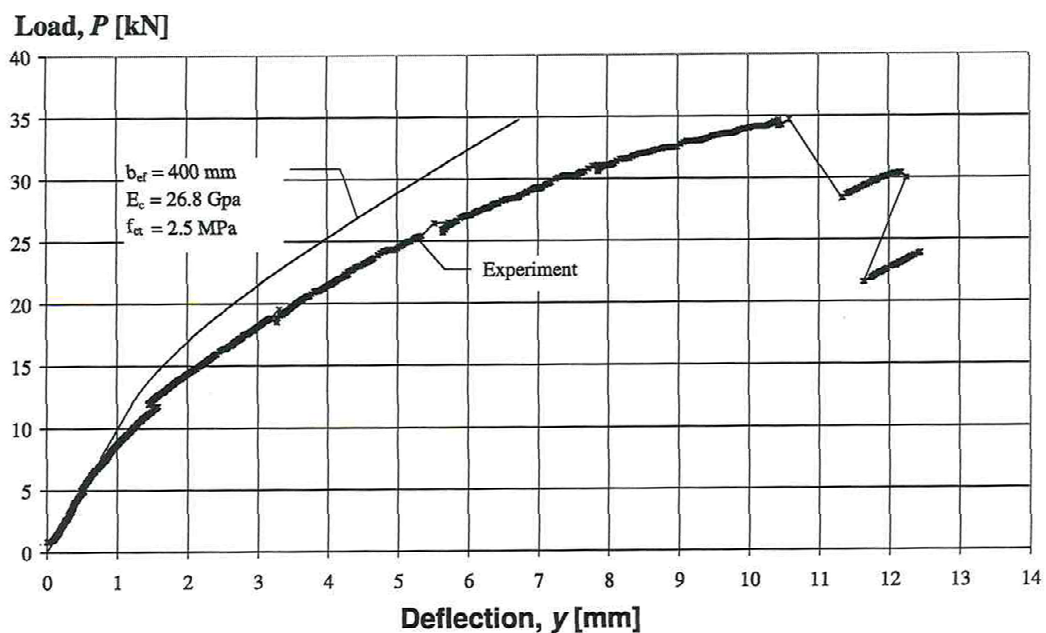


Figure 2-25 Comparison of experimental result and analytical model [49]

In 2003, Löfgren published a report [52] on further experimental and numerical studies on lattice girder planks. The report focused primarily on the behaviour of the precast floor at construction stage and was based on research conducted by Harnisch [53] and Verdugo [54] in Chalmers University. The report notes the desire

Chapter 2. Background

of contractors to increase the spacing of props for lattice girder floors so that there would be less congestion and disturbance on site and to minimise the need for temporary propping and associated costs. Löfgren stated that the contribution of the concrete to the structural behaviour of the lattice girder floor was not well known and that this limited the further development of the precast concrete lattice girder floor product. The analysis of a lattice girder plank is complex as both time-dependent effects (creep and shrinkage) and time-dependent material properties (gain in strength and modulus of elasticity) which are affected by environmental conditions must be considered.

A series of tests was conducted by Verdugo [54] on twelve lattice girder planks. The main parameters varied were the height of the truss and the diameter of the top chord of the lattice girder and the truss geometry was selected to represent the standard trusses used in practice in Sweden at that time. All planks tested had the same outer dimensions (2.6m long, 1.18m wide and 50mm thick), the steel girders were cold-worked steel and the embedded reinforcement was hot-rolled. The planks were tested in four-point bending (Figure 2-26), deflection was measured at specific locations (midspan and load points) and the strains in the top and bottom chord of the lattice girder were measured. The load-deflection behaviour (Figure 2-27) was characterised as having an initial almost linear relationship until the onset of micro-cracking. This is followed by a series near-linear ranges in which the flexural stiffness of the plank reduces as the macro-cracks develop into primary cracks and cracking propagates and become well-developed. Failure and peak load was recorded when buckling of the top chord occurred. The observed crack widths and recorded strains in the longitudinal reinforcement were relatively small. Crack widths were typically less than 0.1mm at peak load and were not visible until about 60% of the peak load. From the experimental tests, it was proposed that the structural behaviour of the lattice girder plank was governed by three main mechanisms:

- (i) buckling of the top of the lattice girder at peak load
- (ii) cracking of the concrete
- (iii) tension stiffening of the concrete (ability of concrete to carry tensile stresses after initial cracking)

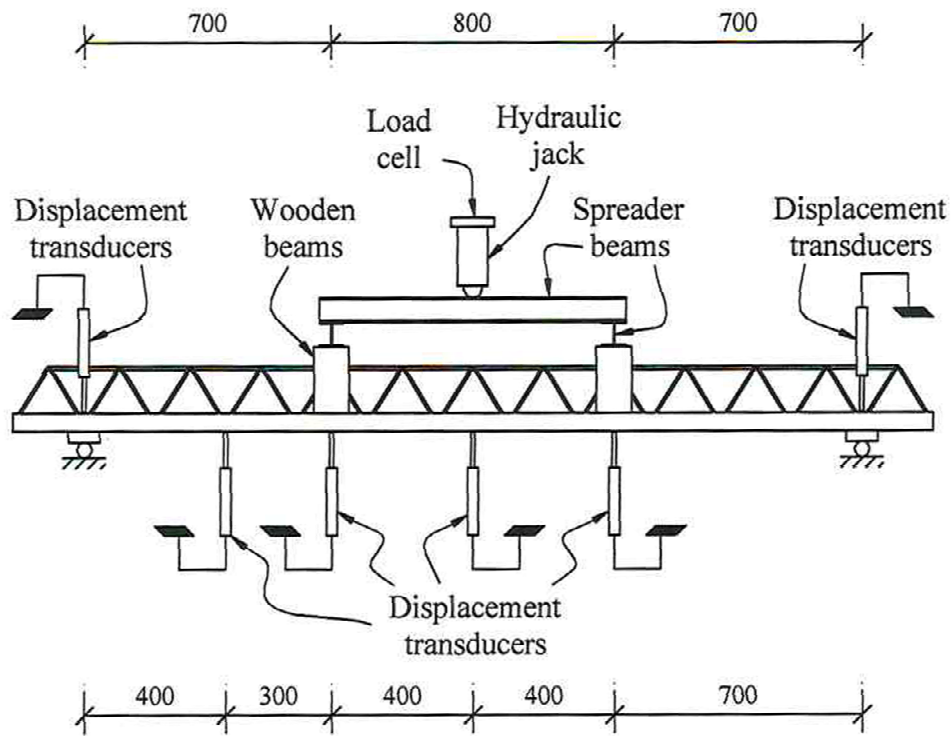


Figure 2-26 Test set-up used by Verdugo [52]

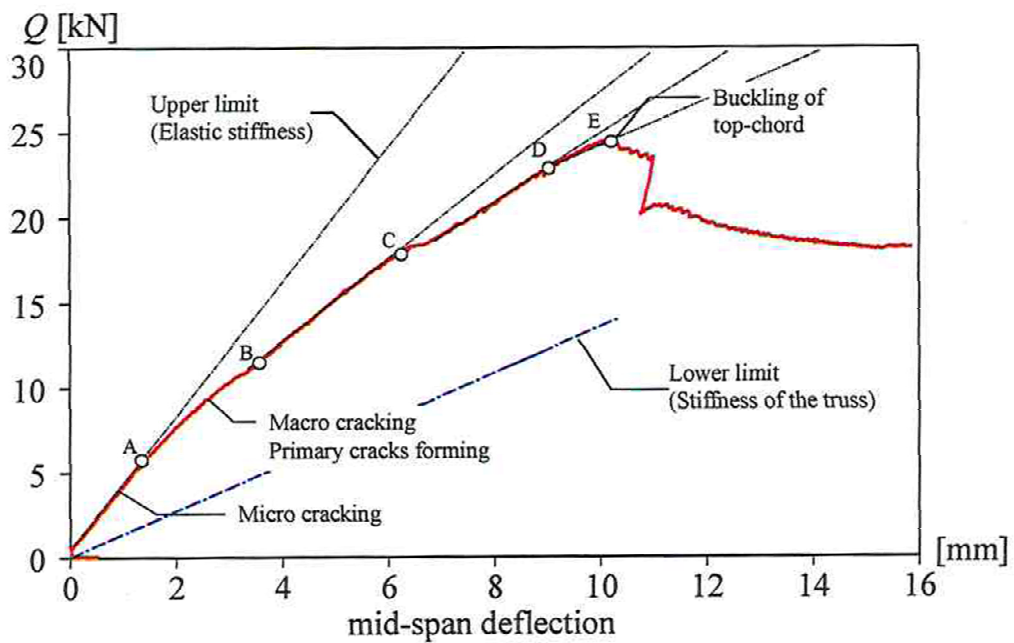


Figure 2-27 Typical load-deflection curve for lattice girder plank [52]

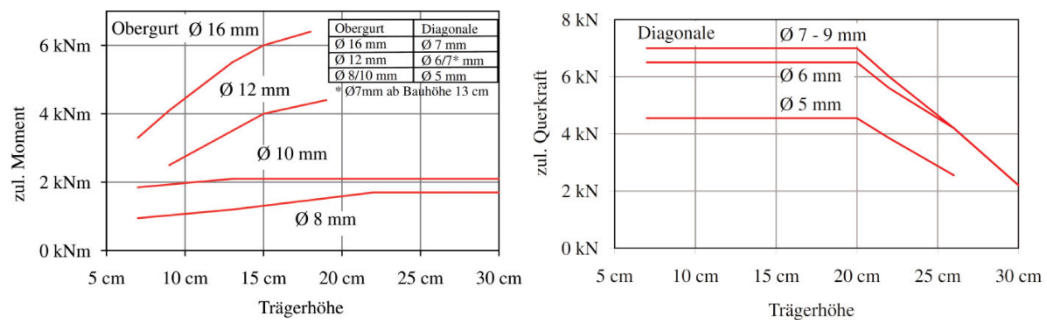
This research project in Sweden presented very promising data with respect to analysing the behaviour of lattice girder planks at construction stage. However, the experimental study was limited to shallow girders (200mm high or less), the steel in the lattice girders was cold worked and there was no attempt to develop design tools which could be used by designers to estimate erection spans for specific lattice girder planks. No further testing was reported by Chalmers University since 2003. It is not clear why additional testing was not conducted on lattice girder slabs or further development of the numerical model was not considered.

2.4.3 Filigran

Filigran Trägersysteme GmbH & Co. is a German company who manufacture steel reinforcement products for the concrete industry. One of their primary products is steel lattice girders used to manufacture lattice girder precast planks for floors and walls. Their primary market is Germany but they also sell their products in Ireland and the UK. In Germany, Technical Approvals of the German Institute for Construction Technology (DIBt) [55] apply to the use of lattice girders in construction. Beyond the material properties of the lattice girders, these stipulate the dimensioning and application conditions of the components with lattice girders. The company provides a range of consulting and technical advice services to their customers and they have developed design tools (tables and programmes) which can be used by their customers to design lattice girder slabs using their products. The Technical Approvals which Filigran have obtained for their lattice girders and design tools which they have developed are based on research undertaken by the company and in conjunction with several German Universities. Much of the research has concentrated on erection spans of lattice girder planks, punching shear resistance of hybrid concrete lattice girder flat slabs and validation of their product (hybrid concrete lattice girder floor) with various codes of practice (Eurocodes) and European/German Technical Approvals (ETA). Much of the experimental testing undertaken by Filigran in conjunction with universities in Germany is not published ([56]–[60]) and this limits the current knowledge of how the floor product components interact during construction stage and the potential scope for development of numerical models which could use the experimental data for validation.

Chapter 2. Background

The erection span is determined by ensuring that the permissible moment of the lattice girder and permissible shear force of the lattice girder plank are not exceeded when subject to uniform variable loading or concentrated variable loads. The use of lattice girders in precast planks is regulated by Technical Approvals of DIBt and they require testing to confirm the shear and bending resistance of lattice girder planks. In addition, the erection spans quoted in Technical Approvals for the lattice girder planks are based on testing of the plank in the single span condition. However, the majority of lattice girder planks erected on site are such that they are continuous over temporary props. This means that the quoted erection spans for the lattice girder planks are overly conservative. An example of the permissible bending moments and shear forces for a particular lattice girder are shown in Figure 2-28. The permissible bending moments and shear force can be used to determine erection spans for precast planks and these are noted in the Technical Approval for the specific lattice girder.



Note: Obergurt = Top chord; Diagonale = Diagonal, Trägerhöhe = Girder height, zul. Moment = Permissible moment per girder, zul. Querkraft = Permissible shear force per girder

Figure 2-28 Approved bending moments and shear force of one type of lattice girder from DIBt Technical Approval [61]

Furche noted in 2009 [62] that investigations on erection spans of lattice girder planks was limited and that the erection spans quoted in German technical approvals were based on tests performed decades ago. He stated that buckling of the top chord typically defined the moment of resistance of planks. He also commented that for tall lattice girders, the lateral resistance of the top chord becomes 'softer' and the moment of resistance no longer increases or increases only to a limited degree with increasing girder height.

Chapter 2. Background

In 2011, Bertram *et al.* [63] and Furche and Bauermeister [42] reported on 78 bending and shear tests conducted in The Institute of Structural Concrete at RWTH Aachen University to investigate the permissible span of lattice girder planks during construction. Previous experimental testing conducted by Filigran to determine erection spans of lattice girder planks was not published. In particular, the testing reported in 2011 was focused on investigating the behaviour of lattice girder planks with larger diagonal bars and thicker slabs (i.e. taller lattice girders) to improve the erection spans during construction. At that time (2011), Filigran had Technical Approval for a number of lattice girders but the objective of this experimental programme was to increase the range of possible lattice girders (larger top chords, larger diagonals and greater height girders) that could be used for hybrid concrete construction of flat slabs. The authors noted that behaviour of the lattice girder plank cannot be described with common bending and shear design methods because of the divided cross section and a slender compression chord (top chord of lattice girder). They also stated that there is no numerical model available which accurately predicts the behaviour of the lattice girder planks for the different possible configurations of the product.

Full scale tests were undertaken by Bertram *et al.* on precast planks ranging in width from 10cm to 66cm and the majority had only one lattice girder in the plank. This means that the distribution of load between lattice girders in a precast plank was not considered and this was deemed by the authors to be on the “safer side” than is the case with typical precast planks which contain several lattice girders. The length of the planks were 4.45m and the thickness of the precast planks tested were 5cm. The concrete age at the time of testing was between 3 and 9 days and the cylinder compressive strength at the time of testing varied between 18-28N/mm². It is not stated if any material testing was conducted on the steel in the lattice girder or the longitudinal reinforcement. The planks were tested firstly in four-point bending where the span was 4.0m and the distance between the loading points was 1.0m. Subsequently, the planks were tested in shear in which the span of the planks was 1.7m and the load was applied 0.4m from the support. The test configuration for both tests are shown in Figure 2-29 and a summary of the test programme is presented in Table 2-2. It is not reported what measures were undertaken to ensure that the bending test on the planks had no effect on the subsequent shear tests.

Chapter 2. Background

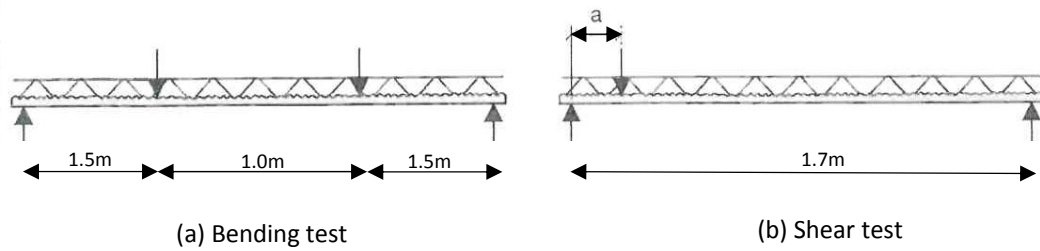


Figure 2-29 Test configuration for tests conducted by Bertram et al. [63]

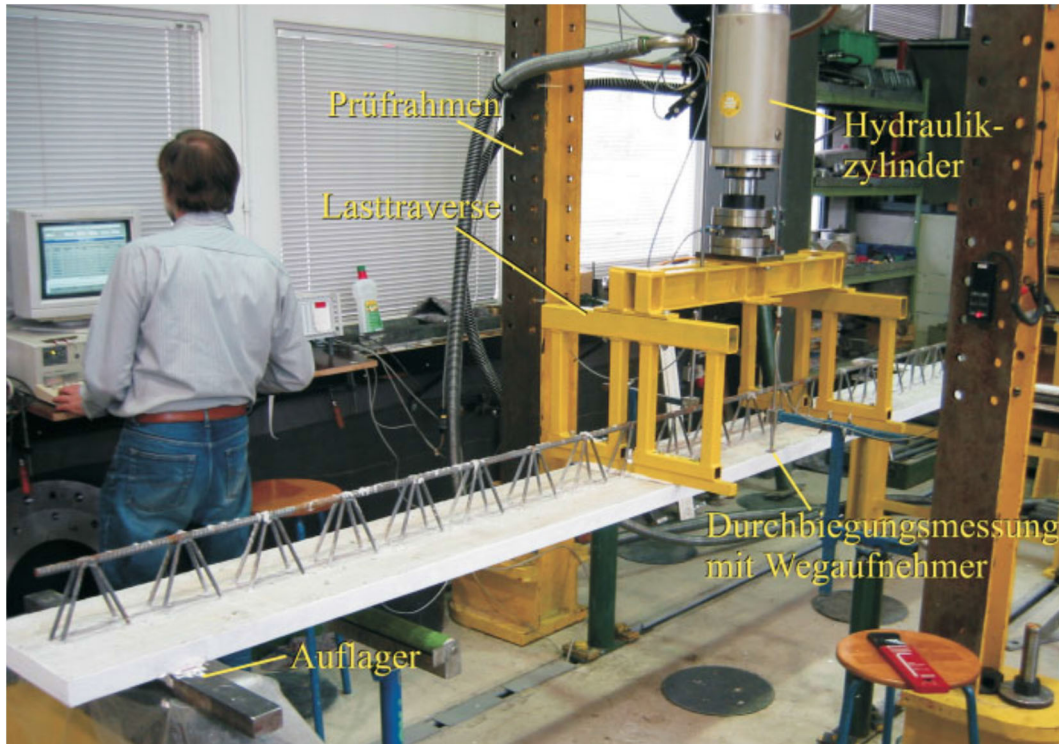


Figure 2-30 Test set-up for 4-point bending [63]

Table 2-2 Test programme conducted by Bertram et al. [63]

Plattenbreite (Plank Width)	Gitterträgerhöhe und -bezeichnung (Girder Height)			
	18 cm EV18-06916	20 cm EV20-06916	24 cm EV24-06916	30 cm EV30-06916
10 cm	4 B + 8 Q		4 B + 8 Q	4 B + 8 Q
33 cm	4 B + 8 Q		4 B + 8 Q	4 B + 8 Q
66 cm ^{a)}		1B + 2Q		1 B + 2 Q
$\Sigma = 26 B + 52 Q = 78$ Versuche				

B = 4-point bending test

Q = shear test

Chapter 2. Background

An example of the moment-deflection curve generated from one of the four-point bending tests on a 33cm wide plank with 18cm high girder is shown in Figure 2-36. Failure of the bending tests occurred in general due to buckling of the top chord of the lattice girder. It was observed that buckling of the top chord predominantly occurred in the horizontal plane but buckling was also observed in the vertical plane in some tests. In the tests conducted on the taller girders (24cm and 30cm) with 10cm wide planks, lateral buckling of the top chord of the girder was observed (Figure 2-32). With the exception of the narrow width planks (10cm wide), the buckling length of the top chord did not exceed 200mm (distance between nodes on the top chord). The ultimate moments for one of the girders tested with a plank width of 33cm is shown in Figure 2-38 for different girder heights. The permissible moment for the lattice girder in accordance with the Technical Approval is also indicated (solid line) and the factor of safety employed between the test data and the values used in the product Technical Approval can be observed.

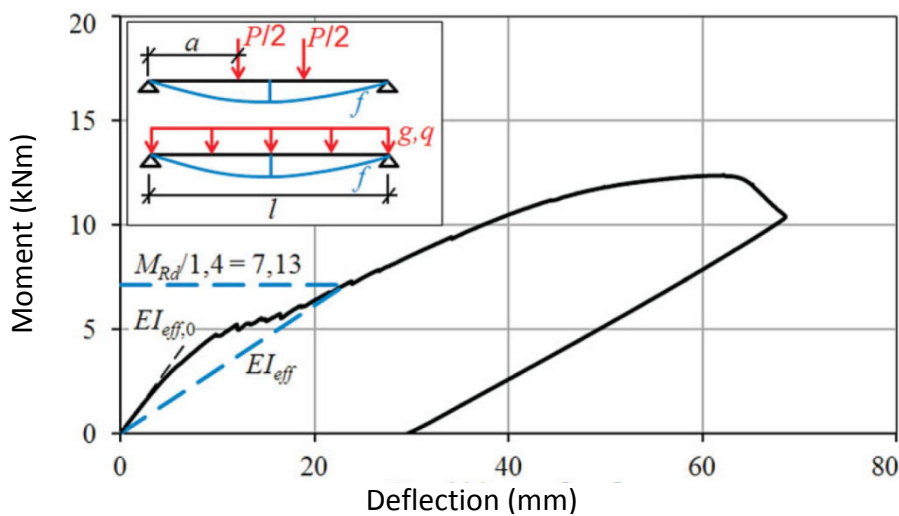


Figure 2-31 Moment-deflection diagram for lattice girder plank [63]



Figure 2-32 Buckling of top chord in bending tests [63]

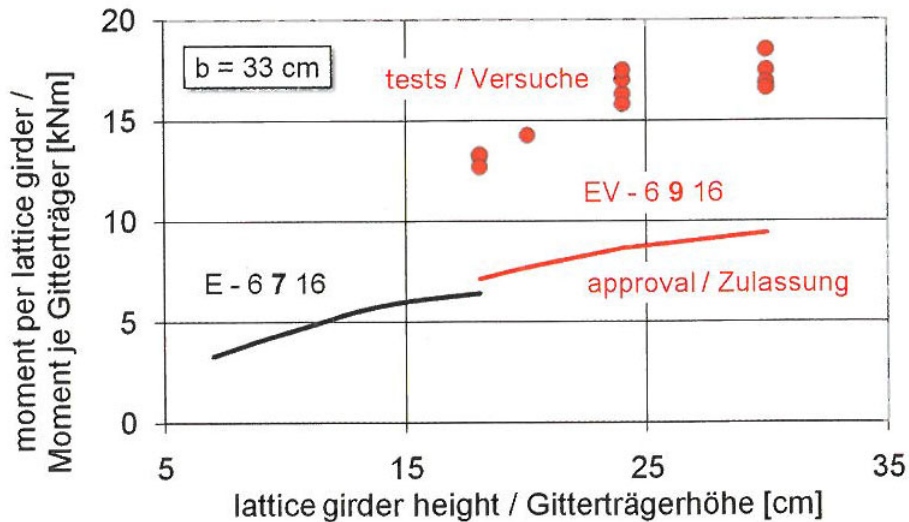


Figure 2-33 Ultimate moment per lattice girder in tests [42]

In the shear tests, typical failure occurred due to buckling of the compression diagonal between the support and the load point. The ultimate shear tests for the tests conducted on the 33cm wide planks are presented in Figure 2-39 for two identical girders except for the diameter of the diagonal. The increased shear resistance for the taller girders with the 9mm diameter diagonal in comparison with the 7mm diameter diagonal when the girder height exceeds 18cm is clearly shown. The permissible shear force per girder specified in the Technical Approval for this girder (EV-6 9 16) is 7.7kN and this is independent of the girder height. Buckling of the diagonals was the predominant shear failure mode for lattice girders exceeding 25cm in height (Figure 2-35a). For smaller height girders, the failure mode in the shear tests was concrete failure (Figure 2-35b & Figure 2-35c) and this is largely influenced by the characteristic compressive strength of the concrete. It was also found that the ultimate shear forces for the 10cm wide planks was approximately 25% lower than the 33cm wide planks.

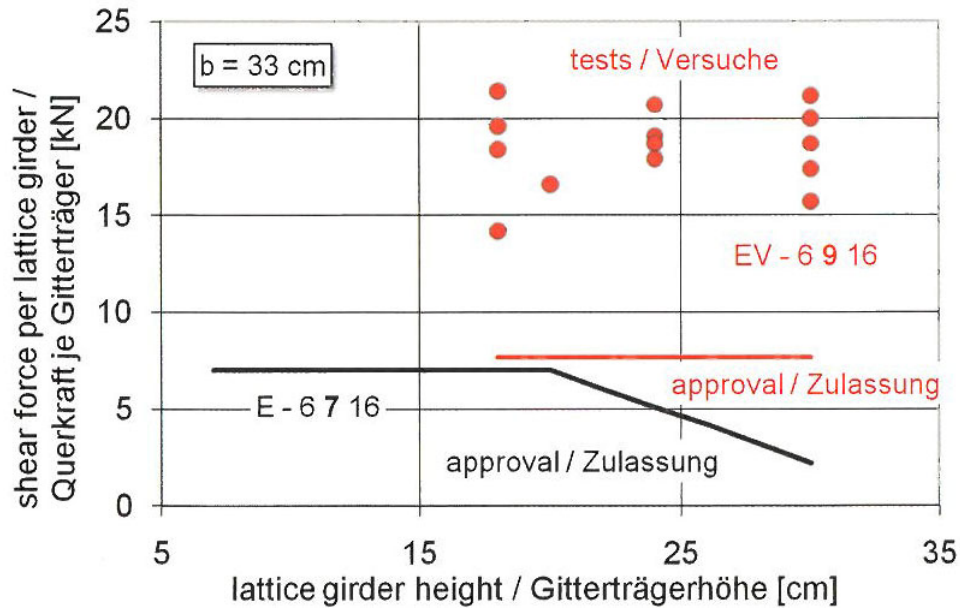


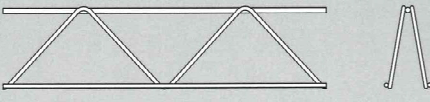
Figure 2-34 Ultimate shear force per lattice girder in tests [42]



Figure 2-35 Shear failure modes at supports [63]

Using the test data (lowest ultimate load in three tests on same lattice girder configuration) and applying partial safety factors to the loads (actions) and partial safety factors to the materials, Filigran are able to determine permissible moments and shear forces for different lattice girders and these are then used to calculate permissible erection spans which are stated in Technical Approvals which the company obtains for their lattice girder products (Figure 2-36). An example of the tabular data provided in the DIBt technical approvals are shown in Table 2-3.

Chapter 2. Background



Z-15.1-147
Elementdecke
Filigran-E- und Filigran-Ev-Gitterträger
 2. Januar 2019 - 2. Januar 2024

FILIGRAN
TRÄGERSYSTEME

www.filigran.de

Deutsches Institut für Bautechnik
DIBt

Zulassungszentrale für Bauprodukte und Bauarten
 Bautechnisches Prüfamt
 Eine vom Bund und den Ländern
 gemeinsam getragene Anstalt des öffentlichen Rechts
 Mitglied der EOTA, der UKA und der WFTRG

Bescheid

über die Verlängerung der Geltungsdauer der
 allgemeinen bauaufsichtlichen Zulassung/
 allgemeinen Bauartgenehmigung
 vom 11. Juni 2018

Datum: 05.11.2019 Beschließelzeichen: I 13-1.15-1-25/19

Nummer: **Z-15.1-147** Geltungsdauer
 vom: **2. Januar 2019**
 bis: **2. Januar 2024**

Antragsteller:
 Filigran Trägersysteme GmbH & Co. KG
 Zoppenberg 6
 31633 Leese

Gegenstand dieses Beschlades:
Filigran-E-Gitterträger und Filigran-Ev-Gitterträger für Fertigplatten
 mit statisch mitwirkender Oberbetondecke

Dieser Bescheid verlängert die Geltungsdauer der allgemeinen bauaufsichtlichen
 Zulassung/allgemeinen Bauartgenehmigung Nr. Z-15.1-147 vom 11. Juni 2018.
 Dieser Bescheid umfasst eine Seite. Er gilt nur in Verbindung mit der oben genannten allgemeinen
 bauaufsichtlichen Zulassung/allgemeinen Bauartgenehmigung und darf nur zusammen mit dieser
 verwendet werden.

Dr.-Ing. Lars Eckfeldt
 Referatsleiter



DIBt | Kolonnenstraße 30 B | D-10589 Berlin | Tel.: +49 (0) 30 767 61 0 | Fax: +49 (0) 30 767 61 500 | E-Mail: info@DIBt.de | www.DIBt.de

Figure 2-36 Technical approval for Filigran lattice girder [64]

Table 2-3 Permissible bending moment and shear forces for a Filigran lattice girder to determine erection spans (based on testing) [64]



Allgemeine bauaufsichtliche Zulassung/
 Allgemeine Bauartgenehmigung
 Nr. Z-15.1-147

Seite 9 von 13 | 11. Juni 2018

Tabelle 2c: Zulässige Momente und Querkräfte zur Ermittlung der Montagestützweiten bezogen auf den einzelnen Filigran-Ev-Gitterträger

Trägerhöhe [mm]	Ober-gurt-ø [mm]	Diagonalen-ø [mm]	Zul. M [kNm] bei einer Einflussbreite b [cm]				Zul. V [kN]	Zulagebewehrung min As [cm ²] je Gitterträger
			10	33	50	62,5		
180	10	7	2,58	2,61	2,61	2,61	7,0	-
200			2,78	2,82	2,83	2,84	7,0	
240			3,13	3,22	3,24	3,25	5,5	
300			3,49	3,72	3,76	3,78	5,2	
400		8	-	4,81	4,98	5,15	5,2	
180	16	9	6,89	7,13	7,18	7,20	7,7	1,53
200			7,31	7,70	7,77	7,80		1,48
240			7,79	8,63	8,80	8,87		1,38
300			7,41	9,38	9,81	10,00	1,23	
400			8,49	9,61	9,61	9,61	6,4	0,87

Die zulässigen Querkräfte und Momente gelten für den rechnerischen Gebrauchszustand im Montagefall mit $\gamma_F = 1,0$.
 Es müssen mindestens 2 Gitterträger in jeder Fertigteilplatte vorhanden sein.

Chapter 2. Background

Failure of the lattice girder planks due to the tension chord (bottom chord) was not observed in the tests conducted by Bertram *et al.* [63]. To avoid tension failure of the lattice girder plank, a minimum area of tension reinforcement must be provided in the precast plank. This can be provided by a combination of the bottom chords of the lattice girder and the longitudinal reinforcement in the plank. The minimum area of tension reinforcement (A_s) is noted in the Technical Approvals for the lattice girder and it is based on the permissible moment per girder determined using the load tests (Eqn. 2-1).

$$A_s = \frac{\gamma M}{(H-1cm)f_{yk}} \quad (\text{Eqn. 2-1})$$

where:

A_s required tension reinforcement (cm^2) per lattice girder (including the lower chords)

γ global safety factor ($\gamma = 1.75$)

M moment (kNm) per lattice girder ($\gamma_f = 1.0$, service moment)

H lattice girder height (cm)

f_{yk} characteristic yield stress of tensile reinforcement ($f_{yk} = 50\text{kN/cm}^2$ for Grade B500A)

For calculating deflection of lattice girder planks during construction, Filigran use the stiffness determined from the experimental bending tests. An effective bending stiffness (EI_{eff}) can be determined from knowledge of the load-deflection characteristics of the lattice girder plank using Eqn. 2-2. The effective bending stiffness can be used to determine the deflection of the plank when subject to uniform loading using Eqn. 2-3. This can be used to determine the maximum permitted loading on the plank during construction stage to ensure that the deflection of the plank does not exceed 1cm. The effective bending stiffness varied between 850kNm^2 to 2000kNm^2 in the tests conducted and this was dependent on the plank width and the girder characteristics. All tests were conducted on single span planks but on most projects lattice girder planks are erected such that they are

Chapter 2. Background

continuous (i.e. multi-span) over a number of temporary props. Therefore, the bending stiffness used by Filigran to comply with allowable deflection criteria is conservative.

$$EI_{eff} = \frac{PL^3}{24\delta} \left(3\frac{a}{L} - 4\left(\frac{a}{L}\right)^3 \right) \quad (\text{Eqn. 2-2})$$

where:

EI_{eff} effective bending stiffness

P test load

δ measured deflection at midspan

L span

a distance between support and load transfer

$$\delta = \frac{5gL^4}{384EI_{eff}} \quad (\text{Eqn. 2-3})$$

where:

EI_{eff} effective bending stiffness (based on testing)

g self-weight of precast plank and insitu topping (wet concrete)

Based on the testing conducted by Filigran in 2011, they obtained several Technical Approvals from DIBt for new lattice girders with larger diameter top chords and diagonals which increased their range of products and allowed larger erection spans to be achieved. Table 2-4 illustrates the tabular data for permitted erection spans which Filigran generated based on the testing for one such lattice girder and this is also included in the technical approvals for the lattice girder. The erection spans are a function of the total slab thickness, girder spacing and girder height. The table also states the minimum tensile longitudinal reinforcement which is required in the plank.

Chapter 2. Background

Table 2-4 Permitted spans during erection for girder [63]

Spacing	Girder Height	Permissible erection span (m) for EV-Girder with 16mm ϕ top chord and 9mm ϕ diagonal For a total slab thickness h (cm) of													
Trägerabstand [cm]	Trägerhöhe [cm]	Zulässige Montagestützweiten [m] für EV-Gitterträger mit Obergurt ϕ 16 mm und Diagonalen ϕ 9 mm bei einer Gesamtdicke h [cm] von													
		22	24	26	28	30	32	34	36	38	40	42	44		
62,5	18	3,52	3,29	3,08	2,90	2,74	2,59	2,46	2,35	2,24	2,14	2,05	1,97		
	20		3,29	3,08	2,90	2,74	2,59	2,46	2,35	2,24	2,14	2,05	1,97		
	22			3,08	2,90	2,74	2,59	2,46	2,35	2,24	2,14	2,05	1,97		
	24				2,90	2,74	2,59	2,46	2,35	2,24	2,14	2,05	1,97		
	26					2,74	2,59	2,46	2,35	2,24	2,14	2,05	1,97		
	28						2,59	2,46	2,35	2,24	2,14	2,05	1,97		
50	18	4,05	3,91	3,79	3,62	3,42	3,24	3,08	2,93	2,80	2,68	2,57	2,46		
	20		4,07	3,85	3,62	3,42	3,24	3,08	2,93	2,80	2,68	2,57	2,46		
	22			3,85	3,62	3,42	3,24	3,08	2,93	2,80	2,68	2,57	2,46		
	24				3,62	3,42	3,24	3,08	2,93	2,80	2,68	2,57	2,46		
	26					3,42	3,24	3,08	2,93	2,80	2,68	2,57	2,46		
	28						3,24	3,08	2,93	2,80	2,68	2,57	2,46		
33	18	4,53	4,44	4,35	4,27	4,20	4,13	4,07	4,01	3,96	3,88	3,80	3,72		
	20		4,59	4,50	4,42	4,36	4,29	4,23	4,16	4,10	4,03	3,89	3,73		
	22			4,70	4,62	4,54	4,47	4,40	4,34	4,24	4,06	3,89	3,73		
	24				4,76	4,68	4,61	4,54	4,44	4,24	4,06	3,89	3,73		
	26					4,80	4,72	4,64	4,44	4,24	4,06	3,89	3,73		
	28						4,83	4,67	4,44	4,24	4,06	3,89	3,73		
20	18	5,04	4,93	4,83	4,74	4,66	4,59	4,52	4,45	4,39	4,34	4,29	4,24		
	20		5,12	5,01	4,92	4,84	4,76	4,69	4,62	4,56	4,50	4,45	4,40		
	22			5,22	5,13	5,04	4,96	4,88	4,81	4,75	4,69	4,63	4,58		
	24				5,29	5,20	5,12	5,04	4,97	4,90	4,84	4,78	4,73		
	26					5,32	5,23	5,16	5,08	5,01	4,95	4,89	4,83		
	28						5,35	5,26	5,19	5,12	5,06	4,99	4,94		
10	18	5,89	5,77	5,65	5,55	5,45	5,37	5,28	5,21	5,14	5,07	5,01	4,95		
	20		5,97	5,85	5,75	5,66	5,57	5,48	5,41	5,34	5,27	5,20	5,14		
	22			6,11	5,99	5,89	5,80	5,71	5,63	5,55	5,48	5,42	5,35		
	24				6,19	6,08	5,98	5,89	5,81	5,73	5,66	5,59	5,52		
	26					6,21	6,11	6,02	5,94	5,86	5,78	5,71	5,65		
	28						6,24	6,14	6,06	5,97	5,90	5,83	5,76		
	30						6,26	6,17	6,09	6,01	5,93	5,87			
Trägerabstand [cm]	Trägerhöhe [cm]	erforderliche Feldbewehrung ¹⁾ [cm ² /m] bei einer Gesamtdicke h [cm] von										Required tension reinforcement ¹⁾ (cm ² /m) For a total slab thickness h (cm) of			
		22	24	26	28	30	32	34	36	38	40	42	44		
62,5	18	2,30	2,15	2,02	1,90	1,79	1,70	1,61	1,54	1,47	1,40	1,34	1,29		
	20		1,92	1,80	1,69	1,60	1,52	1,44	1,37	1,31	1,25	1,20	1,15		
	22			1,63	1,53	1,45	1,37	1,30	1,24	1,18	1,13	1,09	1,04		
	24				1,39	1,31	1,24	1,18	1,12	1,07	1,03	0,98	0,94		
	26					1,21	1,15	1,09	1,04	0,99	0,95	0,91	0,87		
	28						1,06	1,01	0,96	0,92	0,88	0,84	0,81		
50	18	3,06	3,06	3,06	2,98	2,81	2,66	2,53	2,41	2,30	2,20	2,11	2,02		
	20		2,96	2,83	2,66	2,51	2,38	2,26	2,15	2,06	1,97	1,89	1,81		
	22			2,57	2,41	2,28	2,16	2,05	1,95	1,87	1,78	1,71	1,64		
	24				2,20	2,07	1,96	1,87	1,78	1,70	1,62	1,56	1,49		
	26					1,93	1,83	1,73	1,65	1,58	1,51	1,45	1,39		
	28						1,70	1,61	1,54	1,47	1,40	1,34	1,29		
33	18	3,86	3,96	4,06	4,16	4,25	4,34	4,44	4,53	4,62	4,64	4,64	4,64		
	20		3,80	3,89	3,99	4,11	4,19	4,30	4,37	4,45	4,48	4,46	4,49		
	22			3,87	3,97	4,06	4,15	4,23	4,32	4,33	4,15	3,97	3,81		
	24				3,86	3,95	4,03	4,12	4,15	3,96	3,79	3,63	3,48		
	26					3,88	3,96	4,03	3,88	3,71	3,55	3,40	3,26		
	28						3,88	3,82	3,63	3,47	3,32	3,18	3,05		
20	18	4,86	4,98	5,11	5,23	5,35	5,47	5,58	5,69	5,81	5,92	6,03	6,13		
	20		4,85	4,97	5,09	5,21	5,32	5,44	5,55	5,66	5,76	5,87	5,97		
	22			4,99	5,11	5,23	5,34	5,45	5,57	5,67	5,78	5,89	5,99		
	24				5,03	5,15	5,26	5,37	5,48	5,59	5,70	5,80	5,90		
	26					5,17	5,28	5,39	5,50	5,61	5,72	5,82	5,93		
	28						5,28	5,39	5,50	5,61	5,71	5,82	5,92		
10	18	6,75	6,92	7,09	7,26	7,43	7,59	7,75	7,91	8,06	8,22	8,37	8,52		
	20		6,76	6,93	7,11	7,29	7,45	7,61	7,77	7,94	8,07	8,22	8,36		
	22			7,06	7,23	7,40	7,56	7,72	7,88	8,03	8,19	8,34	8,48		
	24				7,20	7,37	7,53	7,69	7,84	8,00	8,15	8,30	8,45		
	26					7,54	7,70	7,86	8,03	8,18	8,34	8,49	8,64		
	28						7,84	8,01	8,17	8,33	8,49	8,65	8,80		
	30							8,12	8,29	8,45	8,61	8,77	8,92		

¹⁾ einschließlich Gitterträgeruntergurte

²⁾ vorhandene Biegezugbewehrung der zwei Gitterträgeruntergurte ϕ 6 mm

³⁾ Erhöhungsfaktor für erf. As bei Passplatten mit 2 Gitterträgern

The technical approval document for the lattice girder states that the use of Table 2-4 is subject to the following conditions:

Chapter 2. Background

- compressive strength at the time of erection of at least $f_{ck} = 25\text{N/mm}^2$
- minimum plank thickness of 5cm
- nodal points of the lower chords of the lattice girder diagonals are positioned above the support
- a minimum required tensile reinforcement
- every precast plank is provided with at least two lattice girders
- the spot weld strengths of the lattice girder meet the specification of the Technical Approval

As noted previously, much of the research conducted by Filigran is not published and the data reported related to determination of erection spans are primarily focused on the ultimate bending moment and shear force data for some of the girders tested. The majority of tests conducted are primarily on planks with only one lattice girder and, therefore, they are not representative of the typical configuration of lattice girder planks used in real projects and do not allow load distribution between lattice girders to be investigated. The technical approval document which Filigran obtained from DIBt requires a minimum of two lattice girders in every plank for compliance. In the tests conducted and published by Filigran, the primary outputs from the testing are deflection and load. Whilst these two properties are very important in relation to the behaviour of the lattice girder plank, there is little information on how the various components of the lattice girder plank (top chord, bottom chord, diagonals, longitudinal reinforcement and concrete) behave and interact during the load test. Without this information, it is very difficult for numerical models to be developed which could be used to predict accurately the behaviour of the lattice girder plank during construction. Whilst the current tabular data provided by Filigran (and certified by DIBt) on erection spans of lattice girder planks is easy to use and understand, it is clear that there is potential to further improve the knowledge of how the floor product behaves during construction and increase the efficiency of the floor system. This can be primarily achieved by optimising the permissible erection spans that can be achieved during construction. The global factor of safety which Filigran uses to specify erection spans in its technical approval documents is typically at least 1.75 and this is based primarily on testing simply supported testing planks with one lattice girder. This suggests that the global factor of safety of continuous planks with at least two lattice

girders is significantly greater than 2.0. As the construction industry strives to improve the sustainability of its products, improving the efficiency and material economy of its products is a key requisite. This research project involved testing precast planks with two lattice girder planks and analysing the erection span characteristics of the lattice girder plank when it is continuous over at least one temporary support. In recent years, the majority of published research by Filigran has focused on the punching shear resistance of hybrid concrete flat slabs.

2.4.4 Torre *et al.*

In Spain, Torre *et al.* [65] conducted an experimental study in 2011 to determine the span in construction of precast slabs and beams with lattice girders during the construction phase and to optimise the number of temporary props required. The genesis of the project was the introduction in Spain of the Building Technical Code (CTE) which required manufacturers to guarantee the resistance/strength properties of their products as shown on the certificate of conformity. The study focussed on both precast slabs and beams manufactured with lattice girders to provide stiffness during the construction stage.

Prior to the experimental study, they used the Spanish structural steel standard EA-95 [66] to determine the theoretical compression resistance of the top chord of the lattice girder and the ultimate bending resistance of the lattice girder plank. They assumed a buckling length of 200mm for the top chord (distance between the nodes on the top chord of the lattice girder). Based on a construction loading of 1kN/m^2 and the theoretical ultimate bending resistance, they calculated the required spacing of the temporary props. They also determined the ultimate shear strength of the lattice girder planks and assumed a buckling length of 0.7 times the length of the diagonal to take account of the fixity of the diagonal in the concrete plank.

Four tests (two bending and two shear) were completed on one type of lattice girder slab and four bending tests were conducted on two types of lattice girder beams. Four-point bending was employed in all tests to determine the ultimate bending and shear strength. The lattice girder slab tested was 120cm wide and 5.5cm thick. The slab was manufactured 4.2m long for the bending tests and 2.2m long for the shear test. The slab had three 19cm high girders and the precast slab had a 10mm diameter longitudinal reinforcement at each girder and mesh (Figure 2-37). The two lattice

Chapter 2. Background

girder beams tested were 50cm wide, 5cm thick with three 23cm high girders and 40cm wide, 8.5cm thick with two 23cm high girders, respectively. For the bending tests on the slabs, the distance between supports was 3.8m and the loads were applied 1.5m and 1.3m from the supports, respectively. For the shear strength tests, the distance between supports was 1.8m and the loads were applied 0.7m and 0.3m from the supports, respectively. The four bending tests on the lattice girder beams were based on the distance between the supports of 3.2m and the loads were applied 1.1m from the support. Material testing was also undertaken on the concrete and the top chord and diagonal of the lattice girders. The average cylinder compressive strength of the concrete was 35.4N/mm^2 . The steel for the lattice girder was Grade B500T. The elastic limit for the steel in top chord and diagonal was measured as 500MPa and 766MPa, respectively. The measured material properties were incorporated into the theoretical ultimate bending and shear strength.

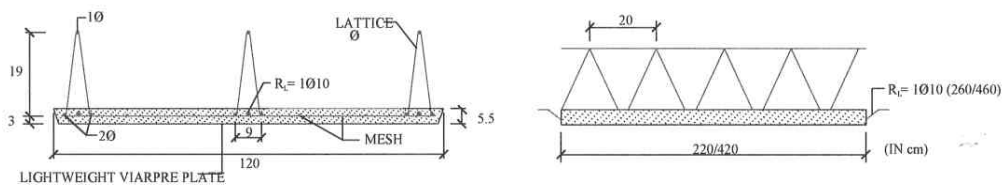


Figure 2-37 Lattice girder slab tested by Torre et al. [65]

Buckling of the top chord of the lattice girder was the failure mode (Figure 2-38) in the two bending tests on the lattice girder slabs. The theoretical moment resistance underestimated the ultimate moment of resistance from the tests by approximately 10%. Buckling of the diagonals was the failure mode for the two shear tests (Figure 2-39) but the theoretical shear resistance significantly underestimated the ultimate shear resistance from the tests by approximately 100%. It was suggested by the authors that a buckling length of 0.5 times the length of the diagonal might be more appropriate as the diagonal has rotational stiffness at both ends (from the embedment in the concrete and the weld connection to the top chord). In the four bending tests on the 50cm wide (3 lattice girders) and 40cm wide beams (2 lattice girders), the theoretical moment resistance underestimated the ultimate moment of resistance from the tests by approximately 47%. The authors suggest that a buckling length of 0.8 times the length of the top chord might be more appropriate so that the theoretical moment resistance would be closer to the value obtained from the load

Chapter 2. Background

tests. In their conclusions, the authors suggest that the larger diameter of the top chord in the beams tested (5mm ϕ) in comparison with the slabs (4mm ϕ) results in some additional rotational stiffness and hence the reduced buckling length ($0.8 \times$ length). However, this approach with respect to the buckling length of the top chord and diagonal does not appear to be consistent and appears to be based on calculating the required buckling length so that the theoretical moment and shear resistance are close to the ultimate values obtained from the tests conducted.

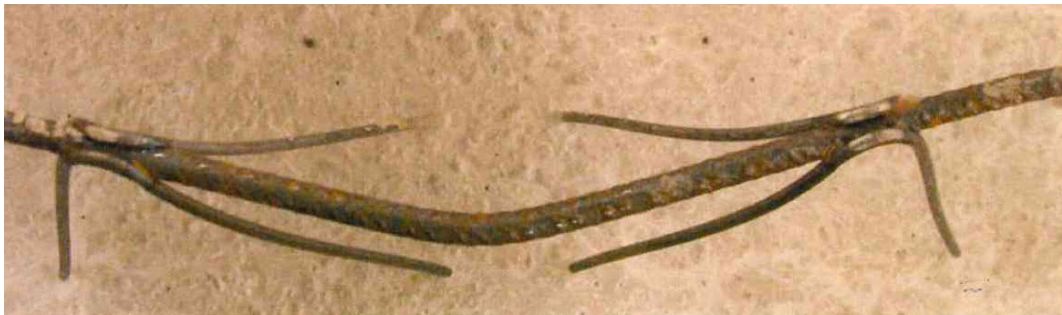


Figure 2-38 Buckling of top chord in bending test [65]



Figure 2-39 Buckling of diagonal in shear test [65]

In the tests conducted in the University of Burgos by Torre *et al.*, the applied load and deflection of the precast plank are the only parameters measured during the load test. Buckling of the lattice girder is based on visual observation, and therefore, there is considerable scope for errors in determining when a component (top chord, diagonal) has buckled. The paper only provides a load-deflection plot graph for two of the 8 tests conducted and there is no consideration of the stiffness or deflection of the precast planks tested. A further limitation of this study is the number of types

of lattice girder planks tested. No further published data is reported by any of the authors in this area since 2011.

2.4.5 Cheng *et al.*

In 1994, Cheng and Fan [67] (Hong Kong Polytechnic) conducted experimental tests on lattice girder planks and proposed a new numerical model derived from analysis of strain, principle of virtual work and coordinate transformation. The authors state that the analysis of the lattice girder plank is difficult because of the complicated shape and orientation of the steel. They also note, that at that time, engineers use approximate methods for analysis because of the difficulties in modelling a lattice girder plank accurately. Engineers neglect the contribution of the concrete and this leads to a very conservative design and adds to construction costs.

Although the research was primarily focused on developing a three-dimensional computational model, the authors provided some limited information on the experimental tests. The experimental programme consisted of two load tests on the steel lattice girder on its own (i.e. no concrete) and three load tests on the same lattice girder plank. The plank was 2m long and 1m wide (Figure 2-40) and a uniform line load was applied along the centre of the plank (three-point bending). The plank was 70mm thick and the height of the lattice girder was such that the majority of the girder was embedded in the concrete (Figure 2-40) which would not be typically of conventional lattice girder planks. They note that the planks tested were similar to the precast planks manufactured in Hong Kong at the time in which the plank would be 70-75mm thick and the overall slab thickness is typically around 200mm. Strain gauges were installed in the concrete and on the longitudinal reinforcement at midspan and at one third span.

A comparison of the load-deflection relationship, maximum compressive stress in the concrete and maximum tensile stress in the reinforcement for the average of the load tests and the numerical model are shown in Figure 2-41. Despite the limited experimental data, the results from the proposed numerical model were relatively accurate and suggested that it could potentially be used to accurately predict the behaviour of the lattice girder plank at construction stage. The authors noted that after initial formation of cracks in the concrete, stress redistribution occurs so that

Chapter 2. Background

the nonlinearity will increase as deflection increases. It was also observed that the tensile stress in the longitudinal reinforcement increases rapidly when the cracking of the concrete becomes significant (at approximately 10kN/m). They stated that failure appeared to be precipitated by crushing of the concrete in the compressive zone of concrete. They also claim that there is an over-use of bottom reinforcement and the majority are located near the neutral axis for the planks that were tested.

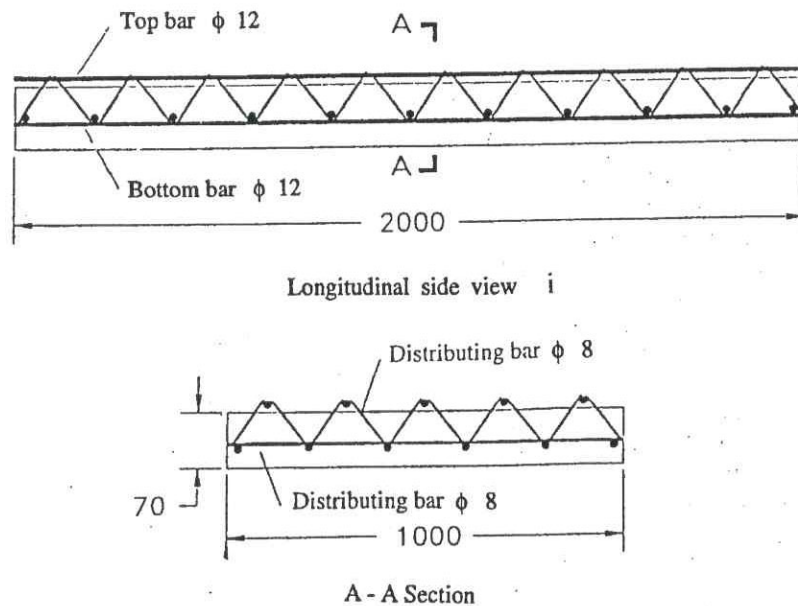
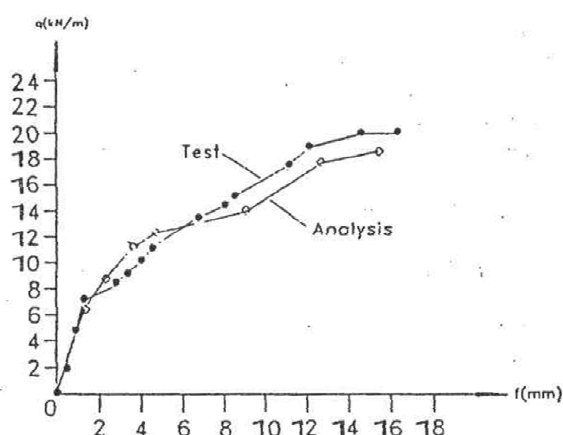


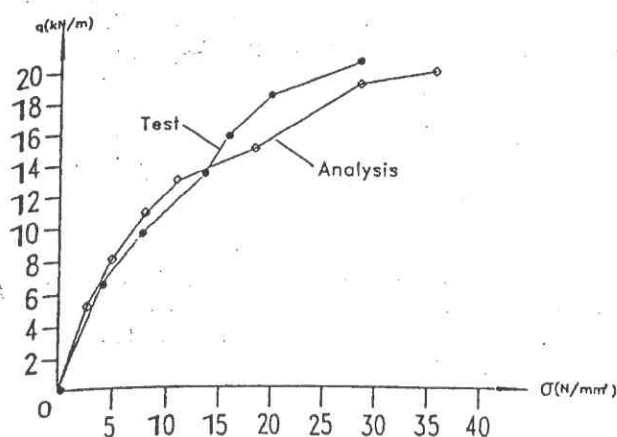
Figure 2-40 Lattice girder plank tested by Cheng & Fan [67]

A follow-on study by Cheng [68] described a non-linear optimisation design model for the lattice girder plank. In this model, it was assumed that the moment was resisted by the top chord and bottom chord of the lattice girder, the diagonals resisted the shear force and the action of the concrete was ignored on the basis of safety. Minimum reinforcement weight was the basic criterion for the optimisation of the structural system. The optimisation study suggested that there was potential for reducing the amount of reinforcement in the plank in comparison to the typical reinforcement used in Hong Kong for the hybrid concrete lattice girder slabs. Furthermore, they suggested that the diameter of the diagonals is dictated by manufacturing requirements rather than structural considerations and that smaller diameter diagonals could be used in the lattice girders. Whilst the point about manufacturing constraints is valid, the resistance of the diagonals in the lattice girder planks is not critical because the majority of the diagonal is embedded in the

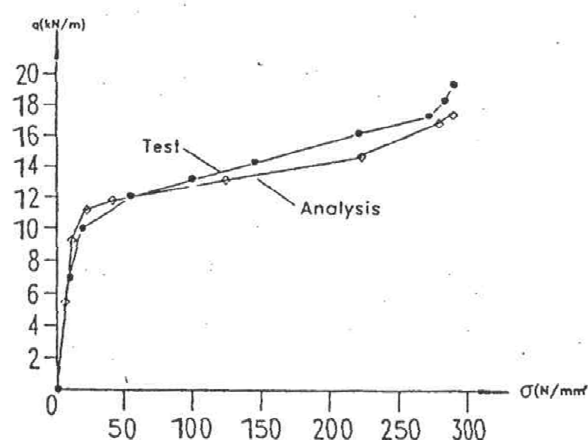
concrete plank tested in this study. This would not be valid for the majority of lattice girder planks, particularly for thick slabs with tall lattice girders. The planks tested and analysed by Cheng and Fan would not be representative of the type of planks used in construction projects in Europe.



(a) Load v Maximum displacement of lattice girder precast plank



(b) Maximum compressive stress in concrete



(c) Maximum tensile stress in reinforcement

Figure 2-41 Comparison of test and numerical model by Cheng & Fan. [67]

2.4.6 Miscellaneous

Park and Yoon in 1991 [69] reported on an experimental investigation on hybrid concrete slabs conducted in Korea in which the lattice girders were replaced by folded wire fabric mesh which was folded in a V-shape to replicate the lattice girder and reinforcement in a traditional Omnia slab (Figure 2-42). Three tests were conducted on planks (1m wide x 3.1m long x 6cm thick) with longitudinal reinforcement ratio of 0.67% to investigate their non-composite behaviour. During the tests (4-point bending), load, deflection and strains in the concrete and reinforcement were recorded. In all three tests, initial cracking of the concrete slab developed at midspan between 19 and 30% of the ultimate load of the plank and additional flexural cracks appeared along the span as the load increased. Failure of the plank in all three tests was initiated by buckling of the top chord. It was concluded that the precast plank was found to be safe during construction stage and could support the insitu concrete topping and construction loading.

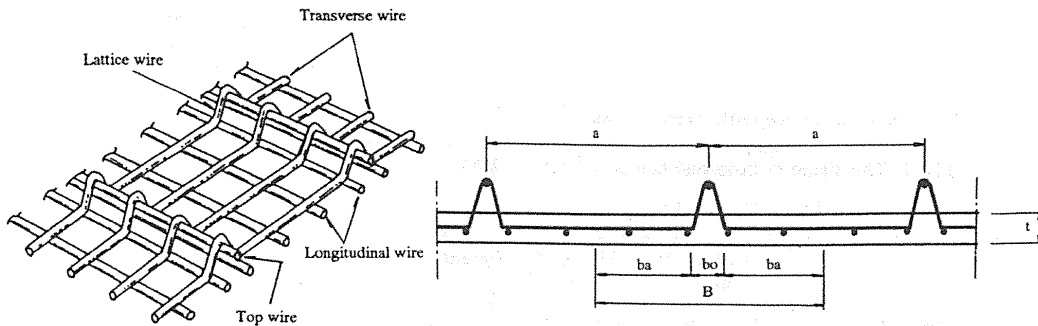


Figure 2-42 Precast plank with folded wire fabric mesh [69]

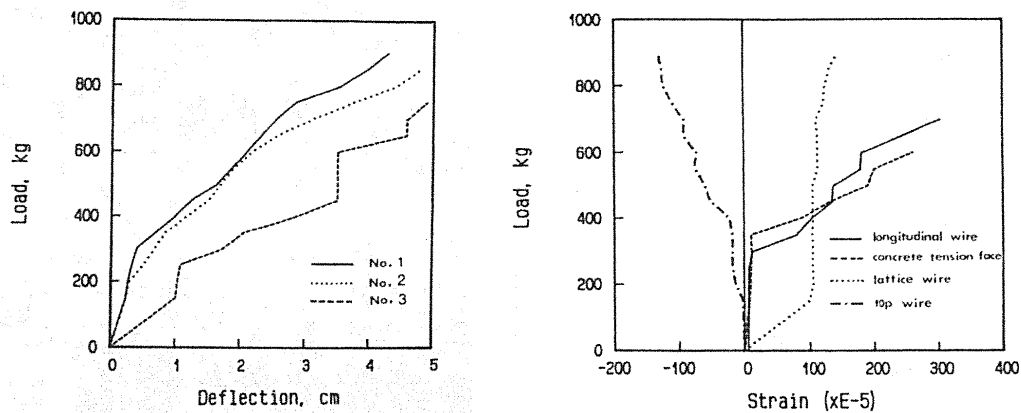


Figure 2-43 Load-deflection and strain data from tests conducted by Park and Yoon [69]

Chapter 2. Background

It should also be noted that experimental testing has also been carried out to investigate the behaviour of the hybrid concrete lattice girder slab (composite floor consisting of precast concrete lattice girder plank and insitu concrete topping). In 2011, Stehle *et al.* [40] conducted a series of tests on lattice girder slabs which was sponsored by Laing O'Rourke plc in the UK to investigate the two-way spanning action and how the bending moments are transferred across the joints. They concluded following the study that further work should be completed 'to optimise and understand the importance of all the design parameters more fully'. Similarly, Lundgren *et al.* [70]–[72] at Chalmers University in Sweden conducted research into the load-carrying behaviour of the hybrid concrete lattice girder slab in two directions across the joints. They used both full-scale experimental testing and finite element modelling to study the ultimate behaviour of the hybrid concrete slab. In particular, their research focused on the joint and surface treatment between the precast plank and insitu topping and the transverse reinforcement ('stitching' bar) across the joints between adjacent planks. They concluded that if the transverse reinforcement was omitted across the joint, the failure mode will most likely become brittle and that the load-carrying behaviour of the slab across the joints is very sensitive to the surface treatment (i.e. roughness) of the precast plank if the reinforcement across the joints is omitted. Lundgren *et al.* [71] also suggested that the long term effects of shrinkage and creep on the behaviour of the hybrid concrete slab should be further investigated.

Outside of the research conducted in Chalmers University by Löfgren *et al.* (Section 2.4.2) and in a number of German Universities sponsored by Filigran Trägersysteme GmbH (Section 2.4.3), there is little published research on experimental testing to study the behaviour of lattice girder precast planks during the construction stage when the planks are temporarily propped and must support temporary construction loading and the self-weight of the wet insitu concrete topping. This is somewhat surprising considering the popularity of the hybrid concrete lattice girder floor system and its increasing market share as the construction industry tries to maximise off-site construction to make the construction process more economical, efficient and sustainable. It is probable that some experimental testing has been undertaken on lattice girder planks at construction stage but it has not been published. The reasons for non-publication to

the wider public could be due to commercial considerations. However, without comprehensive test data on how all components in the floor system behave for different configurations, it is likely that erection spans will be based solely on design tables and/or conservative design aids. This research project uses experimental testing of precast concrete lattice girder planks to augment the current published experimental data and address the gap in comprehensive data which can be used to analyse the behaviour of this floor product during construction and develop numerical models.

2.5 Structural health monitoring

There is no agreed definition of ‘Structural Health Monitoring’ (SHM) ([73]–[78]). However, it typically involves the use of some sensor or device to record one or more parameters which can be used to understand how a structure is currently behaving or how it will behave in the future.

SHM is not a new concept in the field of structural engineering. Engineers have always examined the ongoing performance of their structures in an effort to monitor their behaviour, extend their service life or ensure public safety. In early structures, monitoring might have taken the form of regular visual inspections and one of the earliest form of SHM was the tapping of train wheels using a special hammer in the early 20th century to check for signs of damage or defects. Modern developments in SHM can be attributed to the evolution of digital computing and advances in sensor technology. During the 1970s and 1980s, the aeronautical, oil and space industries adopted SHM methods to help monitor the condition of components (condition monitoring) and detect potential defects or damage. It is only in the last 20-30 years that Civil Engineers have started to use and implement SHM technologies in projects. This is evidenced by the increased research focus on SHM ([75], [79], [80]) and the number of academic journals which publish papers related to SHM in the field of Civil Engineering.

Historically, monitoring of buildings was typically motivated by the need to understand how they behaved during earthquakes and/or storms (high winds). However, in recent years, there has been increased interest in using SHM to monitor behaviour of buildings and assess their condition with respect to maintenance

strategies. The requirement for increased service life and durability of structures will mean that SHM systems which allow the existing condition of the structure to be assessed and can detect possible deterioration of components will become increasingly important.

The recent collapses of bridges in Miami (2018) and Genoa (2018) highlight the important role which SHM systems could play in detecting potential failure and/or deterioration of structural components.

2.5.1 SHM components

In 2003, Mufti [81] proposed the new discipline ‘Civionics’ which was the application of electronics systems in civil engineering structures for the purpose of determining the state of their health. He suggested that this new discipline would produce engineers with the knowledge to build “smart” structures containing the necessary SHM sensors to provide the information on the condition of structures and avoid major structural failures [82].

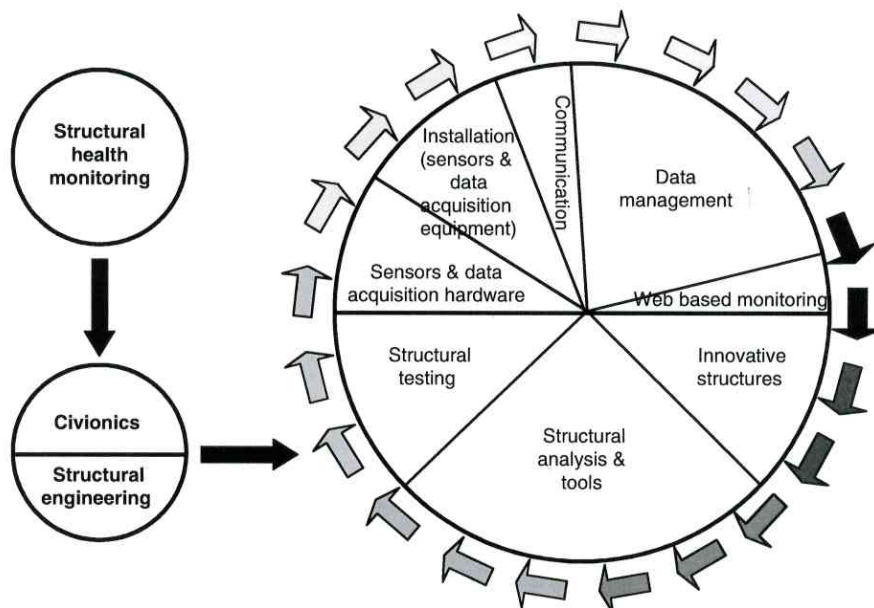


Figure 2-44 Basic components of a SHM system [83]

There is no commonly accepted methodology for designing a SHM system for a particular project. Mufti *et al.* [83] defined ‘SHM as the integration of a system of sensors, a data acquisition system, a data processing system, an archiving system, a communication system, and a damage detection and modelling system to acquire

knowledge, either on demand or on a continual basis, regarding the in-service performance of structures' (Figure 2-44). However, whilst specific details of SHM systems may vary, most SHM systems will have the following common components irrespective of the type of structure:

1. Design of SHM system

The key parameter(s) that will be measured and how they will be measured must be established. Identify damage or deterioration mechanisms that are of concern. Based on the operational and environmental conditions under which the system must function, the type of monitoring system should be determined (type, number and location of sensors; data management; data interpretation).

2. Data acquisition

With advances in technology, the manner by which data from sensors is collected is changing rapidly. Wired sensors were typically the conventional approach but in the last decade, the use of wireless sensors has increased significantly. Similarly, it is now more common for data to be transmitted over the internet (or local network) rather than downloaded periodically by personnel visiting the structure. The big advantage of remote monitoring is that data can be analysed in real-time.

3. Data management

Management of the vast data generated by sensors is one of the most critical components in any SHM system. The raw data are likely to contain unnecessary information or *noise* which is of little use for the purposes of structural health monitoring. Efficient processing of the data is essential so that the data can be interpreted quickly and easily. Some SHM systems use sophisticated algorithms to select and identify specific data such as peak values or data for discrete periods of time.

4. Data analysis

The analysis of the data is the most important component in an SHM system. Analysis of data to produce useful information on the condition or behaviour of the structure requires expert knowledge of the structure and possible damage or deterioration mechanisms. The degree of sophistication of the

analysis will depend on the complexity of the data and needs of the SHM programme.

5. Data storage and maintenance

All SHM systems must have a data storage protocol so that the data is stored for later use in structural health diagnostics. It is important that the data is available in a useable format and is not susceptible to corruption. Ideally, the raw data should be stored rather than the processed data as the raw data allows re-examination at a later time. As many SHM systems will be operational for many years on structures, a maintenance strategy must be implemented to ensure that the data from the sensors is reliable and accurate.

2.5.2 Benefits of SHM

Structural health monitoring which had its origins in condition monitoring, is increasingly becoming a standard feature in large civil engineering projects. Rapid developments in technology with regard to sensors and data acquisition has improved the ease of use of SHM systems. In addition, increased publication of the application of SHM strategies and the benefits accrued has increased the awareness and knowledge of SHM in the civil engineering profession.

The key benefits of SHM to civil engineering and/or society are:

1. Improved understating of insitu structural behaviour

SHM can be used to measure and study the actual behaviour of structures during service. The majority of design codes around the world are based on research conducted in laboratories, in which it is very difficult, if not possible, to replicate the actual behaviour of structures in the real world. The information that can be collected from SHM systems about real structures subject to real loads (structural, environmental, seismic) can be used in development of better codes of practice and design practice. SHM can also be used to detect design flaws or incorrect design assumptions which were not been considered during the design process for structures. SHM can also contribute to the better design of structures in the future as the actual behaviour of the structure can be analysed. Case studies from SHM can also be used in the education of engineers to develop understanding of how real structures behave over time and how the structure

Chapter 2. Background

is designed to resist applied loads. SHM can also be used as a teaching tool in the education of engineers to develop greater understanding of how structures behave and how they interact with their external environment ([84], [85], Appendix C).

2. Increased Safety

Following some notable failures in the recent past (e.g. Genoa bridge in 2018), it is likely in the future that society (backed up by regulations) will require that the condition and risks for all significant structures are certified. Those responsible for certification will require much more information in order to assess the condition and 'health' of a structure and its likely performance in the future. Information from sensors in a SHM system can be analysed remotely to determine the condition of a structure without having to visit the structure. SHM can also be used to detect deterioration and/or damage in a structure at an early stage so that repairs can be made at onset of damage which will reduce maintenance costs and prevent further deterioration. SHM can also be used to provide data on new materials or innovative construction techniques to demonstrate its performance in use. The issue of safety will become increasingly important as the age of much of the developed world's infrastructure (bridges, tunnels, dams, buildings) is approaching or past its intended design life but its actual condition is unclear due to lack of regular monitoring or inspection.

3. Better maintenance and management strategy

SHM systems reduce the requirement for field inspections and allow the condition of structures to be monitored in real time. SHM systems can be used to generate condition databases for structures and formulate maintenance strategies which use their resources efficiently. The data from SHM systems can also be used to predict the remaining service life of components in structures so that future maintenance or replacement of components can be costed and organised efficiently.

4. Cost efficiency

In addition to increased safety and improved working life of structures, SHM can also be used to reduce the cost of site inspections, maintenance, repairs and the potential costs if significant repair necessitating partial or full shut-down of structures was required. As an example, the collapse of

the I-35 bridge in Minneapolis in 2007 resulted in 13 deaths and 147 injuries. In addition to the fatalities, the collapsed bridge cost the state \$400,000 every day and the replacement bridge cost \$234 million [86]. Ironically, because the bridge collapse affected the confidence of the general public in the safety of infrastructure, the replacement bridge has a comprehensive SHM system and is considered one of the first ‘smart’ bridges of its scale [87].

A study by Frangopol and Liu [88] on civil infrastructure comparing two optimal design solutions with and without monitoring concluded that although initial costs are increased if using SHM (cost of SHM system at start of project); that the failure cost is decreased (less risk), and the additional costs are decreased (improved maintenance and management decisions). This is illustrated in Figure 2-45 which shows that the optimal design solution with monitoring results in a reduction of the total life-cycle cost and an improvement in performance.

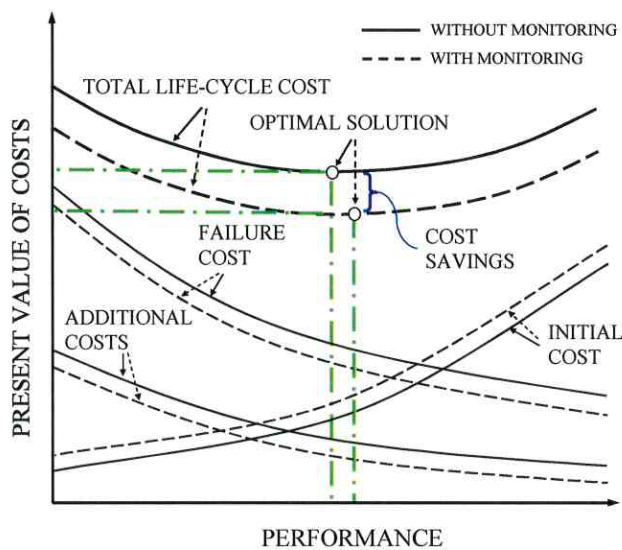


Figure 2-45 Optimum design solution based on life-cycle minimisation with and without monitoring [89]

As the monitoring and assessment capabilities of SHM become more sophisticated, and the list of benefits they provide continues to expand, the application of SHM technology will become more prominent. There are benefits for all stakeholders (client, government, contractor, designer, maintenance operator, student, general public) in a project if a suitable SHM system is implemented as it will result in a

safer and more cost-effective structure with a better decision process for determining maintenance and repair strategies.

2.5.3 SHM of concrete floors

Concrete is the most widely used construction material in the world and as a result society depends on concrete structures in all its forms (buildings, bridges, dams etc.) to function. The service life of concrete structures can typically range from 50 to 120 years and therefore durability of concrete components is an essential property. This is increasingly important as the concrete industry strives to ensure structures are more sustainable and adaptable for future needs of society. In addition, because a large proportion of the existing concrete infrastructure in the developed world is near or past its original service life, the need to determine the existing condition or health of the concrete is critical to the continued functioning of concrete structures.

The majority of SHM systems installed on concrete structures relate to bridges, tunnels and dams (infrastructure). In the literature, there is very little published case studies in which the structural behaviour of concrete floors is monitored or analysed using field data. To illustrate this point, 67 case studies from throughout the world relating to condition monitoring of concrete structures was published in a Department of Trade and Industry (UK) report in 2007 [90] and only one case study directly related to buildings. Historically, SHM of buildings was primarily related to studying the behaviour of buildings during earthquakes and extreme wind events (e.g. [91], [92]). One of the barriers to future implementation of SHM in concrete floors is the lack of case studies which demonstrate the benefits of installing a SHM system and justification of the business case for the SHM system. In 1995, Moss and Mathews [93] outlined some of the motivations for adopting a SHM scheme for buildings:

- (a) modifications to existing structures
- (b) monitoring of structures affected by external works
- (c) monitoring during demolition
- (d) feedback loop to design
- (e) fatigue assessment
- (f) novel systems of construction

Chapter 2. Background

One of the longest continuous SHM schemes of a building is the Punggol building in Singapore which was constructed in 2003 [94]. The scheme consisted of strain gauges embedded in concrete columns and there is now nearly twenty years of SHM data from the sensors. The aims of the SHM scheme which was funded by the Housing and Development board in Singapore was:

- (a) to increase safety,
- (b) verify performance,
- (c) control quality,
- (d) increase knowledge,
- (e) optimise maintenance costs,
- (f) evaluate the condition of the structure after extreme event (earthquake, impact or terrorist act).

This project has yielded some very important insights on the real structural behaviour of tall concrete buildings during construction and in service and will inform future design of tall buildings and implementation strategies for SHM in buildings [95].

Concrete floors utilise the greatest proportion of concrete in most concrete frame buildings but despite their importance to the functioning of the structure, there are still relatively few examples of SHM systems in floors which are used to study and monitor their behaviour in buildings. The possible barriers to the adoption of SHM in concrete floors is that the installation can be slow and labour intensive; and there are very few published case studies demonstrating how a SHM system should be executed and the benefits accruing.

Deterioration or damage to concrete structures can have significant consequences for society, economy, environment and safety. All concrete structures age and deteriorate with time. The dominant cause of premature deterioration of concrete is reinforcement corrosion [96]. Reinforcement corrosion is very costly to repair and can require parts of the concrete structure to be excluded to the public whilst repairs are conducted. The major challenge for detecting reinforcement corrosion is that by the time reinforcement corrosion is visible at the concrete surface (typically in the

form of cracks), the level of deterioration is significant and will require major repairs.

Current methods for monitoring the health or condition of concrete floors are visual inspection, non-destructive testing (NDT) such as the Schmidt Rebound hammer or insitu testing such as core samples. The primary disadvantage of visual inspection is that it is focussed on the concrete surface and it is not possible to inspect buried or clad parts of the floor. NDT and insitu testing are useful but can be time consuming, expensive and will only give information at a specific location and at a specific point in time. Whilst it is not expected that SHM will replace visual inspection for concrete floors, it can make the process more efficient and can be used to identify areas of the floor which may be of concern but which are not accessible. A SHM system in a concrete floor will allow measurements to be recorded automatically for specific parameters at various locations within the depth of the floor and analysed remotely for both short-term and long-term changes. SHM in concrete floors will reduce the requirement for access (not necessary to exclude access to parts of building whilst testing is in progress), can be used to measure properties at specific locations in the floor (sensors can be embedded) and will also allow properties to be studied over time so that possible deterioration can be identified as early as possible. Information from SHM systems in concrete floors will also allow designers to improve their understanding of how concrete floors perform in real structures and this should feed in to the future design of concrete floors. It would be possible to integrate a SHM system with a building management system (BMS) so that the facility manager would get a message (SMS, email) if specific parameter limits were exceeded and this could inform a maintenance or inspection programme.

In the literature, there are very few examples of SHM systems in concrete floors which are installed during the construction phase so that the behaviour of the floor can be analysed for its full life-cycle. Most of the published research on concrete slabs relates to ground-bearing slabs in which either of the strain, temperature or movement in the concrete was measured ([97]–[99]). Some researchers have used SHM techniques in a laboratory to study the behaviour of suspended concrete floors [100] but it is very difficult to replicate field conditions in a laboratory setting. The

Chapter 2. Background

most meaningful and comprehensive project which is applicable to SHM of suspended concrete floors was the European Concrete Building Project (ECBP) in Cardington (UK). A seven-storey insitu concrete frame was constructed in 1998 using commercial developer's standards and all floors were 250mm deep flat slabs with no downstand beams or walls [101]. The aim of the project was to 'improve the efficiency of production and the performance of concrete buildings to meet the needs of clients for reduced costs, better quality and higher speed'[102]. Scott *et al.* [103] used bonded strain gauges on the reinforcement in the flat slab in Cardington and conducted a series of short and long term load tests to study the behaviour of the floor for various loading regimes. Other studies were also conducted in Cardington related to flat slab deflections [104] and back-propping of flat slab formwork [105].



Figure 2-46 Concrete frame in Cardington (ECBP)

At the time of writing, there is no literature on SHM of hybrid concrete lattice girder flat slabs which is the focus of this thesis. This is despite the popularity of flat slabs in concrete frame construction and the promotion of hybrid concrete construction by the precast and concrete industry. The current lack of field data on hybrid concrete lattice girder flat slabs hinders the understanding of how the precast product performs in real buildings and limits potential efficiencies which could be achieved in the design of the floor. If the concrete industry wishes to promote the

potential for fabric energy storage by utilising the thermal mass properties of exposed concrete floors to regulate internal temperatures and reduce energy requirements, it will have to publish more field data and case studies which demonstrates the benefits of this technology. It is also possible that the incorporation of SHM strategies in concrete floors will become more popular if we wish to extend the service life of existing buildings and/or change the use of the buildings so that they become more adaptable and sustainable. For future construction, the implementation of a targeted SHM strategy in concrete floors will allow the existing condition and performance of the floor to be monitored as part of the building management system and give knowledge to the owner of the building if they wish to change the use of the building or increase the life-cycle of the building. As the industry strives for more sustainable construction, SHM will be one of the tools which it can utilise to ensure floors are efficient, economical and adaptable during their operation.

2.5.4 Future of SHM

Although the concept and application of a structural health monitoring strategy is not new, it is still not standard practice in civil engineering. Since the 1970s, there has been considerable research focus on the SHM in civil engineering but to date, it has not become a mainstream discipline within civil engineering. Mufti [106] contends that engineers are typically conservative and risk averse as most structures are unique and their performance during their service life is rarely monitored. However, SHM has the potential for engineers to monitor and evaluate structures in real-time under service conditions improve the reliability, efficiency and safety of structures. Cawley [107] proposes that lack of attention to the business case for SHM, insufficient attention to how the large data flows will be handled and the lack of performance validation of real structures are the primary reasons for the slow transition from research to practical application. In order to encourage more adoption of SHM systems, it is clear that more publication and dissemination of cost-benefit analysis studies on the SHM systems is required which demonstrates the economic case for using a SHM system. The main economic motivations for the use of SHM systems are listed in the SAE standard [108] for the civil aerospace aircraft industry but they are equally applicable to civil engineering:

Chapter 2. Background

- Reduce inspection time and cost;
- Improve repair planning;
- Increase, optimise or customise inspection intervals;
- Extend the economic life of the structure;
- Enable new design principles and maintenance concepts.

Developing intelligent post-processing strategies so that the huge volume of data generated by SHM systems is converted into useful information is critical to the uptake of SHM. As an example, 26 sensors on the Vincent Thomas bridge in California generates 3 terabytes of data per year [109]. In a recent report [110] by CSIC (Centre for Smart Infrastructure and Construction) in the UK, they noted that processing must decrease the data volume and increase the data value and presented the pyramid model (Figure 2-47) which shows that data must be processed to a more manageable form before being passed to the decision making level. The data generated by SHM systems will also provide a rich database for developing and validating new numerical and predictive tools for analysing how structures behave during service and are subject to real loads.

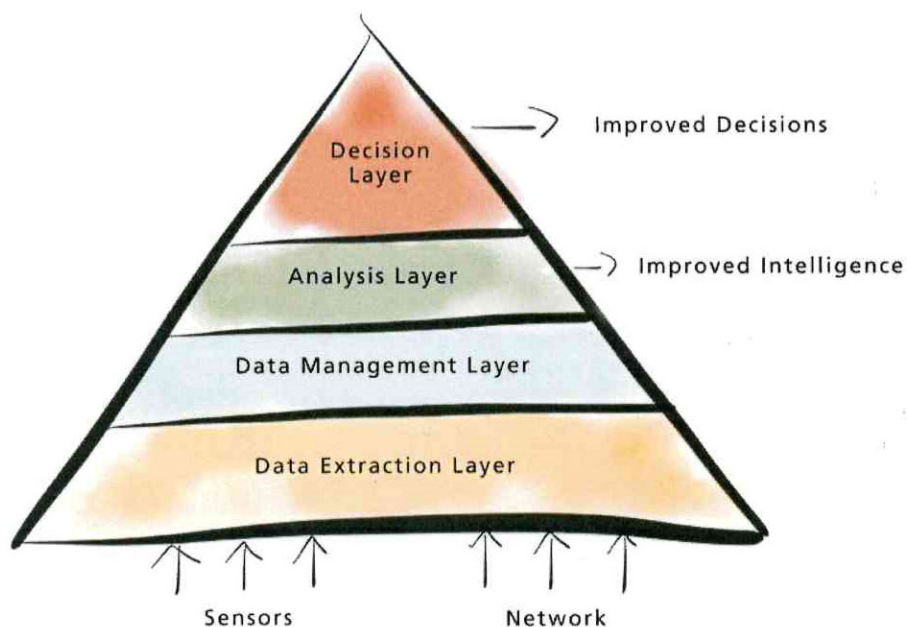


Figure 2-47 Pyramid model of decreasing data volume and increasing data value [111]

Chapter 2. Background

Much of the research conducted on SHM has been based on laboratory testing of simple beam and plate structures in the laboratory. Whilst this research is valid and contributes to the development of SHM, it would be preferable if there was greater consideration of adopting SHM strategies in real structures at design stage which have typical variations in load and environment which are difficult to replicate in a laboratory situation.

It is apparent that in the future, wireless sensors and data acquisition systems will replace wired connections. However, there is still significant development required in wireless technology before they become the norm. The primary challenges with wireless devices are powering the devices, increasing the energy efficiency of devices and durability. The practical problem of embedding sensors in concrete is a subject which also requires further research to develop wireless devices which can operate and transmit a signal at various embedment depths. The other area where considerable research effort is required is the development of tools such as life prediction models which can use the data from SHM models to determine the 'health' of the structure in real time and inform decision making in relation to repair and maintenance.

The development of 'smart materials' or 'smart structures' will be one of the major advances in civil engineering in the coming years and SHM will be integral to the development of this new type of 'intelligent' structures and/or 'intelligent' monitoring. Smart structures utilise active (smart) materials as sensors and actuators to sense and respond to their environment [114]. CSIC define 'smart infrastructure' as the "result of combining physical infrastructure with digital infrastructure, providing improved information to enable better decision making, faster and cheaper." [110]. This concept although relatively new in civil engineering is not new in other fields. For example, Boeing in the 2000s developed software to enable aircraft parts to schedule their own repair and replacement [115]. As mentioned previously, the development of smart structures can be likened to the nervous system in the human body. This will require integration of SHM in building management systems (BMS) and infrastructure management systems (IMS) so that embedded sensors are combined with computer-based decision support so that the structure will effectively 'think for itself' [111]. This rapidly evolving field will

also require education of both professional practitioners and students of civil engineering so that they can utilise this new technology efficiently and appropriately.

In summary, a SHM system (as proposed by Sumitro and Wang [116]) must fulfil ‘AtoE’ characteristics, i.e. accuracy, benefit, comprehensiveness, durability and ease of installation. It is likely that the adoption of SHM will be gradual process. Increased requirement for safety, regulations which require SHM to be part of engineering projects and case studies reporting good practice and tangible benefits of SHM must be collated and disseminated in order to encourage greater adoption of SHM.

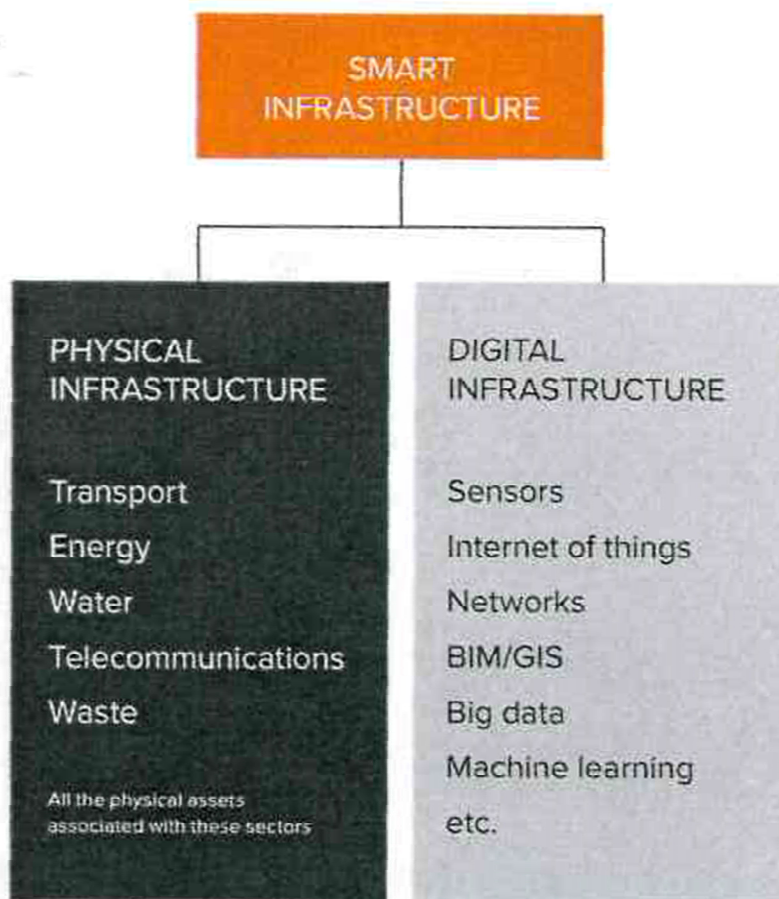


Figure 2-48 Smart Infrastructure [110]

This thesis describes the implementation of SHM strategy for a MMC (hybrid concrete lattice girder flat) and the application of the data generated to study the behaviour of this popular floor product. This addresses the need to publish more case studies which demonstrate the advantages of SHM but also acts as a promoter for future research in this area. The future advancement of ‘smart structures’ will be directly related to the future development in the SHM and sensor technology. Although the technology used in this research project may be different to the technology employed in the future, the methodology, data management and analysis described in this thesis can be incorporated into future SHM schemes and should assist with the development of ‘smart structures’ in the future.

2.6 Conclusions

Despite the increasing popularity of hybrid concrete lattice girder precast floors as an economical option for construction of concrete flat slabs, a number of gaps were identified in the literature in relation to the scarcity of experimental data and understanding of the behaviour of the floor product in real structures during both the construction and operational phases. These gaps have the potential to impact on the efficiency, economy and sustainability of this floor product which is a MMC. In the future, designers will require robust data which demonstrates how any structural product performs in real structures.

With respect to experimental testing of lattice girder planks at construction stage in the literature, there is a dearth of comprehensive test data publicly available on all the components of the precast floor product. Without test data which explores the complex interaction between the concrete plank, steel lattice girder and steel reinforcement, it is unlikely that a numerical model can be developed which can be used to predict accurately the behaviour of lattice girder planks during construction. Many of the previous researchers have commented on the overly conservative approach used to predict erection spans for lattice girder planks during construction. The current design tools are largely based on experimental tests on simply supported planks and do not take account of the propping conditions applied on site. The cost of temporary propping of lattice girder planks is a significant cost element of the floor construction and there is potential for optimisation of erection spans through the application of detailed experimental data and numerical modelling.

Chapter 2. Background

Furthermore, with the increasing trend towards structural health monitoring and rapid technological advances in sensors and data acquisition, there will be an increasing demand from many stakeholders in the construction sector to be able to demonstrate how structural products behave when subject to real structural and environmental conditions. Structural health monitoring (SHM) of hybrid concrete lattice girder floors during construction or operational phase was not in the literature when this research commenced. This is primarily due to the considerable resources required to implement a SHM strategy as almost all current cost-effective technologies require wired sensors connected to data acquisition units. The rich data from SHM can be used to investigate the structural and thermal behaviour of the floor, allowing the behaviour of the real as-built structures to be compared with predicted behaviours using codes of practice, design tools and/or modelling. This research aims to contribute to the improved understanding of the behaviour of hybrid concrete lattice girder floors and also provide a relevant case study which demonstrates the potential of utilising SHM to develop ‘smart structures’ in the near future.

2.7 References

- [1] K. S. Elliott and Z. A. Hamid, *Historical and Chronological Development of Precast Concrete Structures*. Wiley & Sons, 2017.
- [2] FIB, “Precast concrete in mixed construction (fib Bulletin No. 19:),” FIB (The International Federation for Structural Concrete), 2002.
- [3] K. S. Elliott and C. Jolly, *Multi-storey precast concrete framed structures*, 2nd Ed. Wiley Blackwell, 2013.
- [4] The Concrete Centre, “Offsite Concrete Construction - The Benefits (TCC/03/61),” The Concrete Centre (UK), London, UK, 2018.
- [5] Irish Concrete Federation, “Irish Concrete Federation Annual Report 2017,” 2018.
- [6] The Concrete Centre, “Precast Concrete in Buildings. A guide to design and construction (TCC/03/31),” The Concrete Centre (UK) and British Precast, 2007.
- [7] The World Commission on Environment and Development (Brundtland Gro H), *Our Common Future*. Oxford: Oxford University Press, 1987.
- [8] W. M. Adams, “The future of sustainability: Re-thinking environment and development in the twenty-first century,” in *Report of the IUCN renowned thinkers meeting*, 2006, vol. 29, p. 31.
- [9] DEFRA, “Securing the future: delivering UK sustainable development strategy,” Department for Environment, Food & Rural Affairs (UK), 2005.
- [10] DECLG, “Our Sustainable Future – a Framework for Sustainable Development for Ireland,” Dept. of Environment, Community and Local Government (Ireland), Dublin, Ireland, 2012.
- [11] J. Bennett and A. Crudgington, “Sustainable development: Recent thinking and practice in the UK,” *Proc. Inst. Civ. Eng. - Eng. Sustain.*, vol. 156, no. 1, pp. 27–32, 2003.

Chapter 2. Background

- [12] The Concrete Centre, “Thermal Mass Explained (TCC/05/11),” The Concrete Centre (UK), London, UK, 2019.
- [13] British Precast, “Concrete for energy-efficient buildings The benefits of thermal mass,” European Concrete Platform ASBL, 2007.
- [14] The Concrete Centre, “Concrete Credentials. Concrete, concrete products and constituent materials (TCC/05/20),” The Concrete Centre (UK), London, UK, 2018.
- [15] WRAP, “Current Practices and Future Potential in Modern Methods of Construction,” 2007.
- [16] British Precast, “Sustainability Charter,” *British Precast Sustainability Charter*, 2019. [Online]. Available: <https://www.britishprecast.org/Sustainability/Sustainability-Charter.aspx>. [Accessed: 20-Jun-2019].
- [17] British Precast, “Sustainability Matters 2018,” British Precast, Leicestershire, UK, 2018.
- [18] C. H. Goodchild and J. Glass, “Best Practice Guidance for Hybrid Concrete Construction,” The Concrete Centre (UK), London, UK, 2004.
- [19] J. S. Egan, “Rethinking Construction: the Report of the Construction Task Force,” HMSO, London, UK, 1998.
- [20] The Concrete Society, “Formwork. A guide to good practice (CS 030),” The Concrete Society, Camberley, UK, 2012.
- [21] The Concrete Centre, “Concrete Framed Buildings. A guide to design and construction (TCC/03/024),” The Concrete Centre (UK), London, UK, 2016.
- [22] H. Bachmann and A. Steinle, *Precast concrete structures*, 1st Ed. Ernst & Sohn, 2011.
- [23] NSAI, “IS EN 15804: Sustainability of construction works -Environmental product declarations - Core rules for the product category of

Chapter 2. Background

constructionproducts,” NSAI (National Standards Authority of Ireland), Dublin, Ireland, 2012.

- [24] H. Kagermann, W.-D. Lukas, and W. Wahlster, “Industrie 4.0: Mit dem Internet der Dinge auf dem Weg zur 4. industriellen Revolution,” *VDI nachrichten*, vol. 13, no. 1, 2011.
- [25] Acatech - National Academy of Science and Engineering, “Recommendations for implementing the strategic initiative INDUSTRIE 4.0,” Acatech - National Academy of Science and Engineering (Germany), Frankfurt, Germany, 2013.
- [26] C. Roser, “Lean and Industry 4.0,” 2018. [Online]. Available: <https://www.allaboutlean.com/lean-and-industry-4-0/>. [Accessed: 29-Apr-2019].
- [27] J. Furche and U. Bauermeister, “Elementbauweise mit Gitterträgern,” in *Beton-Kalender 2009: Schwerpunkte: Konstruktiver Hochbau-Aktuelle Massivbaunormen*, K. Bergmeister, F. Fingerloos, and J.-D. Wörner, Eds. Berlin: Ernst & Sohn, 2009, pp. 337–498.
- [28] Hanson Building Products, “Omnia and Cobiax Flooring Systems,” 2010.
- [29] P. Peacock, “Integrated eco-floors,” *Struct. Eng.*, vol. 87, no. 9, pp. 12–13, 2009.
- [30] C. H. Goodchild, R. M. Webster, and K. S. Elliott, “Economic Concrete Frame Elements to Eurocode 2 (CCIP-025),” Cement and Concrete Industry Publication (UK), Surrey, UK, 2009.
- [31] J. Burrige, “Flat Slabs Research,” in *Future Infrastructure Forum (17-18th January 2012)*, 2012.
- [32] The Concrete Centre, “Office Cost Study (TCC/03/57),” Concrete Centre (UK), London, UK, 2014.
- [33] K. Cho, Y. Shin, and T. Kim, “Effects of Half-Precast Concrete Slab System on Construction Productivity,” *Sustainability*, vol. 9, no. 7, p. 1268, 2017.

Chapter 2. Background

- [34] NSAI, “IS EN 10080. Steel for the reinforcement of concrete. Weldable reinforcing steel. General,” NSAI (National Standards Authority of Ireland), Dublin, Ireland, 2005.
- [35] NSAI, “IS EN 13369: Common rules for precast concrete products,” NSAI (National Standards Authority of Ireland), Dublin, Ireland, 2013.
- [36] NSAI, “IS EN 206: Concrete - Specification, performance, production and conformity,” NSAI (National Standards Authority of Ireland), Dublin, Ireland, Ireland, 2013.
- [37] The Concrete Centre, “European standards for precast concrete,” 2019. [Online]. Available: <https://www.concretecentre.com/Concrete-Design/Materials/European-standards-for-precast-concrete.aspx>. [Accessed: 19-Mar-2019].
- [38] NSAI, “IS EN 13747: Precast concrete products - Floor plates for floor systems,” NSAI (National Standards Authority of Ireland), Dublin, Ireland, 2010.
- [39] NSAI, “IS EN 1992-1-1: Eurocode 2: Design of concrete structures. Part 1-1: General rules and rules for buildings,” NSAI (National Standards Authority of Ireland), Dublin, Ireland, 2005.
- [40] J. Stehle, A. Kanellopoulos, and B. L. Karihaloo, “Performance of joints in reinforced concrete slabs for two-way spanning action,” *Proc. ICE - Struct. Build.*, vol. 164, no. 3, pp. 197–209, 2011.
- [41] Ebawe GmbH, “Lattice girder floor,” 2019. [Online]. Available: <https://www.ebawe.de/en/lattice-girder-floor>. [Accessed: 01-Aug-2019].
- [42] J. Furche and Bauermeister U, “Load tests: Long erection spans with strengthened lattice girders,” *Betonwerk+ Fert.*, vol. 77, no. 8, pp. 4–17, 2011.
- [43] NSAI, “IS EN 1993-1-1: Eurocode 3: Design of Steel Structures: Part 1-1: General Rules and Rules for Buildings,” NSAI (National Standards

Chapter 2. Background

Authority of Ireland), Dublin, Ireland, 2005.

- [44] L. Gardner and D. A. Nethercot, *Designers' Guide to Eurocode 3: Design of Steel Buildings*, 2nd Ed. London, UK: Thomas Telford (ICE), 2011.
- [45] BSI, "BS 5950-1: 2000: Structural use of steelwork in building-Code of Practice for Design: rolled and welded sections," British Standards Institution, London, UK, 2000.
- [46] NSAI, "IS EN 1991-1-6: Eurocode 1 - Actions on structures - Part 1 -6 : General actions - Actions during execution (Including National Annex)," NSAI (National Standards Authority of Ireland), Dublin, Ireland, 2005.
- [47] NSAI, "IS EN 1990. Eurocode - Basis of structural design," NSAI (National Standards Authority of Ireland), Dublin, Ireland, 2002.
- [48] Steel Construction Institute (SCI), "Advisory Desk (AD 346) Design actions during concreting for beams and decking in composite floors," *New Steel Construction*, no. June, pp. 32–33, Jun-2010.
- [49] I. Löfgren, "Lattice Girder Elements in Four Point Bending – Pilot Experiment (Report No. 01:7)," Chalmers University, Sweden, Göteborg, 2001.
- [50] I. Löfgren and K. Gylltoft, "In-situ Concrete Building-important aspects of industrialised construction," *Nord. Concr. Res.*, vol. 26, no. 1, pp. 61–81, 2001.
- [51] CEB-FIB, "Model Code 1990 (Bulletin No. 213/214)," Comité Euro-International du Béton (CEB) and the Fédération International de la Précontrainte (FIP), Lausanne, Switzerland, 1993.
- [52] I. Löfgren, "Lattice Girder Elements-Investigation of Structural Behaviour and Performance Enhancements," *Nord. Concr. Res.*, no. 29, pp. 85–104, 2003.
- [53] J. Harnisch, "Comparative Studies on Lattice Girder Elements: full-scale Tests and a Finite Element Simulation (Master's Thesis 01:13)," Chalmers

Chapter 2. Background

University, Goteborg, Sweden., 2001.

- [54] G. Verdugo, “Full-scale Tests and Analytical Model for Lattice Girder Elements (Master’s Thesis 01:11),” Chalmers University, Goteborg, Sweden., 2001.
- [55] Deutsches Institut für Bautechnik (DIBt), “German Institute for Construction Technology,” 2019. [Online]. Available: <https://www.dibt.de/en/>. [Accessed: 04-Jun-2019].
- [56] TU Munich, “Ermittlung der aufnehmbaren Momente und Querkräfte bei übergebenen Filigran-Elementplatten im Montagezustand. Report No. 3736 (unpublished),” Munich, Germany, 1980.
- [57] Prüfamts für Baustatik der LGA Bayern, “Gutachterliche Stellungnahme zur Vorlage beim Institut für Bautechnik. Report No. 767/81 (unpublished),” Nuremberg, Germany, 1981.
- [58] J. Hegger, R. Beutel, and F. Hausler, “Versuchsbericht über Tastversuche zum Montagezustand von Elementdecken mit Gitterträgern. Versuchsbericht 168/2006 (unpublished),” Aachen, Germany, 2006.
- [59] J. Hegger and G. Bertram, “Versuche zur Biege- und Querkrafttragfähigkeit von Elementdecken und Balken mit Gitterträgern im Montagezustand. Versuchsbericht 194/2007 (unpublished),” Aachen, Germany, 2007.
- [60] J. Hegger and G. Bertram, “Erweiterung der Zulassung für Filigran Gitterträger Typ E mit Obergurtdurchmessern 10 und 16 im Montagezustand (unpublished),” Aachen, Germany, 2008.
- [61] Deutsches Institut für Bautechnik (DIBt), “Filigran-E-Gitterträger für Fertigplatten mit statisch mitwirkender Ortbetonschicht, Zulassung Z-15.1-147,” Deutsches Institut für Bautechnik (DIBt), 2004.
- [62] J. FURCHE, “Erection state of lattice girder floor slabs: Results of current investigations,” *Betonwerk+ Fert.*, vol. 75, no. 2, pp. 106–108, 2009.
- [63] G. Bertram, J. Furche, J. Hegger, and U. Bauermeister, “Permissible Span of

Chapter 2. Background

Semi-precast Slabs in Case of Erection (Zulässige Montagestützweiten von Elementdecken mit verstärkten Gitterträgern),” *Beton- und Stahlbetonbau*, vol. 106, no. 8, pp. 540–550, 2011.

- [64] Deutsches Institut für Bautechnik (DIBt), “Filigran-E-Gittertrager und Filigran-Ev-Gittertrager für Fertigplatten mit statisch mitwirkender Ortbetonschicht Z-15.1-147,” Deutsches Institut für Bautechnik (DIBt), 2018.
- [65] A. Torre, J. A. M. Martínez, A. R. Saiz, and V. O. Lopez, “Span in Construction of Concrete Precast Products: Bearing Beams and Reinforced Slabs,” *Int. J. Hous. Sci. Its Appl.*, vol. 35, no. 2, pp. 91–102, 2011.
- [66] Ministerio de Fomento, “NBE EA-95 Estructuras de acero en edificación (Steel structures in construction) – Parte 3.2 Piezas de directriz recta sometidas a compresión.,” Ministerio de Fomento, Madrid, Spain, 1996.
- [67] Y. M. Cheng and Y. Fan, “Laboratory and numerical test on concrete plank composite with reinforcement truss,” *J. Struct. Eng.*, vol. 20, no. 4, pp. 207–216, 1994.
- [68] Y. M. Cheng, “Nonlinear optimal design model of a concrete reinforcement truss plank,” *Struct. Optim.*, vol. 9, pp. 250–253, 1995.
- [69] C.-L. Park and S. W. Yoon, “An Experimental Study on the Composite Precast Slab,” 1991.
- [70] K. Lundgren, “Analysis of a lap splice in a lattice girder system (Report 2003:3),” Chalmers University, Sweden, Goteborg, Sweden, 2003.
- [71] K. Lundgren, J. Helgesson, and R. Sylvén, “Joints in lattice girder structures (Report 2005:9),” Chalmers University, Sweden, Goteborg, Sweden, 2005.
- [72] K. Lundgren, “Lap splice over a grouted joint in a lattice girder system,” *Mag. Concr. Res.*, vol. 59, no. 10, pp. 713–727, 2007.
- [73] H. Guan, V. M. Karbhari, and C. S. Sikorsky, “Web-Based Structural Health Monitoring of an FRP Composite Bridge,” *Comput. Civ. Infrastruct. Eng.*,

Chapter 2. Background

vol. 21, no. 1, pp. 39–56, 2006.

- [74] ISIS Canada, “ISIS Canada Educational Module No. 5: An Introduction to Structural Health Monitoring,” ISIS Canada (Intelligent Sensing for Innovative Structures), Winnipeg, MB, Canada, 2005.
- [75] J. M. W. Brownjohn, “Structural health monitoring of civil infrastructure,” *Philos. Trans. R. Soc. a-Mathematical Phys. Eng. Sci.*, no. February, pp. 589–622, 2007.
- [76] P. C. Chang, A. Flatau, and S. C. Liu, “Review Paper: Health Monitoring of Civil Infrastructure,” *Struct. Heal. Monit.*, vol. 2, no. 3, pp. 257–267, 2003.
- [77] A. A. Mufti and ISIS Canada, “Guidelines for Structural Health Monitoring (ISIS Design Manual No. 2),” ISIS Canada (Intelligent Sensing for Innovative Structures), Winnipeg, MB, Canada, 2001.
- [78] J. P. Lynch and K. J. Loh, “A Summary Review of Wireless Sensors and Sensor Networks for Structural Health Monitoring,” *Shock Vib. Dig.*, vol. 38, no. 2, pp. 91–128, 2006.
- [79] S. W. Doebling, C. R. Farrar, M. B. Prime, and D. W. Shevitz, “Damage identification and health monitoring of structural and mechanical systems from changes in their vibration characteristics: A literature review (No. LA-13070-MS),” Los Alamos National Lab, New Mexico, US, 1996.
- [80] H. Sohn, C. R. Farrar, F. Hemez, and J. Czarnecki, “A Review of Structural Health Monitoring Literature 1996 – 2001 (LA-UR-02-2095),” Los Alamos National Laboratory, New Mexico, US, 2002.
- [81] A. A. Mufti, “Integration of sensing in civil structures: development of the new discipline of civionics,” in *In Proceedings of the 1st International Conference on Structural Health Monitoring and Intelligent Infrastructure (SHMII-1/03)*, 2003, pp. 119–129.
- [82] E. Rivera, A. A. Mufti, and D. J. Thomson, “Civionics for structural health monitoring,” *Can. J. Civ. Eng.*, vol. 34, no. 3, pp. 430–437, 2007.

Chapter 2. Background

- [83] A. Mufti, B. Bakht, G. Tadros, A. T. Horosko, and G. Sparks, “Civionics A New Paradigm in Design, Evaluation, and Risk Analysis of Civil Structures,” *J. Intell. Mater. Syst. Struct.*, vol. 18, no. 8, pp. 757–763, 2007.
- [84] J. Goggins, D. Byrne, and E. Cannon, “The creation of a living laboratory for structural engineering at the National University of Ireland, Galway,” *Struct. Eng.*, vol. 90, no. 4, pp. 12–19, 2012.
- [85] S. Newell and J. Goggins, “Embedded instrumentation as a teaching tool for construction students,” *Engineers Journal*. [Online]. Available: <http://www.engineersjournal.ie/2017/04/11/embedded-instrumentation-teaching-tool-construction-engineering/>. [Accessed: 02-Aug-2019].
- [86] Dept. of Transportation Minnesota, “Economic Impacts of the I-35W Bridge Collapse,” Dept. of Transportation, Minnesota, 2011.
- [87] D. Inaudi *et al.*, “Structural Health Monitoring System for the new I-35W St Anthony Falls Bridge,” in *4th International Conference on Structural Health Monitoring on Intelligent Infrastructure (SHMII-4, 22-24 July 2009)*, 2009.
- [88] D. M. Frangopol and M. Liu, “Maintenance and management of civil infrastructure based on condition, safety, optimization, and life-cycle cost*,” *Struct. Infrastruct. Eng.*, vol. 3, no. 1, pp. 29–41, 2007.
- [89] T. B. Messervey, “Integration of Structural Health Monitoring into the Design, Assessment, and Management of Civil Infrastructure (PhD Thesis),” Lehigh University, Bethlehem, 2007.
- [90] R. D. Davies and N. R. Buenfeld, “Automated monitoring of the deterioration of concrete structures,” Department of Trade and Industry, London, UK, 2007.
- [91] A. P. Jeary and B. R. Ellis, “Vibration test of structures at varied amplitudes,” in *Dynamic Response of Structures: Experimentation, Observation, Prediction and Control*, 1981, pp. 281–294.
- [92] D. E. Hudson, “Dynamic tests of full-scale structures,” *J. Eng. Mech. Div.*,

vol. 103, no. 6, pp. 1141–1157, 1977.

- [93] R. M. Moss and S. L. Matthews, “In-service structural monitoring a state-of-the-art review,” *Struct. Eng.*, vol. 73, no. 2, pp. 23–31, 1995.
- [94] B. Glišić, D. Inaudi, J. M. Lau, Y. C. Mok, and C. T. Ng, “Long-term monitoring of high-rise buildings using long-gage fiber optic sensors,” in *In Proceedings of 7th International Conference on Multi-Purpose High-Rise Towers and Tall Buildings, Dubai, UAE, 2005*, pp. 1–13.
- [95] B. Glisic, D. Inaudi, J. M. Lau, and C. C. Fong, “Ten-year monitoring of high-rise building columns using long-gauge fiber optic sensors,” *Smart Mater. Struct.*, vol. 22, no. 5, p. 055030, 2013.
- [96] A. E. K. Jones, “Development of an holistic approach to ensure the durability of new concrete construction,” British Cement Association, 1997.
- [97] S. A. Austin, P. J. Robins, and J. W. Bishop, “Instrumentation and early-age monitoring of concrete slabs,” *Proc. ICE - Struct. Build.*, vol. 159, no. 4, pp. 187–195, 2006.
- [98] H. R. Thomas Rees, S.W., “The thermal performance of ground floor slabs. A full scale in-situ experiment,” *Build. Environ.*, vol. 34, pp. 139–164, 1999.
- [99] W. Hansen and S. Surlaker, “Embedded Wireless Temperature Monitoring Systems For Concrete Quality Control (Whitepaper),” University of Michigan, Michigan, US, 2006.
- [100] B. Martín-Pérez, A. Deif, B. Cousin, C. Zhang, X. Bao, and W. Li, “Strain monitoring in a reinforced concrete slab sustaining service loads by distributed Brillouin fibre optic sensors,” *Can. J. Civ. Eng.*, vol. 37, no. 10, pp. 1341–1349, 2010.
- [101] ECBP, “The European concrete building project,” 2019. [Online]. Available: <http://projects.bre.co.uk/ecbp/index.html>. [Accessed: 24-Jul-2019].
- [102] P. Chana and P. Campbell, “The European Concrete Building Project,” *Struct. Eng.*, vol. 78, no. 2, pp. 12–13, 2000.

Chapter 2. Background

- [103] R. H. Scott, S. G. Gilbert, and R. M. Moss, “Load testing of floor slabs in a full-scale reinforced concrete building,” *Strain*, vol. 38, no. 2, pp. 47–54, 2002.
- [104] R. L. Vollum, R. M. Moss, and T. R. Hossain, “Slab deflections in the Cardington in-situ concrete frame building,” *Mag. Concr. Res.*, vol. 54, no. 1, pp. 23–34, 2002.
- [105] British Cement Association, “Early striking and improved backpropping for efficient flat slab construction,” British Cement Association (BCA), Berkshire, UK, 2001.
- [106] A. A. Mufti, B. Bakht, G. Tadros, A. T. Horosko, and G. Sparks, “Are Civil Structural Engineers ‘Risk Averse’? Can Civionics Help?,” in *Sensing issues in civil structural health monitoring*, F. Ansari, Ed. Dordrecht, Netherlands: Springer, 2005, pp. 3–12.
- [107] P. Cawley, “Structural health monitoring : Closing the gap between research and industrial deployment,” *Struct. Heal. Monit.*, vol. 17, no. 5, pp. 1225–1244, 2018.
- [108] Society of Automotive Engineers, “Guidelines for Implementation of Structural Health Monitoring on Fixed Wing Aircraft (ARP6461),” SAE International, 2013.
- [109] E. Kallinikidou, H.-B. Yun, S. F. Masri, J. P. Caffrey, and L.-H. Sheng, “Application of orthogonal decomposition approaches to long-term monitoring of infrastructure systems,” *J. Eng. Mech.*, vol. 139, no. 6, pp. 678–690, 2013.
- [110] K. Bowers *et al.*, “Smart Infrastructure Getting more from strategic assets,” CSIC (Centre for Smart Infrastructure and Construction), Cambridge, UK, 2017.
- [111] D. McFarlane, A. Parlikad, D. Pocock, S. Parsons, J. Schooling, and C. Jensen, “Intelligent Infrastructure for Tomorrow’s assets: Guiding Principles,” ICE, London, UK, 2017.

Chapter 2. Background

- [112] ISIS Canada, “Guidelines for Structural Health Monitoring (Manual No. 2),” ISIS Canada (Intelligent Sensing for Innovative Structures), 2001.
- [113] P. W. Rucker, D. F. Hille, and D. R. Rohrmann, “Guideline for Structural Health Monitoring (F08b),” SAMCO, Berlin, Germany, 2006.
- [114] A. V. Srinivasan and D. M. McFarland, *Smart Structures, Analysis and Design*. New York, US: Cambridge University Press, 2001.
- [115] A. Brintrup, D. McFarlane, D. Ranasinghe, T. S. López, and K. Owens, “Will intelligent assets take off? Toward self-serving aircraft,” *IEEE Intell. Syst.*, vol. 26, no. 3, pp. 66–75, 2011.
- [116] S. Sumitro and M. L. Wang, “Sustainable structural health monitoring system,” *Struct. Control Heal. Monit.*, vol. 12, no. 3–4, pp. 445–467, 2005.

3 Real-time Monitoring to Investigate Structural Performance of Hybrid Precast Concrete Educational Buildings

Article Overview

This paper describes the structural health monitoring (SHM) methodology which was implemented during the construction phase for three educational buildings built in NUI Galway. The three buildings were constructed in the last ten years (2011, 2014, 2016) and are constructed using predominantly precast concrete elements. In all three buildings, the majority of the floors employed hybrid concrete lattice girder flat slabs. David Byrne and Dr. Magda Hajdukiewicz were responsible for the implementation of the SHM system for the Engineering Building (EB) and the Institute for Lifecourse and Society (ILAS) building, respectively. The author was responsible for the design and implementation of the SHM system for the Human Biology Building (HBB) in 2015. As the first published work of this thesis, this paper introduces the concept of SHM and outlines the motivations and key components of an operational SHM system which can be adapted for any building. Although the data from the SHM system was acquired at regular intervals during the construction phase, the SHM system and technology described permits the data to be acquired in real-time.

For each of the buildings introduced in the paper, the utilisation of the SHM data is demonstrated for a variety of structural applications. The potential for using field data to evaluate the structural capacity of a concrete slab and application of the data to select the most economical design for a potential retrofit and strengthening of the slab is illustrated for one of the buildings (EB). Prediction of strains is extremely difficult in concrete elements. Comparison of the predicted strains using Eurocode 2 in a concrete slab and the measured strains using the embedded sensors from the SHM system is presented in the paper for the first two years after construction of the second building (ILAS). The various components of strain which are present in

Chapter 3. Real-time Monitoring to Investigate Structural Performance of Hybrid Precast Concrete Educational Buildings

the concrete slab are discussed and the significant parameters which can influence the magnitude of predicted strains are reviewed. The behaviour of the hybrid concrete lattice girder slab during construction is analysed for the third building (HBB). The induced strains on a slab due to the construction process whereby self-weight of floors are supported by the floors below is analysed. The SHM data suggests that the slab is uncracked during the construction phase.

This paper should be of interest to other researchers and construction professionals who are considering implementing a SHM strategy on a structure and exploring the possibility of developing ‘smart structures’ in the future in which the data from sensors can be used to add value to the structure. A comprehensive description of the design and installation phase of the SHM system implemented for the HBB is described in **Appendix F**.

This chapter was published in the *Journal of Structural Integrity and Maintenance* (2016).

Abstract

The motivation and implementation of a real-time structural health monitoring strategy to determine the structural performance of a number of educational buildings recently constructed in Ireland is discussed in this paper. In recent years, smart materials with embedded instrumentation has been installed in a number of buildings at the National University of Ireland Galway during the construction phase, which allows continuous monitoring of the behaviour of the structure.

Instrumentation installed on a number of projects, described in this paper, allow many important aspects of structures to be monitored during construction, as well as in the operational phase of the building such as temperature, concrete and reinforcement strain, deflection, and response to the environment.

3.1 Introduction

Structural Health Monitoring (SHM) can be defined as ‘the use of *insitu*, non-destructive sensing and analysis of structural characteristics, including the structural response, for purposes of estimating the severity of the damage and

Chapter 3. Real-time Monitoring to Investigate Structural Performance of Hybrid Precast Concrete Educational Buildings

evaluating the consequences of the damage on the structure in terms of response, capacity, and service-life [1]. SHM typically consists of continuous or periodic monitoring of a structure using sensors that are either embedded in it or attached to its exterior [2]. Historically, monitoring of buildings was motivated by the need to understand their performance in extreme events, such as earthquakes and storms. However, in recent decades, SHM has emerged as an increasingly important tool in Civil Engineering to understand how structures behave during construction and operation. Although SHM is not a new concept, it is only relatively recently that Civil Engineers have adopted SHM for the design, construction and management of buildings which are not likely to be subject to extreme events. The trend towards increased service life and durability of structures means that monitoring systems which permit the condition of the structure to be measured and which detect the possible onset of damage and/or deterioration of the structure will become increasingly important. A SHM system, if correctly designed and implemented, can be used for assessment of current condition of the structure, residual life prediction and detection of deterioration of a structural component [3].

3.2 SHM Strategy

One of the key benefits of SHM is the improved understanding of insitu structural behaviour. This paper presents the SHM strategy which has been developed in National University of Ireland Galway (NUI Galway) in order to monitor the structural and environmental performance of a number of buildings and outlines some of the results from the strategy. Sensors installed during the construction phase of a number of projects allow real-time monitoring of the structure during the construction and operational phase. This paper describes some applications of the data from the insitu instrumentation for a number of educational buildings constructed in recent years.

3.2.1 Methodology

The general SHM methodology (Figure 3-1) which was implemented for the three projects described in this paper is as follows:

- (1) Design and configuration of SHM system

Chapter 3. Real-time Monitoring to Investigate Structural Performance of Hybrid Precast Concrete Educational Buildings

The location, number and type of sensors which allow real-time monitoring of specific variables during the construction and operational phase of the buildings is the first step when implementing a SHM system. It is important for any SHM system that the sensors chosen are robust with respect to their environment to which they are exposed and the purpose and motivation for the SHM is clearly defined.

(2) Data communication

There were a variety of methods through which data can be managed after the sensors were installed. The frequency of measurement of data is determined by the variable being measured (temperature, strain etc.) and the intended use of the data. Typically, less frequent data acquisition can be specified after the construction phase is completed. A Campbell Scientific data acquisition system consisting of data loggers, multiplexers, Ethernet and Compact Flash Module that automatically collects data from the sensors was used in all projects. The datalogger can communicate over a local network or a dedicated internet connection via TCP/IP, transmitted wirelessly to the site office and/or data can also be downloaded manually to a laptop on site. After commissioning of the buildings, data is collected over a local network and saved to a dedicated server in NUI Galway. Wired sensors were predominantly used in these projects due to cost and time constraints. However, it is expected that wireless systems will replace wired monitoring systems in the future as the technology and robustness of wireless sensors improves.

(3) SHM maintenance

Regular maintenance of the SHM system is required to ensure that the data is recorded and reliable. All external sensors and wiring should be inspected periodically to check for damage or failure and replaced if necessary. Embedded sensors in general cannot be inspected and, thus, some redundancy is designed into the SHM system because of the relatively harsh environment when embedded in concrete and possible damage during the construction phase. A system is required to ensure that the data is reviewed regularly and any unexpected anomalies in the data are noted and investigated. Depending on the nature of the data and type of sensors, some processing of the raw data is required to filter the data to remove

Chapter 3. Real-time Monitoring to Investigate Structural Performance of Hybrid Precast Concrete Educational Buildings

unwanted effects ('noise') that is not required for the purposes of SHM. Filtering of raw data makes the post-processing and interpretation phase of the process easier and more efficient. Examples of filtering data include modifying data for thermal effects or removing data where sensors have recorded data outside their allowable range. In addition to maintenance of the SHM system, it is also important to note events (concrete pours, removal of props, application of finishes/cladding etc.) that occur during the construction phase so that they can be related to the raw data during the post-processing phase.

(4) Data management

Adequate memory must be provided for storage of both the raw data and processed data. The SHM strategy for these projects was to monitor the long-term performance of the buildings and, therefore, the raw data is stored on a dedicated server with protected access. The location, type and reference for all sensors must be documented clearly to allow for future interpretation of the data. It is envisaged that the data will be stored for many years and will be available for students and professionals for teaching and research applications. A MySQL database is used to store long term data from sensors and the database is accessible remotely via web using a PHP application, or using MySQL Workbench.

(5) Post-processing

Arguably, the most important component of a SHM strategy is the post-processing of the raw data recorded from the sensors. The purpose of the post-processing is to convert the raw data into useful information about the behaviour of the structure when subject to various external effects (structural, environmental, thermal) during construction and the operational phase of the building. The ultimate goal of SHM is to provide reliable information on the behaviour of the structure which can be calibrated against numerical models and compared with predicted behaviour in codes of practice (e.g. Eurocodes).

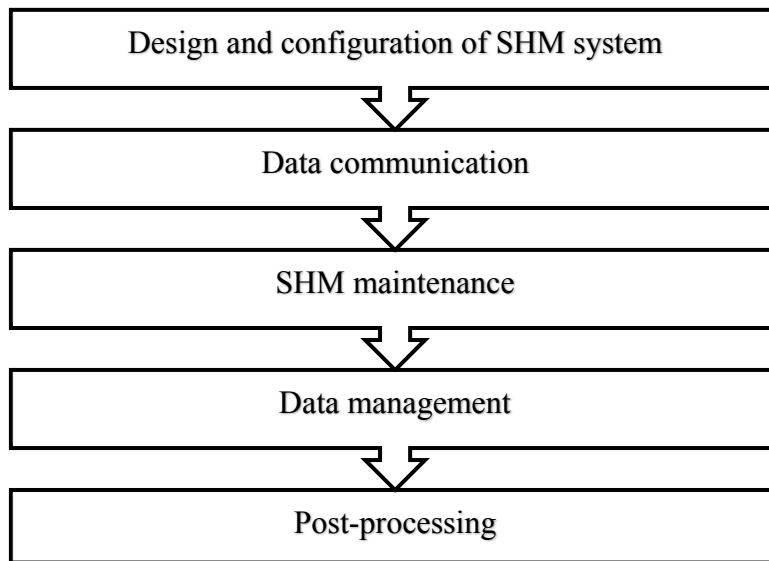


Figure 3-1 Visual schematic of the SHM methodology

3.2.2 Demonstrator buildings

Since 2010, sensors have been installed in three demonstrator buildings (i) the Engineering Building (EB), (ii) the Institute for Lifecourse and Society (ILAS) and (iii) the Human Biology Building (HBB) which are all located at the NUI Galway campus in Galway, Ireland. The three buildings are predominantly constructed using hybrid precast reinforced concrete components and insitu reinforced concrete.

In all buildings, sensors were installed in both precast concrete and insitu concrete elements which provide rich information about the actual building performance when subject to actual structural and environmental loads. Real-time monitoring offers potential benefits in relation to optimisation of structural components by understanding the actual behaviour of components in use and the possibility to develop and calibrate numerical models that predict structural performance. The information from the real-time monitoring also offers the opportunity to compare actual behaviour with predicted behaviour using structural codes, such as Eurocodes. The majority of the instrumentation is embedded within the structure so that long-term effects such as creep and shrinkage of concrete components can also be investigated.

Chapter 3. Real-time Monitoring to Investigate Structural Performance of Hybrid Precast Concrete Educational Buildings

3.2.3 Sensors

The SHM strategy implemented in NUI Galway used a number of sensors embedded in the structural components of the building to monitor and record the various parameters with respect to the structural and environmental performance. These sensors include (Figure 3-2):

- Vibrating Wire (VW) gauges (Gage Technique model TES/5.5/T) which are embedded in concrete and measure strain and temperature.
- Electrical resistance (ER) strain gauges (Tokyo Sokki Kenkyujo model FLA-6-11) bonded to steel reinforcement in concrete, which measure uniaxial strain.
- IP98 rated thermistor sensors (ATC Semitec model IP 68) which are capable of measuring concrete temperature.

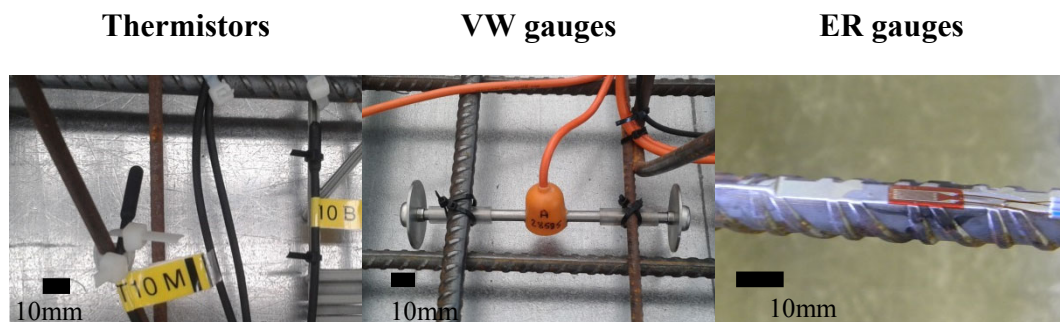


Figure 3-2 Sensors embedded in the buildings' structure

Weather data from the NUI Galway weather station [4] located on the main campus was recorded to provide accurate environmental data (air temperature, relative humidity, wind speed, solar radiation, etc.) for the concrete elements which are monitored using embedded sensors. This data is used to develop and calibrate numerical models predicting the behaviour of the concrete elements. The deformation of some concrete elements was recorded during the construction phase using digital surveying and digital image correlation. In addition, the embedded sensors are also used to investigate the environmental and energy performance of the buildings [5].

3.2.4 Material Testing

To complement the data from the embedded sensors in the concrete, a comprehensive material testing programme was undertaken to measure the properties of the concrete (compressive strength, tensile strength, modulus of elasticity, etc.) in which the sensors are embedded. When predicting the behaviour of concrete elements, it is critical that the properties of the concrete are determined as its properties will change over time depending on loading and environment [6].

3.3 Engineering building

The Engineering Building at NUI Galway integrates all engineering activities on campus and was open to the public in July 2011. It was the first building in which real-time monitoring using embedded sensors was utilised to investigate the performance of buildings at the NUI Galway campus. The 14,250m² building is the largest engineering school in Ireland and accommodates approximately 1100 students and 110 staff. In addition to its teaching and research functions, the building was designed such that it acts as a learning/teaching tool for undergraduate students through the use of the real-time data from the sensors installed throughout the building ('living laboratory') [7]. In the Engineering Building, three key concrete elements were instrumented during construction; a prestressed double tee beam, a prestressed transfer beam and a void form flat slab (VFFS). Further details of these elements and the SHM systems employed may be found in Goggins *et al.* [7]. However, the next section contains some details of the novel void-form flat slab (VFFS) system as an example of how the SHM system has been used within the engineering building.

3.3.1 Void form flat slab (VFFS)

This project utilised a void-form flat slab (VFFS) system for the majority of flooring in this building. This innovative form of flat slab system was implemented for the first time on a large scale project in Ireland in this building. The reinforced concrete slabs contain high-density polyethylene hollow void formers to replace concrete over the middle height of the slab, where the slab primarily experiences bending stresses with relatively low shear stresses (Figure 3-3). Those hollow void formers

Chapter 3. Real-time Monitoring to Investigate Structural Performance of Hybrid Precast Concrete Educational Buildings

not only reduce the structural dead load of the slab (resulting in saving on the material cost and allowing larger slab spans), but also increase the thermal resistance of the slab.

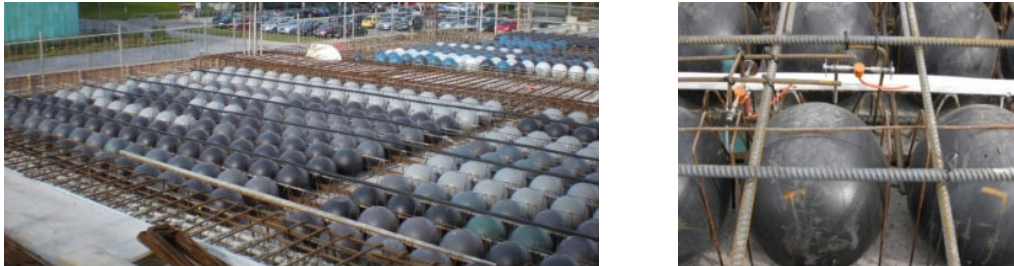


Figure 3-3 Cobiax VFFS system being installed in the EB (left) and with gauges installed (right)

One of the areas of investigation for the VFFS was the measured strain profile through the section of the concrete slab and comparison with the theoretical tensile strain capacities derived using codes of practice such as Eurocode 2 [8] and American Concrete Institute [9]. During the early phases of construction, there is potential for cracking to occur if the tensile strain capacity of the concrete is exceeded. Early-age cracking can lead to problems with respect to durability and loss of serviceability of the floor structure. Strain profiles in the floor structure were calculated and compared with the tensile strain capacities determined using European and American standards. It was found that the measured tensile strain exceeded the theoretical strain capacity at only one instrumented section and this occurred at a mid-span section. The strain profiles at this location for the top, middle and bottom of the slab are shown in Figure 3-4 and compared with the relative tensile strain capacities outlined by the respective standards. Some discussions of the behaviour of the void form flat slab (VFFS) system with respect to strains and potential cracking is available in Hajdukiewicz *et al.* [5].

Chapter 3. Real-time Monitoring to Investigate Structural Performance of Hybrid Precast Concrete Educational Buildings

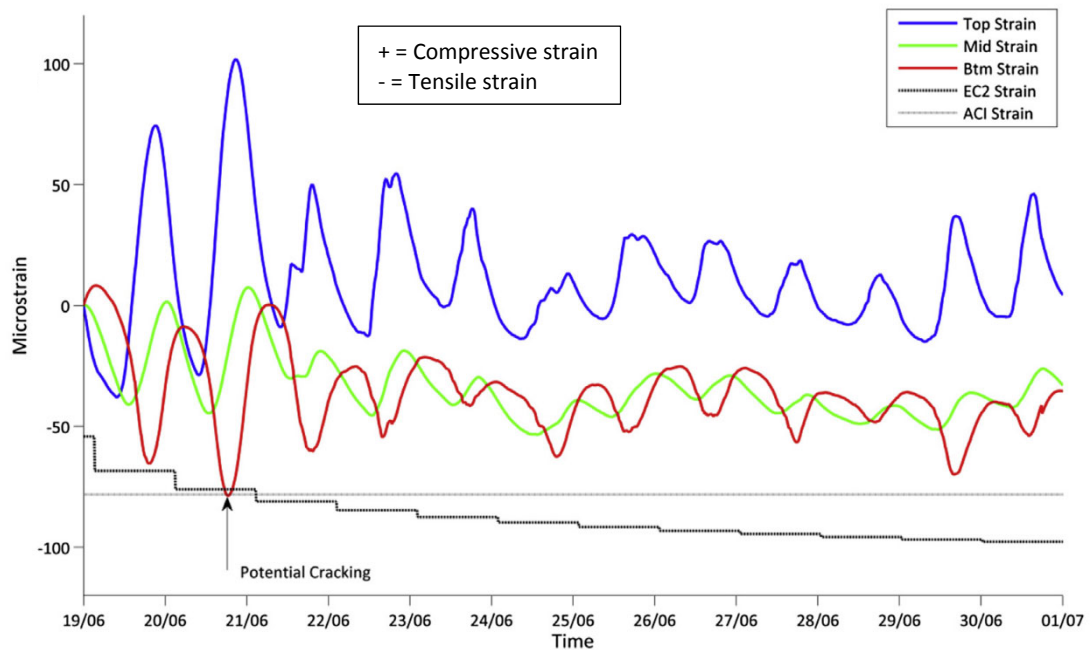


Figure 3-4 Strain profile at one of the instrumented sections in the Engineering Building [5]

3.3.2 Evaluating structural capacity

The application of insitu instrumentation and utilisation of the data was previously demonstrated for the EB in relation to assessing the structural capacity of the floor so that more efficient and economical design can be formulated, particularly for retrofitting and strengthening structures [10]. The insitu data from the VFFS floor structure in the EB building was used to assess the load capacity of the floor for the purpose of assessing the possible increase of the flexural capacity of the floor using fibre reinforced polymers (FRP's) because of a change of use of the floor structure (increase in imposed load). One of the most critical parameters when calculating externally bonded FRP reinforcement for concrete structures is the existing strains on the soffit of the slab. Using the data from the embedded instrumentation, it was possible accurately determine the strains on the slab soffit.

The structural capacity of the slab was calculated using American Concrete Institute [11] and FIB design guidelines [12] and also by substituting the calculated insitu soffit strains from the instrumented slab for their corresponding values in the aforementioned design guides. Design solutions were determined for the three most

Chapter 3. Real-time Monitoring to Investigate Structural Performance of Hybrid Precast Concrete Educational Buildings

common types of externally bonded FRP materials (carbon, glass and aramid). It was found that the layout and shape of the external FRP reinforcement was quite similar for all design solutions, but that there was a significant reduction in the amount of FRP (i.e. number of layers etc.) when utilising the data from the insitu instrumentation. Insitu strains were almost 20% less than those calculated using the design guidelines. Overall, the ACI design procedure required the most externally bonded FRP reinforcement, followed by the FIB design procedure and the least amount of reinforcement was determined using the insitu data. Depending on the FRP material used and the design guideline, the comparative cost saving when using the instrumented data varied between 4% and 25%. Figure 3-5 illustrates the comparative unit cost for the three types of FRP when utilising the design guidelines and the insitu data.

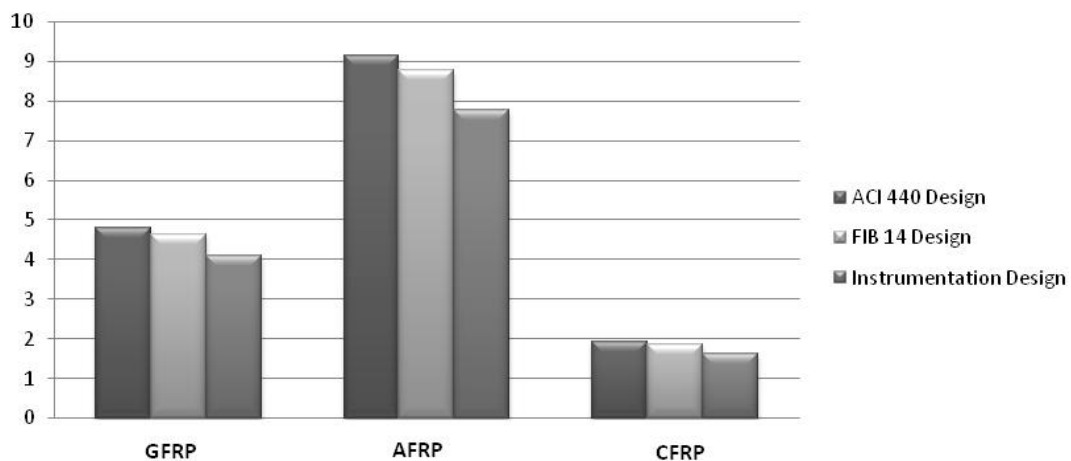


Figure 3-5 Graph showing comparative unit cost of materials for retrofitting of void form flat slab [10]

3.4 Institute for lifecourse and society building

The Institute for Lifecourse and Society (ILAS) building in NUI Galway commenced construction in July 2013 and was completed by September 2014. The building occupies a gross floor area of approximately 3600 m² and has been built with two separate wings (two storeys high East wing and three storeys high West wing) designed around a large central atrium. The building accommodates mainly office spaces, seminar rooms and lecture theatres. The ILAS building is mainly built using precast concrete technology, including the building frame, lattice girder

Chapter 3. Real-time Monitoring to Investigate Structural Performance of Hybrid Precast Concrete Educational Buildings

flooring, twinwall components and hollowcore slabs. In the ILAS building, sensors were installed in the hollowcore ground floor, hybrid concrete lattice girder floor (1st floor and roof) and the structural walls (internal and external). The primary focus of this research project was the heat transfer and storage characteristics of the precast building components [13], although some vibrating-wire gauges were also embedded in the floor structure to monitor strains.

3.4.1 Hybrid concrete lattice girder floor

The 300 mm deep flat slab forming the first floor of the East wing of the ILAS building contains 59 VW gauges installed over 29 designated sections. The instrumented slab was an interior, two way spanning slab (of multiple spans) spanning 8.14 m in one direction and has two spans of 5.81 m and 4.21 m in the orthogonal direction [14]. The floor plate used for the superstructure of the building is a hybrid precast and in-situ concrete flat slab system similar to that used on the EB, but without the hollow void formers.

The prediction of strains for concrete elements systems is extremely difficult to estimate accurately [15]. The behaviour of a slab at service loads varies with time and depends on the extent of cracking, stiffness of the slab, creep, shrinkage and degree of restraint. The slab in the ILAS building is subject to strains from thermal, shrinkage, creep and flexural components. Because the data is recorded from the sensors after the building is operational, the long-term behaviour of the concrete elements can be analysed and compared with design guidelines. One of the difficulties of predicting long-term behaviour of concrete elements is that the properties of concrete change and evolve over time in response to environment and loading conditions.

The predicted strains in the first floor slab due to the various components determined using Eurocode 2 [8] are compared with the measured strains from the embedded VW gauges in Figure 3-6 for the twenty-six months (Oct 2013-Dec 2015 inclusive) after the floor was poured. The measured strains from the VW strain gauges are corrected for thermal effects so that only strain due to shrinkage, flexure and creep is determined from the gauge reading:

Chapter 3. Real-time Monitoring to Investigate Structural Performance of Hybrid Precast Concrete Educational Buildings

$$\mu\epsilon_{\text{load}} = \mu\epsilon_{\text{actual}} - \mu\epsilon_{\text{thermal}} = \Delta\epsilon + \Delta T \cdot \alpha_{\text{vw}} - \Delta T \cdot \alpha_c \quad (\text{Eqn. 3-1})$$

where $\Delta\epsilon$ is the change in measured strain; ΔT is the change in temperature; α_{vw} is the coefficient of thermal expansion of the VW gauge and α_c is the coefficient of thermal expansion of the concrete.

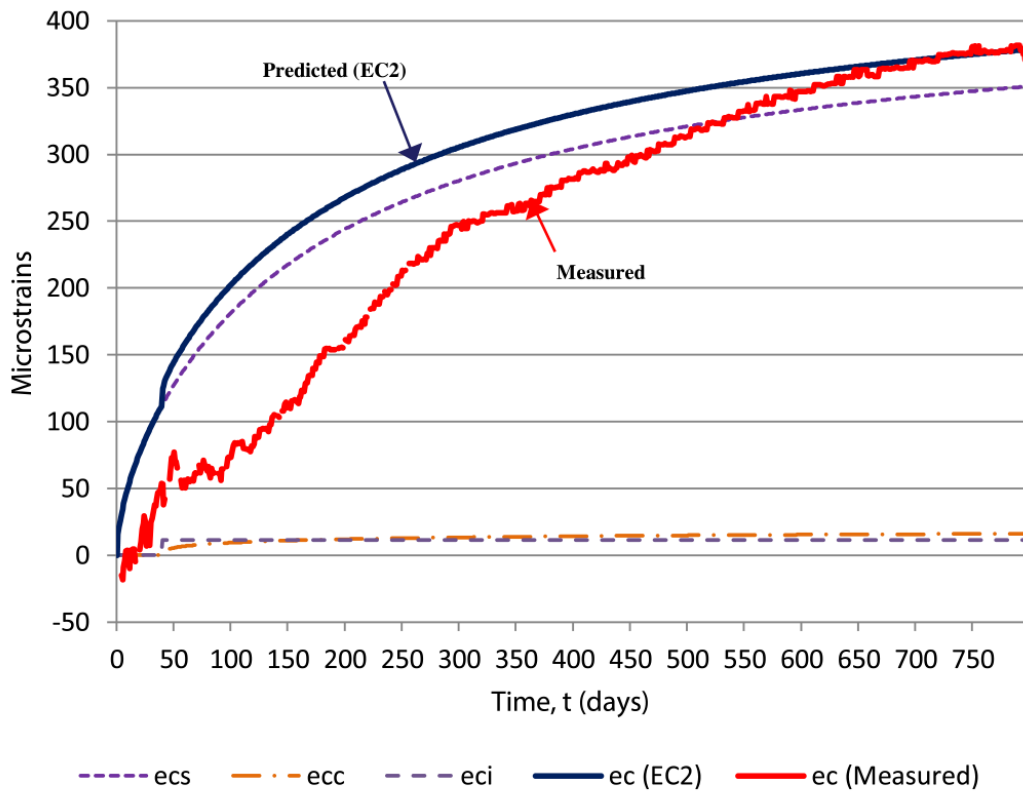


Figure 3-6 Comparison of predicted strain (EC2) and measured strain in ILAS building (*ecs* = shrinkage strain, *ecc* = creep strain, *eci* = flexural strain)

The dominant predicted strain component is shrinkage and this accounts for over 80% of the strain induced on the first floor slab. However, the predicted strain due to flexure and creep is likely to be underestimated as it is very difficult to determine the contribution due to imposed loading acting on the floor after the building is operational. When the ILAS building was completed, approximately 10 months after the first floor slab was poured, the predicted strain (in accordance with Eurocode 2) was 317 microstrains and the measured strain was 262 microstrains. The predicted strains are based on assumed relative humidity of the ambient environment and design values for the concrete properties.

Chapter 3. Real-time Monitoring to Investigate Structural Performance of Hybrid Precast Concrete Educational Buildings

The measured and predicted strain values compare reasonably well considering the relatively large coefficient of variation for both creep (20%) and drying shrinkage (30%) when using the approach of Eurocode 2 [8] for determining strains. The accuracy of predicted strains using Eurocode 2 with the measured strains in the concrete slab appears to improve over time and are less accurate at predicting the early-age strains in the slab during the construction phase. This may suggest the difficulty in modelling the actual slab conditions during construction in which the environment can change relatively quickly. One of the areas of investigation will be to review predictive models for long-term behaviour and their sensitivity to input parameters such as compressive strength, relative humidity and air temperature.

Of the three demonstrator buildings presented in this paper, the ILAS project was the least successful in relation to data acquisition from the embedded sensors. Due to time constraints during the construction phase of this project, there was limited time for installation of embedded sensors and a number of the sensors were damaged during the construction process. Lessons learnt from this project were taken forward to the next project in relation to protection of wiring and sensors during construction, particularly when insitu concrete is poured on site.

3.5 Human biology building

The Human Biology building (HBB) is a four storey building over basement and roof level plant enclosure with a gross floor area of 8200m². This facility will encompass three schools; Anatomy, Physiology & Pharmacology and Therapeutics. The building will be a teaching and research facility with lecture theatres, laboratories, offices and meeting rooms. Construction commenced in January 2015 and the expected construction period is 19 months (July 2016). It is anticipated that the building will achieve an A rating under the Commercial Energy Rating marking scheme and a BREEAM Excellent rating.

The Human Biology building is primarily constructed using precast concrete elements, including the building frame, twinwall system, hybrid concrete lattice girder slabs and hollowcore slabs which were designed, manufactured and installed by Oran Pre-Cast Ltd. Embedded sensors were positioned in the two-way spanning

Chapter 3. Real-time Monitoring to Investigate Structural Performance of Hybrid Precast Concrete Educational Buildings

second floor of the Human Biology building in two zones to monitor the strain and temperature in the concrete floor structure (hybrid concrete lattice girder flat slab) during the construction and operational phase of the building. The overall slab thickness in the second floor is 400mm and this consists of a 65mm thick precast lattice girder plank (Figure 3-7) and 335mm insitu concrete topping. The lattice girder truss that protrudes from the plank provides stiffness in the temporary state and increases composite action with the insitu structural concrete topping. The precast planks are temporarily propped until the structural concrete topping has reached the required compressive strength.



Figure 3-7 Precast Concrete Lattice Girder Plank (with embedded sensors)

The VW gauges were positioned along a number of orthogonal grids in the floor structure at over 30 designated locations so that two-way spanning behaviour of the floor structure could be monitored. At most locations, four VW gauges were positioned through the depth of the slab (1 in the precast plank and 3 in the insitu topping) so that the strain and temperature profile through the slab could be measured (Figure 3-8).

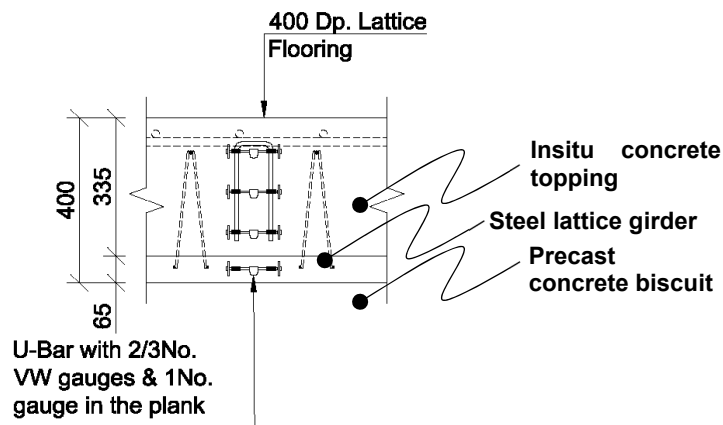


Figure 3-8 Typical section showing locations of vibrating wire gauge installed in the flat slab system.

The embedded sensors in the floor structure allows the actual strains in the slab to be measured during the construction phase, so that the impact of the temporary propping for supporting subsequent pours and their removal can be monitored and assessed. Deflections of the slab is also being monitored using a precise level and digital image correlation system, which will be compared to estimates from the strain measurements. Furthermore, the configuration of embedded sensors in the slab permits the behaviour of the slab to be analysed along a number of gridlines and compared with theoretical behaviour based on codes of practice such as Eurocode 2 [8]. It is envisaged that this research project, in conjunction with laboratory testing of lattice girder precast planks, will be used to optimise this floor system with respect to design and construction. Some preliminary results from this project are discussed in following sections.

3.5.1 Early-age thermal effects

Nine VW gauges, which record strain and temperature, were embedded in one of the 65mm thick precast lattice girder planks prior to manufacture and data was recorded immediately after the plank was cast. Data was continuously recorded for this plank during curing, delivery and erection on site so that strain and temperature history of the precast plank could be analysed throughout the life cycle of the product from cradle to end of life. Figure 3-9 shows the temporal temperature in the precast concrete plank and ambient air temperature (dashed line) for the first week

Chapter 3. Real-time Monitoring to Investigate Structural Performance of Hybrid Precast Concrete Educational Buildings

after its manufacture. Because the planks were cast during the summer, temperature curing was not used by the precast manufacturer in this case. In the first 24 hours after casting (25th June 2015), the peak in the concrete temperature due to the heat of hydration is noted and contrasts with the falling ambient air temperature during the night. The peak in the concrete temperature occurs 10 hours after casting and the maximum difference between the air temperature and the concrete temperature is approximately 5.5°C. It is noted that the peak temperature is slightly less for the three gauges located close to the perimeter of the plank (less than 300mm from plank perimeter) as the plank cools more quickly along its external surfaces. However, because the concrete plank is relatively thin (65mm), after the first 24 hours the concrete temperature in the plank is relatively uniform for all nine VW gauges and correlates with the ambient air temperature.

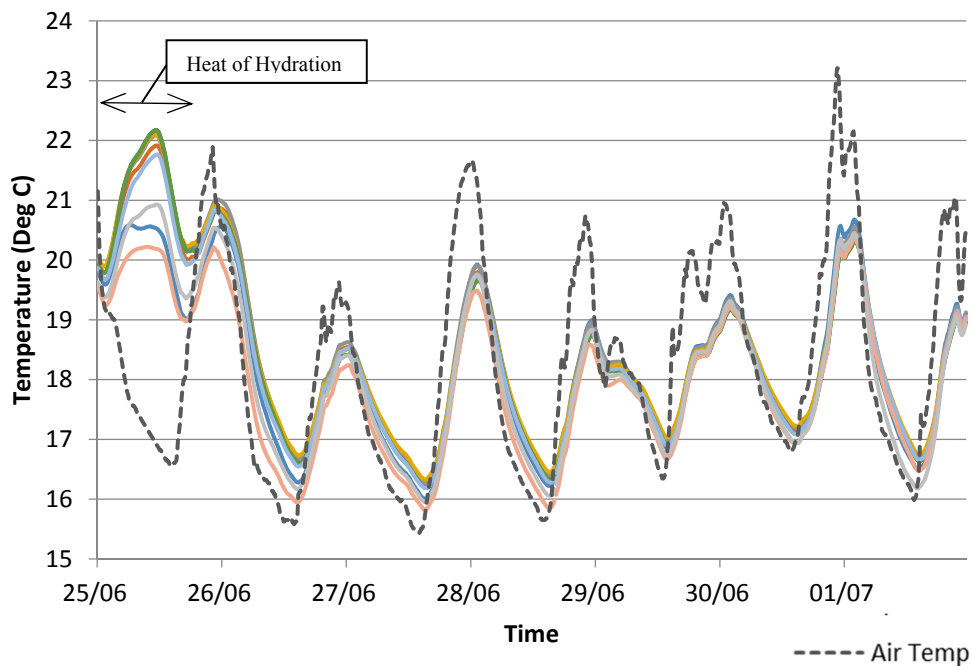


Figure 3-9 Concrete temperatures in the 65mm thick precast plank (7 days after manufacture)

This contrasts markedly with the concrete temperature in the insitu structural topping in which the heat of hydration is more significant because of the thickness of the concrete (335mm thick), as well as the insulating properties of the precast plank resulting in only one surface of the insitu concrete being exposed. The

Chapter 3. Real-time Monitoring to Investigate Structural Performance of Hybrid Precast Concrete Educational Buildings

concrete temperature in the insitu topping at one location in which three VW gauges are embedded to measure strain and temperature through the concrete (top, middle and bottom) are shown in Figure 3-10. The temperature for the VW gauge in the precast plank at this location is also shown. For the first 7 days after pouring, the temperature in the concrete exceeds the ambient air temperature and it is only after 7 days that the heat generated from the hydration process has fully dissipated. The effect of the diurnal temperature changes are clearly visible in the measured temperature in the concrete floor. Similar to the precast plank, the peak in concrete temperature occurs 10 hours after casting and at this point, the maximum temperature differential between the air and concrete temperature is approximately 13°C. As expected, the peak temperature is recorded for the VW gauge in the middle of the insitu topping as the internal section of the slab will be slowest to cool down. The effect of the heat of hydration from the insitu topping on the concrete in the precast plank can be noted almost immediately after pouring and results in a peak increase in temperature of 9°C.

For ‘thick’ concrete sections (typically greater than 500mm), the temperature rise due to the heat of hydration can result in excessive thermal stresses and cracking generated by restraint to thermal movement. For the 335mm thick insitu topping in this project, the temperature differential through the slab is small (Figure 3-10) because of the relatively thin section which allows the concrete to cool comparatively uniformly as the heat is readily lost to the environment. The temperature differential recorded between the VW gauges in top, middle and bottom of the insitu topping did not exceed 3°C and the maximum differential occurred during the cooling phase.

Chapter 3. Real-time Monitoring to Investigate Structural Performance of Hybrid Precast Concrete Educational Buildings

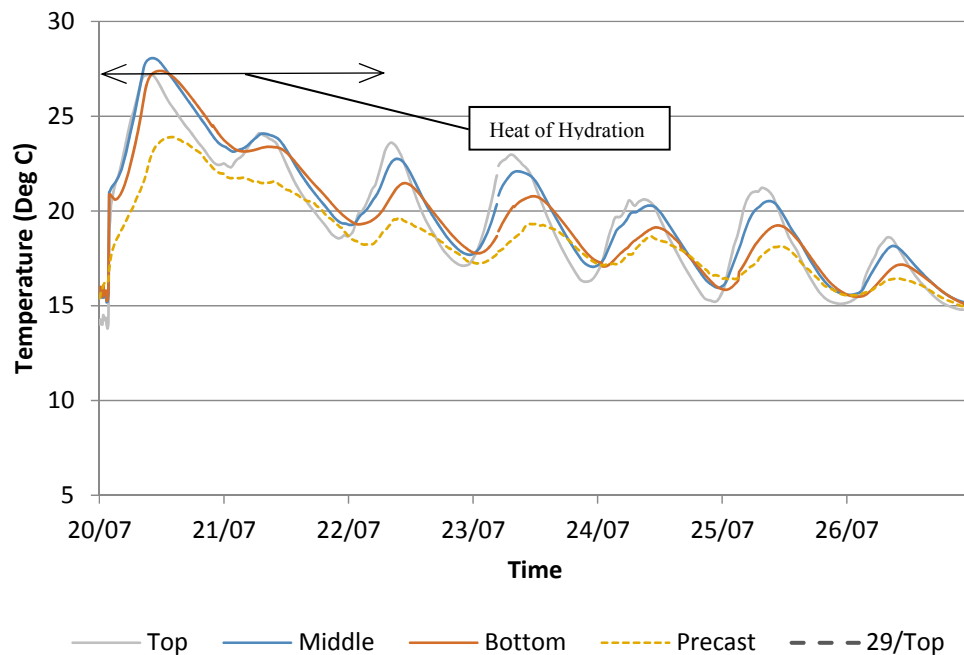


Figure 3-10 Concrete temperature in 335mm insitu structural topping (7 days after pour)

The increasing use of high-performance concrete with higher compressive strengths and lower permeability has seen an increased concern in relation to early age cracking which can affect durability and service life of concrete structures. In addition, discrepancies between performance of construction materials in the laboratory and their observed performance in the field has been reported [16]. Because of this uncertainty, the design of concrete structures to ensure long-term in-service performance can be problematic. Therefore, the use of insitu instrumentation can be used to appraise material properties, construction procedures and design methods with respect to the actual behaviour of concrete structures.

Predicting the potential for early-age thermal cracking is very difficult at the design stage because of numerous factors which affect the behaviour of the concrete and the limited information on the concrete known at design stage. CIRIA Report C660 by Bamforth [17] gives guidance on predicting the early-age thermal behaviour of concrete sections based on a comprehensive testing programme undertaken at University Dundee [18]. However, the report recommends thermal modelling for

Chapter 3. Real-time Monitoring to Investigate Structural Performance of Hybrid Precast Concrete Educational Buildings

reliable predictions which takes account of the formwork and exposure conditions. Based on thermal modelling, it predicts that the maximum temperature differential in the insitu topping would be 13°C, but this figure is highly dependent on the thermal diffusivity of concrete, surface conditions and the environmental conditions (wind and solar gain).

As an upper bound, Fitzgibbon [19] estimated that the peak temperature rise under adiabatic conditions is 12°C/100kg per cubic metre of concrete, regardless of the type of cement used. Therefore, assuming a 100% CEM I cement for the insitu topping, it could be expected that the peak temperature could be as much 40°C (total cement content of insitu topping was 330kg/m³). However, in this project 30% GGBS was used as a cement replacement in the concrete mix and this would help to reduce the heat of hydration generated during curing. The predicted peak temperature differential for the insitu topping using CIRIA Report C660 is approximately 19°C, but other factors which can affect the peak temperature are the variation between cements, placing temperature and actual thermal conductivity of the precast plank. The measured peak temperature of 13°C equates to a temperature rise of 4°C/100kg per cubic metre of concrete. In terms of minimising cracks, the general rule of thumb used by designers is to limit temperature differentials to 20°C, although this figure is dependent on the type of aggregate used in the concrete mix. It can be seen from the above figures that the CIRIA Report C660 provides upper bounds for the peak temperature and temperature differentials for a specific concrete pour.

The strain and temperature profile for three VW gauges through the depth of the insitu topping at one location is shown in Figure 3-11 for the first 7 days after pouring. After the dormant period of the hydration process, which lasted approximately 2 hours, there is a significant step change in tensile strain varying from 20µε near the bottom of the insitu topping to 40 µε at the top of the insitu topping due to the heating phase and the resulting expansive strains. Typically, the measured strains are greater for the gauges near the top of the insitu topping in comparison with the gauges near the bottom of the insitu topping which may be partially explained by the restraining effect of the precast plank. After the cooling

Chapter 3. Real-time Monitoring to Investigate Structural Performance of Hybrid Precast Concrete Educational Buildings

phase of the heat of hydration is finished (approximately 2-3 days), thermal strains are significant and the concrete is subject to daily fluctuations in strains in response to the diurnal ambient air temperature. There are varying recommendations for the coefficient of thermal expansion of concrete (α_c) in the literature. Eurocode 2 [8] recommends a value of $10\mu\epsilon/^\circ\text{C}$ for normal weight concretes although values can typically vary from $8\text{-}13\mu\epsilon/^\circ\text{C}$ depending primarily on the type of aggregate used [20]. The daily changes in strain due to thermal effects can be estimated by multiplying the coefficient of thermal expansion of concrete (α_c) and the measured temperature change in the concrete. It should be noted that whilst the floor structure is propped, the measured strain is a combination of thermal, shrinkage (autogenous and drying) and creep. The thermal strain component is the dominant strain and accounts for the majority of the measured strain in the early-age stages of the concrete floor. For this analysis, the coefficient of thermal expansion of concrete is taken as $10\mu\epsilon/^\circ\text{C}$ in accordance with Eurocode 2 and it is estimated that the magnitude of thermal strain exceeds the magnitude of total strain due other strain components (shrinkage and creep) for the first 7 days after the pour of the insitu topping.

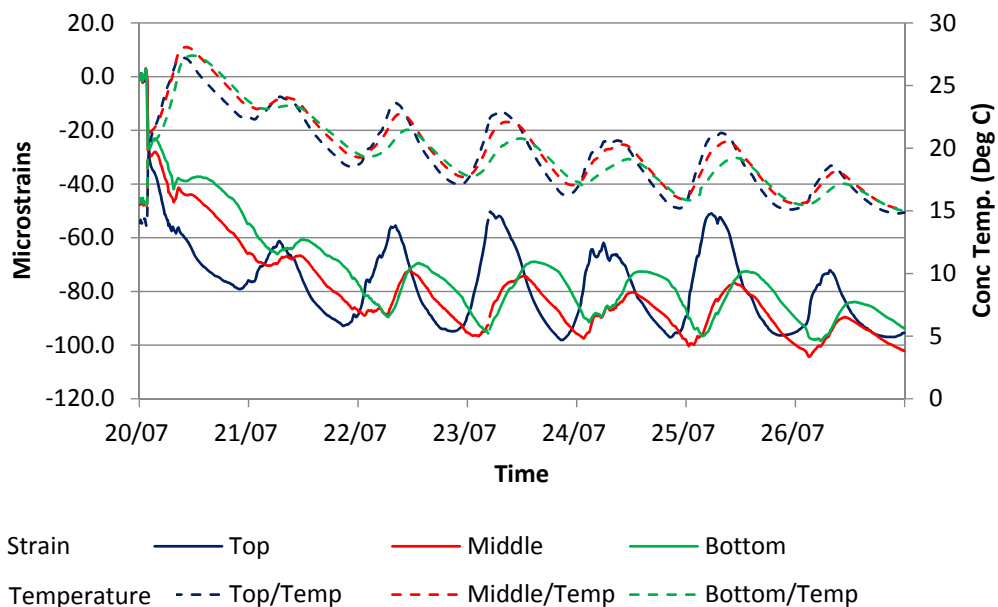


Figure 3-11 Strain and temperature profile in insitu topping (7 days)

Chapter 3. Real-time Monitoring to Investigate Structural Performance of Hybrid Precast Concrete Educational Buildings

The strain which occurs in structures during the early-age thermal effects are rarely measured but actual strain data is of great importance when trying to understand the early-age behaviour of concrete elements and the potential to optimise future design and construction procedures [17].

3.5.2 Construction stage behaviour

During the construction phase, the precast planks are temporarily supported by props which are erected prior to installation of the planks. The precast planks acts as permanent formwork and contain the bottom reinforcement. As the concrete frame is constructed upwards, the floors constructed below the floor under construction must support the self-weight of the next floor. When the compressive strength of the insitu concrete had reached a specified strength, the supporting props were dropped and re-applied so that each floor was supporting its own self-weight. The embedded sensors in the slab at second floor allow the behaviour of the slab during the construction phase to be monitored and compared with analysis undertaken by the designers.

A linear elastic model finite element (FE) model was developed by the designers which models the precast floor as a 400mm thick slab with 65mm high and 130mm wide recess along all joints between precast planks. The material properties for the slab are assumed to be uniform and the same as the insitu section of the slab. During the construction stage, the measured changes in strain through the 400mm thick section can be analysed. The strain profile in the middle of the second floor slab when the third floor is poured (13th August 2015) and when the props (supporting the third floor) are dropped (28th August) is shown in Figure 3-12. At this location, there are three VW gauges located in the insitu topping and one VW gauge in the precast plank. The measured strain profile suggests that the slab is still linear elastic and therefore can be considered ‘uncracked’. As expected, the change in strain on the 28th August is a reversal of the change in strain on the 13th August as the second floor partially supports the self-weight of the third floor above and then the load is removed as the props are dropped to the third floor.

Chapter 3. Real-time Monitoring to Investigate Structural Performance of Hybrid Precast Concrete Educational Buildings

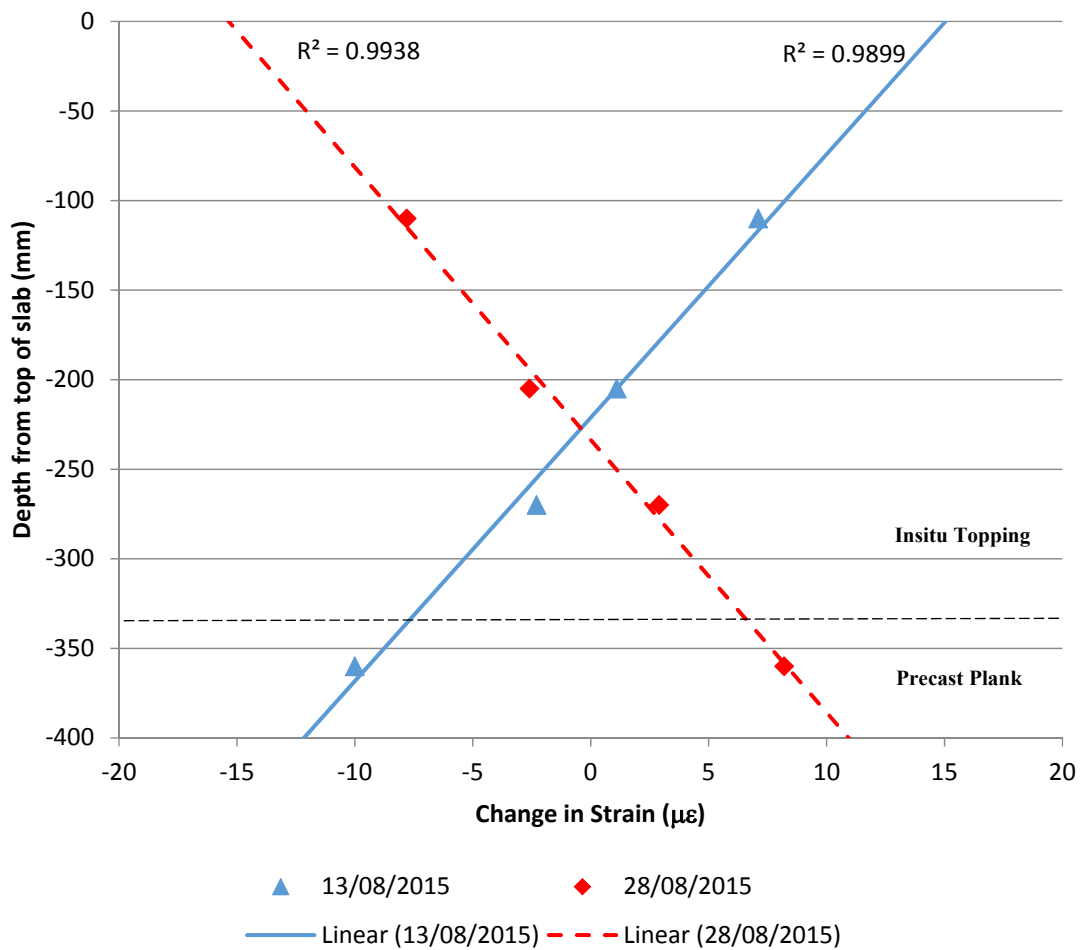


Figure 3-12 Strain profile through second floor

The measured changes in strain when the props to the second floor were dropped and when the props were removed can be summated and compared with the predicted behaviour when the slab supports its own self weight. The measured changes in strain along sections of the slab were converted to bending moments assuming the slab is uncracked and using the concrete properties derived from material testing conducted on the concrete used on site for the second floor. The predicted bending moment using the finite element model and the bending moment derived using the measured strain is shown in Figure 3-13 along a gridline (GL H) in second floor. The measured strains were converted to bending moment for the case of no creep and creep (creep coefficient determined in accordance with Eurocode 2). In both cases, it is observed that the embedded sensors measured restraint at the edge of the slab (GL 27) where a simple support was assumed in

Chapter 3. Real-time Monitoring to Investigate Structural Performance of Hybrid Precast Concrete Educational Buildings

design. Because of the hogging moment at the edge of the slab, the measured sagging moment at midspan is less than the design moment from the FE analysis. This illustrates why many design codes require additional torsional reinforcement at the edge of slabs to resist bending which may occur in real structures but is not determined during analysis.

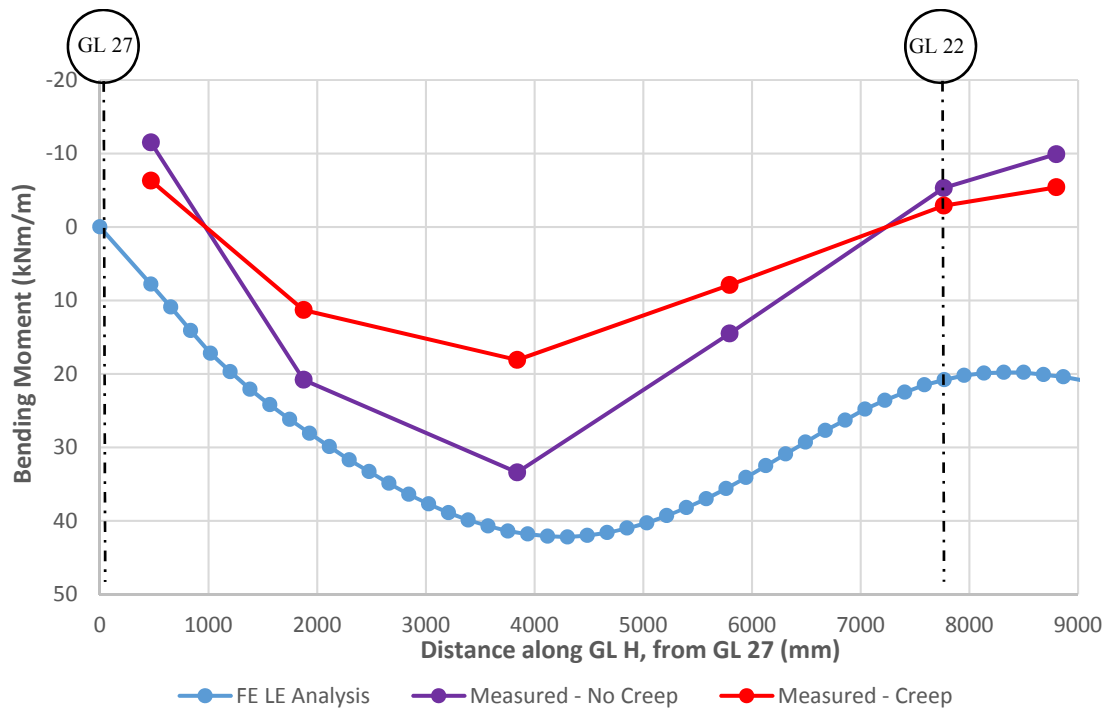


Figure 3-13 Bending moment in second floor along GL H

3.6 Conclusions

This paper presents the methodology and implementation of a real-time structural health monitoring strategy for a number of educational buildings at National University of Ireland Galway (NUI Galway). The sensors installed allow many important aspects of the performance of the buildings (structural, environmental and energy) to be monitored during the construction and operational phase of the building. In combination with the material testing, weather monitoring station and laboratory testing, this SHM strategy provides rich information about the buildings' performance. This real-time information is also available to students and researchers in NUI Galway to study and investigate environmental, energy and structural performance of the buildings.

Chapter 3. Real-time Monitoring to Investigate Structural Performance of Hybrid Precast Concrete Educational Buildings

Real-time monitoring offers potential benefits in relation to optimisation of structural components by understanding the actual behaviour of components in use and the possibility to develop and calibrate numerical models that predict structural performance. The information from the real-time monitoring also offers the opportunity to compare actual behaviour with predicted behaviour using codes of practice. The majority of the instrumentation is embedded within the structure so that long-term effects such as creep and shrinkage of concrete components can also be investigated.

With the rapid development in wireless and sensor technologies, the use of such technology to monitor the performance of structural elements will be an increasingly important tool for the design, construction and management of buildings in the future.

Acknowledgements

The authors would also like to thank the National University of Ireland Galway and particularly the Department of Civil Engineering in the College of Engineering and Informatics for the help with the instrumentation in the demonstration buildings. They also wish to thank all the construction personnel and building professionals involved in the demonstrator buildings who facilitated and helped with installing the structural health monitoring systems. The authors would like to acknowledge the financial support of the European Commission through the Horizon 2020 project Built2Spec (637221). The second author would like to acknowledge the support of Science Foundation Ireland through the Career Development Award programme (Grant No. 13/CDA/2200).

3.7 References

- [1] H. Guan, V. M. Karbhari, and C. S. Sikorsky, “Web-Based Structural Health Monitoring of an FRP Composite Bridge,” *Comput. Civ. Infrastruct. Eng.*, vol. 21, no. 1, pp. 39–56, 2006.
- [2] ISIS Canada, “ISIS Canada Educational Module No. 5: An Introduction to Structural Health Monitoring,” ISIS Canada (Intelligent Sensing for Innovative Structures), Winnipeg, MB, Canada, 2005.
- [3] N. R. Buenfeld, R. Davies, A. Karimi, and A. Gilbertson, “CIRIA Report C661: Intelligent monitoring of concrete structures,” CIRIA, London, UK., 2008.
- [4] IRUSE Weather, “IRUSE Weather,” *Informatics research unit for sustainable engineering NUI Galway weather website*. [Online]. Available: <http://weather.nuigalway.ie/>. [Accessed: 20-Jul-2019].
- [5] M. Hajdukiewicz, D. Byrne, M. M. Keane, and J. Goggins, “Real-time monitoring framework to investigate the environmental and structural performance of buildings,” *Build. Environ.*, vol. 86, pp. 1–16, 2015.
- [6] A. M. Neville, *Properties of concrete*, 5th Ed. Upper Saddle River, NJ, USA: Prentice Hall, 2011.
- [7] J. Goggins, D. Byrne, and E. Cannon, “The creation of a living laboratory for structural engineering at the National University of Ireland, Galway,” *Struct. Eng.*, vol. 90, no. 4, pp. 12–19, 2012.
- [8] NSAI, “IS EN 1992-1-1: Eurocode 2: Design of concrete structures. Part 1-1: General rules and rules for buildings,” NSAI (National Standards Authority of Ireland), Dublin, Ireland, 2005.
- [9] American Concrete Institute, “ACI 209R-92 Prediction of Creep, Shrinkage and Temperature Effects in Concrete Structures (Reported by ACI Committee 207),” American Concrete Institute, Farmington Hills, MI, USA., 1992.

Chapter 3. Real-time Monitoring to Investigate Structural Performance of Hybrid
Precast Concrete Educational Buildings

- [10] D. Byrne and J. Goggins, “Evaluating the Structural Capacity of Concrete Elements through In Situ Instrumentation,” in *Key Engineering Materials*, 2013, vol. 569–570, pp. 382–389.
- [11] American Concrete Institute, “Guide for the design and construction of externally bonded FRP systems for strengthening concrete structures (ACI 440.2R-08),” American Concrete Institute, Farmington Hills, MI, USA, 2002.
- [12] S. A. Altoubat and D. A. Lange, “Creep, Shrinkage and Cracking of Restrained Concrete at Early Age,” *ACI Mater. J.*, vol. 98, no. 4, pp. 323–331, 2001.
- [13] J. Goggins and M. Hajdukiewicz, “The influence of heat transfer and storage in structural precast building components on indoor environments,” in *Proceedings of Civil Engineering Research in Ireland (CERI 2014, Queens University Belfast, 28-29 August 2014)*, 2014, pp. 161–166.
- [14] J. Goggins, S. Newell, D. King, and M. Hajdukiewicz, “Real-time monitoring of a hybrid precast and in situ concrete flat slab system,” in *Proceedings of Civil Engineering Research in Ireland (CERI 2014, Queens University Belfast, 28-29 August 2014)*, 2014, pp. 321–326.
- [15] R. I. Gilbert, “Shrinkage, cracking and deflection-the serviceability of concrete structures,” *Electron. J. Struct. Eng.*, vol. 1, no. 1, pp. 2–14, 2001.
- [16] E. W. Gulis, D. Lai, and B. Tharambala, “Performance and Cost Effectiveness of Substructure Rehabilitation/Repair Strategies (Draft Report),” Ministry of Transportation of Ontario, Downsview, Canada, 1998.
- [17] P. B. Bamforth, “CIRIA Report C660: Early-age thermal crack control in concrete,” CIRIA, London, UK, 2007.
- [18] R. K. Dhir, K. A. Paine, and L. Zheng, “Design Data for Use where Low Heat Cements are Used (Report No. CTU2704),” Concrete Technology Unit, University of Dundee, Dundee, UK, 2006.

Chapter 3. Real-time Monitoring to Investigate Structural Performance of Hybrid
Precast Concrete Educational Buildings

- [19] M. E. FitzGibbon, “Large pours for reinforced concrete structures. Current Practice Sheet 2P/15/1, NO. 28,” *Concrete*, vol. 10, no. 3, p. 41, 1976.
- [20] P. Bamforth, D. Chisholm, J. Gibbs, and T. Harrison, “Properties of concrete for use in Eurocode 2 (CCIP-029),” Cement and Concrete Industry Publication (UK), London, UK, 2008.

4 Real-time Monitoring of Concrete–Lattice-girder Slabs during Construction

Article Overview

This paper reports on the real time monitoring of a hybrid concrete lattice girder slab during the construction phase. A variety of sensors were embedded in the precast plank and insitu concrete topping of the floor in the Human Biology Building (HBB) which was constructed in 2015-16. Although the data from the SHM system was acquired at regular intervals during the construction phase, the SHM system and technology described permits the data to be acquired in real-time. The design, installation and supervision of the SHM system in the HBB was undertaken by the author. A review of the literature presented in **Chapter 2** revealed a lack of published case studies in relation to the SHM systems installed in buildings and this is a barrier to the future implementation of SHM systems in concrete floors.

The paper demonstrates many of the potential applications of the data with respect to the structural behaviour of the concrete floor and how it can be used to enhance our understanding of the actual behaviour of the floor. The temperature and strain data are used to investigate the potential for early-age thermal cracking and derive restraint factors for the concrete floor. The imposed strains acting on the second floor of the HBB during construction when the third floor overhead is poured and supported by temporary propping are analysed. The provision of formwork and supporting of subsequent pours by floors below is critical to the efficient and economical construction of flat slabs and therefore this study provides data on the load transfer mechanism in the floors during construction.

The measured bending moments (based on measured strains) are compared with predicted bending moments generated by the finite element model which was created by the designers of the HBB. It is very rare that designers have the opportunity to compare actual behaviour of structural elements with the predicted behaviour. Time dependent effects in concrete, which are very difficult to predict

Chapter 4. Real-time Monitoring of Concrete–Lattice-girder Slabs during Construction

accurately, are also investigated in this paper for the first six months of the floor slab using the data from the SHM system implemented.

The main contribution to the literature from this chapter consists of the application of SHM data to analyse the structural behaviour of the hybrid concrete lattice girder slabs during the construction stage. This research should assist designers and researchers and provide the basis for improved understanding of how the floor behaves during the construction phase. The rich field data reported in this paper can also be used to develop numerical models or improved design guides.

Photographs from the structural health monitoring installation phase is presented in in **Appendix A**. This chapter was published in the journal *Proceedings of the Institution of Civil Engineers - Structures and Buildings* (2017).

Abstract

This paper reports on the instrumentation, monitoring and some preliminary results from a real-time monitoring scheme of a hybrid concrete–lattice-girder slab flooring system. One of the key benefits of this monitoring project is improved understanding of in situ structural behaviour. Sensors were embedded in both the precast and in situ components of the floor system and were used to monitor various aspects of the behaviour of the floor during the manufacturing, construction and operational phases. Concrete strains and temperatures were measured, while environmental conditions were also monitored to assess their effects on the floor structure. The information from the real-time monitoring offered the opportunity to compare actual and predicted behaviour using structural codes, such as Eurocodes. Results on the early-age behaviour of the floor slab during the construction phase (strain, thermal cracking, restraint factors) are described in this paper.

4.1 Introduction

This paper describes the implementation of a real time structural health monitoring (SHM) scheme on a new building (Human Biology Building) under construction at the National University of Ireland Galway (NUI Galway). This project is one of a number of projects which forms part of a measurement framework strategy developed at NUI Galway to continuously monitor the structural and environmental

Chapter 4. Real-time Monitoring of Concrete–Lattice-girder Slabs during Construction

performance of buildings during construction and operation ([1]–[3]). The general SHM methodology for these projects is described in more detail by Newell *et al.* [3]. In previous projects constructed on the NUI Galway campus, the structural behaviour of a void form flat slab was monitored in the Engineering Building (EB) [4] and the environmental and thermal performance of precast components was monitored in the Institute for Lifecourse and Society Building (ILAS) [2]. The Engineering Building, completed in 2011, also acts as a ‘Living Laboratory’ for engineering students [5]. Although the HBB is under construction at the time of writing, some preliminary results from the project are presented in this paper, primarily focussing on the early-age behaviour of a hybrid concrete precast concrete lattice girder flat slab during the construction phase. This project is part of the Built2Spec European project in which the structural and environmental performance of buildings are continuously monitored using smart sensor-embedded construction elements (smart building components).

Although the majority of sensors and monitoring equipment are predominantly used on civil infrastructure projects, the use of instrumentation for the design, construction and management of buildings has increased in recent decades. The trend towards increased service life and durability of structures means that monitoring systems which permit the condition of the structure to be measured and which detect the possible onset of damage and/or deterioration of the structure will become increasingly important. A SHM system, if correctly designed and implemented, can be used to assess the current condition of the structure, residual life prediction and detection of deterioration of a structural component [6]. One of the key benefits of insitu instrumentation is the improved understanding of insitu structural behaviour. The majority of design codes have been developed following research conducted in engineering laboratories, where it can be very difficult to replicate the behaviour of real structures insitu. Consequently, testing and analysis is typically conducted on small-scale specimens which only partially represent the overall structure. Real time monitoring can be used to provide rich information on how real structures behave when subject to actual structural and environmental loads [7].

Chapter 4. Real-time Monitoring of Concrete–Lattice-girder Slabs during Construction

A variety of sensors were embedded in the hybrid concrete floor structure of the building and are used to monitor various aspects of the behaviour of the floor during the manufacture, construction and operational phase of the building.

The overall objectives of this research project are to:

- compare actual and predicted behaviour of the floor.
- analyse the long term behaviour of the floor.
- investigate construction and design parameters for potential optimisation of hybrid concrete floor systems.
- develop and calibrate numerical models that predict the performance of the hybrid concrete floor system.

4.2 Human Biology Building

The Human Biology building (HBB) is a four storey building over basement and roof level plant enclosure with a gross floor area of 8200m² (Figure 4-1). This building will house the existing university disciplines of Anatomy, Physiology & Pharmacology and Therapeutics. The building has been designed as a teaching and research facility with accommodation including teaching and research laboratories, offices, anatomy and mortuary facilities, meeting rooms, lecture theatres and other ancillary areas. Construction commenced in January 2015 and the building was handed over to the client in March 2017. It is anticipated that the building will achieve an A rating under the Commercial Energy Rating marking scheme and a BREEAM Excellent rating. The HBB is primarily constructed using precast concrete elements, including the building frame, twinwall system, hybrid concrete lattice girder slabs and hollowcore slabs, which were designed, manufactured and installed by Oran Pre-Cast Ltd. in Galway, Ireland.

Chapter 4. Real-time Monitoring of Concrete–Lattice-girder Slabs during Construction



Figure 4-1 Human Biology Building (under construction)

4.2.1 Hybrid concrete lattice girder flat slab

A two-way spanning hybrid precast concrete lattice girder flat slab system is used for the floor structure. The majority of the floor plate is 400mm thick and consists of a 65mm thick precast lattice girder plank (Figure 4-2) and 335mm insitu concrete topping. The lattice girder truss, which protrudes from the plank, provides stiffness in the temporary state and increases composite action with the insitu structural concrete topping. The bottom layer of reinforcement is contained within the precast concrete plank and the top layer of reinforcement is placed on site, together with a layer of stitching reinforcement across the joint between slabs, prior to pouring the insitu concrete topping. The precast planks are temporarily propped until the structural concrete topping has reached the required compressive strength.

A reinforced concrete twin wall system is the primary lateral resisting system in the building, as well as transferring gravity loads to the ground. The twin wall system consists of two plates of 65mm thick concrete connected by means of cast-in lattice girders to form a core between the plates. The cavity between the plates is filled with concrete on site after the panel has been erected to complete the composite wall. Precast reinforced concrete columns and downstand beams are also employed in the building.



Figure 4-2 Precast Concrete Lattice Girder Plank (with embedded sensors)

Flat slabs are one of the most widely used forms of floor construction providing minimum structural depths, fast construction and uninterrupted service zones. Transportation and site handling limitations generally dictate the allowable sizes of the precast planks. The use of steel moulds results in a high-quality finish, which can be left exposed if required. The quality of the factory produced soffits also provides the opportunity to take advantage of the thermal mass properties of the concrete slab by exposing them. The main advantages of this floor system to the contractor are in terms of programme, reduction in steel fixing and formwork requirements on site.

4.3 Instrumentation

The SHM strategy implemented in the HBB employed sensors embedded in the floor structure to monitor the environmental and structural behaviour of the hybrid concrete lattice girder flat slab. Two zones in the second floor of the HBB were selected for instrumentation using a combination of vibrating-wire (VW) strain gauges, electrical resistance (ER) strain gauges and thermistors (Figure 4-3 and Figure 4-4).

Chapter 4. Real-time Monitoring of Concrete–Lattice-girder Slabs during Construction

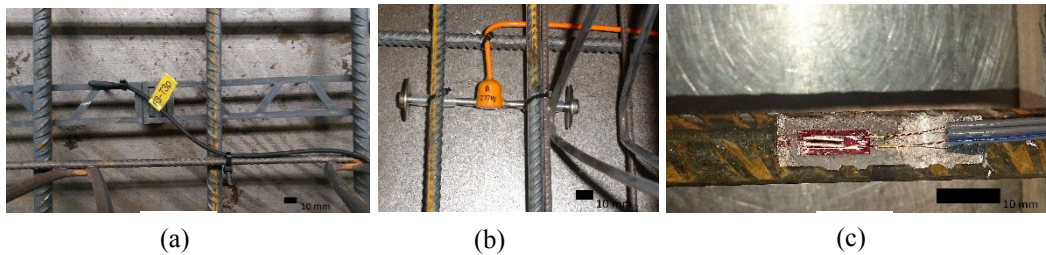


Figure 4-3 Sensors embedded in the building's structure: (a) thermistors; (b) VW gauges; (c) ER gauges

In total, 112 embedment VW strain gauges, manufactured by Gage Technique (Type TES/5.5/T), were installed in both the precast plank prior to manufacture and in the insitu concrete topping prior to pouring. The VW gauges measure both temperature and longitudinal strain in the concrete. These type of gauges were initially developed by the Transport and Road Research laboratory (TRRL) in the UK and are used extensively in bridge sections, tunnel linings and dam projects. They have a range of greater than 300 microstrain and resolution better than 1 microstrain. The temperature can be measured between -20°C and $+80^{\circ}\text{C}$. These VW gauges are very robust and their stability makes them suitable for monitoring time dependent effects in concrete such as creep and shrinkage.

The strain gauge operates on the principle that a tensioned wire, when plucked, vibrates at a frequency that is proportional to the strain in the wire. The gauge is constructed so that a wire is held in tension between two end flanges. Loading of the concrete structure changes the distance between the two flanges and results in a change in the tension of the wire. An electromagnet is used to pluck the wire and measure the frequency of vibration. Strain is then calculated by applying calibration factors to the frequency measurement. In order to interpret the data from the VW strain gauges, it is very important that strain readings are corrected for temperature effects. The internal temperature of the concrete in the floor, as well as causing expansion and contraction of the concrete, will also change the temperature of the VW gauge which will affect the readings from the VW strain gauges. The coefficient of thermal expansion of the VW strain gauges is $11\mu\epsilon/^{\circ}\text{C}$ and for this project it was assumed that the coefficient of thermal expansion of the concrete was $9\mu\epsilon/^{\circ}\text{C}$, as limestone aggregates were used for the concrete in the precast plank and insitu topping [8]. Therefore, in order to measure the strain of the concrete due to

Chapter 4. Real-time Monitoring of Concrete–Lattice-girder Slabs during Construction

load effects only, the difference in thermal expansion between the gauge and host material must be accounted for ($2\mu\epsilon/^\circ\text{C}$, in this instance).

The VW gauges were positioned along a number of orthogonal grids in the floor structure at over 30 designated locations so that two-way spanning behaviour of the floor structure could be monitored. At most locations, four VW gauges were positioned through the depth of the slab (1 in the precast plank and 3 in the insitu topping) so that the strain and temperature profile through the slab could be measured (Figure 4-4). The location of the embedded sensors in one zone of the second floor is shown in Figure 4-5.

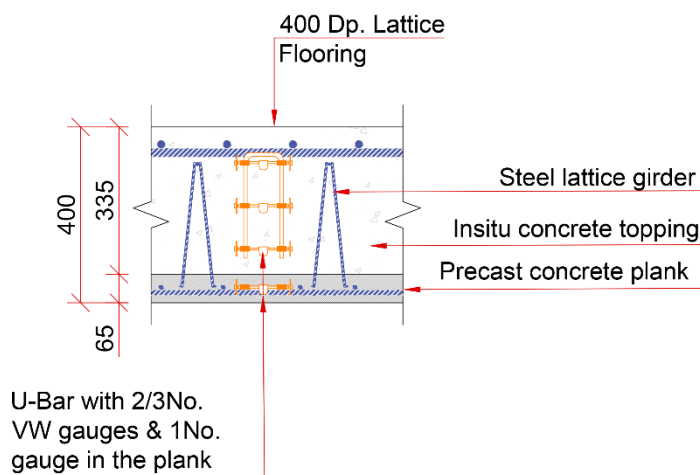


Figure 4-4 Typical section showing locations of vibrating wire gauge installed in the flat slab system (dimensions in mm)

4.3.1 Material testing

To accurately predict the behaviour of concrete elements, it is critical that the properties of the concrete are determined as they will change over time depending on the environment and loading [9]. A comprehensive material testing programme was undertaken to measure the properties of the precast and insitu concrete used in the floor structure. The information from the material testing is used to interpret the data from the instrumentation and can also be used for modelling of the behaviour of the floor structure. Concrete cylinders, cubes and prisms specimens were made and cured in water and in air (to match the environmental conditions of the floor structure).

Chapter 4. Real-time Monitoring of Concrete–Lattice-girder Slabs during Construction

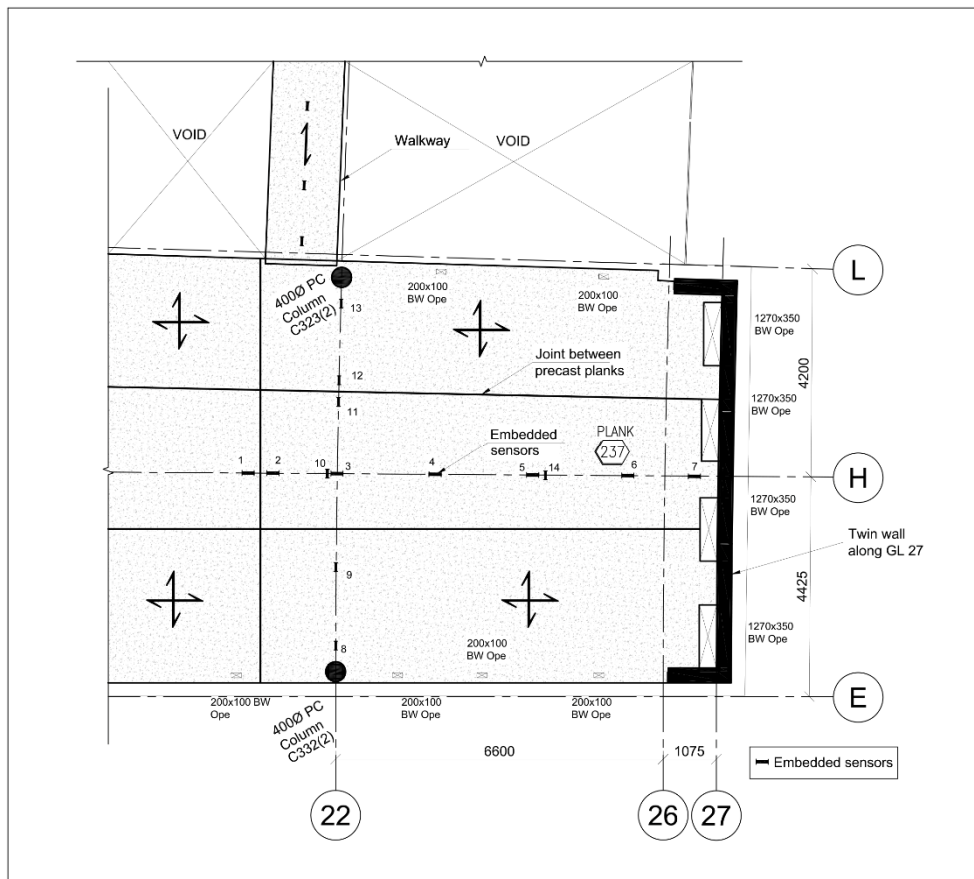


Figure 4-5 Part of second floor slab of HBB with insitu instrumentation

The precast planks were manufactured using a C40/50 concrete mix [10] with a CEM II A-V cement (370kg/m^3 typically or 425kg/m^3 of self-compacting concrete used). The mix design for the insitu concrete topping was C30/37 with 230kg/m^3 of CEM I cement and 100kg/m^3 of GGBS (i.e. 30%).

4.3.2 Environmental conditions

The environmental conditions around the floor structure will impact on the behaviour of the concrete slab, particularly at early stages of curing. Air temperature and relative humidity in the vicinity of the instrumented slab were measured using the weather data from the NUIG weather station (located approximately 1km from the site) [11]. When building was enclosed a sensor was positioned inside the building to record the air temperature and relative humidity.

4.4 Results

As mentioned previously, the HBB is still under construction but all of the insitu instrumentation will continue to monitor the behaviour of the floor structure during the operational phase of the building. This will allow long-term effects of creep and shrinkage of concrete elements to be further investigated. This paper presents some of the results from the sensors focussing on the early-age behaviour of the hybrid concrete lattice girder flat slab during the construction phase.

4.4.1 Temperature rise and temperature differentials

Predicting the temperature rise and temperature differentials are key parameters when determining the early-age behaviour of concrete elements and the potential for thermal cracking. However, at design stage, this can sometimes be difficult as there are numerous factors which affect the early-age behaviour of concrete. Guidance in relation to predicting the early–age thermal behaviour of concrete sections is provided in the CIRIA Report C660 by Bamforth [12]. However, the report recommends thermal modelling for reliable predictions which take account of the formwork and exposure conditions. Insitu instrumentation can also be used to determine parameters, such as peak temperature and temperature differentials in concrete pours, to improve the accuracy of prediction models for early-age thermal cracking.

Nine VW strain gauges were embedded in one of the 65mm thick precast planks (Plank 237, Figure 4-5) prior to manufacture and data was recorded immediately after the plank was cast. The concrete temperature for the nine VW gauges embedded in the plank and the air temperature (dashed line) are shown in Figure 4-6 for the 7 days after the plank is manufactured. The peak in the concrete temperature occurs approximately 10 hours after casting, which is typical of the heat generation phase during cement hydration [13] and contrasts with the falling ambient air temperature during the night. The max recorded difference between the air temperature and the concrete temperature is approximately 5.5°C. The peak temperature for the three gauges (No. 2, 7 and 11) located close to the perimeter (less than 300mm) are slightly less as the concrete adjacent to the external surface cools at a faster rate. Within 24 hours after manufacture, the concrete temperature

Chapter 4. Real-time Monitoring of Concrete–Lattice-girder Slabs during Construction

in the plank is relatively uniform for all nine VW gauges and they correlate with the ambient air temperature because the plank is relatively thin (65mm).

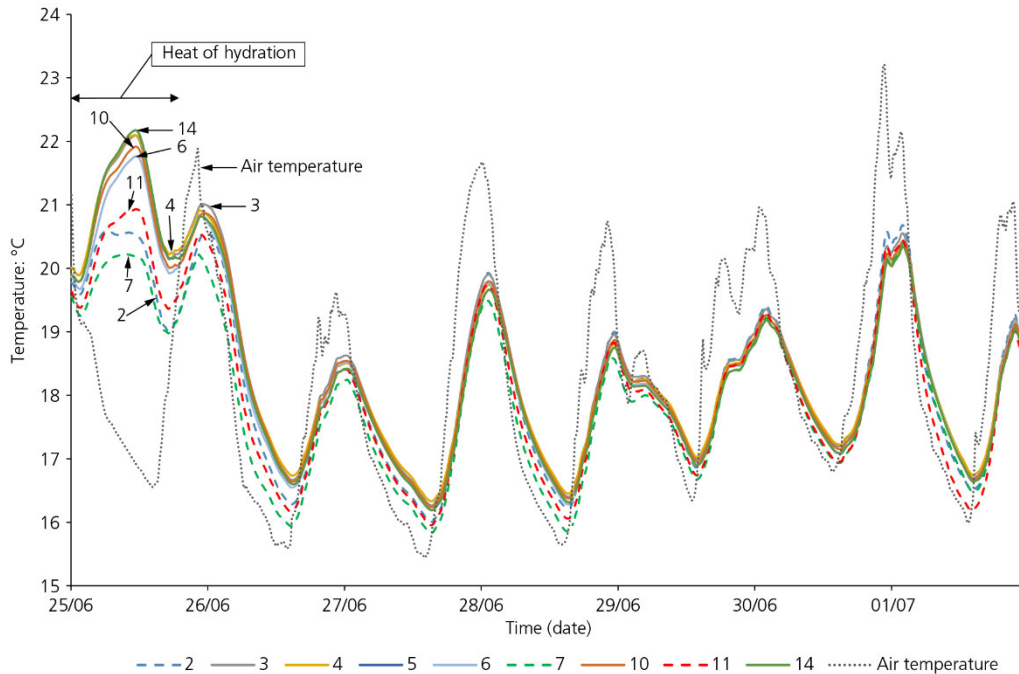


Figure 4-6 Concrete temperature in a 65mm thick precast plank (7d after manufacture)

The concrete temperatures in the insitu topping at one location in which three VW gauges are embedded to measure strain and temperature through the insitu topping (top, middle and bottom) and precast plank are shown in Figure 4-7. The peak temperatures recorded in the insitu topping are more significant than the precast plank because of the thickness of the concrete (335mm thick) and the insulating effect of the precast biscuit which means that only one surface of the insitu topping is directly exposed to air. Similar to the precast plank, the peak in concrete temperature occurs approximately 10 hours after casting and at this point, the maximum temperature differential between the air and concrete temperature is approximately 13°C. It takes approximately 7 days for the heat generated from the hydration process to dissipate. The temperature in the insitu topping exceeds the ambient air temperature for approximately 7 days after the pour. The effect of the diurnal temperature changes are also clearly visible in the measured temperature in the concrete floor. The peak temperature is recorded for the VW gauge in the middle

Chapter 4. Real-time Monitoring of Concrete–Lattice-girder Slabs during Construction

of the insitu topping as the internal section of the slab will be slowest to cool down. The effect of the heat of hydration from the insitu topping on the concrete in the precast plank can be noted almost immediately after pouring and results in a peak increase in temperature of 9°C.

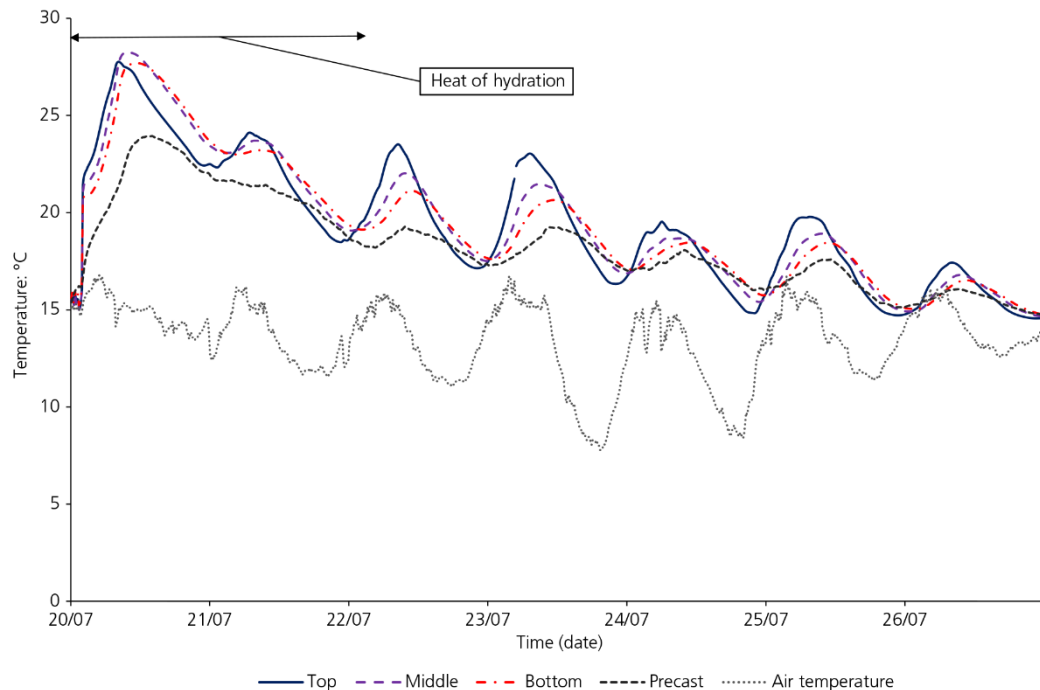


Figure 4-7 Concrete temperature in the 335mm insitu precast plank (7d after pour)

As expected, the peak temperature in the concrete during the initial hydration phase was recorded in the middle section of the insitu topping and the lowest temperature is recorded in the top section due to heat loss to the surrounding air. The concrete in the bottom section of the insitu is partially insulated by the precast plank but the heat transfer to the plank is noted as the temperature of the precast plank increases during the hydration phase. After the initial hydration phase, the concrete temperature in the slab is primarily in response to the diurnal temperature changes. The time lag between the concrete temperatures in the insitu topping and the ambient air temperature are shown in Figure 4-7. The time lag increases from top to bottom through the 335mm thick insitu topping as the top of the slab is exposed and is subject to radiant heating from the sun. In contrast, the time lag recorded between the ambient air temperature and the concrete in the precast plank (Figure 4-6) after manufacture is much smaller because it is only 65mm thick and

Chapter 4. Real-time Monitoring of Concrete–Lattice-girder Slabs during Construction

consequently has a much smaller thermal mass in comparison with the insitu topping.

One of the main concerns with large volume pours is the heat generated as the cement hydrates and the potential thermal stresses generated by restraint to thermal movement. In terms of minimising cracks, the general rule of thumb used by designers is to limit temperature differentials to 20°C, although this figure can be revised depending on the type of aggregate used in the concrete mix. For the insitu topping in this project, the temperature differential through the slab is small (Figure 4-7) because of the relatively thin section which allows the concrete to cool comparatively uniformly as the heat is readily lost to the environment. The temperature differential recorded by the VW gauges in top, middle and bottom of the insitu topping did not exceed 3°C and the maximum differential occurred during the cooling phase. Using CIRIA Report C660 [12], the predicted maximum temperature differential in the insitu topping is 13°C, but this figure is highly dependent on the thermal diffusivity of concrete, surface conditions and the environmental conditions (wind and solar gain). The predicted peak temperature differential for the insitu topping using CIRIA Report C660 [12] is approximately 19°C, but other factors which can affect the peak temperature are the variation between cements, placing temperature and actual thermal conductivity of the precast plank. The measured peak temperature of 13°C equates to a temperature rise of 4°C/100kg per cubic metre of concrete. In this project, the mix design for the insitu concrete topping was C30/37 with 230kg/m³ of CEM I cement and 100kg/m³ of GGBS (i.e. 30%). Fitzgibbon [14] estimated that the peak temperature rise under adiabatic conditions is 12°C/100kg per cubic metre of concrete, regardless of the type of cement used. This figure can be considered as an upper bound, but does not take into account the reduced heat of hydration because of the 30% GGBS used as a cement replacement in the concrete mix.

4.4.2 Early-age thermal cracking

During the early stages of curing, there is potential for cracking to occur if the tensile strain capacity of the concrete is exceeded. Some research has shown that microcracks can form even if 50% of the tensile strength of the concrete is exceeded

Chapter 4. Real-time Monitoring of Concrete–Lattice-girder Slabs during Construction

[15]. The coefficient of thermal expansion of concrete (α_c) will determine the magnitude of thermal strain associated with a particular temperature change. Values for concrete vary from 8-13 $\mu\epsilon/^\circ\text{C}$ depending primarily on the aggregate used. EN 1992-1-1 [16] recommends a value of 10 $\mu\epsilon/^\circ\text{C}$ for normal weight concretes, if measured values are not available. However, a design value of 9 $\mu\epsilon/^\circ\text{C}$ may be used for limestone aggregates [8], which were used for the concrete on the HBB project. Using the measured peak recorded temperature of 13 $^\circ\text{C}$, this equates to thermal strains of approximately 117 $\mu\epsilon$ in the insitu topping. Observations have shown that early-age cracking is most likely to occur within three to six days [17].

The tensile strain capacity of concrete, ϵ_{ctu} , is the maximum strain that the concrete can withstand without the formation of a continuous crack. Tensile strain capacity is not dealt with in EN 1992-1-1, but can be derived from values of the tensile strength and elastic modulus of the concrete provided in EN 1992-1-1. Tensile strain capacity under short-term loading can be approximated as the ratio of the mean tensile strength of concrete f_{ctm} to its mean elastic modulus E_{cm} and this has been shown to represent lower bound values [12].

$$\epsilon_{ctu} = f_{ctm}/E_{cm} \quad (\text{Eqn. 4-1})$$

The values derived for tensile strain capacity are increased by 23% to take account of the relaxation of stress due to creep and reduction in tensile strength under a sustained load [12]. The aggregate type is of particular significance to the tensile strain capacity as aggregate comprises about 70% of the concrete volume.

The strain profile in the insitu topping at one location in the slab for the first seven days is compared in Figure 4-8 with the theoretical tensile strain capacity given in Equation 4-1. The graph indicates the measured strain is close to or exceeds the theoretical strain capacity during the first 3 days after the pour. No cracking was observed in the location of the slab in which strain gauges were embedded and the actual tensile strain capacity of the insitu topping is at least 20-30% greater than the theoretical tensile strain capacity based on material testing conducted on concrete samples at 3 Days and 7 Days, which were air cured to match the environmental conditions on site. This illustrates the difficulty of predicting early-age cracking

Chapter 4. Real-time Monitoring of Concrete–Lattice-girder Slabs during Construction

without accurate knowledge of the environment or material properties. Similar research based on the embedded sensors in the void form flat slab in the Engineering Building [4] also noted locations where the measured strain exceeded the theoretical strain capacity but that no cracking was observed on site.

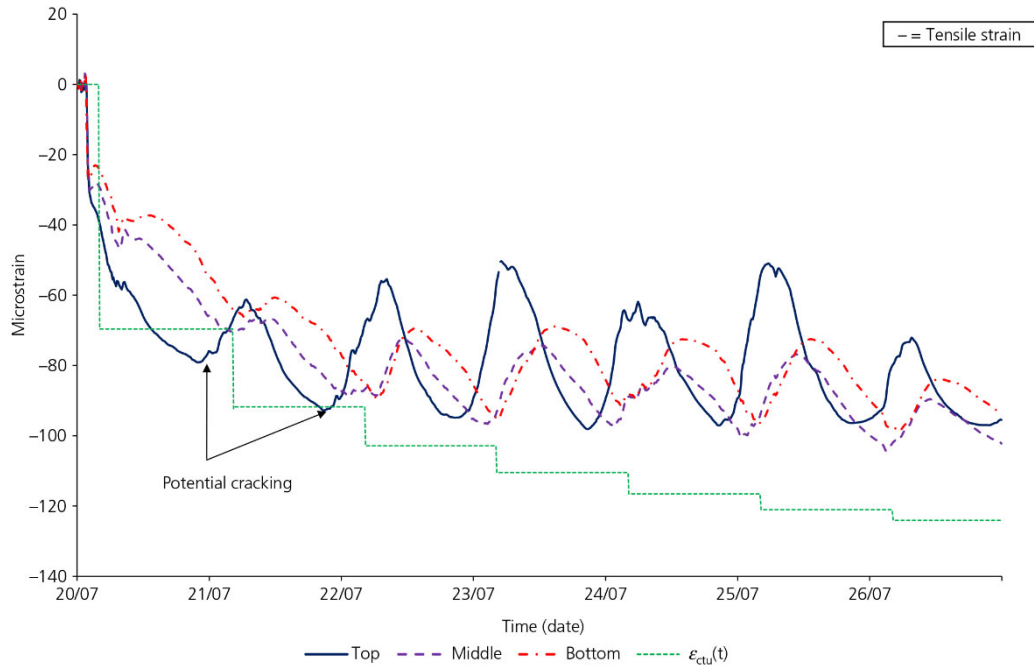


Figure 4-8 Comparison of measured strain and theoretical strain capacity (7d)

4.4.3 Deriving restraint factors

Restraint to movement can occur both externally and internally. External restraint can occur due to continuous edge restraint, end restraint and intermittent restraint. Internal restraint is where one part of a concrete pour expands or contracts relative to another part of the same section. In general, internal restraint will typically dominate for ‘thick’ concrete sections and external restraint will dominate for thinner sections. In this project, the hybrid concrete slab was subject to intermittent external restraint from the supporting columns and walls and internal restraint should not be critical as the insitu topping was only 335mm thick.

Early-age thermal cracking will occur if the restrained strain, ϵ_r , exceeds the tensile strain capacity of the concrete, ϵ_{ctu} . In order to estimate a value for the restrained strain, one must determine a restraint factor (R) which represents the amount of

Chapter 4. Real-time Monitoring of Concrete–Lattice-girder Slabs during Construction

restraint to lateral and shrinkage movement which is actually provided to the structural element under consideration ($R=0.0$ unrestrained; $R = 1.0$ full restraint). Various publications provide guidance on values to be adopted for different restraint conditions, although there is little guidance with respect to suspended slabs. Information for determining restraint factors are given in Annex L of EN 1992-3 [18] for common construction configurations. It should be noted that the values in EN 1992-3 include a modification factor of 0.5 for creep. When calculating the risk of early-age thermal cracking, the restraint factor to use at design stage can be difficult to determine, particularly if there is the potential for internal and external restraint. Choosing an incorrect restraint factor can result in uneconomical over-design, or under-design leading to unacceptable cracking.

Insitu instrumentation can be very informative, on large projects with similar pours, to determine restraint factors. In this project, the embedded vibrating wire strain gauges were used to estimate the restraint factors for the 335mm thick insitu topping which was poured on top of the precast concrete lattice girder plank. The restraint factor is determined by comparing the observed strain in the element and the free strain that would have occurred with no restraint.

The restraint factor (R) is determined as follows [12];

$$R = \frac{(\alpha_c - \alpha_r)}{\alpha_c} \quad (\text{Eqn. 4-2})$$

where α_c is the coefficient of thermal expansion of unrestrained concrete (derived using a Hot Box test in which in which the temperature and strain change are measured for an insulated unrestrained specimen as suggested in CIRIA Report C660) and α_r is the insitu restrained coefficient of expansion strain which is measured during the cooling phase after the concrete has reached its peak temperature after pouring. It was assumed that the free strain (α_c) or coefficient of thermal expansion of the unrestrained insitu concrete was $9\mu\epsilon/^\circ\text{C}$ [8]. The insitu strain-temperature curves were plotted for the strain gauges embedded in the insitu topping and insitu restrained coefficient of expansion (α_r) is determined by measuring the slope of the strain-temperature curve during the cooling phase of the

Chapter 4. Real-time Monitoring of Concrete–Lattice-girder Slabs during Construction

concrete. The strain-temperature curve for three VW strain gauges in the top, middle and bottom at one location in the insitu topping is shown in Figure 4-9. From the chart, it is observed that the restrained coefficient of thermal expansion varies between $5.7\text{--}7.6\mu\epsilon/^\circ\text{C}$. Using Equation 4-2, this equates to a restraint factor of 0.16–0.37, which would be considered low-moderate restraint.

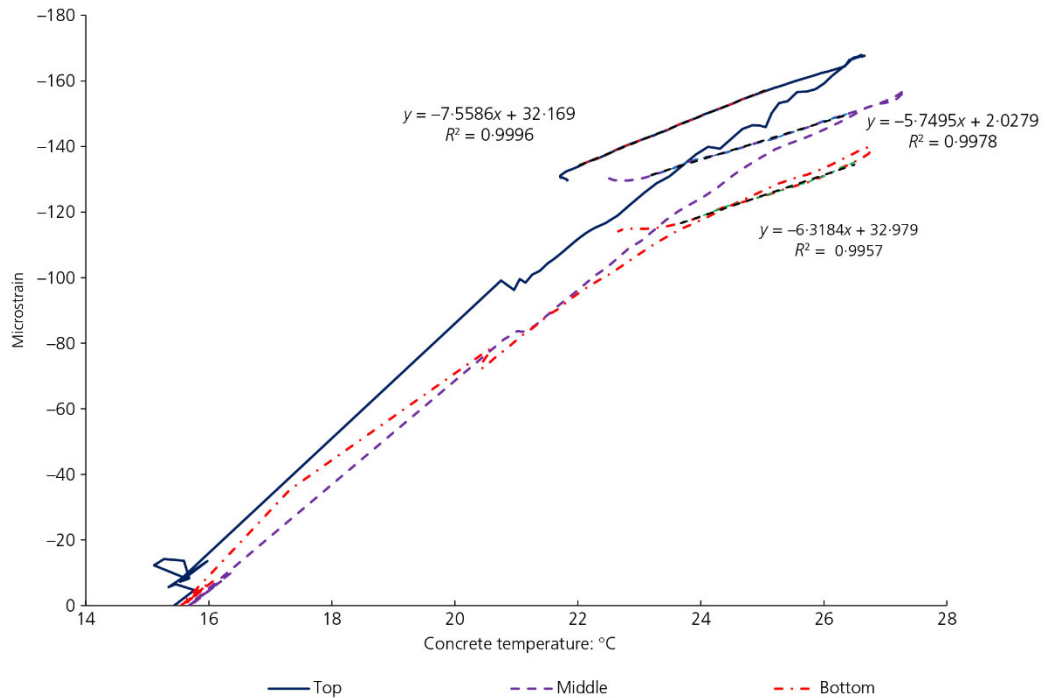


Figure 4-9 Insitu strain-temperature curve for insitu topping in hybrid concrete slab

The average measured restraint factor for the 335mm insitu topping was 0.27 with a coefficient of variation (Cv) of 36%. In general, the restraint factors were generally higher for the gauges in the middle of the slab (average R = 0.37, Cv = 19%) in comparison with the gauges located in the top and bottom of the insitu topping (average R = 0.23, Cv = 32%). There was no noticeable increase in the measured restraint for the gauges located close to the supporting columns or walls, which is expected as the reinforced concrete core walls in this project were constructed using the twin wall system and the insitu core of the walls were typically poured with the insitu topping so that the walls had limited stiffness during the early-age stages of the insitu topping. Using restraint factors determined using

Chapter 4. Real-time Monitoring of Concrete–Lattice-girder Slabs during Construction

embedded instrumentation and comparison with assumed (design) values may highlight potential changes to the design that can result in more economical and cost-effective design, particularly with respect to early-age thermal cracking and resulting crack widths.

4.4.4 Construction stage behaviour of hybrid concrete flat slab

A hybrid concrete lattice girder flat slab structure was used to construct the ground to fourth floor of the HBB (the basement was constructed using insitu concrete). As mentioned previously, the precast planks are temporarily supported by props which are erected prior to installation of the planks. The precast planks act as permanent formwork and contain the bottom reinforcement for the floor structure. As the concrete frame progressed upwards, the floors constructed below the floor under construction were used to support the self-weight of the next floor. A temporary works engineer was employed by the contractor to determine a back propping sequence for the floor structure at each level as construction progressed. The back propping sequence must ensure that the load from the wet concrete is transferred to a sufficient number of floors below so that no slabs are overloaded. When the compressive strength of the insitu topping had reached a specified strength, the supporting props were removed and reproped so that each slab was supporting its own self-weight (also known as striking and reproping).

During the construction phase of the HBB, the changes in strain when props were dropped, back-propped and removed can be analysed, as well as when floors were poured above second floor. The deformation of the slab soffit during the construction phase was also recorded using a digital level (accuracy $\pm 0.6\text{mm}$). The change in strain along a gridline (GL H) in the second floor for a series of VW strain gauges in the top of the insitu topping at two loading events is shown in Figure 4-10. The solid line is the change in strain when the third floor was poured (13th August 2015) and the second floor partially supported the newly cast floor above and the dashed line is the change in strain when the props were dropped and reproped 15 days later (28th August 2015). When the third floor is poured, its self-weight is transferred down to the floors below (ground, first and second floor) using the system of backpropping. The recorded strains shows that when the props were

Chapter 4. Real-time Monitoring of Concrete–Lattice-girder Slabs during Construction

removed from the third floor, so that it supports its own self-weight, that the imposed strains (and stresses) on the second floor from the third floor pour are reversed. The magnitudes of the change in strain when the third floor was poured when compared with the measured changes in strain when the second floor was poured suggest that the second floor supported approximately 70% of the self-weight of the third floor until the props were removed. The self-weight of the third floor is not equally distributed between the supporting floors below because of each slab has a different stiffness due to the sequence of construction and also the elasticity of the supporting props. This percentage agrees with the research from the European Concrete Building Project (ECBP) in Cardington [19] which demonstrated that the supporting floor below the falsework takes the majority of the load when backpropping and correlates closely with the load transfer mechanism used by temporary works designers [20].

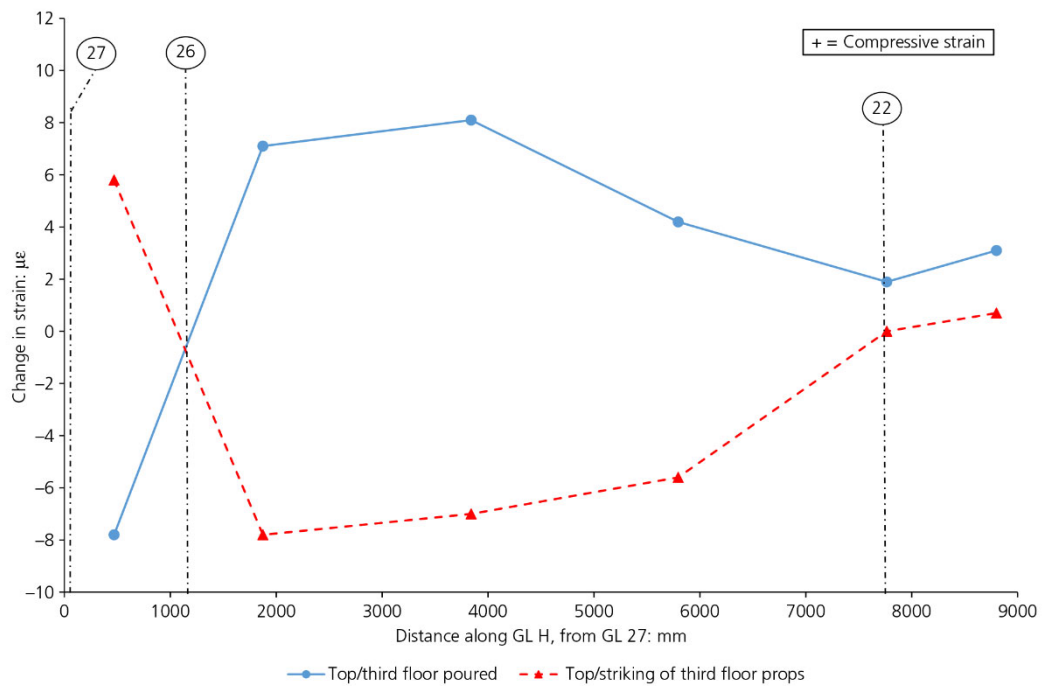


Figure 4-10 Measured change in strain in the second floor when (i) when the third floor was poured and (ii) striking of props

4.4.5 Strain profile

The measured changes in strain through the 400mm thick floor structure at one location along gridline H is shown in Figure 4-11 when the third floor is poured (13th August 2015) and when the props supporting the third floor are dropped (28th August 2015). At this location, there are three VW gauges in the insitu topping and one VW gauge in the precast plank. The strain profile illustrates the composite nature of the hybrid concrete floor structure and also that the slab appears to exhibit linear elastic behaviour at this stage of construction and could be considered ‘uncracked’. Similar to the behaviour observed in Figure 4-10, the measured change in strains through the concrete floor in second floor when the 3rd floor is poured above are reversed when the props supporting the 3rd floor are removed.

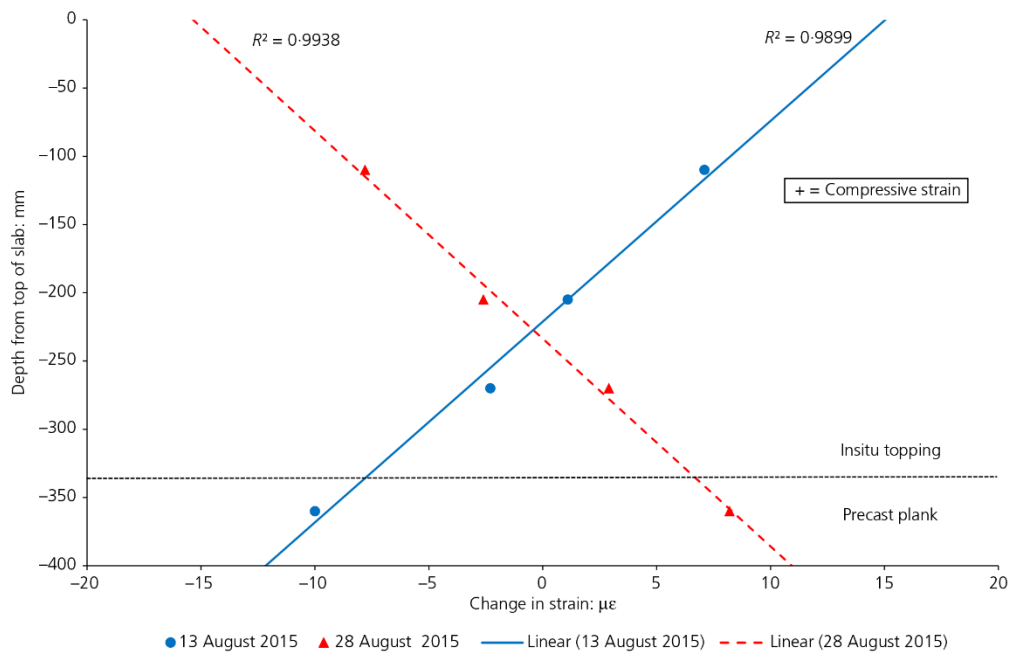


Figure 4-11 Measured change in strain in the second floor when (i) when the third floor was poured and (ii) striking of props

The measured change in strains from the embedded VW strain gauges after striking props to the second floor and repropping (to let slab support its own self weight) and when the props were removed permanently are assumed to be broadly equivalent to when the second floor supports its own self-weight. The applied load on the slab when it supports its self-weight is approximately 67% of the total design

Chapter 4. Real-time Monitoring of Concrete–Lattice-girder Slabs during Construction

service load on the slab. The measured changes in strain along sections of the slab were converted to bending moments assuming the slab is uncracked (as suggested by measured changes in strain in Figure 4-11) and using the concrete properties derived from material testing conducted on the concrete used on site for the second floor. The concrete test results for the air-cured specimens were used when determining moments from the measured strains as they were cured in a similar environment to the concrete on site and are more representative of the insitu concrete in the floor slab. Although the specification for the insitu topping was C30/37 ($f_{ck} = 30.0 \text{ N/mm}^2$), the average 28 day compressive strength (f_{ck}) from material testing was 36.5 N/mm^2 and 41.5 N/mm^2 for air cured and water cured specimens respectively (cylinders and cubes were tested). This illustrates one of the challenges of predicting behaviour of concrete structures at design stage, as typically assumed values for concrete properties will have to be assumed which may not be representative of the insitu concrete on site.

During the design process, a linear elastic finite element (FE) model was developed by the designers (precast manufacturer was responsible for the design of the hybrid lattice girder floor) in order to model the floor structure. In the analysis, the floor is modelled as 400mm thick insitu flat slab and the joints between the precast planks are modelled as a 65mm high and 130mm wide recess in the slab soffit. For the purposes of design, the material properties for the slab are assumed to be uniform throughout the depth and are taken as that for the insitu topping of the slab (C30/37, $f_{ck} = 30 \text{ N/mm}^2$). The moments determined were compared with the moments from the model on second floor when it supports its own self-weight along gridlines (GL) H and 22 (Figure 4-5). The location of embedded sensors in the floor are noted in Figure 4-5 and typically consist of three or four VW gauges through the depth of the 400mm thick hybrid flat slab at each location as detailed in Figure 4-4 previously.

The bending moments determined using the measured strain data and the concrete material testing are compared with predicted bending moments from the linear elastic finite element analysis in Figure 4-12 for both gridlines H and 22 (orthogonal to each other). The measured strains were converted to bending moments for both

Chapter 4. Real-time Monitoring of Concrete–Lattice-girder Slabs during Construction

the case of no creep and creep (creep coefficient determined in accordance with Eurocode 2). There is relatively good correlation between the predicted bending moments and moments derived using the measured strain from the insitu instrumentation and the comparison can be used to highlight differences between assumed and actual behaviour of the floor structure. The FE model is conservative (upper bound) as it does not take account that the 65mm thick precast plank was manufactured 25 days prior to the insitu topping and using a higher grade of concrete (C40/50) than the insitu topping (C30/37). Therefore, the actual floor slab is stiffer than modelled and we would expect that the moments derived from the measured strains would be less than the moments from the FE analysis. In addition, the model is based on a linear elastic behaviour and does not take account of creep in the concrete. Along GL H (Figure 4-12a), the insitu instrumentation records a hogging moment adjacent to the slab edge (GL 27) where the slab is supported by a reinforced concrete wall (twin-wall construction). In the FE model, the support condition was modelled as pinned and the bending moment is zero at the slab edge, but the embedded instrumentation indicates that the wall provides some torsional restraint. For this reason, many structural design codes require additional torsional reinforcement at slab edges to resist bending which may occur in real structures, but are not determined during analysis or where simply supported end conditions are assumed. If the ‘measured’ bending moment along GL H is shifted downwards by the magnitude of the hogging moment at GL 27, there is good agreement between the analysis and insitu instrumentation.

During the striking, repropping and permanent removal of props to the second floor, the walkway slab along GL 22 (250mm thick, hybrid concrete lattice girder slab) adjacent to the slab at GL L was continuously propped and, therefore, the predicted hogging moment over the column at GL 22-L from the FE analysis would not be as large in the actual floor structure. Similar to GL H, there is relatively good correlation for the sagging moment at midspan along GL 22 (Figure 4-12b), and as expected the ‘measured’ hogging moment at GL L is less than the predicted moment.

Chapter 4. Real-time Monitoring of Concrete–Lattice-girder Slabs during Construction

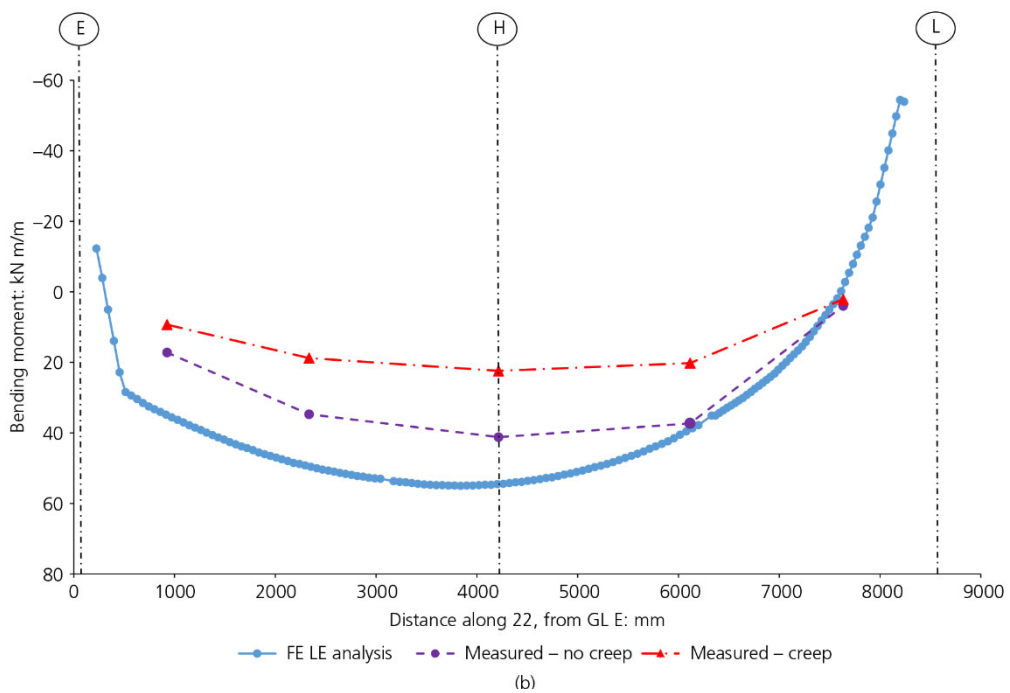
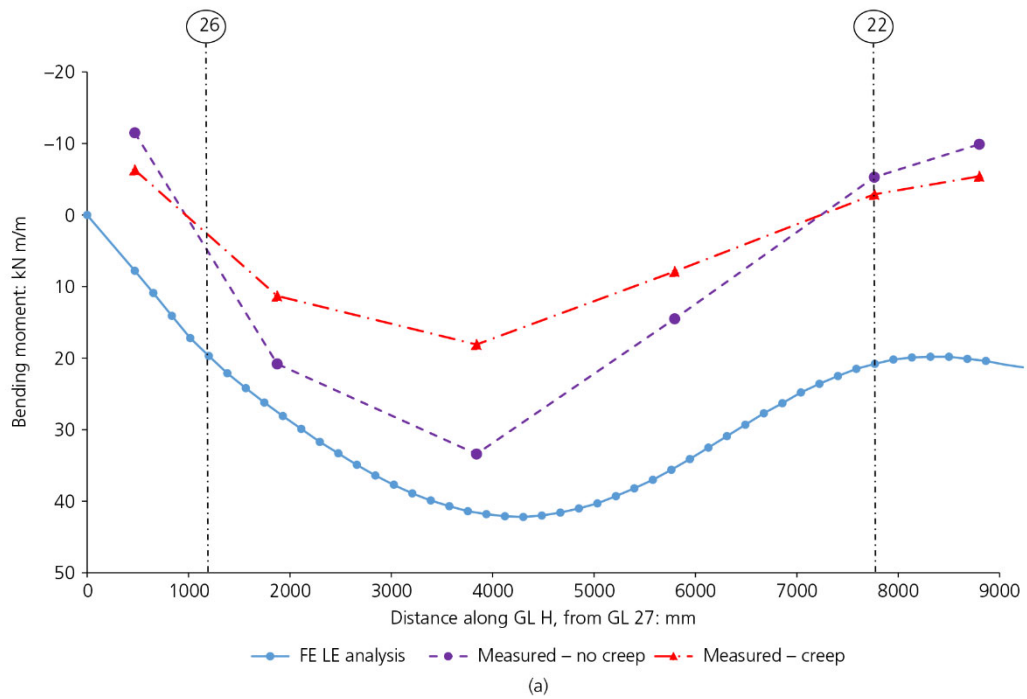


Figure 4-12 Predicted and measured bending moments in second floor of HBB; (a) Along GL H, (b) Along GL 22

The embedded sensors in the walkway slab did record moment transfer after striking the props for repropping and permanent removal of props in the adjacent 400mm thick slab and this would reduce the hogging moment over the column at

Chapter 4. Real-time Monitoring of Concrete–Lattice-girder Slabs during Construction

GL 22-L. The difference between the predicted moment over the column at GL L and the ‘measured’ moment may also be due to the fact that FE software can over-estimate peak moments over columns depending on the mesh size and how the column is modelled.

4.4.6 Time dependent effects

The prediction of strains for concrete elements systems is extremely difficult to estimate accurately [21]. The behaviour of a slab at service loads varies with time and depends on the extent of cracking, stiffness of the slab, creep, shrinkage and degree of restraint. A range of +15% to -30% between calculated and actual deflections is suggested in The Concrete Society publication on deflections in concrete slabs [22]. One of the key goals of this project is to monitor the time dependent effects (TDE) on the slab in HBB through the use of the insitu instrumentation. In this project, data will continue to be recorded from the sensors after the building is operational so that the long-term behaviour of the slab can be analysed and compared with various predictive models. There are numerous predictive models in the literature and design codes ([16], [23], [24]) for predicting TDE but there is still a large degree of uncertainty for predicting accurately the long-term behaviour of concrete structures at serviceability limit states. One of challenges when predicting TDE is that the properties of concrete change with time and at design stage it is very difficult to accurately know the insitu properties of the concrete as they evolve over time in response to environment and loading.

The slab in the HBB is subject to strains from thermal, shrinkage, creep and flexural components. The predicted strains in the second floor slab due to the various components determined using Eurocode 2 [16]) are compared with the measured strains from an embedded VW gauge at midspan along GL 22 in Figure 4-13 for the first six months (June 2015- Dec. 2015 inclusive) after the floor was poured. The predicted strains are determined using assumed values for the concrete properties and relative humidity. The applied loading due to self-weight and creep are assumed to commence after striking the props and repropping, which was 8 days after the insitu topping was poured. The measured strains from the VW strain

Chapter 4. Real-time Monitoring of Concrete–Lattice-girder Slabs during Construction

gauges are corrected for thermal effects so that only strain due to shrinkage, flexure and creep is determined from the gauge readings:

$$\mu\epsilon_{\text{load}} = \mu\epsilon_{\text{actual}} - \mu\epsilon_{\text{thermal}} = \Delta\epsilon + \Delta T \cdot \alpha_{\text{vw}} - \Delta T \cdot \alpha_c \quad (\text{Eqn. 4-3})$$

where $\Delta\epsilon$ is the change in measured strain; ΔT is the change in temperature; α_{vw} is the coefficient of thermal expansion of the VW gauge and α_c is the coefficient of thermal expansion of the concrete.

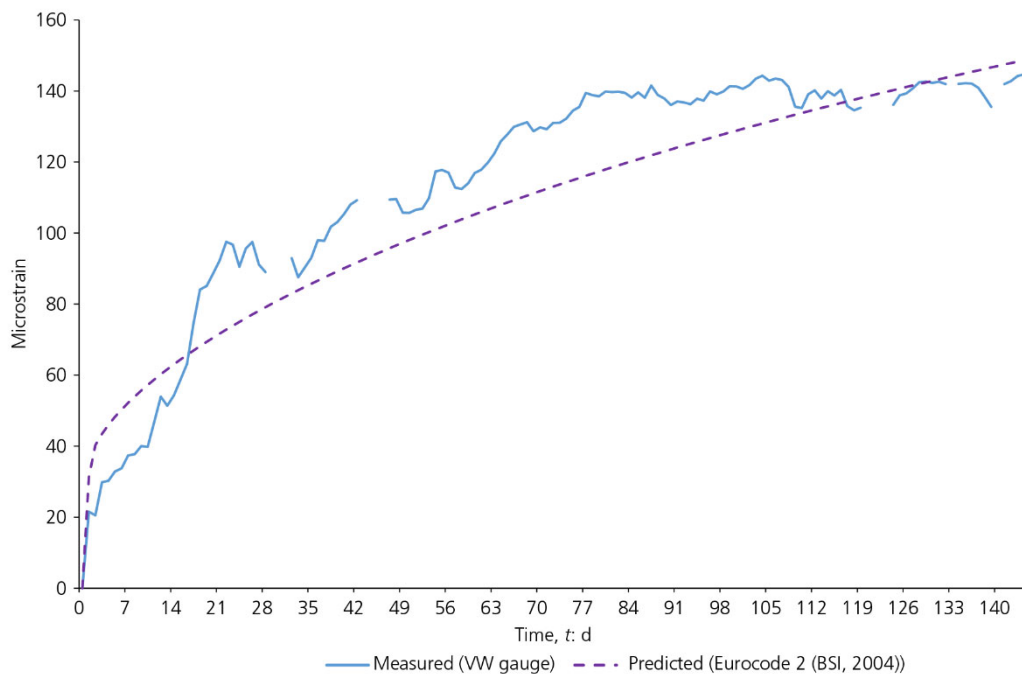


Figure 4-13 Comparison of predicted and measured strains in second floor of HBB

The dominant strain component is shrinkage and this accounts for approximately 60% of the strain induced on the second floor slab. For the strain gauge shown in Figure 4-13, there is relatively good correlation between the measured and predicted strain values considering the relatively large coefficient of variation for both creep (20%) and drying shrinkage (30%) when using the approach of Eurocode 2 [16] for determining strains. The next stage in this process is to incorporate actual concrete properties determined from testing and environmental data from the NUIG weather station (RH and temperature) and internal sensors to compare the effect of using assumed design values and actual data when calculating predicted strains. As there are over 100 VW gauges embedded in the second floor slab, it will allow a

Chapter 4. Real-time Monitoring of Concrete–Lattice-girder Slabs during Construction

meaningful study of the correlation between measured and predicted strain using a variety of models. The data from the sensors will continue to be collected from the sensors so that TDE in the floor slab (such as creep) can be studied and compared with predictive models.

4.5 Practical applications

The use of SHM, as implemented in this research project, has considerable practical relevance for Structural Engineering practitioners and many potential applications. Design guidelines are typically approximations which simplify the behaviour of the structure so that it can be analysed relatively quickly and simply. However, these approximations and simplifications have the potential to introduce errors or inaccuracies to the design process. The insitu instrumentation provides performance data on actual behaviour which can be used to verify design methods. Real time monitoring offers potential benefits in relation to optimisation of structural components by understanding the actual behaviour of components in use and the possibility to develop and calibrate numerical models that predict structural performance.

This paper illustrates the important role which real time monitoring (SHM) and the use of sensors can play for more accurate prediction and understanding of the actual structural behaviour of concrete components. Some of the practical applications demonstrated in this paper include:

- The use of sensors to accurately predict the temperature rise and temperature differentials in concrete components which can lead to more accurate predicting of early-age behaviour.
- The significance of accurate knowledge of material properties and environmental conditions to predict precisely early-age thermal cracking. The paper shows that basing design decisions on theoretical properties or assumed conditions can potentially lead to inappropriate design decisions.
- The determination of the restrained insitu coefficient of expansion in concrete components leading to more realistic restraint factors. Incorrect

Chapter 4. Real-time Monitoring of Concrete–Lattice-girder Slabs during Construction

restraint factors can result in uneconomical over-design or under-design leading to unacceptable cracking.

- The striking of formwork and backpropping is a critical part of the efficient and economic construction of flat slab structures. Embedded sensors can be used to measure the actual load transfer mechanism and assist with improved temporary works design and more efficient construction techniques.
- SHM can be used to improve understanding of actual structural behaviour and information from SHM programmes can be used to improve prediction models and codes of practice. In addition, with the increasing use of new construction materials and innovative construction practices, sensors can be used to provide confidence for designers in relation to actual performance of structures.
- Predicting time dependent effects (TDE) in concrete is one of the most difficult tasks in structural engineering. The use of sensors as described in this research project can be used to study the relationship between measured strain and the various prediction models.

4.6 Conclusions

This paper presents the motivation and implementation of a real time SHM strategy for a hybrid concrete lattice girder flat slab floor system. The embedded sensors in combination with the material testing and weather monitoring allow the performance of the floor structure to be monitored and the effect of various factors such as temperature, relative humidity and construction method to be studied. This project is such that data is recorded during the manufacture, construction and operational phase of the building so that early-age performance, construction behaviour and long-term effects can be analysed. It is envisaged that the rich information about the performance of the floor can be used to study the various design parameters of the hybrid concrete lattice girder flat slab floor system and identify potential optimisation of the floor system.

Discrepancies between performance of construction materials in the laboratory and their observed performance in the field has been reported [25], particularly with

Chapter 4. Real-time Monitoring of Concrete–Lattice-girder Slabs during Construction

respect to serviceability limit states of concrete (durability, deflection etc.). Therefore, insitu instrumentation can be used to assess the actual performance structural elements and assist designers during the design process of concrete structures to achieve long-term in-service performance criteria.

Acknowledgements

The authors would also like to thank the National University of Ireland Galway and particularly Mr. Colm Walsh, Senior Technical Officer in the Department of Civil Engineering for his help with the instrumentation in the demonstration buildings. They also wish to thank all the construction personnel and building professionals involved in the demonstrator buildings who facilitated and helped with installing the structural health monitoring systems, with a special thanks to Brian Holmes and Noel Waters of BAM Construction. The authors would like to acknowledge the financial support of the European Commission through the Horizon 2020 project Built2Spec (637221). The second author would like to acknowledge the support of Science Foundation Ireland through the Career Development Award programme (Grant No. 13/CDA/2200).

4.7 References

- [1] J. Goggins, S. Newell, D. King, and M. Hajdukiewicz, “Real-time monitoring of a hybrid precast and in situ concrete flat slab system,” in *Proceedings of Civil Engineering Research in Ireland (CERI 2014, Queens University Belfast, 28-29 August 2014)*, 2014, pp. 321–326.
- [2] M. Hajdukiewicz, D. Byrne, M. M. Keane, and J. Goggins, “Real-time monitoring framework to investigate the environmental and structural performance of buildings,” *Build. Environ.*, vol. 86, pp. 1–16, 2015.
- [3] S. Newell, M. Hajdukiewicz, and J. Goggins, “Real-time monitoring to investigate structural performance of hybrid precast concrete educational buildings,” *J. Struct. Integr. Maint.*, vol. 1, no. 4, pp. 147–155, 2016.
- [4] D. Byrne, J. Goggins, and E. Cannon, “The analysis of time dependent effects of concrete systems through in-situ structural health monitoring,” in *In IABSE Symposium Report (Vol. 98 No. 8) - Global Thinking in Structural Engineering: Recent Achievements. (IABSE Conference, Sharm El Sheikh, Egypt)*, 2012, pp. 27–34.
- [5] J. Goggins, D. Byrne, and E. Cannon, “The creation of a living laboratory for structural engineering at the National University of Ireland, Galway,” *Struct. Eng.*, vol. 90, no. 4, pp. 12–19, 2012.
- [6] N. R. Buenfeld, R. Davies, A. Karimi, and A. Gilbertson, “CIRIA Report C661: Intelligent monitoring of concrete structures,” CIRIA, London, UK., 2008.
- [7] ISIS Canada, “ISIS Canada Educational Module No. 5: An Introduction to Structural Health Monitoring,” ISIS Canada (Intelligent Sensing for Innovative Structures), Winnipeg, MB, Canada, 2005.
- [8] P. Bamforth, D. Chisholm, J. Gibbs, and T. Harrison, “Properties of concrete for use in Eurocode 2 (CCIP-029),” Cement and Concrete Industry Publication (UK), London, UK, 2008.

Chapter 4. Real-time Monitoring of Concrete–Lattice-girder Slabs during Construction

- [9] A. M. Neville, *Properties of concrete*, 5th Ed. Upper Saddle River, NJ, USA: Prentice Hall, 2011.
- [10] NSAI, “IS EN 206: Concrete - Specification, performance, production and conformity,” NSAI (National Standards Authority of Ireland), Dublin, Ireland, Ireland, 2013.
- [11] IRUSE Weather, “IRUSE Weather,” *Informatics research unit for sustainable engineering NUI Galway weather website*. [Online]. Available: <http://weather.nuigalway.ie/>. [Accessed: 20-Jul-2019].
- [12] P. B. Bamforth, “CIRIA Report C660: Early-age thermal crack control in concrete,” CIRIA, London, UK, 2007.
- [13] S. Mindess, Y. Young, and D. Darwin, *Concrete*, 2nd Ed. Upper Saddle River, NJ, USA: Prentice Hall, 2002.
- [14] M. E. FitzGibbon, “Large pours for reinforced concrete structures. Current Practice Sheet 2P/15/1, NO. 28,” *Concrete*, vol. 10, no. 3, p. 41, 1976.
- [15] FIB, “Externally bonded FRP reinforcement for RC structures (fib Bulletin No. 14),” FIB (The International Federation for Structural Concrete), Lausanne, Switzerland, 2001.
- [16] NSAI, “IS EN 1992-1-1: Eurocode 2: Design of concrete structures. Part 1-1: General rules and rules for buildings,” NSAI (National Standards Authority of Ireland), Dublin, Ireland, 2005.
- [17] S. J. Alexander, “Why does our concrete still crack and leak?,” *Struct. Eng.*, vol. 84, no. 23–24, pp. 40–43, 2006.
- [18] NSAI, “IS EN 1992-3: Eurocode 2 - Design of Concrete Structures - Part 3 : Liquid Retaining and Containment Structures,” NSAI (National Standards Authority of Ireland), Dublin, Ireland, 2006.
- [19] A. Beeby, “BRE 394: A radical re-design of the in-situ concrete frame process, Task 4: Early striking of formwork and forces in backprops,”

Chapter 4. Real-time Monitoring of Concrete–Lattice-girder Slabs during
Construction

Building Research Establishment (BRE), 2000.

- [20] The Concrete Society, “Formwork. A guide to good practice (CS 030),” The Concrete Society, Camberley, UK, 2012.
- [21] R. I. Gilbert, “Shrinkage, cracking and deflection-the serviceability of concrete structures,” *Electron. J. Struct. Eng.*, vol. 1, no. 1, pp. 2–14, 2001.
- [22] The Concrete Society, “Deflections in concrete slabs and beams (TR No. 58),” The Concrete Society, Camberley, UK, 2005.
- [23] American Concrete Institute, “ACI 209R-92 Prediction of Creep, Shrinkage and Temperature Effects in Concrete Structures (Reported by ACI Committee 207),” American Concrete Institute, Farmington Hills, MI, USA, 1992.
- [24] G. Ranzi and R. I. Gilbert, *Time-dependent behaviour of concrete structures*, 1st Ed. London, UK: CRC Press, 2010.
- [25] E. W. Gulis, D. Lai, and B. Tharambala, “Performance and Cost Effectiveness of Substructure Rehabilitation/Repair Strategies (Draft Report),” Ministry of Transportation of Ontario, Downsview, Canada, 1998.

5 Investigation of Thermal Behaviour of a Hybrid Precasted Concrete Floor using Embedded Sensors

Article Overview

This paper can be read in conjunction with the paper presented in the previous chapter. This paper also relates to the real time monitoring of the hybrid concrete lattice girder floor in the Human Biology Building which was constructed in 2015-2016. Whereas, **Chapter 4** focused on the structural behaviour of the concrete floor, this chapter focusses on the thermal behaviour of the concrete floor for the first year after construction.

Sensors were embedded in the lattice girder plank during manufacture of the precast floor products and sensors were also embedded in the insitu concrete topping so that the thermal response of the floor during the manufacture and construction phases could be studied. Environmental conditions such as ambient temperature, relative humidity, solar irradiance and wind speed were also monitored, as they can have a significant effect on the thermal behaviour of concrete structures. In some structures, thermal strains can be significantly greater than the strains due to service loading and can cause cracking and affect long-term durability of concrete structures. The early-age thermal effects when the heat of hydration from the cement is dominant is studied and the prediction of peak temperature rise and peak temperature differential using CIRIA Report C660 is explored. The response of the hybrid concrete slab to changes in ambient temperature (daily and seasonal) and solar radiation over one year is reviewed in the paper. In addition, the potential application of monitoring data to determine restraint factors and insitu coefficient of thermal expansion of the concrete is studied in the paper.

The paper also describes the development of a one-dimensional finite difference model to examine the temperature profile through the hybrid concrete slab. The model takes account of four modes of heat transfer: conduction, convection, solar radiation and thermal irradiation. The temperature profile from the 1-D model is

Chapter 5. Investigation of Thermal Behaviour of a Hybrid Precasted Concrete Floor using Embedded Sensors

compared with the measured temperatures using the sensors and found to be relatively accurate. The rich field thermal data in this paper can also be used for further development of numerical models.

Currently, there is a lack of field data related to thermal behaviour of concrete floors. The author believes that the concrete industry needs to publish more case studies with robust field data if the thermal mass of concrete floors is to be harnessed effectively for more sustainable structures. The novelty of this work is that it relates to a hybrid concrete floor and explores the thermal behaviour of both the precast plank and insitu topping during the manufacture and construction stages using field data and environmental data. This paper will be of interest to the designers of concrete floors who wish to understand and predict how concrete floors will behave in response to the heat of hydration, ambient temperature and solar radiation.

More information on the 1-D numerical model described in the paper is presented in **Appendix C**. This chapter was published in the *International Journal of Concrete Structures and Materials* (2018).

Abstract

Concrete structures expand and contract in response to temperature changes which can result in structural strain and cracking. However, there is a limited amount of robust field data on hybrid concrete floor structures. Shortage of such data impacts on our understanding of how concrete structures respond to thermal effects and ultimately the overall design of concrete structures. Thus, a comprehensive structural and environmental monitoring strategy was implemented by the authors during the construction of an educational building. Sensors were embedded in the precast and in situ components of a hybrid concrete lattice girder flat slab so that the thermal response of the floor during the manufacture, construction and operational stages could be investigated. Many aspects of the thermal behaviour of the floor during the construction phase were monitored using the embedded sensors. The early-age thermal effects during curing and the impact of the variation of ambient temperature (daily and seasonal) and solar radiation on the behaviour of concrete floor is explored in the paper. Values for restraint factors and the in situ

Chapter 5. Investigation of Thermal Behaviour of a Hybrid Precasted Concrete Floor using Embedded Sensors

restrained coefficient of thermal expansion of concrete are calculated using the data from the embedded sensors. Numerical modelling of the thermal behaviour of the hybrid concrete floor was undertaken and validated using the real-time field measurements. The data presented and analysed in this paper can be used to improve the understanding and modelling of the thermal behaviour of a hybrid concrete floor. This will assist with improved design of sustainable buildings as it allows the environmental performance of the floor to be optimised with respect to controlling the internal environment, thermal mass and energy efficiency.

5.1 Introduction

Most concrete structures are subjected to frequent temperature changes during their design life. In fact, the internal temperature of a reinforced concrete element and relative humidity can be considered as two of the key indicators to monitor and evaluate the condition of the material and detect structure deterioration [1]–[3]. For example, Hover [4] explored the similarity between concrete and the human body in regard to the influence of temperature and moisture conditions on health and performance. The expansion and contraction of concrete structures in response to temperature can result in structural strain and cracking. The strain through a winter/summer cycle can be up to ten times greater than that due to service loading [5]. Furthermore, consideration of thermal effects is particularly important for designers checking the possibility of early-age thermal cracking. Movement of concrete elements due to thermal effects is unavoidable due to the heat of hydration as the concrete hardens. During the hydration process, the concrete expands as the heat of hydration exceeds the rate at which heat is dissipated, but then the concrete contracts as the concrete cools down to ambient temperature. These volume changes would be of little consequence if the concrete was unrestrained and free to expand and contract without creating any stresses. However, in real structures, most concrete elements have some form of restraint (internal or external) and, therefore, stresses are generated which have the potential to cause cracking which can affect the long-term performance and durability of concrete structures. Hence, it is very important to understand the thermal response of concrete components (concrete temperature, thermal strain etc.) so that better prediction models may be developed.

Chapter 5. Investigation of Thermal Behaviour of a Hybrid Precasted Concrete Floor using Embedded Sensors

Knowledge of the thermal behaviour of concrete components can also be used to improve the energy performance of buildings and the thermal comfort of the occupants [6]. For example, Høseggen *et al.* [7] found that exposed concrete in the ceiling of an office building on the Nord-Trøndelag College (HiNT) campus in Norway both considerably reduces the number of hours with excessive temperatures and created a better and more stable thermal environment during the working day when compared to utilising a suspended ceiling.

Many modern buildings have a building management system (BMS) that monitors and controls the environmental conditions and energy consumption during the operational phase of the building life cycle. The use of embedded sensors to monitor the actual behaviour of components within the building complements the data from the BMS and allows a more holistic evaluation of the performance of the building. Linking data from embedded temperature sensors in the concrete floor slabs with the room air temperature and external weather conditions in the BMS could assist with making the most effective use of thermal mass within a building in controlling internal comfort conditions and minimising energy consumption. The additional advantage of the embedded sensors is that they can be used to study the behaviour of components at all stages of its life cycle (manufacture, construction, operation).

Ge *et al.* [8] conducted an experimental study investigating the accuracy of various embedded strain sensors (vibrating-wire strain gauge, electrical resistance gauge, Fibre Bragg grating sensor and Brillouin optical fibre sensor) to measure the response of concrete beams subjected to thermal loading. They concluded that vibrating-wire strain gauges produced the most stable and reliable results (compared to theoretical calculations) among the four sensors. In addition, following an experimental and numerical study of VW strain gauges with metallic and plastic housing, Azenha *et al.* [9] recommended the use of metallic VW strain gauges for early-age concrete strains as they are more robust than those that use plastic housing and present lower temperature sensitivity.

Observations and findings from embedded instrumentation in a hybrid precast concrete flat slab floor in a recently constructed educational building are presented in this paper. The embedded sensors permitted real-time monitoring of the floor during the manufacture, construction and operational phases of the building. The

Chapter 5. Investigation of Thermal Behaviour of a Hybrid Precasted Concrete Floor using Embedded Sensors

embedded sensors in this project are part of a structural health monitoring (SHM) strategy which has been developed in the National University of Ireland Galway (NUI Galway) to monitor the structural and environmental performance of a number of educational buildings ([6], [10], [11]). SHM can be defined as a non-destructive in-situ structural evaluation method that uses any of several types of sensors which are attached to, or embedded in, a structure [12]. A schematic summarising the SHM methodology which was implemented for this project is shown in Figure 5-1. The data from the sensors can be used to assess the safety, integrity, strength, or performance of the structure, and to identify damage at its onset.

In this paper, details are provided of a case study building, floor structure and the extensive instrumentation installed in the floor. Monitoring of the floor using the embedded sensors is ongoing with automatic data logging at frequent time intervals. This paper presents the results for the first twelve months of the building prior to the operational phase of the building. The results show the transient, seasonal and diurnal thermal response of the concrete floor.

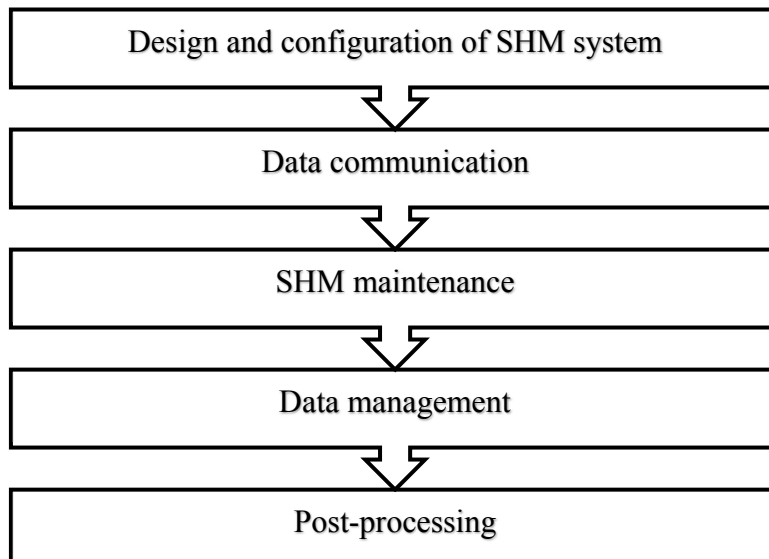


Figure 5-1 Visual schematic of the SHM methodology [10]

5.2 Methodology

5.2.1 Case study building

The Human Biology Building (HBB) on the NUI Galway campus is the new home to three existing schools: Anatomy, Physiology & Pharmacology and Therapeutics (Figure 5-2). The building is a teaching and research facility for undergraduate and postgraduate students and incorporates laboratories, lecture theatres and meeting rooms. The building is a five storey building including basement and two storey plant enclosure at roof level. The building has a gross floor area of 8200m² and the project cost is in excess of €30 million. Construction commenced in January 2015 and the construction period was 22 months.



Figure 5-2 Human Biology Building

The basement was constructed using insitu concrete and above ground the majority of the structure was constructed using precast concrete components such as twinwall system, hybrid concrete lattice girder slabs and hollowcore slabs. All precast components were designed, manufactured and installed by Oran Pre-Cast Ltd., who is located 10km from the site.

The majority of the floor structure in the HBB was constructed using two-way spanning hybrid concrete lattice girder flat slab floor system (either 400mm or 250mm thick). This floor system was selected by the contractor to reduce construction time, reduce steel fixing on site, minimise formwork, improved safety and because of its high quality finish. The lattice girder plank (Figure 5-3) consists of a 65mm thick concrete slab, which contains the bottom layer of reinforcement of

Chapter 5. Investigation of Thermal Behaviour of a Hybrid Precasted Concrete Floor using Embedded Sensors

the slab and a steel lattice girder which protrudes from the plank. The lattice girder planks are temporarily propped when erected on site and the top layer of reinforcement is placed on site prior to pouring the structural concrete topping. Steel reinforcement ‘stitching’ bars are also required to be placed across adjacent precast planks to compensate for the discontinuity caused by discrete planks, whose size is limited by transportation logistics. Thus, two-way spanning action is achieved by positioning these ‘stitching’ bars across the joints between adjacent planks. The steel lattice girder is required to provide stiffness to the plank during construction and also to improve the composite action between the plank and structural topping. The props are removed when the structural topping has reached the required compressive strength.



Figure 5-3 Precast Concrete Lattice Girder Plank

5.2.2 Embedded sensors and data acquisition

This project used a number of sensors (Figure 5-4) which were embedded in the floor structure to monitor the environmental and structural performance of the hybrid concrete lattice girder flat slab:

- Vibrating Wire (VW) gauges (Gage Technique model TES/5.5/T) embedded in concrete that measure strain and temperature. The range of the measured strains is greater than 3000 microstrains and the resolution is

Chapter 5. Investigation of Thermal Behaviour of a Hybrid Precasted Concrete Floor using Embedded Sensors

better than 1 microstrain. The measured temperature range is -20°C to $+80^{\circ}\text{C}$ with an accuracy of $\pm 1^{\circ}\text{C}$.

- Electrical resistance (ER) strain gauges (Tokyo Sokki Kenkyujo model FLA-6-11) bonded to steel reinforcement in concrete, which measure uniaxial strain. The ER gauges have a strain limit of 5% and the gauge resistance is $120\Omega (\pm 0.3\Omega)$.
- IP68 rated thermistor sensors (ATC Semitec model IP 68) which are capable of measuring concrete temperature. The thermistors have a temperature range of -50°C to $+110^{\circ}\text{C}$ with a 1% tolerance.

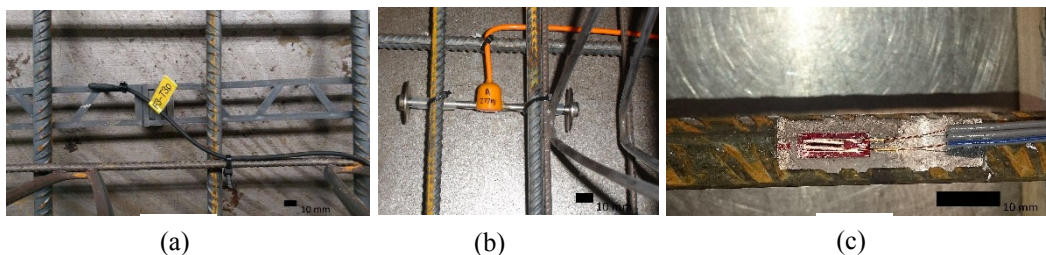


Figure 5-4 Sensors embedded in the building's structure: (a) thermistors; (b) VW gauges; (c) ER gauges

The embedded sensors are located within two zones of the second floor of the HBB along a number of orthogonal grids. The location of the embedded sensors in one zone of the second floor slab is shown in Figure 5-5. Sensors were installed prior to manufacture of some of the precast lattice girder planks to allow the behaviour of the floor to be monitored during the manufacturing process. The VW gauges are typically arranged such that there are four gauges through the depth of the floor (Figure 5-6). This allows the three-dimensional profile of the change in strain and temperature in the floor slab to be monitored.

To collect data from the sensors, a data acquisition system consisting of CR1000 data loggers, AM16/32B multiplexers and AVW200 vibrating wire interface from Campbell Scientific were used to collect and store real-time data from the embedded instrumentation. This system has automatically recorded data from the precast planks since manufacture and the insitu concrete topping since the concrete pour on site. During the construction phase, data was manually downloaded onto a laptop, but after commissioning of the building, data is downloaded over a local network using Campbell Scientific's NL116 Ethernet interface and compact flash

Chapter 5. Investigation of Thermal Behaviour of a Hybrid Precasted Concrete Floor using Embedded Sensors

module. This allows long term monitoring of the behaviour of the floor during the operational phase of building. This data is being stored on a dedicated server and is available for students for both teaching and research applications.

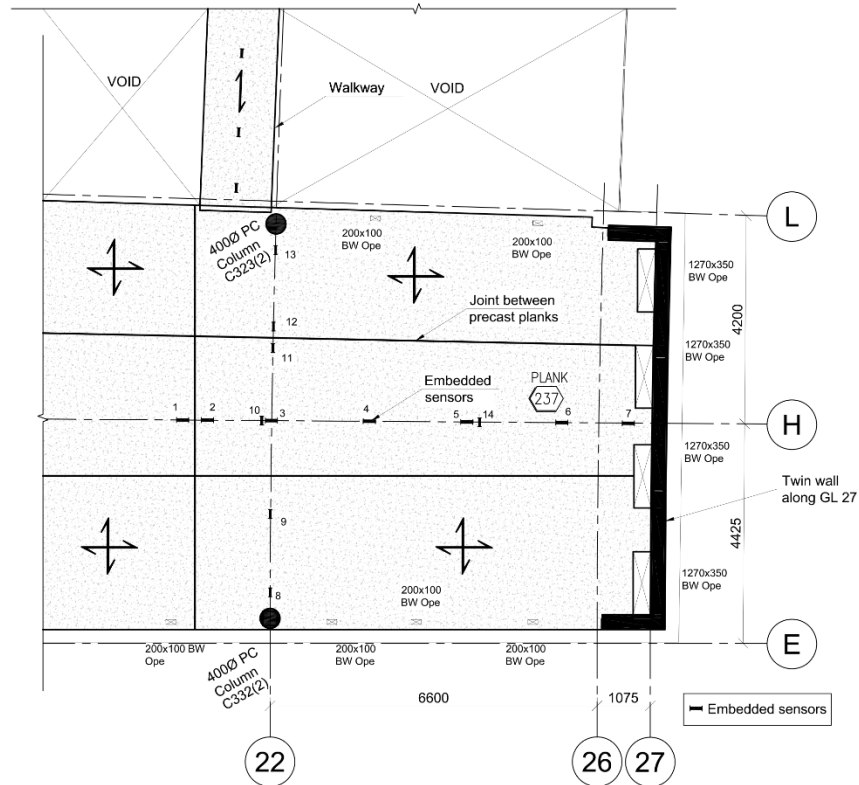


Figure 5-5 Embedded sensors in one zone of the second floor of HBB [13]

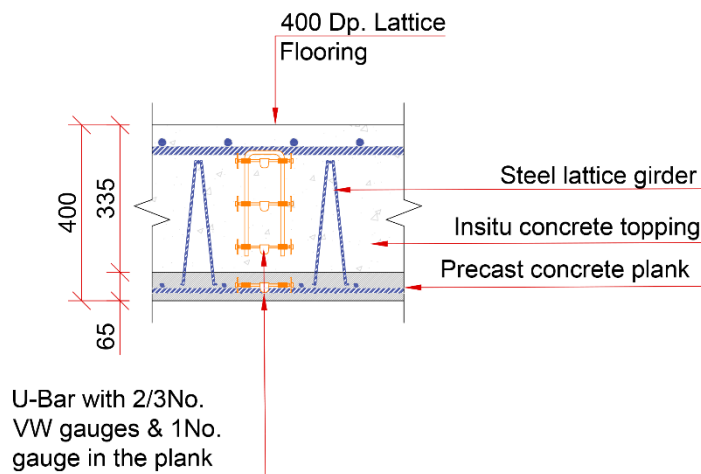


Figure 5-6 Typical section showing locations of vibrating wire gauge installed in the flat slab system [13]

Chapter 5. Investigation of Thermal Behaviour of a Hybrid Precasted Concrete Floor using Embedded Sensors

5.2.3 Material testing

A comprehensive material testing programme was undertaken to measure the properties of the concrete (precast and insitu) in the floor over time. Concrete specimens (cubes, cylinders and prisms) were made and cured in water (in accordance with EN 12390-2 [14]) and in air (to replicate environmental conditions on site). The properties of concrete will change over time, and therefore, it is very important to accurately measure the properties which are required to (i) interpret the data from the embedded sensors and (ii) as inputs when modelling the behaviour of the floor. Testing of concrete used in the second floor of HBB was undertaken for one year after the insitu topping was poured on site.

5.2.4 Environmental conditions

Changes in the environmental conditions surrounding any concrete element will have a significant effect on its behaviour with respect to deformation, strength, durability and service life [15]–[17]. Outdoor weather conditions were provided by the automatic weather station [18] (IRUSE 2017) at the NUI Galway campus which is located less than 1km from the HBB building. This weather station records air temperature, relative humidity, wind speed and direction, solar irradiance and rainfall at one minute intervals. As construction proceeded and the erection of the external façade commenced, a standalone data logger (Easy Log EL-USB-2+) which measures ambient temperature and relative humidity was positioned on site in December 2015 so that the precise internal environmental conditions around the second floor were recorded. This is important as the building became weathertight and the commissioning phase of the heating system for the building commenced. In the long term, the internal environment will be monitored using the building management system. When comparing the ambient air temperature readings from the external weather station and internal data logger, the difference is not significant until after August 2016, when the façade of building is fully complete.

5.2.5 Data post-processing

The embedded vibrating wire strain gauges (Gage Technique model TES/5.5/T) measure both change in strain and temperature (via thermistors) in the concrete slab. Changes in the internal temperature of the concrete slab will cause expansion and

Chapter 5. Investigation of Thermal Behaviour of a Hybrid Precasted Concrete Floor using Embedded Sensors

contraction of both the concrete and vibrating wire gauge that is used to measure change in strain in the concrete. Failure to correct for the thermal effects in the VW strain gauges would lead to erroneous strain readings. The difference between the coefficient of thermal expansion of the concrete and VW strain gauge will give rise to an apparent change in strain in the concrete. The coefficient of thermal expansion of the VW strain gauges is $11\mu\epsilon/^\circ\text{C}$ and for this project it was assumed that the coefficient of thermal expansion of the concrete was $9\mu\epsilon/^\circ\text{C}$. The measured strain readings (apparent strain) from the VW gauges are corrected for thermal effects using the following equation so that only strain due to shrinkage, flexure and creep is determined:

$$\mu\epsilon_{\text{load}} = \mu\epsilon_{\text{actual}} - \mu\epsilon_{\text{thermal}} = \Delta\epsilon + \Delta T \cdot \alpha_{\text{vw}} - \Delta T \cdot \alpha_{\text{c}} \quad (\text{Eqn. 5-1})$$

where $\Delta\epsilon$ is the change in measured strain; ΔT is the change in temperature; α_{vw} is the coefficient of thermal expansion of the VW gauge and α_{c} is the coefficient of thermal expansion of the concrete.

The effect of the thermal correction can be seen in Figure 5-7, where the temporal apparent and corrected strains are shown with the slab's internal temperature for the first month after the insitu topping is poured. Without the temperature correction, the strain data would apparently indicate a tensile strain when the actual strain in the concrete is compressive. The measured strains from the VW strain gauges will record strain due to shrinkage, flexure and creep. Strain due to flexure and creep will not be significant until the supporting props are removed and re-propped. The dominant strain component is shrinkage during the early stages. Further analysis of the measured strains from the embedded sensors and comparison with predicted strains using Eurocode 2 [19] is provided in a paper by the same authors focussing on the structural behaviour of the floor during construction [13].

In the literature, there is no agreement on the time at which the concrete stiffness has exceeded that stiffness of the strain gauge so that measured strains are consistent with the strains in the concrete (Time Zero). Prior to this time, the concrete is not sufficiently stiff to transfer strains to the embedded strain gauge or to restrain the gauge under applied thermal loads. Boulay and Paties [20] conducted a laboratory and numerical study of the interaction between early-age concrete and VW strain

Chapter 5. Investigation of Thermal Behaviour of a Hybrid Precasted Concrete Floor using Embedded Sensors

gauges and found that once the concrete modulus exceeded 1500MPa, the errors between measured and imposed deformations, due to thermal or structural loads were less than 5%.

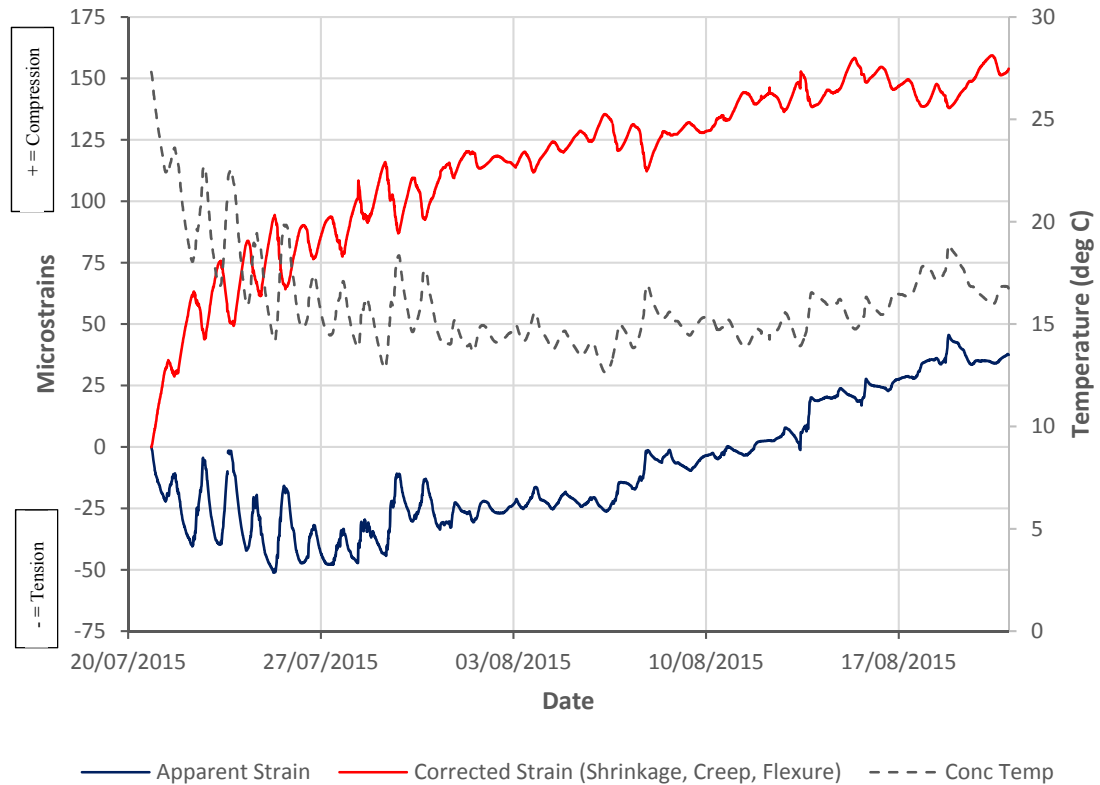


Figure 5-7 Comparison of apparent and corrected strains from VW strain gauges

In this study, the zero point for strain readings is assumed to be time at which the maximum concrete temperature is reached. Prior to the concrete reaching its maximum temperature, the concrete can be assumed to be in, or near to, a zero stress state due to creep [21]. The insitu concrete topping for second floor slab in HBB in which the sensors were embedded was poured on the 20th July 2015 at 10.00 and the peak concrete temperature was recorded approximately 8-11 hours after the pour. Therefore, it is assumed that the zero point is 20.00 on the 20th July 2015. This may be considered conservative as Cusson and Hoogeveen [22] proposed that that ‘Time Zero’ should be determined when the rate of temperature in the concrete increases sharply. Figure 5-8 plots the temporal rate of temperature change (left axis) and the measured temperature change (right axis) developing in the concrete after casting from one of the embedded VW strain gauges located in the middle of

Chapter 5. Investigation of Thermal Behaviour of a Hybrid Precasted Concrete Floor using Embedded Sensors

the slab. This suggests that 'Time Zero' occurs somewhere between four and ten hours after casting.

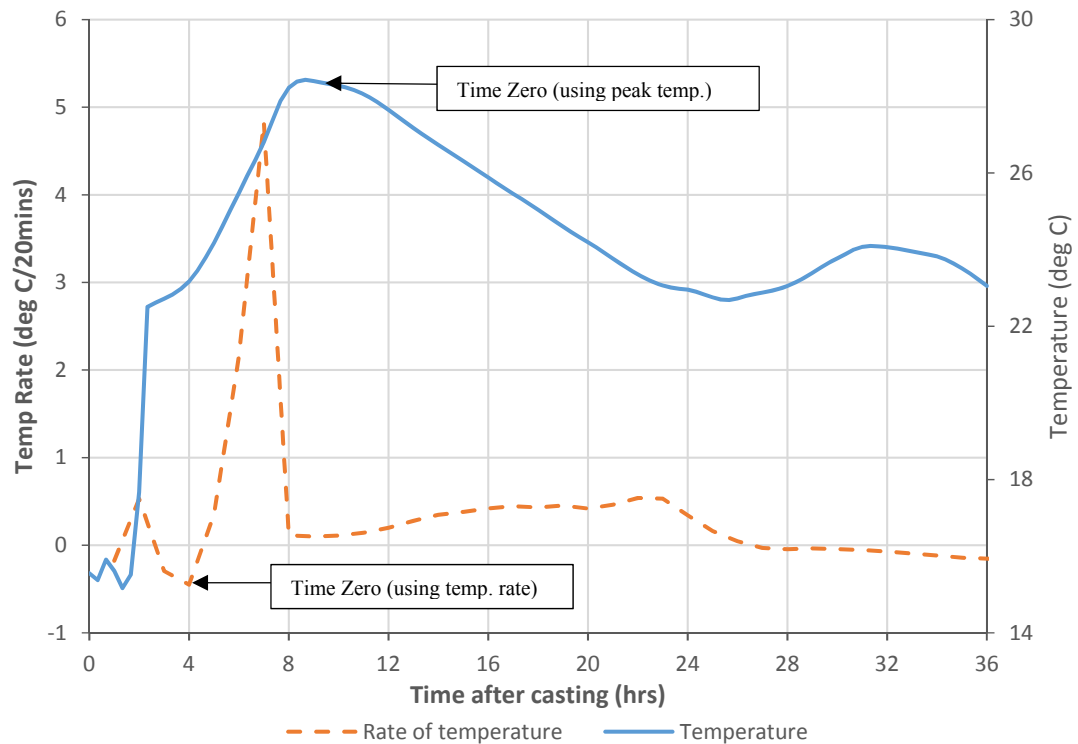


Figure 5-8 Determination of Time Zero from measured temperature in the concrete

5.2.6 Numerical model

A one-dimensional finite difference model was developed to model the temperature profile in the hybrid concrete slab. It was assumed that a one-dimensional model through the slab thickness was applicable for the internal sections of the slab and the model is validated against embedded sensors located internally in the slab. The model is based on the numerical method developed by Ross and Bray [23] and uses heat diffusion theory described by Crank [24]. The model developed is similar to the model described in CIRIA Report C660 [25] and uses the two component model developed by Dhir et al. [26] based on test data to predict the heat of hydration. The 400mm overall thickness of the hybrid slab was modelled with a spatial resolution of 20mm. At the top surface, four modes of heat transfer are considered: conduction into the concrete, convection, solar radiation (absorption) and thermal irradiation to the surroundings. At the bottom surface, it is assumed that there is no heat transfer due to solar radiation.

Chapter 5. Investigation of Thermal Behaviour of a Hybrid Precasted Concrete
Floor using Embedded Sensors

The following equations are used in the model to describe heat transfer through the concrete slab:

(i) Conduction: $q_{\text{cond}} = k (T_0 - T_1)/\Delta x$ (Eqn. 5-2)

where k is the thermal conductivity of the concrete, T_0 and T_1 are the surface and internal temperature at the first internal node, and Δx is the space increment in the model (through the depth of the concrete).

(ii) Convection: $q_{\text{conv}} = h (T_0 - T_a)$ (Eqn. 5-3)

where h is the convection coefficient (thermal conductance) of the concrete surface (wind speed has a significant effect), T_0 is the concrete surface temperature, and T_a is the ambient temperature.

(iii) Solar Radiation $q_{\text{sol}} = \gamma_{\text{abs}} Q_{\text{inc}}$ (Eqn. 5-4)

where γ_{abs} is the solar absorptivity of the concrete and Q_{inc} is the incident solar radiation (measured from weather station).

(iv) Thermal Irradiation: $q_{\text{irr}} = \sigma \epsilon (T_{0k}^4 - T_{\text{sky}}^4)$ (Eqn. 5-5)

where σ is the Stefan-Boltzmann constant, ϵ is the emissivity of the concrete, T_{0k} is the concrete surface temperature (in Kelvins), and T_{sky} is the sky temperature.

The difference-calculation remains numerically stable, if the following is valid for the time increment:

$$\Delta t \leq (C\rho/2k) \cdot \Delta x^2 \quad (\text{Eqn. 5-6})$$

where Δt is the time increment, Δx is the space increment, C is the specific heat of the concrete, ρ is the density of the concrete and k is the thermal conductivity of the concrete.

At the commencement of the pour, the precast plank is assumed to be the same temperature as the ambient temperature (15.1°C) and the placing temperature of the concrete is assumed to be 20°C (5°C difference is typical based on previous studies in the UK ([27], [28])). Environmental conditions, measured from the nearby

Chapter 5. Investigation of Thermal Behaviour of a Hybrid Precasted Concrete Floor using Embedded Sensors

automatic weather station [18], such as ambient temperature, wind speed and solar irradiation are used as input parameters in the model. The thermal properties (thermal conductivity, specific heat, diffusivity) of the concrete (insitu topping) and precast plank are assumed constant. The specific heat of the concrete (C) in the model was assumed to $1.0\text{kJ/kg}^\circ\text{C}$ and the thermal conductivity of the reinforced concrete (k) was assumed to be $2.34\text{W/m}^\circ\text{C}$; both values were determined based on the mix design, aggregates (limestone) and percentage reinforcement used in the floor slab in the HBB. The convection coefficient (or thermal conductance) of the surface (h) used in the model at the top and bottom of the slab is based on the measured wind speed [29]. When the external cladding was installed, it was assumed that the wind speed was zero for the purposes of determining the convection coefficient and there was no heat transfer due to solar radiation or thermal irradiation.

5.3 Results

The results presented in this paper focus on the manufacture and construction phases of the HBB and relate to a time period of approximately one year. The use of sensors to monitor the temperature of concrete during the first few days is common practice, but long-term monitoring is not always implemented. Knowledge of the temperature profile within concrete elements can be used to determine maturity, strength development, when formwork can be removed and potential for early-age thermal cracking. In addition, many sensors are affected by temperature and require temperature correction and, therefore, temperature is a very common parameter in structural monitoring. In this project, the concrete temperature was monitored during the manufacture of the precast plank and pouring of the second floor insitu concrete topping. As outlined previously, the ambient temperature was also monitored during manufacture of the precast plank and during the construction phase of the HBB. The temperature of the concrete slab is being continuously monitored during the operational phase of the HBB using the embedded sensors.

5.3.1 Early-age thermal effects

Predicting early-age thermal cracking is very complex as there are numerous factors which affect the potential for cracking and properties of the concrete (elastic

Chapter 5. Investigation of Thermal Behaviour of a Hybrid Precasted Concrete Floor using Embedded Sensors

modulus, compressive strength, tensile strength) are rapidly changing during the early stages of curing. The use of insitu instrumentation in this project allowed the thermal behaviour of the second floor slab to be recorded and this data can be used during the design process for checking early-age thermal cracking. Two important temperature considerations for control of early-age thermal cracking are [25]:

a) the temperature rises above the adjoining concrete or substrate and this is applicable to conditions of external restraint. External restraint occurs where an external element restrains the early thermal movements of a member being cast. External restraint can be classified as continuous edge restraint, end restraint or intermittent restraint (more than one type of external restraint may apply). The degree of external restraint will depend on the member being cast (wall, slab, beam and their dimensions) and the construction process (supporting elements, reinforcement and construction sequence).

(b) the maximum temperature differential and thermal gradient within the section. This is the condition of internal restraint and occurs where one part of a concrete pour expands or contracts at a different rate to another part of the same section. It typically occurs in thick sections in which there can be a large temperature differential across the section and can lead to both surface cracking and internal cracking (which may not be observable from the surface). Internal restraint can also occur when there is large percentages of reinforcement restraining the concrete.

Usually either external or internal restraint dominates but there are some situations in which both types of restraint need to be considered.

The second floor slab in the HBB consists of a 65mm thick lattice girder plank and 335mm insitu concrete topping (400mm overall thickness). As noted previously, at most locations there were four VW strain gauges positioned through the depth of the slab (top insitu, middle insitu, bottom insitu and precast). The temperature in the concrete at one location in the slab is shown in Figure 5-9 for the first two weeks after the pour. The heat of hydration effect on the concrete temperatures is clearly observed during the early days of curing. The peak temperature occurs approximately ten hours after pouring when the difference between the concrete temperature and ambient air is approximately 13°C. Concentrating on the three VW

Chapter 5. Investigation of Thermal Behaviour of a Hybrid Precasted Concrete Floor using Embedded Sensors

gauges in the insitu structural topping, the ‘middle’ gauge records the highest concrete temperature (28°C) as it is insulated by the surrounding concrete and is slowest to cool down. As expected, the ‘top’ gauge in the insitu topping records the lowest peak temperature because of heat transfer from/to the external concrete surface to air through convection. The effect of heat transfer through conduction between the insitu topping and the precast plank is also noted as the temperature in the precast plank increases by approximately 9°C after approximately fourteen hours since the pour commenced. The relatively low maximum temperature differential (13°C) between the concrete and ambient air can be partially explained by the mix design for the concrete topping in the HBB. The mix design for the insitu structural topping was 70% CEM I cement and 30% GGBS (ground granulated blast-furnace slag) with total cement content of 330kg/m³. It is common to blend GGBS (typically 30-50%) with CEM I cements to reduce the heat of hydration and likelihood of early-age thermal cracking. CIRIA Report C660 by Bamforth [25] provides guidance on controlling cracking due to early-age thermal cracking, but it states that direct measurement is the most reliable method for determining the temperature rise during the heat of hydration because of the large number of parameters which can affect its value. The CIRIA document is primarily focussed on construction of walls and does not provide explicit guidance for determining the temperature rise for concrete topping poured on top of a precast plank. The predicted maximum temperature rise using the CIRIA document is approximately 19°C and this is determined assuming the insitu topping is similar to a suspended floor slab with an uninsulated top surface (the thickness of the wall is increased by a factor of 1.3 and steel formwork is assumed).

The end of the hydration phase is difficult to determine precisely, but after the first few days it appears that the thermal response of the slab is primarily driven by the ambient air temperature and solar gain (Section 5.3.5). After the first day, the maximum and minimum concrete temperatures were recorded in the gauges located near the top of the insitu topping. The peak daily concrete temperatures after the first day decrease through the depth of the slab, the highest in the top and lowest in the precast plank at the bottom of the slab. Similarly, the time lag between the peak ambient temperature and peak concrete temperature increases from top to bottom through the 400mm thick slab. This illustrates that the top surface of the slab is

Chapter 5. Investigation of Thermal Behaviour of a Hybrid Precasted Concrete Floor using Embedded Sensors

subject to radiant heating from the sun and the potential of the concrete slab to act as a thermal mass to store and release heat. The time lag between the peak ambient temperature and the peak concrete temperature in the top of the slab in the first few days after the initial heat of hydration varies between two and six hours. It is noted that after the 30th July 2015 (Figure 5-9) that the differential between the concrete and ambient air temperature is significantly reduced. This is explained by the fact that the precast planks for the third floor (over the second floor with embedded sensors) were erected on the 31st July 2015 and, therefore, shaded the second floor slab which reduced heat gain from the summer sun.

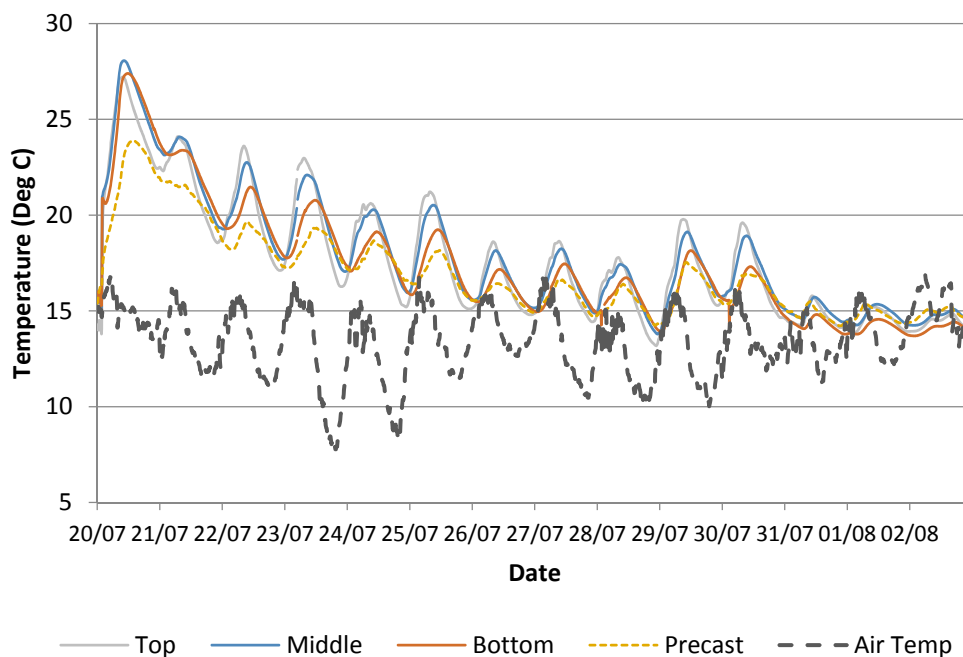


Figure 5-9 Concrete temperature in the 335mm insitu structural topping (14 days after pour)

Large temperature differentials between the surface and centre of concrete elements can lead to internal restraint, which can lead to cracking and this is of critical importance for thick concrete elements. Quantifying and controlling the temperature differential within the concrete section is one of the critical design checks when considering early-age thermal cracking. The maximum recorded temperature differential within the 335mm thick concrete topping in the second floor slab in HBB never exceeded 3°C. Using the CIRIA Report C660 [25], the predicted maximum temperature differential is 13°C, but this figure is based on

Chapter 5. Investigation of Thermal Behaviour of a Hybrid Precasted Concrete Floor using Embedded Sensors

applying temperature data for walls and adjusting for suspended floor slab with an uninsulated top surface. The CIRIA report recommends thermal modelling for reliable predictions of thermal behaviour of concrete elements. This paper highlights the advantages of using embedded instrumentation to record the actual thermal behaviour of concrete elements and that it can be used to improve the design process for controlling early-age thermal cracking.

The temperature profile through the depth of the slab (400mm overall thickness) at a location in the middle of the slab is shown for the first 24 hours after pouring in Figure 5-10. The ambient air temperature at the time of the pour was approximately 15°C and it is noted that the concrete temperature in the precast plank before the pour of the concrete topping is approximately the same (ambient temperatures shown at bottom of Figure 5-10). The peak concrete temperature during the curing phase occurs 10 hours after the pour at 20.00 and the highest temperatures are recorded in the middle of the slab. The temperature in the precast plank lags behind the temperatures in the insitu topping and the lowest temperatures in the insitu topping are recorded in the top of the slab as heat is lost to the exposed top surface. During the cooling phase, it is observed that after 24hrs the middle of the slab has the highest temperatures as it is the slowest section of the slab to cool down. During the first 24hrs, the temperature differentials between the VW gauges never exceeds 3°C, but it is likely that the maximum differentials between the top surface of the concrete slab and middle of the insitu topping were significantly higher. They are relatively low as the thickness of the insitu topping (335mm) is relatively thin and allows the heat to dissipate relatively quickly. For mass concrete, a temperature differential limit of 20°C is often used, but concrete can crack at higher or lower temperature differentials.

As noted previously, in Figure 5-9, there are temperature variations through the depth of the slab during the curing phase and at all subsequent stages of construction. Temperatures recorded by the VW strain gauges embedded through the depth of the slab show that they reach different maximum and minimum temperatures and that they occur at different times.

Chapter 5. Investigation of Thermal Behaviour of a Hybrid Precasted Concrete Floor using Embedded Sensors

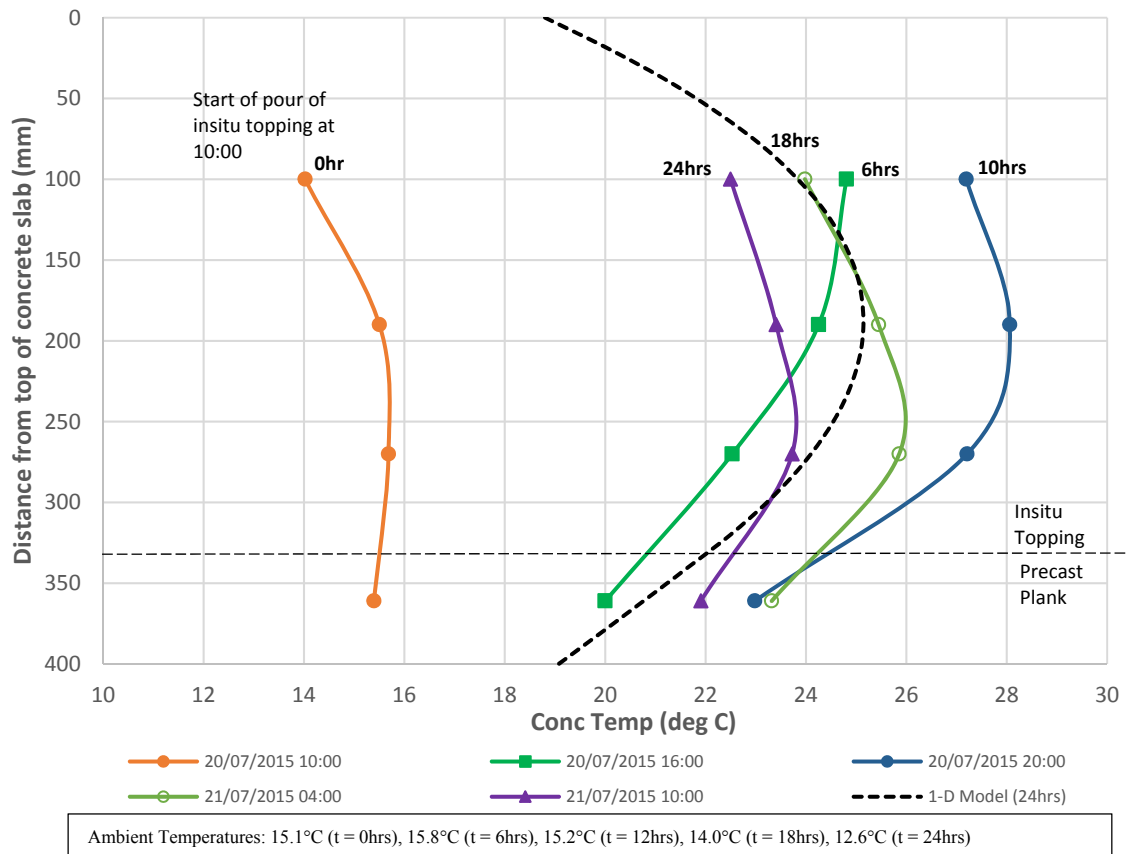


Figure 5-10 Temperature profile in concrete slab for first 24 hours

The predicted temperature profile through the slab using the 1-D numerical model after 24 hours is also shown in Figure 5-10. The model predicts a maximum temperature in the insitu topping of 30°C at 10hrs after the pour commenced and a maximum temperature differential of 8°C. As noted previously, the maximum measured concrete temperature of 28°C was recorded after approximately ten hours and the maximum recorded temperature differential was 3°C. A number of factors could be put forward for the 7% error (~2°C) in predicting the maximum temperature using the 1-D model:

- Similar to other models, the numerical model described in this paper uses adiabatic hydration models (i.e. heat transfer is not lost to/or gained from the surrounding). Previous studies ([25], [30]) have shown that models based on adiabatic hydration models are more reliable when predicting temperature rises in thick sections rather than thin sections. The insitu topping in HBB was 335mm thick and would be considered a ‘thin’ section.

Chapter 5. Investigation of Thermal Behaviour of a Hybrid Precasted Concrete Floor using Embedded Sensors

- The thermal properties of the concrete (specific heat, thermal conductivity and diffusivity) were assumed to be constant in the model and were based on typical values from the literature. However, the thermal properties of concrete change during the hardening process [31] and the accuracy of the temperature prediction is dependent on the thermal properties used in numerical model.
- The numerical model assumes that the insitu topping and hydration process commences at a specific time interval. In practice, the insitu topping was poured on site in layers over approximately one hour and therefore may introduce some discrepancies between the predicted and measured temperature in the concrete.
- The accuracy of VW strain gauges for measuring temperature in the concrete is accuracy of $\pm 1^{\circ}\text{C}$.

5.3.2 Thermal gradients

Temperature differentials or thermal gradients between the top and bottom of the slab during the curing phase causes internal restraint in the concrete which may lead to surface or internal cracking (early-age thermal cracks). During the construction phase of the HBB, both the top and bottom of the slab are exposed and, therefore, are affected by daily and seasonal environmental changes. The thermal gradients may lead to slab curvature (curling or warping of the slab) and because typically the slab is subject to some form of external restraint, additional temperature-induced stresses are developed which may create cracks in the concrete. The curvature is upward if the thermal gradient is positive (temperature decreasing from top to bottom) and downward if it is negative. Restraint to slab curvature is the cause of most early-age thermal cracking in pavements [25].

Distinct differences can be observed in the daily thermal gradients in the slab in response to the changes in the ambient air temperature. The thermal gradient in the slab is typically non-linear through the depth of the slab and approximately parabolic in shape at peak differentials. Temperature profiles through the slab are shown in Figure 5-11 for two days in which there is a negative temperature differential (30th December 2015) and a positive temperature differential (19th July 2016). On the 30th December 2015, the ambient air temperature falls by 5°C and

Chapter 5. Investigation of Thermal Behaviour of a Hybrid Precasted Concrete Floor using Embedded Sensors

on the 19th July 2016, the ambient air temperature increases by 15°C. It can be seen that when the ambient air temperature decreases significantly (typically during night-time in winter months) that the temperature gradient is convex as both the top and bottom exposed surfaces of the slab cool quicker than the inner core of the slab. On the 30th December, the thermal gradient changes from concave to convex as the ambient air temperature decreases and the temperature of exposed surfaces of the slab become lower than the inner core of the slab. Conversely, when the ambient air temperature increases significantly (typically during day-time in summer months) the temperature gradient is concave as both the top and bottom exposed surfaces of the slab heat up quicker than the inner core of the slab. The recorded thermal gradients in the slab are rarely linear or uniform during the construction phase as the temperature of the slab is continuously changing in response to the diurnal temperature cycle.

The predicted temperature profiles on the 30th December 2015 and 19th July 2016 using the 1-D model are also shown in Figure 5-11 (a and b respectively). The input temperatures for the concrete for the initial time step on each day were based on the temperatures measured by the four embedded sensors in the slab. The ambient temperature was based on the internal temperature in the building measured by a sensor that was positioned adjacent to the slab when the external cladding commenced (Section 5.3.3). The predicted temperatures by the model indicate similar developments to the measured temperatures and in both cases the predicted temperature are within 1°C of the measured temperatures after 24hrs (Note: accuracy of the VW gauges is $\pm 1^\circ\text{C}$). Similar to the measured profiles, the predicted temperature profile changes from concave to convex on the 30th Dec 2015 over the duration of the day as the ambient temperature decreases.

Chapter 5. Investigation of Thermal Behaviour of a Hybrid Precasted Concrete Floor using Embedded Sensors

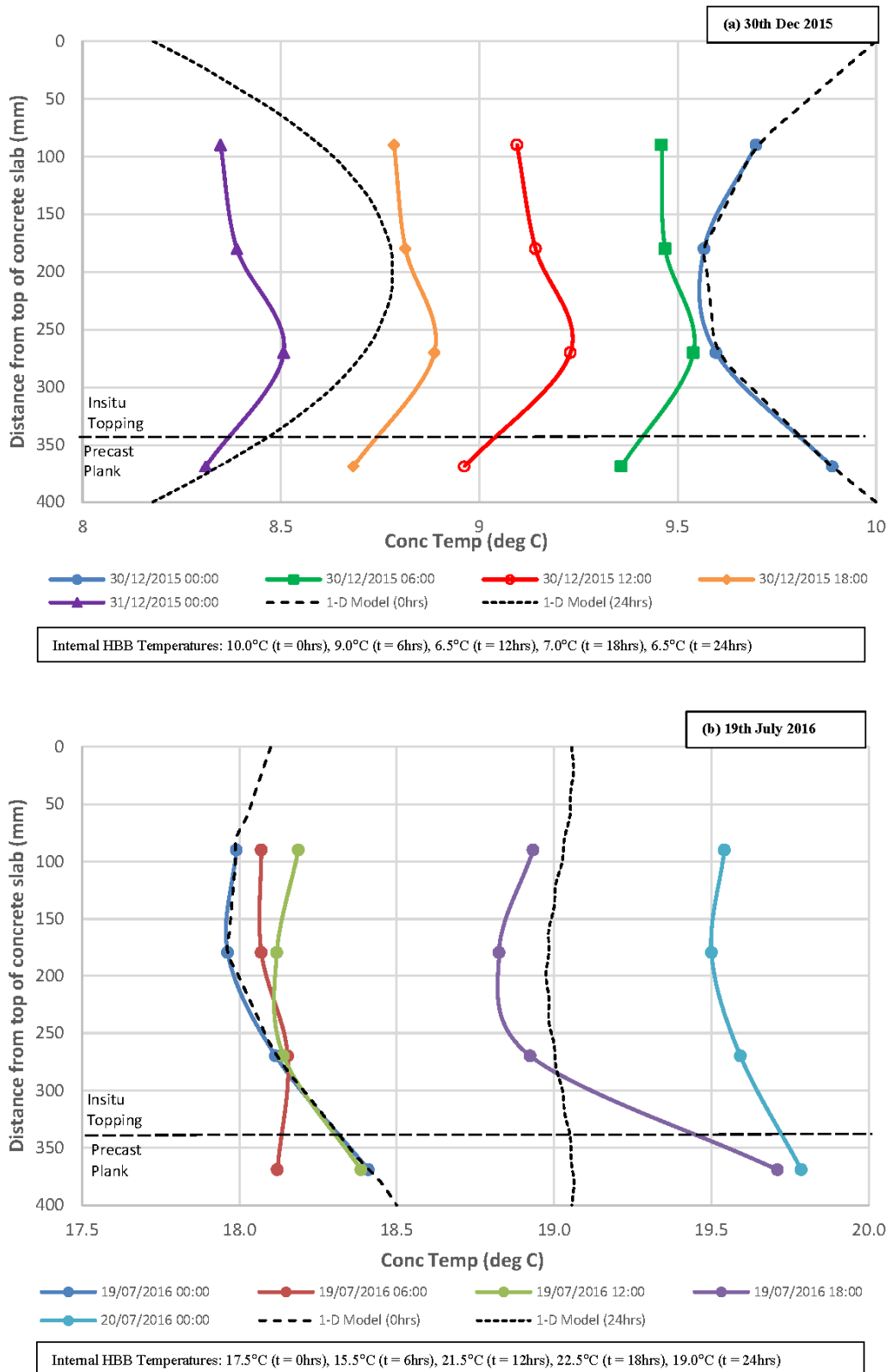


Figure 5-11 Temperature profile in concrete slab for (a) negative temperature differential on 30th Dec 20 15, and (b) positive temperature differential on 19th July 2016

Chapter 5. Investigation of Thermal Behaviour of a Hybrid Precasted Concrete Floor using Embedded Sensors

Although the 1-D finite-difference numerical model described in this paper is relatively simple, it can be used to predict the temperature profile during the early-age heat of hydration phase and at later stages when the environmental conditions are the dominant factor on the temperature in the concrete slab. During curing of the concrete slab, the model will tend to predict temperature rises which are conservative but could be used to identify potential early-age thermal cracking. Accurate prediction of the concrete temperatures in slabs is critical if the thermal mass of the concrete is used as one of the passive design strategies to control comfort (heating and cooling) in a sustainable manner. Exploiting the potential of exposed concrete in buildings can lead to enhanced energy efficiency and carbon savings over the lifetime of the building.

5.3.3 Horizontal spatial temperature distribution

Thermal gradients were also recorded horizontally in the slab in addition to vertically through the depth of the slab as outlined above. The temperature distribution along gridline (GL) H (Refer to Figure 5-5) recorded by VW gauges located in the top, middle and bottom of the structural topping and in the precast plank are shown in Figure 5-12, ten hours after the insitu topping is poured (10.00 20th June 2015). This time period (20.00) is approximately the peak temperature in the concrete slab during the hydration phase. The lag in temperature increase in the precast plank is clearly shown after the insitu topping is poured and as noted previously, the maximum temperatures in the concrete slab are recorded in the middle of the slab.

After the curing phase, the horizontal temperature distributions in the instrumented section of the second floor concrete slab are relatively uniform and do not exceed 3°C difference between sensors along GL H or GL 22 (embedded sensors positioned along approximately 9m length of slab in orthogonal directions). However, local deviations in the horizontal temperature distributions are noted in the slab perimeter along GL 22. The horizontal temperature distributions for the slab along GL 22 are shown in Figure 5-13 for the 19th July 2016 (18.00), which corresponds to the highest recorded daily ambient temperature during the construction phase. There is a noticeable decrease in the slab temperature along GL 22 and this is typical of the horizontal temperature distribution on days of high

Chapter 5. Investigation of Thermal Behaviour of a Hybrid Precasted Concrete Floor using Embedded Sensors

ambient temperature during the construction phase. On the 19th July 2016, there is a recorded temperature differential of 3°C across the width of the slab (total width along GL 22 = 8.5m from GL E to L) which equates to a horizontal temperature gradient of 0.37°C/m. The slab perimeter along GL E is on the South-West external elevation of the building and the slab perimeter along GL L is internal (adjacent to atrium). It is assumed that the higher temperatures recorded in the slab perimeter adjacent to GL E are due to solar gain during the day (Section 5.3.5 provides further analysis of solar irradiance) as there is continuous glazing along GL E. This suggests that the orientation of structural elements and exposure conditions can have a significant effect on the spatial temperature distribution in concrete slabs, particularly in regions which may be subject to significant solar radiation.

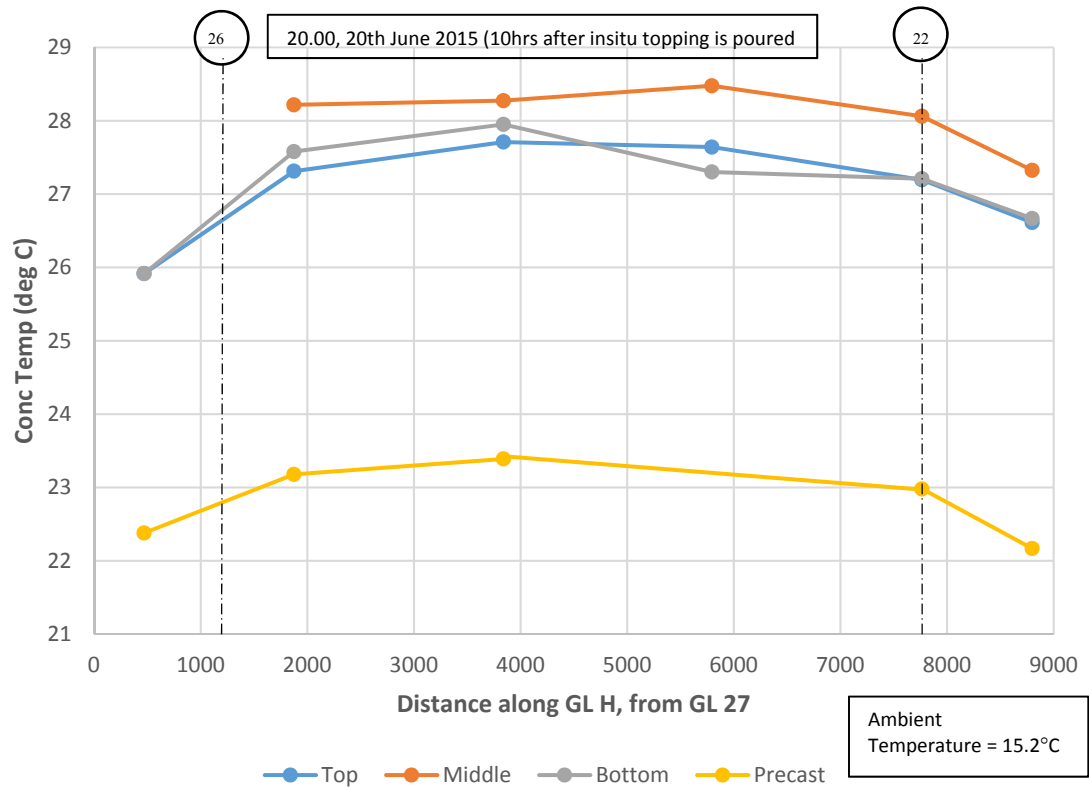


Figure 5-12 Temperature distribution in concrete slab along GL H at approximately peak temperature during hydration phase (20.00, 20th June 2015)

Chapter 5. Investigation of Thermal Behaviour of a Hybrid Precasted Concrete Floor using Embedded Sensors

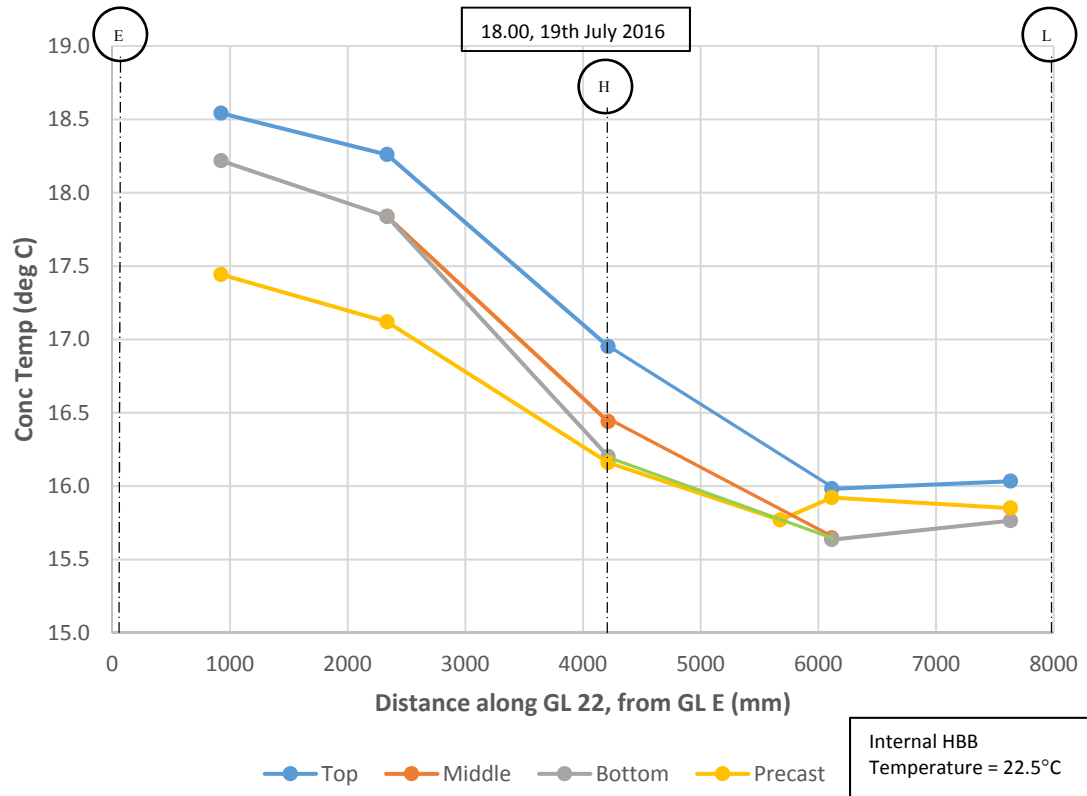


Figure 5-13 Temperature distribution in concrete slab at 18.00, 19th July 2016 along GL 22

5.3.4 Coefficient of thermal expansion

The coefficient of thermal expansion of concrete (α_c) is a measure of the free strain (unrestrained concrete) produced by a unit change in temperature and its magnitude will control the expansion and contraction of the concrete in response to a given temperature change. In design of concrete structures, the value of α_c can influence the control of early-age thermal cracking, provision of movement joints and construction tolerances for elements connected to concrete. A concrete with a low coefficient of thermal expansion is desirable when trying to control the risk of early-age thermal cracking; the type of aggregate used in the concrete is the dominant factor with respect to the coefficient of thermal expansion of concrete. The value of α_c can vary from $8\text{-}13\mu\epsilon/\text{°C}$ depending on the type of aggregate used in the mix. Eurocode 2 [19] recommends a value of $10\mu\epsilon/\text{°C}$ for normal weight concretes if no information is available. In the HBB project, limestone aggregates were used for the concrete for both the lattice girder precast plank and the insitu structural topping and, therefore, a value of $9\mu\epsilon/\text{°C}$ was assumed for the concrete based

Chapter 5. Investigation of Thermal Behaviour of a Hybrid Precasted Concrete Floor using Embedded Sensors

recommendations by Bamforth et al. [32]. It should also be noted that α_c changes over time and with moisture content.

There is no standard method for determining the coefficient of thermal expansion of concrete in CEN, although there is a method provided in BS EN 1770 [33] related to repair materials. For large projects, particularly when thermal cracking is critical, it is advisable to accurately determine the insitu thermal properties of the concrete so that the design is based on actual concrete properties rather than assumed behaviour. The embedded VW strain gauges in the concrete floor in the HBB allow the insitu restrained coefficient of thermal expansion of concrete (α_r) to be measured for the insitu topping that is poured on top of the precast plank. The slope of the insitu strain-temperature relationship during the cooling phase of the temperature cycle can be used to determine α_r at a number of locations in the slab and at different depths in the slab. In Figure 5-14, the strain-temperature curves are plotted for three VW strain gauges in the top, middle and bottom at one location in the insitu topping. It is observed that α_r is lower in the middle ($4.7\mu\epsilon/^\circ\text{C}$) of the concrete in comparison with the top ($6.0\mu\epsilon/^\circ\text{C}$) and bottom ($5.9\mu\epsilon/^\circ\text{C}$) and this finding was consistent at all locations in the slab.

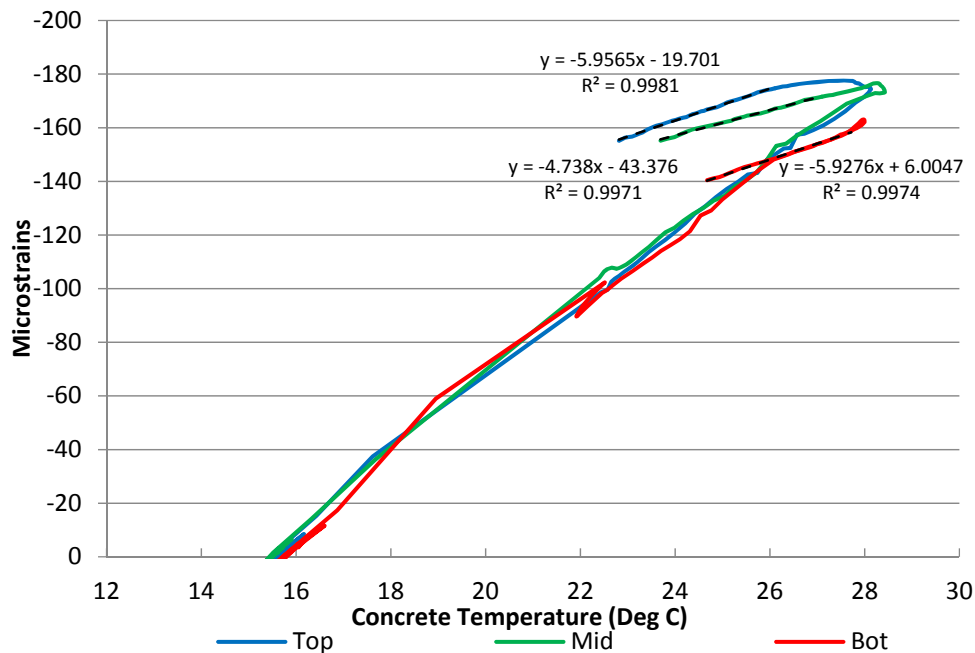


Figure 5-14 Insitu strain-temperature curve for the insitu topping at one location in the slab

Chapter 5. Investigation of Thermal Behaviour of a Hybrid Precasted Concrete Floor using Embedded Sensors

The variation of α_r through the depth of the slab is shown in Figure 5-15 based on the values of α_r determined in strain-temperature plot previously (Figure 5-14). The average insitu restrained coefficient of thermal expansion of concrete (α_r) using the embedded sensors in the 335mm thick insitu topping was $6.6\mu\epsilon/^\circ\text{C}$ with a coefficient of variation (Cv) of 13% (max = $8.1\mu\epsilon/^\circ\text{C}$, min = $4.7\mu\epsilon/^\circ\text{C}$). The average α_r for gauges located in the middle of the insitu topping was $5.7\mu\epsilon/^\circ\text{C}$ (Cv = 11%) and the average α_r for gauges located in the top and bottom of the insitu topping was $6.9\mu\epsilon/^\circ\text{C}$ (Cv = 10%).

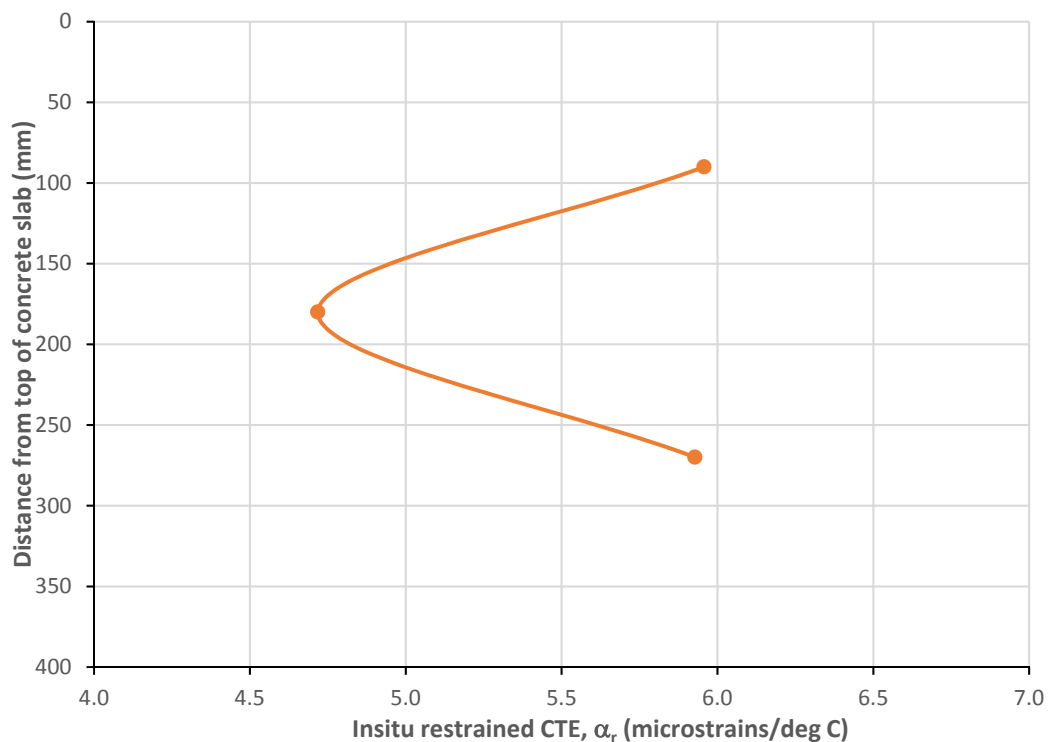


Figure 5-15 Variation of insitu restrained coefficient of thermal expansion in slab

In previous experimental studies on mass concrete foundations [34], the variation of α_r with depth of pour was found to be approximately represented by a parabolic curve and this correlates with the insitu data from the slab in the HBB even though the top of the insitu topping is exposed and the bottom of the insitu topping is partially insulated by the precast plank. The variation of α_r with depth correlates with the variation in concrete temperature, the central core being subjected to the greater temperature rise and imposing movement on the cooler surface regions. The reduced value of the restrained coefficient of thermal expansion of concrete (α_r) in

Chapter 5. Investigation of Thermal Behaviour of a Hybrid Precasted Concrete Floor using Embedded Sensors

the middle of the insitu topping in comparison with the top and bottom (Figure 5-15) indicates that the central core of the slab is subject to more restraint during the cooling phase. As the core of the concrete cools, its thermal contraction is restrained by the already cooler external sections of the insitu topping and the potential for internal cracking. Early-age thermal cracking will occur in the concrete if the restrained strain exceeds the tensile strain capacity of the concrete.

Restraint factors (R) are used in many design codes to quantify the degree of restraint when two concrete elements are cast against each other (R = 0.0 unrestrained; R = 1.0 full restraint). Annex L of Eurocode 2-Part 3 [35] provides guidance for determining restraint factors for common construction situations, but there is little guidance on suspended slabs; however, BS 8110-Part 2 [36] (superseded standard) suggested a restraint factor of between 0.2-0.4 should be used for suspended slabs. There is no information on restraint factors for hybrid concrete slabs such as precast concrete lattice girder flat system used in HBB. Incorrect values of restraint factors used in design can lead to inefficient over-design or under-design with potential cracking. Therefore, accurate estimation of restraint factors is critical for design and control of early-age thermal cracking.

CIRIA Report C660 [25] outlines how the restraint factors can be determined using measured insitu data. The restraint factor (R) can be calculated using:

$$R = \frac{(\alpha_c - \alpha_r)}{\alpha_c} \quad (\text{Eqn. 5-7})$$

where α_c is the coefficient of thermal expansion of unrestrained concrete (free strain) and α_r is the insitu restrained coefficient of expansion strain which can be measured as outlined above. Assuming that α_c was $9\mu\epsilon/^\circ\text{C}$ for the insitu topping in the HBB using limestone aggregates, values for the restraint factors can be determined using the insitu values for restrained coefficient of expansion strain (α_r). The average restraint factor at the bottom of the insitu topping which is cast on top of the precast plank was 0.25 ($C_v = 34\%$). A method for estimating the restraint factor at a joint (R_j) was proposed by ACI [21]:

$$R_j = \frac{I}{I + \frac{A_n E_n}{A_o E_o}} \quad (\text{Eqn. 5-8})$$

Chapter 5. Investigation of Thermal Behaviour of a Hybrid Precasted Concrete Floor using Embedded Sensors

where:

A_n is the cross-sectional area of the new (restrained) pour

A_o is the cross-sectional area of the old (restraining) concrete

E_n is the modulus of elasticity of the new pour concrete

E_o is the modulus of elasticity of the old concrete

It is recommended that for a slab cast against an existing slab that the relative area (A_n/A_o) is in proportion to the relative thicknesses of the two slabs (h_n/h_o). Using the above equation, the estimated restraint at the interface of the insitu topping and the precast plank after 12 hours is calculated as $R_j = 0.24$. This compares favourably with the restraint factor determined using the insitu data ($R = 0.25$) from the embedded instrumentation during the cooling phase after the heat of hydration even though there is a large variability. Thus, the equation developed by the ACI could be a useful method for determining restraint factors in hybrid concrete slabs.

5.3.5 Solar irradiance

In addition to consideration of ambient air temperature, the effect of solar radiation on the behaviour of concrete floors must be considered, particularly in regions in which exposed concrete may be subject to high levels of solar radiation during construction and/or in service. Better understanding and prediction of the thermal behaviour of concrete slabs and their ability to store and release heat is also very important with respect to better design of buildings with exposed concrete surfaces (using thermal mass).

The automatic weather station [18] at the NUI Galway campus measures both total and diffuse solar irradiance (W/m^2) and this allowed the daily total solar irradiance (kJ/m^2) to be determined and compared with the thermal behaviour of the precast plank and hybrid concrete lattice girder flat slab during construction. The total area of the second floor slab which was instrumented had limited exposure to solar radiation during construction because eleven days after the insitu topping was poured (31st July 2015), precast planks for the third floor were erected. The third floor precast planks located directly over the second floor provided shading for the

Chapter 5. Investigation of Thermal Behaviour of a Hybrid Precasted Concrete Floor using Embedded Sensors

majority of the slab, except at the perimeter which was still subject to partial solar radiation.

The 65mm thick precast planks for the second floor were erected on the 6th July 2015 and data was recorded after the 10th July 2015. Nine VW strain gauges were embedded in one of the 65mm thick precast planks (Plank 237, Figure 5-5) and this allowed the thermal behaviour of the precast plank to be analysed for the nine days prior to pouring the insitu topping on the 20th July 2015. The concrete temperature in plank 237 and the daily solar irradiance is shown in Figure 5-16 for the nine days prior to the pour of the insitu topping. On the days of low solar irradiance (11th July, 16th July and 18th July), the concrete temperature and ambient air temperature are closely aligned and the maximum difference between the concrete temperature and ambient air temperature is less than 2 degrees. On these days, there is very good correlation between the diurnal temperature cycle and concrete temperature because the plank is relatively thin and there is little solar radiation.

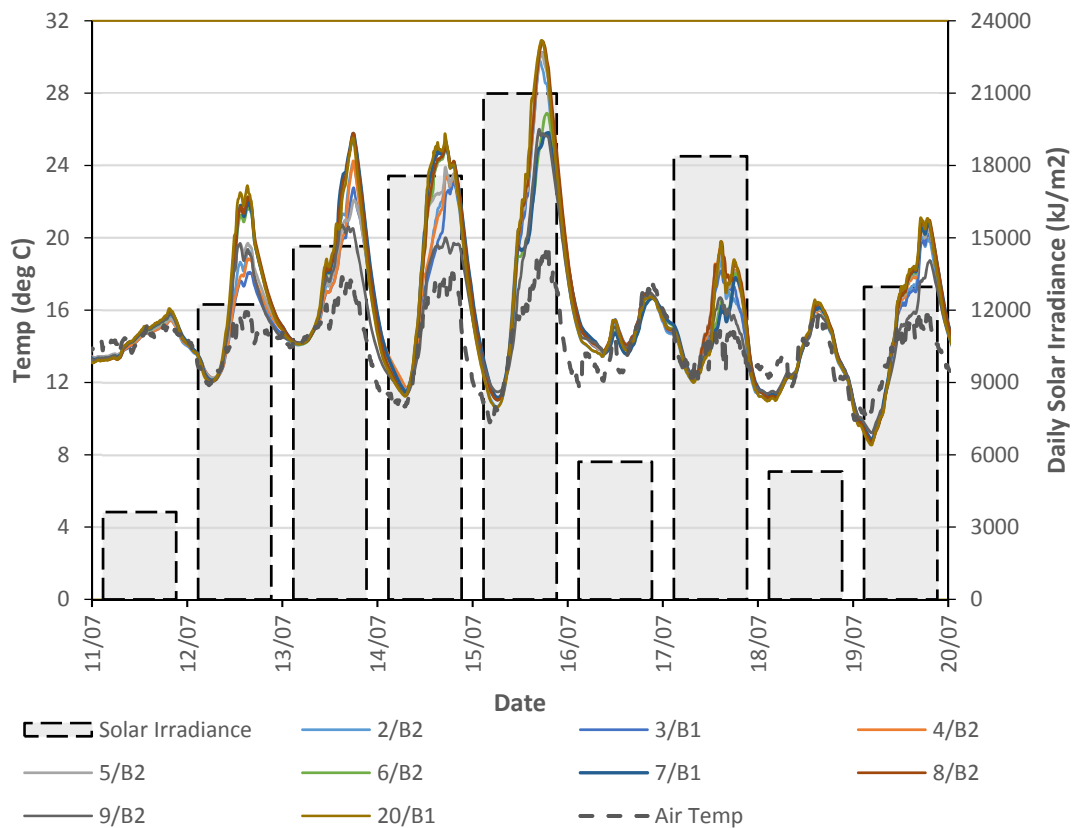


Figure 5-16 Comparison of concrete temperature and solar irradiance in the precast plank

Chapter 5. Investigation of Thermal Behaviour of a Hybrid Precasted Concrete Floor using Embedded Sensors

This contrasts with days of high solar irradiance, when the concrete temperature in the plank is significantly greater than the ambient temperature. On the 15th July, which had the highest solar irradiance prior to pouring the insitu topping, the temperature in the plank was almost 12 degrees higher than the ambient temperature. This highlights the potential for generation of significant induced thermal strains in concrete elements during construction, particularly in regions of high solar radiation. At night-time, the precast plank returns to ambient temperature and this illustrates the effectiveness of concrete with respect to exchanging heat with the environment (admittance) and potential of using concrete to manage thermal energy flows in a building.

The concrete temperature in the insitu topping in the centre of the slab and the daily solar irradiance is shown in Figure 5-17 for the sixteen days after the pour of the insitu topping (20th July - 4th August 2015). The exposed surface of the insitu topping of the floor slab was not covered during any stage of the construction. This is typical of concrete slabs poured during the Summer in Ireland and the UK if high temperatures or strong winds are not anticipated. The impact on solar heat gain can be observed on the 22nd July 2015 (3 days after the pour) when the peak temperature in the top of the slab exceeds the peak temperature of the previous day (21st July 2015) even though the ambient temperature was broadly similar for the two days. As the heat of hydration dissipates, it would be expected that the concrete temperatures would reduce at this stage and correlate with the ambient temperature; however, the high solar irradiance on the 22nd July 2015 increases the concrete temperature in the top of the floor slab. As expected, because the top of the slab is directly exposed to the sun, the temperatures through the depth of the slab decrease from top to bottom and the lowest concrete temperatures are recorded in the precast plank at the bottom of the slab. The highest daily solar irradiance is recorded on the 29th July 2015 and there is a noticeable increase in concrete temperatures on this day. The peak concrete temperature of 21°C is recorded in the top VW gauge (90mm below top surface of the slab) at 18:20 and this is approximately 6°C higher than the ambient temperature (15°C). At this time, the temperature in the precast plank is almost 4°C lower and this represents a vertical temperature gradient of 0.13°C/cm through the depth of the slab. The significant shading effect of the third floor precast planks after the 31st July 2015 is very noticeable as after this date, the

Chapter 5. Investigation of Thermal Behaviour of a Hybrid Precasted Concrete Floor using Embedded Sensors

concrete temperature stabilises through the depth of the slab and temperature does not exceed the ambient temperature even though there was high solar irradiance on the 1st and 3rd August 2015.

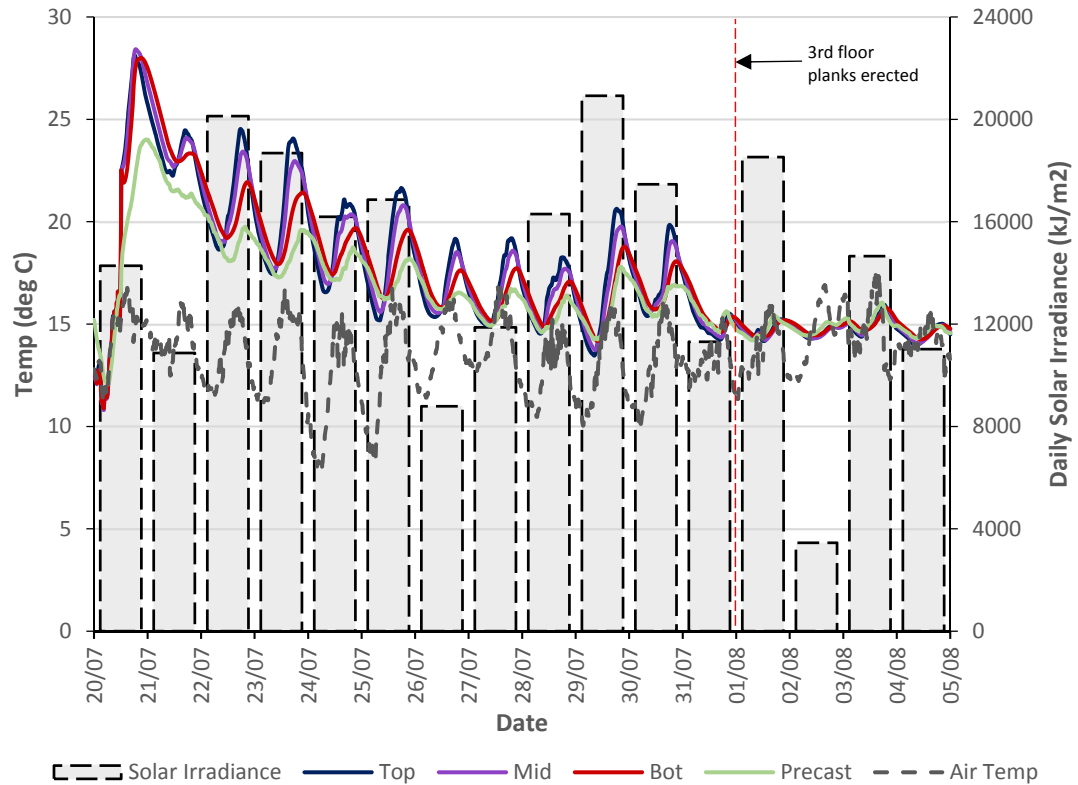


Figure 5-17 Comparison of concrete temperature and solar irradiance in the insitu topping

5.3.6 Thermal loadings

The magnitude and source of thermal induced loadings will vary during the lifetime of concrete structures. Initially, the heat generated during the heat of hydration phase can cause strains which may result in cracks which will affect the durability and performance of concrete elements. After the curing phase, interaction of the concrete with the environment (ambient temperature and solar radiation) can lead to daily and seasonal temperature changes within the structure which will cause the material to expand and contract. If movement in the structure is restrained, stresses may be induced which may contribute to cracking in the structure. In some cases, the thermal induced stresses may exceed the stresses induced by service loads (permanent and variable loading).

Chapter 5. Investigation of Thermal Behaviour of a Hybrid Precasted Concrete Floor using Embedded Sensors

An estimate of the thermal strains induced in the concrete slab may be determined by assuming a coefficient of thermal expansion of the $9\mu\epsilon/^\circ\text{C}$ for the concrete. As noted in Section 5.3.1, the measured peak temperature during concrete curing was 13°C and, therefore, this equates to thermal strains of approximately $117\mu\epsilon$ in the insitu topping. Cracking will occur in the concrete if the tensile strain capacity of the concrete at that time is less than the strains induced by the temperature change during the hydration phase. After the initial curing period (first 7 days), cracking due to early-age thermal cracking is unlikely as the tensile strain capacity of the concrete increases over time.

Exposed concrete surfaces are subject to temperature increases due to solar radiation which can induce curvature in the slab due to the creation of temperature differentials through the concrete (Section 5.3.5) and also increase the average temperature of the whole section which will increase the linear expansion in comparison to expansion due to ambient temperature alone (concrete in the shade). Thermal induced stresses due to solar radiation are particularly important for structures with exposed concrete such as multi-storey car parks, bridges and reservoirs. The embedded sensors in the slab of the HBB indicate that consideration of solar radiation during construction may also need to be considered during design in regions of high levels of sunshine.

5.4 Conclusions

A detailed account of a real-time monitoring programme is described which allows the thermal behaviour of a hybrid concrete floor during the construction phase to be investigated. The project involved embedding sensors in the precast concrete plank during manufacture and the insitu topping during construction so that the response of a hybrid concrete floor to temperature variations for one year could be monitored. The relationship between concrete floor and external environmental conditions was investigated using data from an automatic weather station located close to the building.

The data from the embedded sensors demonstrates that thermal behaviour of the concrete changes during the construction process. For the first few days after the insitu topping is poured, the heat of hydration is the dominant factor and has the

Chapter 5. Investigation of Thermal Behaviour of a Hybrid Precasted Concrete Floor using Embedded Sensors

potential to cause thermal cracks if the tensile strains generated in the concrete exceed the tensile strain capacity of the concrete. Although the concrete slab monitored in this project was exposed to direct solar radiation for a short period of the time, the significant effect of solar radiation on the concrete temperatures in the slab were recorded. High levels of solar radiation have the potential to cause curvature of the slab and also increase the average temperature of the concrete section. During the monitoring period described in this paper (1 year), differences in the thermal response of the slab to diurnal and seasonal temperature variations were observed and time lag between ambient temperature and concrete temperatures were noted. Variations in concrete temperatures in the concrete slab were recorded vertically through the depth of the slab and horizontally in the region of the slab which was monitored.

A one-dimensional finite-difference model is described which takes account of the various heat transfer components acting on the slab and allows prediction of the temperature profile in the slab during construction and operational phase of the building. Although the model is conservative when predicting the temperature rise during the heat of hydration, it can be used to model the temperature rise and temperature differential in a hybrid concrete floor when the insitu structural topping is poured. The thermal response of the floor to the diurnal and seasonal changes in the ambient temperature is also modelled using the numerical model.

This paper demonstrates the important role which embedded sensors can play for better understanding and prediction of thermal behaviour of concrete components in real buildings. The comprehensive thermal information from the embedded sensors described in this paper have many potential applications for designers of concrete buildings:

- The data presented in this paper can be used in conjunction with laboratory experiments to develop and validate numerical models which will allow designers to simulate the thermal behaviour of concrete components. This is particularly important in buildings in which the thermal mass of exposed concrete is used to regulate the internal environment and reduce energy consumption.

Chapter 5. Investigation of Thermal Behaviour of a Hybrid Precasted Concrete Floor using Embedded Sensors

- Although, hybrid concrete construction is increasingly popular in concrete structures, there is little data available on the actual thermal behaviour of concrete components. The data presented in this paper can be used in conjunction with laboratory experiments to develop and validate numerical models which will allow designers to simulate the thermal behaviour of concrete components. This is particularly important in buildings in which the thermal mass of exposed concrete is used to regulate the internal environment and reduce energy consumption.
- The effect of solar gain on exposed concrete components can be significant in regions which have high levels of solar radiation and needs to be considered at design stage. Thermal strains induced by solar irradiance can induce additional curvature and moments in slabs. The thermal data presented in this paper is related to actual weather data and can be used for analysing the effect of solar irradiance on concrete slabs.
- Guidelines for designers in codes of practice in relation to restraint for suspended slabs is limited. At design stage, it is very difficult to determine the degree of restraint and the nature of restraint (internal, external or a combination of both). The methodology described in this paper for determining the restraint factors based on the measured restrained coefficient of thermal expansion is applicable to similar hybrid precast concrete slabs.

Thermal effects during the construction and operational phase of concrete, if not considered during the design process, can have a significant negative effect on the performance of concrete structures. As performance requirements of buildings continue to increase, designers must adopt a holistic approach to design and be able to demonstrate how the various components and materials work in unison to enhance the overall performance of the building. If implementing a passive design strategy, designers will require accurate numerical models validated using field data from buildings to predict the thermal behaviour of concrete floors so that it can be optimised with respect to controlling the internal environment, thermal mass and energy efficiency.

Chapter 5. Investigation of Thermal Behaviour of a Hybrid Precasted Concrete
Floor using Embedded Sensors

Acknowledgements

The authors would also like to thank the National University of Ireland Galway and particularly the Department of Civil Engineering in the College of Engineering and Informatics for the help with the instrumentation in the demonstration buildings. They also wish to thank all the construction personnel and building professionals involved in the demonstrator buildings that facilitated and helped with installing the structural health monitoring systems. The authors would like to acknowledge the financial support of the European Commission through the Horizon 2020 project Built2Spec (637221). The second author would like to acknowledge the support of Science Foundation Ireland through the Career Development Award programme (Grant No. 13/CDA/2200).

5.5 References

- [1] Y. Xia, H. Hao, G. Zanardo, and A. Deeks, “Long term vibration monitoring of an RC slab: Temperature and humidity effect,” *Eng. Struct.*, vol. 28, no. 3, pp. 441–452, 2006.
- [2] G. S. Duffó and S. B. Farina, “Development of an embeddable sensor to monitor the corrosion process of new and existing reinforced concrete structures,” *Constr. Build. Mater.*, vol. 23, no. 8, pp. 2746–2751, 2009.
- [3] K. V. Yuen and S. C. Kuok, “Ambient interference in long-term monitoring of buildings,” *Eng. Struct.*, vol. 32, no. 8, pp. 2379–2386, 2010.
- [4] K. C. Hover, “Using human senses to guide concrete construction practice, with examples from the climate of New Zealand,” *Constr. Build. Mater.*, vol. 24, no. 5, pp. 854–861, 2010.
- [5] N. R. Buenfeld, R. Davies, A. Karimi, and A. Gilbertson, “CIRIA Report C661: Intelligent monitoring of concrete structures,” CIRIA, London, UK., 2008.
- [6] M. Hajdukiewicz, D. Byrne, M. M. Keane, and J. Goggins, “Real-time monitoring framework to investigate the environmental and structural performance of buildings,” *Build. Environ.*, vol. 86, pp. 1–16, 2015.
- [7] R. Hoseggen, H. M. Mathisen, and S. O. Hanssen, “The effect of suspended ceilings on energy performance and thermal comfort,” *Energy Build.*, vol. 41, no. 2, pp. 234–245, 2009.
- [8] Y. Ge, M. Z. E. B. Elshafie, S. Dirar, and C. R. Middleton, “The response of embedded strain sensors in concrete beams subjected to thermal loading,” *Constr. Build. Mater.*, vol. 70, pp. 279–290, 2014.
- [9] M. Azenha, R. Faria, and D. Ferreira, “Identification of early-age concrete temperatures and strains: Monitoring and numerical simulation,” *Cem. Concr. Compos.*, vol. 31, no. 6, pp. 369–378, 2009.
- [10] S. Newell, M. Hajdukiewicz, and J. Goggins, “Real-time monitoring to

Chapter 5. Investigation of Thermal Behaviour of a Hybrid Precasted Concrete Floor using Embedded Sensors

investigate structural performance of hybrid precast concrete educational buildings,” *J. Struct. Integr. Maint.*, vol. 1, no. 4, pp. 147–155, 2016.

- [11] S. Newell, J. Goggins, M. Hajdukiewicz, and D. Holleran, “Behaviour of hybrid concrete lattice girder flat slab system using insitu structural health monitoring,” in *Proceedings of Civil Engineering Research in Ireland (CERI 2016, NUI Galway, 29-30 August 2016)*, 2016, pp. 623–629.
- [12] ISIS Canada, “ISIS Canada Educational Module No. 5: An Introduction to Structural Health Monitoring,” ISIS Canada (Intelligent Sensing for Innovative Structures), Winnipeg, MB, Canada, 2005.
- [13] S. Newell and J. Goggins, “Real-time monitoring of concrete – lattice-girder slabs during construction,” *Proc. Inst. Civ. Eng. - Struct. Build.*, vol. 170, no. 12, pp. 885–900, 2017.
- [14] NSAI, “IS EN 12390-2: 2009 Testing hardened concrete - Part 2: Making and curing specimens for strength tests,” NSAI (National Standards Authority of Ireland), Dublin, Ireland, 2009.
- [15] P. Liu, Z. Yu, F. Guo, Y. Chen, and P. Sun, “Temperature response in concrete under natural environment,” *Constr. Build. Mater.*, vol. 98, pp. 713–721, 2015.
- [16] M. Pour-Ghaz, O. B. Isgor, and P. Ghods, “The effect of temperature on the corrosion of steel in concrete. Part 1: Simulated polarization resistance tests and model development,” *Corros. Sci.*, vol. 51, no. 2, pp. 415–425, 2009.
- [17] M. Sofi, P. Mendis, D. Baweja, and S. Mak, “Influence of ambient temperature on early age concrete behaviour of anchorage zones,” *Constr. Build. Mater.*, vol. 53, pp. 1–12, 2014.
- [18] IRUSE Weather, “IRUSE Weather,” *Informatics research unit for sustainable engineering NUI Galway weather website*. [Online]. Available: <http://weather.nuigalway.ie/>. [Accessed: 20-Jul-2019].
- [19] NSAI, “IS EN 1992-1-1: Eurocode 2: Design of concrete structures. Part 1-

Chapter 5. Investigation of Thermal Behaviour of a Hybrid Precasted Concrete
Floor using Embedded Sensors

- 1: General rules and rules for buildings,” NSAI (National Standards Authority of Ireland), Dublin, Ireland, 2005.
- [20] C. Boulay and C. Paties, “Mesure des deformations du beton au jeune âge,” *Mater. Struct.*, vol. 26, no. 5, pp. 307–311, 1993.
- [21] American Concrete Institute, “ACI 207.2R-95 Effect of Restraint , Volume Change , and Reinforcement on Cracking of Mass Concrete (Reported by ACI Committee 207),” American Concrete Institute, Farmington Hills, MI, USA, 1995.
- [22] D. Cusson and T. Hoogeveen, “An experimental approach for the analysis of early-age behaviour of high-performance concrete structures under restrained shrinkage,” *Cem. Concr. Res.*, vol. 37, no. 2, pp. 200–209, 2007.
- [23] A. D. Ross and J. W. Bray, “The prediction of temperatures in mass concrete by numerical computation,” *Mag. Concr. Res.*, vol. 1, no. 1, pp. 9–20, Jan. 1949.
- [24] J. Crank, *The mathematics of diffusion*, 2nd Ed. London, UK: Oxford University Press, 1975.
- [25] P. B. Bamforth, “CIRIA Report C660: Early-age thermal crack control in concrete,” CIRIA, London, UK, 2007.
- [26] R. K. Dhir, L. Zheng, and K. a Paine, “Measurement of early-age temperature rises in concrete made with blended cements,” *Mag. Concr. Res.*, vol. 60, no. 2, pp. 109–118, 2008.
- [27] M. Anson and P. M. Rowlinson, “Early-age strain and temperature measurements in concrete tank walls,” *Mag. Concr. Res.*, vol. 40, no. 145, pp. 216–226, Dec. 1988.
- [28] The Concrete Society, “In situ concrete strength. An investigation into the relationship between core strength and standard cube strength (CS 126),” The Concrete Society, Camberley, UK, 2004.
- [29] D. P. Bentz, “A computer model to predict the surface temperature and time-

Chapter 5. Investigation of Thermal Behaviour of a Hybrid Precasted Concrete
Floor using Embedded Sensors

of-wetness of concrete pavements and bridge decks (NISTIR 6551),” National Institute of Standards and Technology (NIST), Maryland, USA, 2000.

- [30] K. Vitharana, N; Sakai, “Early-age behaviour of concrete sections under strain-induced loadings,” in *Proceedings of the 2nd International Conference on Concrete under Severe Conditions (CONSEC '95) Sapporro, Japan, 2-4 August 1995*, 1995, pp. 1571–1581.
- [31] G. DeSchutter, L. Taerwe, “Specific heat and thermal diffusivity of hardening concrete,” *Mag. Concr. Res.*, vol. 47, no. 172, pp. 203–208, 1995.
- [32] P. Bamforth, D. Chisholm, J. Gibbs, and T. Harrison, “Properties of concrete for use in Eurocode 2 (CCIP-029),” Cement and Concrete Industry Publication (UK), London, UK, 2008.
- [33] NSAI, “IS EN 1770: Products and systems for the protection and repair of concrete structures. Test methods - Determination of the coefficient of thermal expansion,” NSAI (National Standards Authority of Ireland), Dublin, Ireland, 1998.
- [34] P.B Bamforth, “In situ measurement of the effect of partial Portland cement replacement using either fly ash or ground granulated blast-furnance slag on the preformance of mass concrete,” *Proc. Inst. Civ. Eng.*, vol. 69, no. 2, pp. 777–800, 1980.
- [35] NSAI, “IS EN 1992-3: Eurocode 2 - Design of Concrete Structures - Part 3 : Liquid Retaining and Containment Structures,” NSAI (National Standards Authority of Ireland), Dublin, Ireland, 2006.
- [36] BSI, “BS 8110-2: Structural use of concrete — Part 2: Code of practice for special circumstances,” British Standards Institution, London, UK, 1985.

6 Experimental Study of Hybrid Precast Concrete Lattice Girder Floor at Construction Stage

Article Overview

The scarcity of published experimental data on hybrid concrete lattice girder planks was identified in the literature review presented in **Chapter 2**. In addition, a number of commentators noted that the specified erection spans for lattice girder planks are conservative. This paper relates the experimental testing conducted on six lattice girder planks in 2015 and 2018. Bonding of sensors prior to testing and all experimental testing was conducted by the author. The four-point bending load tests were undertaken to investigate the behaviour of the lattice girder plank at construction stage when the plank must support its own self-weight, self-weight of the concrete insitu topping and construction loads. Instrumentation was used to monitor strain in the lattice girder, concrete and the embedded steel reinforcement so that interaction between the key parameters in a lattice girder plank could be studied.

The characteristics of the moment-deflection behaviour of the lattice girder planks is reviewed and the development of strain through the lattice girder plank during the load tests are analysed. An analytical model of the plank is devised using the transformed area method and the accuracy of the model to predict the initial stiffness and deflection of the plank during the linear elastic phase is discussed. The experimental data is used to investigate the deflection characteristics of the lattice girder planks for different propping arrangements and suggest that efficiencies are possible by allowing for the multi-span propping arrangements which are used typically on construction projects. The possible failure modes of lattice girder planks are discussed and prediction of the ultimate load of the lattice girder plank using Eurocode 3 is evaluated. Finally, recommendations for further research related to the experimental testing undertaken is presented.

Chapter 6. Experimental Study of Hybrid Precast Concrete Lattice Girder Floor at Construction Stage

This research is a significant addition to the literature on the experimental testing of lattice girder precast planks during construction. The key novelty of this work is that it analyses all the components of the lattice girder plank during testing so that the critical design parameters which control its behaviour can be analysed. The results from the experimental testing suggest that there is scope to improve the prediction of the failure of lattice girder planks and that the buckling length of the top chord and diagonals in the lattice girder are critical parameters. This research can be used to develop numerical models to predict the behaviour of the concrete lattice girder plank accurately and will be of interest to both contractors and designers who use this popular MMC for construction of flat slabs.

Photographs from the experimental testing is presented in **Appendix B**. This chapter was published in the journal *Structures* (2019).

Abstract

As part of an on-going research project on the hybrid precast lattice girder floor system, a series of six specimens were physically tested in the laboratory to investigate the behaviour of the floor at construction stage. The purpose of the experimental tests was to improve the understanding of the floor system at construction stage and examine the key parameters which influence its behaviour at both serviceability and ultimate limit states. The results suggest that there is scope for further optimisation of the lattice girder floor system and that the current design methods may be overly conservative.

The lack of comprehensive test data on this floor system limits the development of accurate models which can predict the behaviour of the floor during construction. In this paper, the development of strain in the various components of the floor system (lattice girder, concrete plank and reinforcement) are measured for a range of lattice girder planks. The use of the transformed area method and Eurocode 3 to predict the behaviour of the plank are investigated in this paper. The analytical model developed is shown to be relatively accurate for predicting the initial stiffness and deflection of planks with tall girders but is not appropriate for planks with low height girders. Areas requiring further research are recommended in this

Chapter 6. Experimental Study of Hybrid Precast Concrete Lattice Girder Floor at Construction Stage

paper to allow formulation of a generic model which would predict the behaviour of the floor system accurately at construction stage.

6.1 Introduction

The cost of formwork is a significant component of the total cost of an in-situ concrete frame. In recent years, contractors have attempted to rationalise construction by implementing offsite construction methods to minimise the amount of formwork required and reduce the quantity of reinforcement installed on site. Offsite construction offers many advantages in terms of efficiencies, quality control, time saving and health and safety. One such method is the use of hybrid concrete lattice girder slabs as an alternative to in-situ flat slab construction. Lattice girder precast planks (Figure 6-1) may be designed and detailed for both one-way and two-way spanning action.

Hybrid concrete construction (HCC) combines in-situ and precast concrete to utilise the many advantages of both forms of construction. HCC offers increased prefabrication, faster construction times, improved quality control and significant cost savings. To maximise the benefits of HCC, the design and construction decisions in relation to any project must be finalised at design stage. This will allow precast elements to be manufactured and stored at the precast factory and delivered 'just-in-time' to site. Traditional formwork traditionally accounts for 40 per cent of in-situ frame costs and is dependent on weather and labour [1]. The use of HCC means that a percentage of the frame is manufactured in a weather-proof factory, resulting in faster construction and reduced formwork costs.

6.1.1 Precast concrete lattice girder floor

One of the most popular forms of hybrid concrete floors is the lattice girder slab system. The major advantage of this system is that it is an 'in-situ structure' (one-way or two-way spanning); fully continuous and tied together without the need for shuttering on site [1]. The lattice girder floor system is also known as Omnia slab, Filigree slab or half-finished slab in the construction industry.

The floor system consists of steel lattice girders which are cast with the precast plank (typically 50-70mm thick), as shown for example in Figure 6-1, and an in-

Chapter 6. Experimental Study of Hybrid Precast Concrete Lattice Girder Floor at Construction Stage

situ concrete topping, which when hardened, forms a composite concrete slab. The lattice girder trusses which protrude from the precast plank serve a number of functions. The girders (i) provide stiffness to the precast plank during the construction stage until the in-situ topping has reached sufficient strength to ensure composite action, (ii) increase composite action between the precast plank and in-situ topping, (iii) act as a spacer for the top layer of reinforcement in the slab which is placed on site and (iv) are used as lifting points when unloading the planks on site. The bottom layer of reinforcement is embedded in the precast plank and two-way action between adjacent planks is created by the use of a ‘stitching bar’ which is laid perpendicular to the joint between precast planks.



Figure 6-1 Precast concrete lattice girder plank

The precast planks are manufactured using steel moulds which ensures a high-quality finish and gives the option to leave exposed soffits, if required. The top surface of the plank is roughened to ensure bond between the precast plank and in-situ topping (see, for example Figure 6-1). The planks can be manufactured up to 3400mm wide and 12000mm long, depending on transport restrictions to the site. Lattice girder floors require temporary propping until there is sufficient strength gain in the in-situ topping. The spacing and configuration of propping is generally

Chapter 6. Experimental Study of Hybrid Precast Concrete Lattice Girder Floor at Construction Stage

dictated by the load/span characteristics, spacing of the lattice girders and the diameter of the top chord bar in the lattice girder. The height of the lattice girder is based on the overall thickness of the hybrid concrete slab, as the lattice girder supports the top layer of reinforcement.

Lattice girders are three-dimensional industrially manufactured elements constructed using steel reinforcement. The steel used for lattice girders in Europe is typically grade B500A and they consist of a top chord, two bottom chords and diagonal bars. The diagonal bars are welded to the top and bottom chord by electric resistance welding. The standard distance between diagonal bars along the top chord is 200mm. The diameter of the bars in the lattice girders typically range from 5mm to 16mm and height of the girders required for most slabs will generally be between 100mm and 300mm (Figure 6-2).

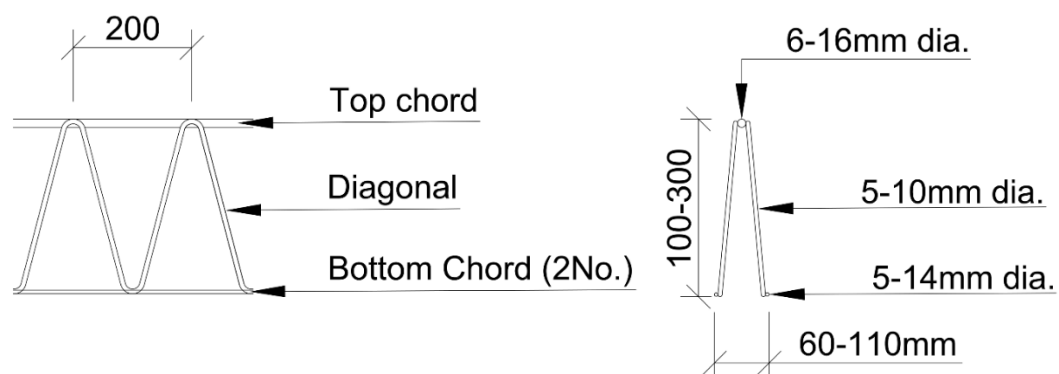


Figure 6-2 Typical dimensions of lattice girders

At construction stage, the lattice girder plank must be able to support the self-weight of the plank, construction loading and the weight of the in-situ concrete topping. In addition, the deflection of the plank during construction must be controlled. The European standard EN 13747 [2] requires mid-span deflection between props or temporary supports to not exceed 10mm for spans up to 4m. Typically, contractors erect temporary propping at specified maximum centres (determined by lattice girder plank designer) before the lattice girder planks are erected on site (Figure 6-3). At midspan (between props and/or supports), the top chord of the lattice girder must resist the compressive forces and the tensile forces are resisted by a

Chapter 6. Experimental Study of Hybrid Precast Concrete Lattice Girder Floor at Construction Stage

combination of the reinforcement in the plank, bottom chord of the lattice girder and the concrete in the plank. At the location of the temporary props, the top chord is subject to tensile forces and the compression forces are resisted by the concrete in the plank, embedded reinforcement and the bottom chords of the girders. During design of the lattice girder floors, four checks for the construction stage must be undertaken: (1) demand does not exceed the compression buckling resistance of the top chord (bending failure mode), (2) demand does not exceed the compression buckling resistance of the diagonal (shear failure mode), (3) maximum permitted deflection is not exceeded and (4) maximum crack width is not exceeded. The configuration of the lattice girders (spacing and diameter of the reinforcement in the girder truss) largely determines the behaviour of the plank at construction stage. For most girders, the top chord compression resistance and deflection are the critical design checks at the construction stage. However, for taller girders (greater than 200mm height), the diagonal compression resistance can be critical as the length of the diagonal increases.



Figure 6-3 Temporary props prior to erection of lattice girder planks

Chapter 6. Experimental Study of Hybrid Precast Concrete Lattice Girder Floor at Construction Stage

The behaviour of the lattice girder floor at the construction stage is relatively complex because of the interaction between the concrete plank and steel lattice girder trusses. Although some experimental testing has been conducted on the behaviour of precast concrete lattice girder planks at construction stage [3]–[7], there is relatively little experimental data available in the literature on the floor system during construction in view of the popularity of the floor as a viable and efficient alternative to in-situ flat slab construction. The laboratory testing programme described in this paper utilised a comprehensive range of sensors to measure the deformation of the plank and the strain characteristics of all the key parameters (top chord, diagonals, bottom chord, reinforcement and, concrete) which effect the behaviour of the lattice girder floor during construction. Without this knowledge in relation to the interaction of the various components of the floor system, the development of accurate modelling of the lattice girder plank and potential optimisation is difficult.

6.2 Experimental set-up

A series of physical tests was undertaken on six precast concrete lattice girder planks in the heavy structures laboratory in NUI Galway. The planks were manufactured by Oran Pre-Cast in Galway, Ireland. This experimental study is part of an on-going research project which is investigating the behaviour of the lattice girder floor system using experimental testing and embedded sensors [8]–[13] in real buildings. The concrete plank for all six tests was similar, except for the type of lattice girders used, which varied in each test. All planks were 3650mm long, 65mm thick, 550mm wide and were manufactured with two lattice girders at 250mm centres (Figure 6-4). Many precast manufacturers require temporary propping at a maximum of 2.4 metres to limit deflection during construction. The span of planks was 3.6m (measured from centre of bearing) in this experimental study and this was selected so that the possible optimisation of the spacing of temporary propping could be investigated. It was considered that manufacturing the planks with two lattice girders would allow the interaction between the girders to be studied and is more representative of the lattice girder planks used in the industry. The steel reinforcement in all planks (Grade B500B) was H12 at 100mm spacing in both the longitudinal and transverse directions and the cover to the

Chapter 6. Experimental Study of Hybrid Precast Concrete Lattice Girder Floor at Construction Stage

reinforcement at the plank soffit was 25mm. The concrete planks were tested between 45-69 days after manufacture.

The configuration of the lattice girders used in the experimental testing is provided in Table 6-1. The convention for identifying girders is the letter designating the type of girder ('S' for slab, 'W' for wall), the height of the lattice girder in centimetres, the diameter of the top chord, diameter of the diagonal and diameter of the bottom chord (all expressed in millimetres). For example, S29-14/07/06 refers to a slab lattice girder plank with a height of 29cm, top chord diameter of 14mm, diagonal bar diameter of 7mm and a bottom chord diameter of 6mm.

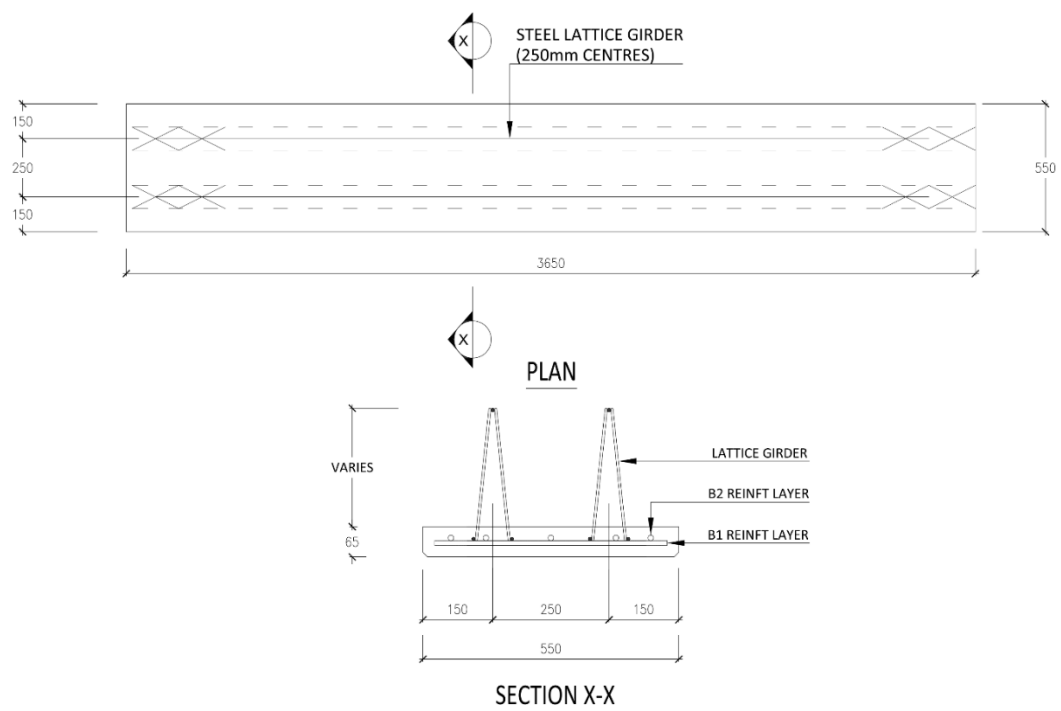


Figure 6-4 Configuration of precast lattice girder plank tested

Chapter 6. Experimental Study of Hybrid Precast Concrete Lattice Girder Floor at
Construction Stage

Table 6-1 Details of test planks

Plank Reference	Ø Top Chord (mm)	Ø Diagonal (mm)	Ø Bottom Chord (mm)	Girder Height (mm)	Longitudinal Reinforcement	Plank Thickness (mm)
S29-14/07/06 2015	14	7	6	290	H10-100 B2	65
S29-14/07/06 2018	14	7	6	290	H10-100 B2	65
S22-14/07/06 2018	14	7	6	220	H10-100 B2	65
S10-14/07/06 2018	14	7	6	100	H10-100 B2	65
W22.5- 08/05/05 2018	8	5	5	225	H10-100 B2	65
W10-10/06/06 2018	10	6	6	100	H10-100 B2	65

The lattice girder planks were loaded in four point bending using a 240kN hydraulic actuator and spreader beam, as shown in Figure 6-5 and Figure 6-6. The load was transferred to the plank from the spreader beams through 2 No. 40 x 5mm square hollow sections (SHS) located at approximately one-third span to ensure a constant moment within the central third of the plank. A compressible board was located between the top of the plank (textured profile) and the SHS to ensure uniform load is applied to the plank during the test. At the end supports, the precast plank was supported on rollers, where the load was transferred through 50mm wide x 10mm thick steel bearing plates. To create a low friction slip membrane at the bearing of the precast plank, two sheets of PTFE (Polytetrafluoroethylene) were positioned between the plank soffit and bearing plates. Initially, a ‘seating load’ of approximately 10% of the expected load followed by a return to zero was applied to the plank. The test was carried out using displacement control, with a midspan displacement rate of 0.01mm/sec. The test was terminated when the midspan displacement reached 40mm ($> \text{span}/100$).

Chapter 6. Experimental Study of Hybrid Precast Concrete Lattice Girder Floor at Construction Stage

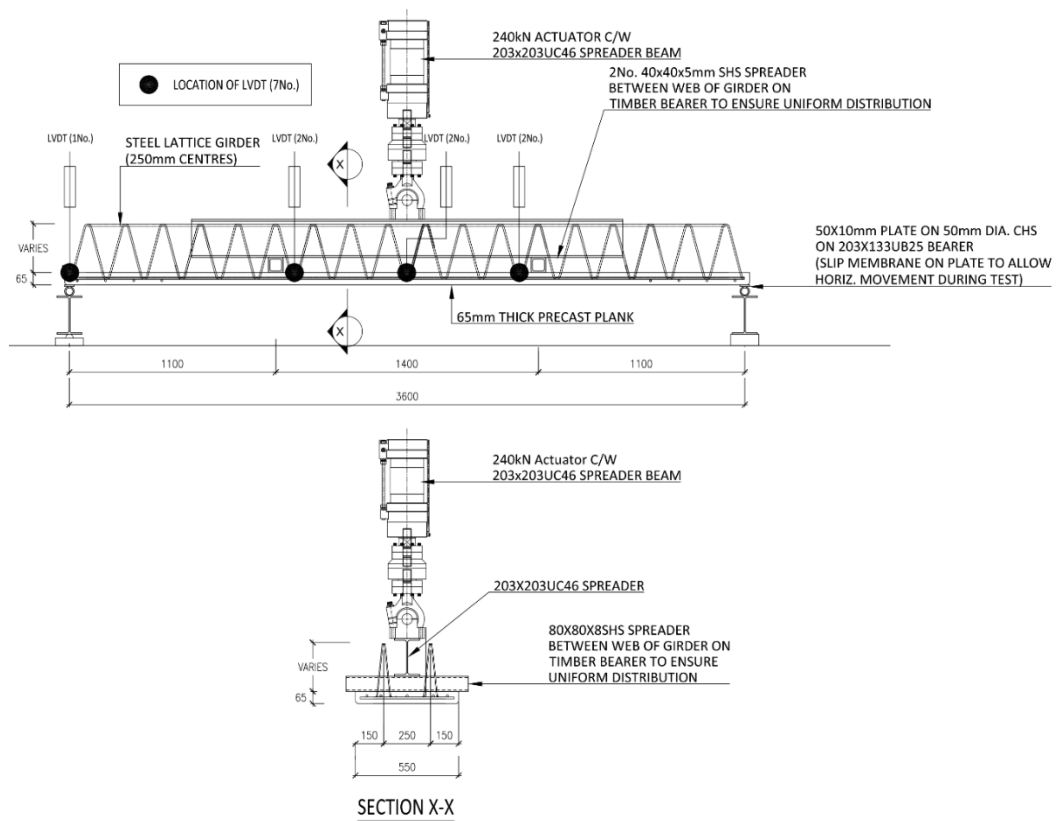


Figure 6-5 Four point bending of precast plank

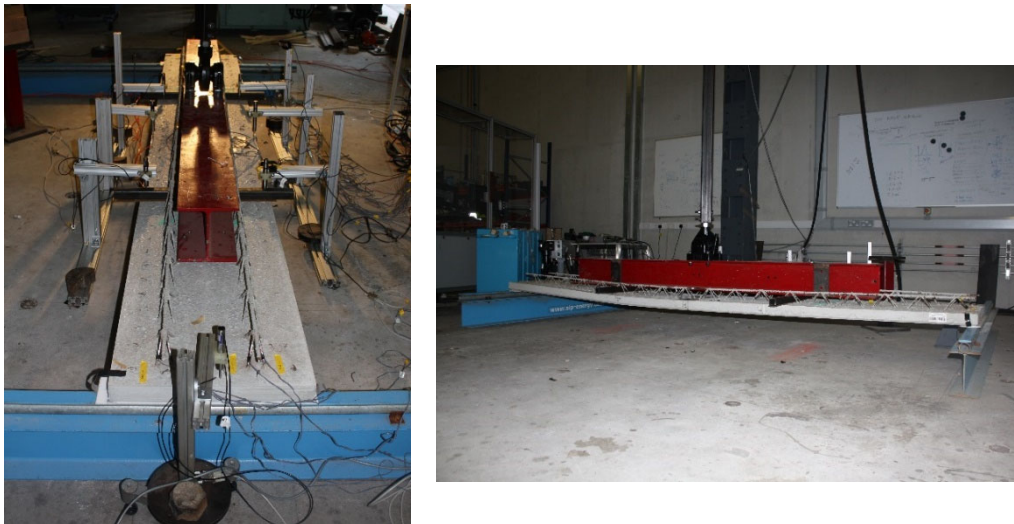


Figure 6-6 Experimental test set-up in laboratory

6.2.1 Instrumentation

Seven LVDTs (Linear variable differential transformers) were used in each test to record the vertical displacement of the plank at midspan, at the two load points on

Chapter 6. Experimental Study of Hybrid Precast Concrete Lattice Girder Floor at Construction Stage

both sides of the plank and at one of the supports. In addition, digital image correlation (DIC) was used in one of the tests to measure the midspan deflection of the plank to investigate the accuracy and feasibility of using DIC for subsequent load tests in the laboratory.

In order to study the interaction of the various components in the lattice girder plank, a total of twenty three electrical resistance (ER) strain gauges were bonded to the longitudinal reinforcement, steel lattice girder and the concrete surface of the precast plank. Five ER gauges were bonded to one of the internal longitudinal reinforcement bars (3.6m long, H10 at 100mm centres) prior to manufacture of the precast plank (Figure 6-7a). The gauges are located at 200mm from either end of the reinforcement bar and at 800mm centres along the reinforcement bar (B2 reinforcement layer). One ER strain gauge was bonded to each of the bottom chords of both lattice girders in each plank at midspan (Figure 6-7b). The ER gauges embedded in the concrete were sequentially coated in wax, butyl coating tape and vinyl-mastic (VM) tape prior to casting of the concrete to protect the gauges from water ingress (Figure 6-7).

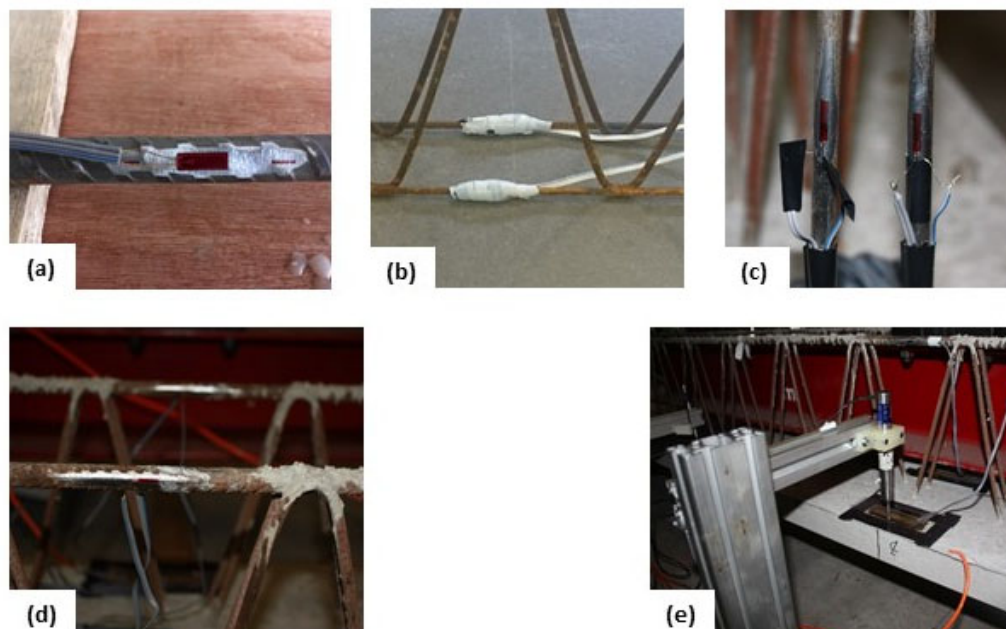


Figure 6-7 ER strain gauges bonded to (a) longitudinal reinforcement, (b) bottom chord, (c) diagonal, (d) top chord and (e) concrete surface

Chapter 6. Experimental Study of Hybrid Precast Concrete Lattice Girder Floor at Construction Stage

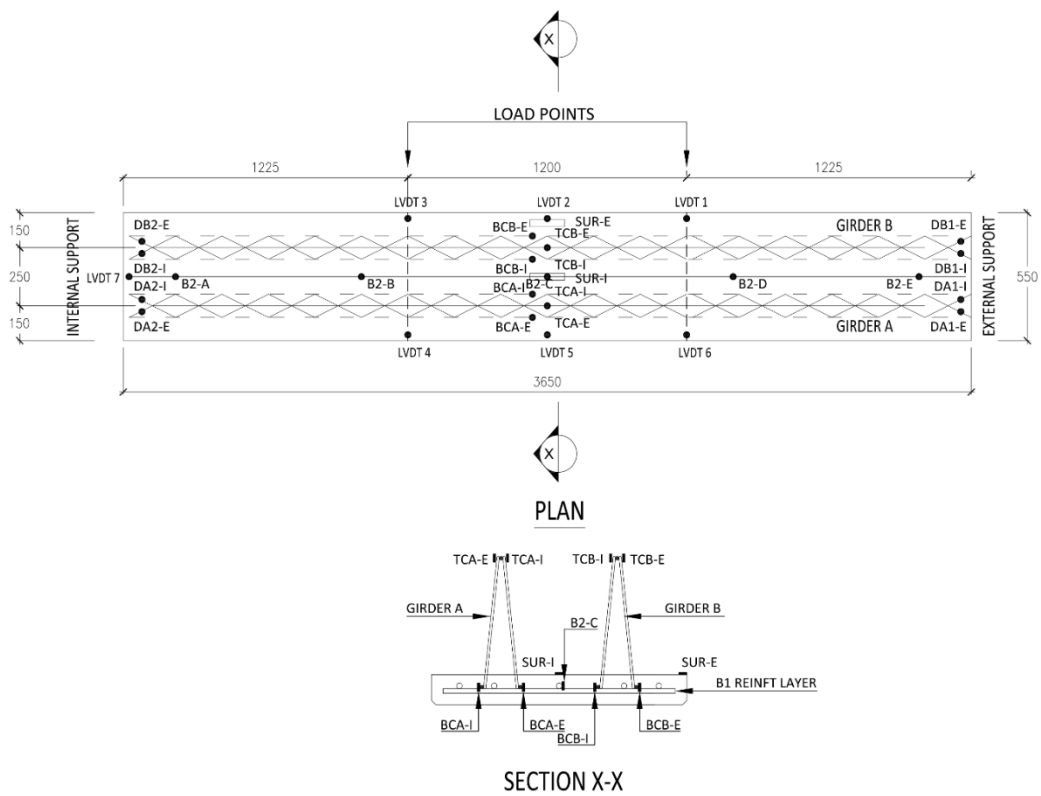


Figure 6-8 Schematic of instrumentation

After manufacture of the plank, ER gauges were bonded to the diagonals of the both lattice girders at the supports, as shown in Figure 6-7c (8 No. in total). Two ER gauges were bonded to the top chord of both lattice girders at midspan (Figure 6-7d). These gauges were positioned at 180 degrees to each other so that the buckling behaviour of the top chord could be recorded during the test. Two ER gauges were bonded to the top surface of the precast concrete plank at midspan to directly measure the strain at the top surface of the concrete plank (Figure 6-7e). Data from the sensors were recorded every second during the testing. Two fixed location webcams and a camcorder were also used to record the deformation of the precast planks during the testing. The instrumentation used for the experimental testing of the lattice girder planks are detailed in Figure 6-8 and Table 6-2.

Chapter 6. Experimental Study of Hybrid Precast Concrete Lattice Girder Floor at Construction Stage

Table 6-2 Table of Instrumentation

(Refer to Figure 6-8 for drawing showing location of instrumentation)

Instrumentation	Reference	Location	Quantity
LVDT	LVDT 1-7	At one support; at midspan and both load points on either side of the plank.	7
Surface ER Gauge (GL = 60mm)	SUR-E, SUR-I	On top surface (SUR) of plank at midspan, at edge of plank and between the two lattice girders	2
Diagonal ER Gauge (GL = 6mm)	DA1-I/E, DA2-I/E DB1-I/E, DB2-I/E	On diagonals (D) on both girders at both supports (external support = 1, internal support = 2)	8
Top Chord ER Gauge (GL = 6mm)	TCA-I/E, TCB-I/E	On top chord (TC) at midspan on both girders. Two gauges on each top chord at 180° to each other.	4
Bottom Chord ER Gauge (GL = 6mm)	BCA-I/E, BCB-I/E	On bottom chords (BC) at midspan on both girders.	4
Reinft. ER Gauge (GL = 6mm)	B2-A-E	On longitudinal reinforcement (B2), 3600mm long. Gauges positioned at 200mm, 1000mm, 1800mm, 2600mm and 3400mm respectively from end of bar.	5

Note: GL = Gauge Length; E = external side of girder; I = internal side of girder

6.2.2 Concrete properties

The tensile resistance of the concrete used to manufacture the concrete plank will determine the nature of cracking (width, extent) and the stiffness of the plank during construction stage. When the tensile stresses at the plank soffit exceed the tensile resistance of the concrete, the concrete will crack and the tensile strains are resisted by the embedded reinforcement and the bottom chord of the lattice girders. The concrete used to manufacture the precast planks in the factory is strength class C40/50. A CEM II A-V cement (370kg/m³) and limestone aggregates are the primary constituents in the concrete mix (Table 6-3). The precast planks are thermal cured for approximately 10-12 hours at a minimum temperature of 32°C after manufacture so that they can be removed from their steel moulds and stored at the precast factory.

Chapter 6. Experimental Study of Hybrid Precast Concrete Lattice Girder Floor at Construction Stage

Concrete cylinders and cubes were made and tested to measure the compressive strength (EN 12390-Part 3 [14]) and modulus of elasticity (EN 12390-Part 13 [15]). The cylinders and cubes were cured in water and in air to match the environmental conditions of the concrete planks that were tested in the laboratory. The mean characteristic compressive strength based on testing cubes and cylinders (cured in water) at 28 days was 52.3 MPa (f_{cm}), with a standard deviation (σ) of 1.44 MPa (The compressive strength of the concrete cubes were multiplied by 0.8 to convert them to an equivalent cylinder compressive strength). Concrete cylinders which were air cured and stored with the precast planks were tested on the same day that the planks were tested in the laboratory. The planks were tested between 45 and 69 days after manufacture and the mean cylinder compressive strength was 54.1 MPa ($\sigma = 2.17$ MPa), which was very favourable when compared with values measured from the concrete specimens stored in water (high ambient air temperatures at this time might partially explain the compressive strength of the air cured specimens) . The mean secant modulus of elasticity of the concrete cylinders cured in water at 28 days was 49.5GPa ($\sigma = 1.54$ GPa). The measured values for the compressive strength and modulus of elasticity indicate the importance of using actual characteristic material properties rather than assumed properties based on the specified grade of concrete used. In both cases, the measured modulus of elasticity and compressive strength were significantly greater than those assumed if the properties were based on a C40/50 grade of concrete.

Table 6-3 Concrete mix design for precast concrete planks (1m³)

C40/50 mix for lattice girder planks, w/c = 0.35, D _{max} = 10mm				
Cement (II-A-V 42.5)	Aggregate (8-14mm)	Sand (0-2mm)	Water	Plasticiser
(kg)	(kg)	(kg)	(litre)	(litre)
370	900	950	130	2.2

6.2.3 Steel properties

The mechanical properties of the steel reinforcement in the lattice girder will typically govern the stiffness of the lattice girder plank at construction stage and the failure mode. Depending on the configuration of the lattice girder plank, the failure

Chapter 6. Experimental Study of Hybrid Precast Concrete Lattice Girder Floor at Construction Stage

mode for the lattice girder plank will be compression buckling of the top chord or the diagonals in the lattice girder. Samples of the top chords (12No.) of all lattice girders in the precast planks tested in this project were cut after the planks were tested and the material properties were evaluated by means of a tensile test (EN ISO 15630-Part 1 [16]). The samples of top chord were taken close to the support, where no buckling of the top chord had occurred during the load tests. The reinforcement used to manufacture the lattice girder is grade B500A (characteristic yield strength = 500 MPa). The mean yield strength of the reinforcement in the top chords tested was 569MPa (minimum = 518 MPa, maximum = 639 MPa, standard deviation = 45.8MPa). The mean modulus of elasticity of the top chords was 202 GPa ($\sigma = 17.4$ GPa). The mean ratio of tensile ultimate strength to yield strength based on the tensile tests undertaken was 1.09.

6.3 Test results

The results and findings from six laboratory tests are presented in this section. An initial test (Specimen ID S29-14/07/06 2015) was undertaken in 2015 to assess the experimental set-up and to investigate the optimum number of sensors required to accurately model the behaviour of the lattice girder precast plank. The remaining tests were undertaken in 2018. Cracking and crack propagation in the concrete plank was visually observed during all tests. However, many cracks were difficult to observe because of the relatively small width of the cracks. At the end of the test, the cracking pattern on the precast plank soffit was also recorded.

6.3.1 Moment-deflection behaviour

The moment of resistance per girder (two girders in each plank) is plotted against the average midspan deflection in Figure 6-9. The moment-deflection behaviour of the planks is characterised by a linear relationship initially until the onset of micro-cracking of the concrete, which was visible on the soffit (or at the side originating at the soffit) of the plank. As the cracks continue to grow and propagate, the stiffness of the lattice girder plank reduces until peak load/moment is reached. Failure (and peak load) is typically initiated by buckling of the top chord (bending failure) or buckling of the diagonals (shear failure). Up to peak load, it is observed that the moment-deflection curve consists of a series of near-linear phases and load

Chapter 6. Experimental Study of Hybrid Precast Concrete Lattice Girder Floor at Construction Stage

steps which represent a loss of stiffness of the plank caused by either cracking of the concrete, buckling of top chord or buckling of diagonal. Initial cracking was typically observed adjacent to one of the load points (Figure 6-10a) and as the test developed cracking would develop along the soffit of the plank at a number of locations in the middle third of the plank (constant moment zone).

In all tests conducted, it is noted in the moment-deflection plots (Figure 6-9) that the first significant reduction in stiffness typically occurs at approximately the same midspan deflection (3.0-4.5mm). When the concrete cracks, load redistribution occurs and the stiffness and resistance of the plank is reduced suddenly. As the test is displacement control, the actuator maintains the same displacement rate of loading (0.01mm/sec) but the rate of loading is lower to take account of the reduced stiffness of the plank.

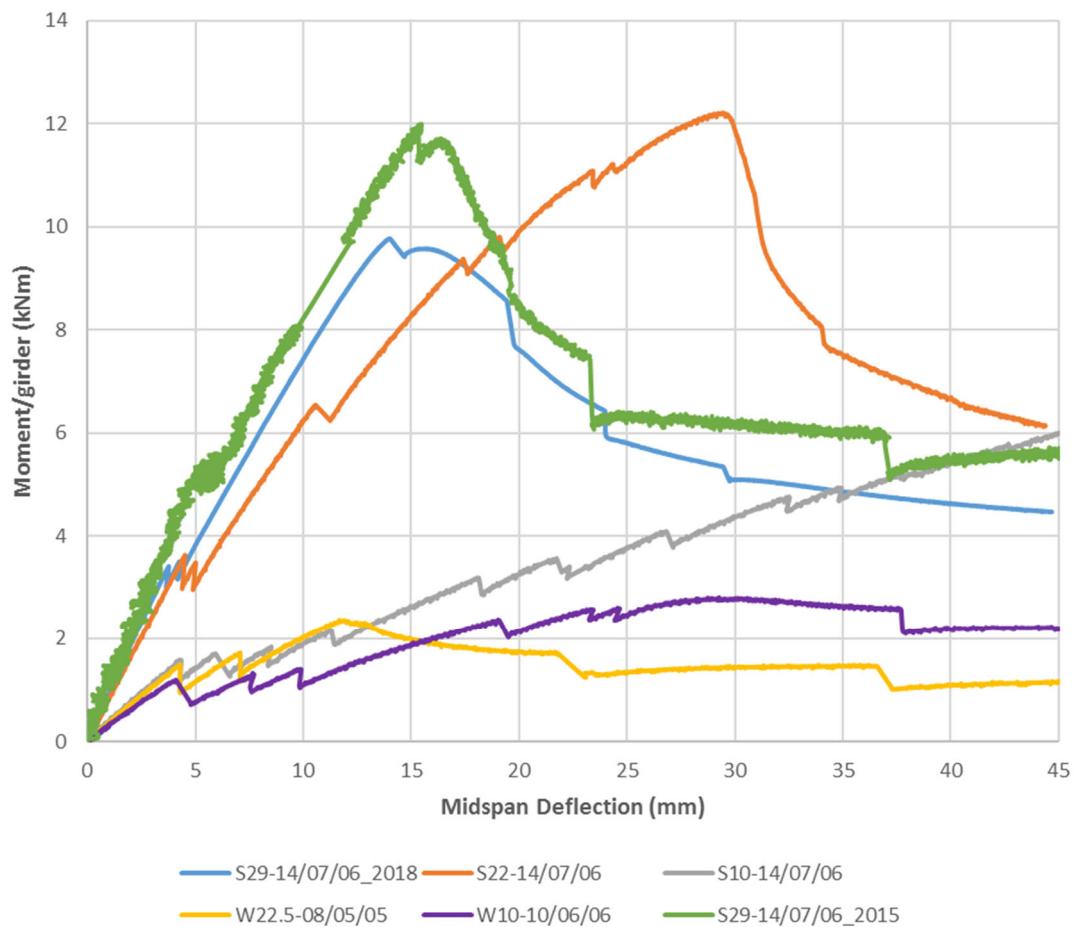


Figure 6-9 Moment-deflection behaviour of lattice girder planks

Chapter 6. Experimental Study of Hybrid Precast Concrete Lattice Girder Floor at Construction Stage

The vertical deformed shape of the planks during the tests was typically symmetrical until peak load. After peak load, relatively larger deflections of the planks occurred at the location of failure/damage (i.e. top chord, diagonal etc.) in the planks. The average vertical displacement at midspan and the two load points (measured by LVDTs on either side of the plank) is shown in Figure 6-11 for the plank S29-14/07/06-2018.

The moment-deflection characteristics for the two planks tested in 2015 and 2018 with the same lattice girder configuration (S29-14/07/06) are very similar for the initial stages of the load test. The behaviour of the two planks are slightly different at ultimate limit state and this can be attributed to construction imperfections and differences in material properties for the steel reinforcement, steel lattice girder and concrete. Although both planks have similar configurations, small differences in the location of the girders (spacing, edge distance etc.), geometry of the girders and material properties of the components of the lattice girder planks will impact the behaviour of the plank at failure.

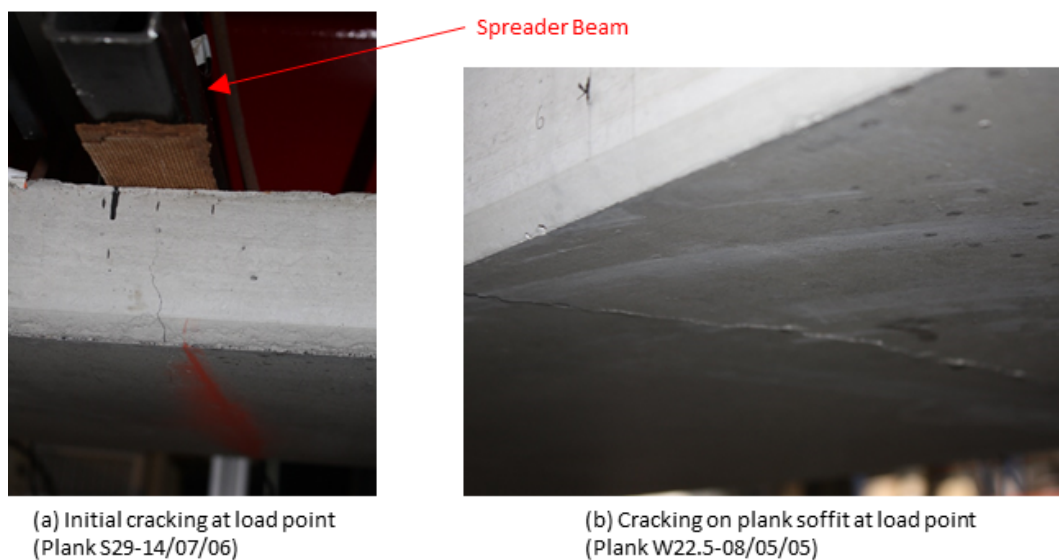


Figure 6-10 Cracking on concrete plank

Chapter 6. Experimental Study of Hybrid Precast Concrete Lattice Girder Floor at Construction Stage

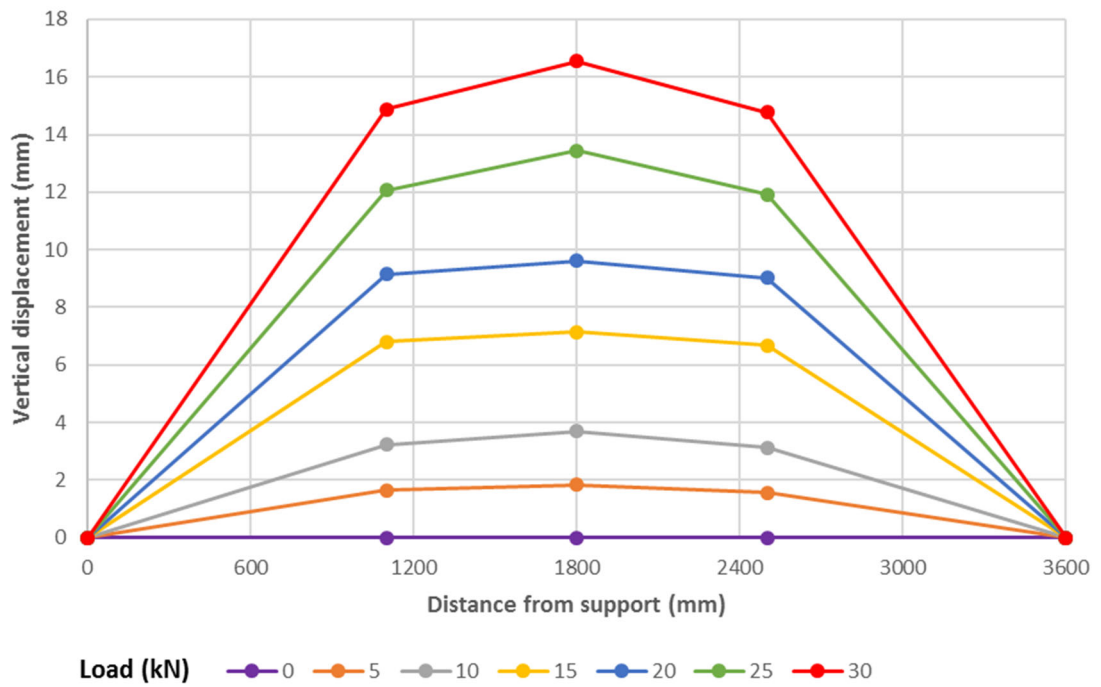


Figure 6-11 Vertical displacement of lattice girder planks at different load levels

6.3.2 Initial cracking

During the tests, a number of audible cracks were noted in the laboratory during the load tests and it is believed that these correspond to points at which the stiffness of the planks are reduced due to cracking of the concrete plank. It is proposed that the first audible crack is the onset of the first micro-cracks during the load test. Typically, at a later stage during the test cracking was observed in the concrete plank at the location of the load points. From a theoretical viewpoint, cracking would be expected to occur on the plank when the tensile strain capacity of the concrete (ϵ_{ctu}) was exceeded during the load test. Some research has shown that microcracks can form even if 50% of the tensile strength of the concrete is exceeded [17]. Although not explicitly mentioned in Eurocode 2 [18], the tensile strain capacity can be determined by dividing the mean tensile strength of the concrete (f_{ctm}) and the mean elastic modulus of elasticity of the concrete (E_{cm}).

$$\epsilon_{ctu} = f_{ctm} / E_{cm} \quad (\text{Eqn. 6-1})$$

Based on the testing undertaken on samples made from the concrete used to manufacture the precast planks, the mean compressive strength (f_{cm}) of the concrete

Chapter 6. Experimental Study of Hybrid Precast Concrete Lattice Girder Floor at Construction Stage

when the planks were tested was 54.1 MPa ($\sigma = 2.17$ MPa). The compressive strength was determined using cylinders tested on the day of the tests and cured in the same environmental conditions as the planks tested (cylinders and planks were cured side by side until testing). The mean tensile strength and elastic modulus can be derived using the mean compressive strength (Eqn 3.4 and 3.5 in Eurocode 2:Pt 1-1) so that an estimate of tensile strain capacity of the concrete plank can be calculated. Using equation 6-1, the tensile strain capacity of the concrete was estimated to range from 88-125 microstrains. The lower and upper value for the tensile strain capacity depends on whether the measured value for the elastic modulus is used (49.5 GPa, $\sigma = 1.54$ GPa) or the value derived using the mean compressive strength (34.8 GPa).

An estimation of the tensile strain at the bottom of the plank during the test can be determined by plotting the measured strains on the top surface of the plank and in the bottom chord of the girder and extrapolating the strain to the soffit of the plank. Theoretically, for the initial stages of the load test, the lattice girder plank should be linear elastic and, therefore, the strain profile from the top of the plank to the bottom of the plank should be linear. The strain profile for the 65mm thick plank (S22.5-08/05/05 girder) is shown in Figure 6-12 during the linear elastic phase of the test. The graph plots the average strain at the top of the plank (measured by two surface ER gauges bonded to the concrete surface at midspan) and the average strain in the bottom chords (measured by four ER gauges bonded to the four bottom chords at midspan) with increasing load. The graph is typical of the strain profile in all the concrete planks and indicates that the top of the plank is subject to compressive strains and that the neutral axis for the precast lattice girder plank lies within the concrete section. An estimate of the tensile strain at the soffit of the plank is found by extrapolating the measured linear strain profile to the bottom of the plank. For this plank, the first reduction in stiffness and audible crack was noted at an applied loading of 4.98kN and Figure 6-12 shows the change in strain profile in the concrete plank up to the point immediately before the first change in stiffness.

Chapter 6. Experimental Study of Hybrid Precast Concrete Lattice Girder Floor at Construction Stage

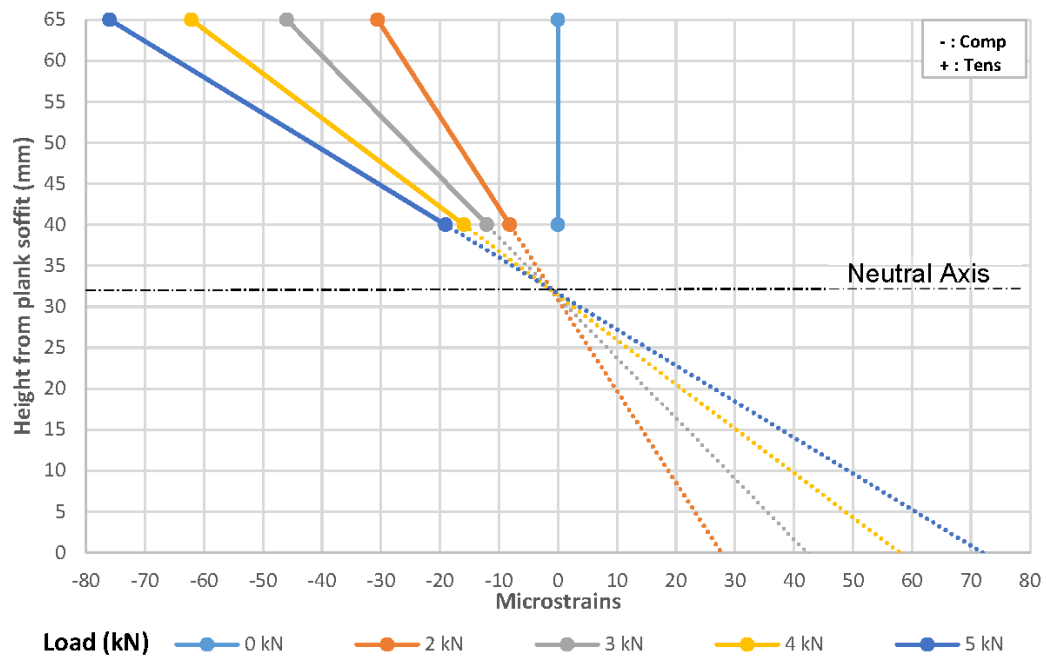


Figure 6-12 Measured strain profile in concrete plank (S22.5_08/05/05)

By reviewing the video and measured data, it was found that the first audible crack in the tests occurred at approximately the load which equates to the tensile strain at the plank soffit to be in the range of 37-102 microstrains. Therefore, this suggests that the first reduction in stiffness in the plank due to microcracking on the plank soffit occurs when the tensile strain in the bottom of the plank exceeds 50% of the tensile strain capacity of the concrete in the lattice girder plank. This concept has the potential for designers to offer a conservative predictor for first reduction in stiffness of the plank and the likelihood of microcracking on the plank soffit during construction.

6.3.3 Initial Stiffness

In order to accurately predict the behaviour of the lattice girder plank during construction stage, the initial stiffness (EI) of the plank must be known. Prior to the onset of micro cracking in the concrete plank, there is a linear relationship between load and midspan deflection which can be measured (Figure 6-9) to determine the initial stiffness of the lattice girder plank. The lattice girder plank is a hybrid system and, therefore, its initial stiffness is due to the composite action between the lattice girders, concrete and steel reinforcement. When significant cracking in the concrete

Chapter 6. Experimental Study of Hybrid Precast Concrete Lattice Girder Floor at Construction Stage

plank occurs, the composite action ceases and the stiffness of the floor system is primarily provided by the lattice girder and the reinforcement.

An analytical model of the lattice girder plank may be developed using the transformed section method such that the steel components in the girder and steel reinforcement are transformed to the equivalent concrete section. The modular ratio (ratio of the modulus of elasticity of the steel (202 GPa) to the modulus of elasticity of the concrete (49.5 GPa)) used is based on the material testing undertaken on the concrete and steel in the girder. The top chord, diagonals, bottom chord and longitudinal reinforcement are transformed to the equivalent concrete section. The stiffness provided by the diagonals will vary along the length of the plank as the diagonals are inclined with respect to the neutral axis of the lattice girder plank. An average stiffness provided by the diagonals at mid-height of the lattice girder is used in the analytical model (elliptical cross-section for diagonal is used). This allows the stiffness of the lattice girder plank to be determined using conventional beam theory. The comparison of measured initial stiffness in the plank (from testing) and the predicted initial stiffness using the analytical model (transformed section) are shown in Table 6-4. In addition, secondary stiffness of the plank after the initial formation of first cracking measured during the test is compared with the analytical model by omitting the stiffness of the concrete plank in the model. This is a conservative estimate and a measure of the lower bound of the secondary stiffness, as the concrete will still have some tensile and compressive strength after initial crack formation. It is expected that there will be some discrepancy between the measured and predicted stiffness as the analytical model is sensitive to the material properties and does not take account of shrinkage, creep or tension stiffening when cracking starts.

Chapter 6. Experimental Study of Hybrid Precast Concrete Lattice Girder Floor at Construction Stage

Table 6-4 Stiffness of lattice girder planks

Plank Reference	Girder Height (mm)	Measured Initial Stiffness K_{im} (kN/mm)	Predicted Initial Stiffness K_{ip} (kN/mm)	Ratio of $\frac{K_{ip}}{K_{im}}$	Measured Secondary Stiffness K_{2m} (kN/mm)	Predicted Secondary Stiffness K_{2p} (kN/mm)	Ratio of $\frac{K_{2p}}{K_{2m}}$	Estimated contribution of plank to overall stiffness (%)
S29-14/07/06 2015	290	1.53	2.35	1.54	1.33	1.49	1.12	15%
S29-14/07/06 2018	290	1.54	2.35	1.53	1.18	1.49	1.26	15%
S22-14/07/06 2018	220	1.35	1.37	1.02	1.06	0.79	0.74	20%
S10-14/07/06 2018	100	0.62	0.42	0.67	0.52	0.13	0.25	50%
W22.5-08/05/05 2018	225	0.59	0.69	1.18	0.46	0.39	0.85	31%
W10-10/06/06 2018	100	0.50	0.32	0.65	0.33	0.09	0.26	62%

For planks with tall girders (greater than 200mm), the analytical model calculated the initial stiffness and consequently the elastic deflection of the lattice girder planks to an accuracy of between +2 and +53%. Although, the scope of this study is limited to comparison with five types of lattice girders, the analytical model has the potential to be used as a tool for predicting the initial stiffness and elastic deflection of tall lattice girder planks at construction stage. It should be noted that the Concrete Society [19] estimated that even the most sophisticated analysis can only estimate deflection with an error of between +15% and -30% because of the number of factors which cannot be accurately assessed. Similarly for the tall girders, the analytical model predicts the secondary stiffness after the onset of initial cracking with an accuracy of +26% to -26%. It is expected that the accuracy of the analytical model for the secondary stiffness would be a lower bound, as it does not take account of the degree of cracking, tension stiffening and residual stiffness of

Chapter 6. Experimental Study of Hybrid Precast Concrete Lattice Girder Floor at Construction Stage

the concrete plank after the first cracks form. As the analytical model after initial cracking ignores the stiffness of concrete plank, the predicted stiffness is more representative of the lattice girder plank when the concrete has fully cracked and behaviour is governed by the stiffness of the steel lattice girder and the longitudinal reinforcement.

However, for the two planks with low height girders (100mm) that were tested, the analytical model underestimates the initial stiffness by approximately -34% and the secondary stiffness by approximately by -74%. It is proposed that accuracy of the analytical model for planks with small height girders is diminished because the contribution of the concrete plank to the stiffness of the composite plank is more significant for planks with small height girders. For the two planks with 100mm high girders, the contribution of the concrete to the overall stiffness of the lattice girder plank is 50% (S10-14/07/06) and 62% (W10-10/06/06) respectively. This contrasts with the three tall lattice girders tested in which the average contribution of the concrete to the overall stiffness of the lattice girder plank is 22%. This suggests that the analytical model is less accurate at modelling the bending behaviour of the concrete plank because of the various properties which are not included in the model such as creep, shrinkage and tension stiffening. In particular, accurate determination of the material properties is critical to the accuracy of the analytical model. Because the model is based on the transformed section method, the modular ratio (ratio of modulus of elasticity of steel and concrete) is a very important factor with respect to the predicted stiffness. Another possible reason for the discrepancies between the analytical model and measured stiffness is that the concrete plank may be considered a wide slender flange, so the assumption of plane cross-sections remaining planar during bending for beam theory may not be applicable. The low height girders are typically used for the production of twin-wall precast wall panels.

6.3.4 Deflection at construction stage

The cost of temporary propping lattice girder planks during the construction phase is a significant element for the contractor (€20-50/m²; based on information supplied by precast manufacturer in Ireland). The higher figure would apply to

Chapter 6. Experimental Study of Hybrid Precast Concrete Lattice Girder Floor at Construction Stage

projects with very high floor to ceiling heights and, hence, the requirement for longer props. The props must be left in place until the concrete in the in-situ topping reaches a specified compressive strength and the hybrid concrete slab can support its own self-weight and construction loading. The spacing of the props is dictated by limiting the deflection of the planks during construction. Typically, lattice girder planks are manufactured in lengths such that they are continuous over at least one line of temporary props (i.e. multi-span behaviour). The European standard for precast concrete floor products, EN 13747 [2], states that the midspan deflection of precast floors during construction should not exceed 10mm for spans up to 4m. EN 13747 recommends that a uniformly distributed load of 1kN/m^2 should be used for temporary loads (variable) during construction. EN 1991-1-6 [20] covers actions during construction and provides guidance in relation to construction loads for various types of construction activities and equipment and also for construction loads during casting of concrete. It recommends a uniformly distributed load of 1kN/m^2 for construction personnel and hand tools. For casting of concrete, it recommends a minimum uniformly distributed load of 0.75kN/m^2 with an additional of 10% of the slab self-weight or 0.75kN/m^2 whichever is greater, over a $3\text{m} \times 3\text{m}$ working area. Typically in Ireland and the UK, a uniformly distributed of 1.5kN/m^2 is allowed for construction loads and this figure is based on previous Irish and British codes of practice which were superseded with the introduction of the Eurocodes in 2010.

Many designers when checking the behaviour of the lattice girder plank at construction assume the plank is single span, ignore the stiffness of the concrete plank and assume the plank is simply supported between supports and/or props. This implies that there is potential for optimisation of the propping system if the behaviour of the floor at construction stage and the critical design parameters are better understood. Using the initial stiffness determined from the load tests, it is possible to determine the maximum span of the lattice girder plank (single span) during construction supporting the self-weight of the in-situ topping and a construction load of 1.5kN/m^2 . In Table 6-5, the maximum span and corresponding midspan deflection for each of the planks tested is determined based on the plank resisting an applied moment equivalent to bending moment at which the first

Chapter 6. Experimental Study of Hybrid Precast Concrete Lattice Girder Floor at Construction Stage

cracking of the plank (M_{crack}) was recorded in the plank during the load test (i.e. first reduction in plank stiffness). In addition, the deflection of the plank for various propping arrangements can also be investigated. The predicted deflection of the plank for the single span arrangement of 2.4m (common spacing of temporary prop systems) and double span arrangement of 3.6m (7.2m long plank) is also provided in Table 6-5 to illustrate the application of the test data to generate useful design data for the floor system (predict deflection for various propping arrangements). The applied loading in all cases is the self-weight of the in-situ topping and the construction load (1.5kN/m^2). It is noted in Table 6-5 where the cracking moment (M_{crack}) is exceeded and the expected deflection would therefore be larger than the figure quoted in the table as the lattice girder plank would have reduced stiffness after cracking occurs. The importance of the diameter of the top chord to control deflection at construction is highlighted by the fact that the two planks with similar heights (100mm and 220/225mm) have significantly different deflection characteristics.

The most critical parameter for controlling the deflection of the plank is the diameter of the top chord. The deflection characteristics of planks S22-14/07/06 and W22.5-08/05/05, whose girders are approximately the same height are significantly different because the cross-sectional area of the former is approximately three times greater than the latter (i.e. 14mm and 8mm diameter bars in the top chords, respectively). For the two propping arrangements examined (single span, $L = 2.4\text{m}$; double span, $L = 2 \times 3.6\text{m}$), the midspan deflection of the plank W22.5-08/05/05 is approximately 4.5 times the deflection of the plank S22-14/07/06. The difference in the deflection characteristics of the two planks with girders which are 10cm high (i.e. planks S10-14/07/06 and W10-10/06/06) were not as sizeable because the top chords are 14mm and 10mm, respectively. However, as expected, the deflection of the plank with the 14mm top chords is approximately 20% less than the planks with 10mm top chords for the two propping arrangements examined.

Chapter 6. Experimental Study of Hybrid Precast Concrete Lattice Girder Floor at Construction Stage

Table 6-5 Deflection characteristics of lattice girder planks during construction

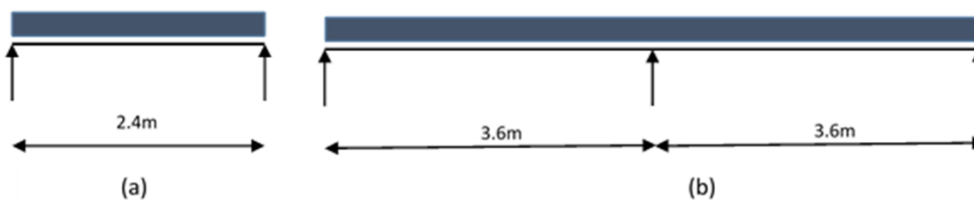
Plank Reference	Girder Height (mm)	Top chord diameter (mm)	Max Span ¹ (single span) (m)	Midspan deflection at Max Span ¹ (mm)	(a) Midspan deflection when propping at L = 2.4m (single span) ² (mm)	(b) Midspan deflection when propping at L = 3.6m (double span) ² (mm)
S29-14/07/06 2018	290	14	3.17	2.05	1.55	0.97
S22-14/07/06 2018	220	14	3.61	2.19	1.46	0.91
S10-14/07/06 2018	100	14	2.99	4.99	4.00	2.49
W22.5-08/05/05 2018	225	8	2.30	6.48	6.77 ³	4.22 ³
W10-10/06/06 2018	100	10	2.60	5.38	4.96	3.09 ³

Notes

1) Maximum span for the plank based on initial cracking of the plank in the test (single span and supporting self-weight of insitu concrete topping and construction loading (1.5kN/m²)).

2) Propping arrangements: (a) 2.4m Single span, (b) 7.2m Double span

 Self-weight of insitu concrete topping and construction loading (1.5kN/m²)



3) Cracking moment is exceeded and therefore expected deflections would be larger than the figure quoted in the table.

6.3.5 Strain distribution

The development of strain in the top chords was broadly similar for all planks tested. Increasing compressive strains (negative) were recorded during the load test. The two strain gauges bonded on each top chord (girder A and B in each plank, refer to Figure 6-8) allowed buckling behaviour of the top chord to be measured.

Chapter 6. Experimental Study of Hybrid Precast Concrete Lattice Girder Floor at Construction Stage

The measured strains in the top chords for the plank S29-14/07/06-2018 are shown in Figure 6-13a and the buckling of the top chord in girder A is clearly observed at peak load (approximately 32kN) causing excessive tensile strains on one side of the top chord and excessive compressive strains on the other side of the top chord. In contrast, no buckling was observed in the top chord for S10-14/07/06-2018 (Figure 6-14a) when the midspan deflection was 50mm.

Strain gauges were bonded to each of the diagonals at the supports and in all tests the intersection of first diagonal of the girder and bottom chord of the girder was located over the support (50mm wide). The measured strains from the diagonals in the tests are not consistent, which suggests that imperfections in the diagonals may influence the induced strains in the diagonals during the load tests. In an idealised lattice girder plank, it would be expected that the diagonals would be subjected to increasing compressive strains as the load increases. However, in some tests, the measured strains between diagonals at opposite supports and at the same support are inconsistent. The measured strains up to peak load for the diagonals at each support for one girder in plank S29-14/07/06 are shown in Figure 6-13b. Initially, increasing compressive strains (negative) are recorded but at approximately 25kN load, tensile strains are recorded in the diagonals up to peak load. This may indicate that buckling of the top chord of girder A commences at this point and induces tensile strains in the diagonals as the top chord buckles laterally in response to the increasing load. To contrast, the measured strains up to peak load for the diagonals at each support for one girder in plank S10-14/07/06 are shown in Figure 6-14b. At both supports, one diagonal experiences tensile strains (positive) and one support experiences compressive strains (negative). There is no change in the nature of the induced strains during the load test and this is primarily due to the fact that buckling of the top chord had not commenced at the end of the test. Similar findings were reported by Lofgren [4] in which he conducted load tests on two similar lattice girder planks and measured inconsistent strains in the diagonals similar to the findings as reported herein.

It is also noted that the strains in the diagonals suggest that the load transfer in the lattice girder is not shared equally between the diagonals and this may be due to

Chapter 6. Experimental Study of Hybrid Precast Concrete Lattice Girder Floor at Construction Stage

imperfections and also the geometric layout of the diagonals (angle of inclination with respect to the horizontal and vertical axis, distance from the support, distance from edge of plank). During the manufacture of lattice girder planks, it is not uncommon because of tolerances and manufacturing practices that the girder may not be perfectly symmetrical and, therefore, this can result in non-symmetrical load transfer within the girder.

The measured strains on the top surface of the concrete planks tested were generally consistent and there was little difference between strains from the two ER gauges bonded to the concrete surface in the middle of the plank and at the edge of the plank. This suggests that the transverse strains on the concrete surface are relatively uniform. The strains on the surface of the plank are compressive which confirms that the neutral axis of the lattice girder plank lies within the depth of the concrete plank. The surface strains measured by the two ER gauges on the top surface of planks S29-14/07/06 and S10-14/07/06 are shown in Figure 6-13c and Figure 6-14c, respectively. The reduction in load at the onset of micro-cracking indicating the reduced stiffness of the plank after the onset of cracking of the plank soffit is clearly observed.

The measured strains in the bottom chords of the girders were generally consistent for all tests conducted and had two distinct phases. Initially, up to the onset of the first cracking in the concrete plank, increasing compressive strains are recorded. At first, this may appear surprising but it confirms the strain profile plotted in Figure 6-12 which shows that the neutral axis for the uncracked lattice girder plank lies below the bottom chords of the girder. Hence, in the uncracked state, approximately the top half of the plank (65mm overall thickness) is in compression. The bottom chords are positioned in the top portion of the plank as the girders sit on the transverse reinforcement (H12 bars at 100mm centres) which are located 25mm above the plank soffit to comply with cover requirements. This first phase of increasing compressive strains may be clearly identified in Figure 6-13d, which plots the measured strains in the four bottom chords of the two girders in plank S29-14-07-06 up to peak load. The significant tensile change in strain at approximately 11kN measured in the bottom chords indicates the point at which the concrete plank

Chapter 6. Experimental Study of Hybrid Precast Concrete Lattice Girder Floor at Construction Stage

cracks initially. After cracking of the concrete, the bottom chords in combination with the longitudinal reinforcement in the plank must resist the tensile stresses and this is clearly observed by the increasing tensile strains up to peak load.

The five ER gauges bonded to one of the longitudinal reinforcement bars (B2 layer, H10 reinforcement at 100mm centres, 3.6m long) embedded in the concrete are at 0.8m centres and, therefore, allow the development of strain along the plank to be measured. The measured strains in the instrumented longitudinal reinforcement in plank S29-14/07/06 and S10-14/07/06 are shown in Figure 6-15. The ER gauges on the reinforcement bar are labelled in sequence A-E ('A' is located 200mm from end of the bar, 'C' is in the middle of the bar). Similar to the measured strains at midspan in the bottom chords, the measured strain in the longitudinal reinforcement has two distinct phases. This is expected as both the longitudinal reinforcement and bottom chord are positioned on top of the transverse reinforcement during the manufacture of the lattice girder plank. As described previously, with reference to the strains in the bottom chord, the measured strains in the longitudinal reinforcement were compressive up to the onset of the cracking of the concrete plank. After cracking of the concrete plank, the longitudinal reinforcement is subject to increasing tensile strains up to peak load.

The magnitude of the measured strains in the ER gauges located 200mm from the end of the 3.6m bar (Gauges A and E) at either end is typically small, as they are close to the supports where the bending stresses are relatively small. The three central ER gauges (Gauges B, C and D) are located at approximately midspan and adjacent to the load points on the support side of the plank. The measured strains along the longitudinal reinforcement at the approximate locations of the load points (Gauge 'B' and 'D') show slight differences which indicates that after cracking of the plank commences, the strain distributions along the reinforcement are not symmetrical. This is confirmed by observing the crack formation during the tests as typically cracking is initiated at one of the points and increased crack widths and deflection is noted in the vicinity of the load points.

The strain profile for the longitudinal reinforcement during the load for plank S10-14/07/06 is shown in Figure 6-16. Figure 6-16a plots the measured strains along the

Chapter 6. Experimental Study of Hybrid Precast Concrete Lattice Girder Floor at Construction Stage

longitudinal reinforcement when the concrete plank is uncracked. Up to the first crack (load less than 6kN), the lattice girder plank is linear elastic and the recorded strains along the longitudinal bar are compressive as the bar is located above the neutral axis and broadly symmetrical. When cracking occurs, the longitudinal reinforcement must resist the tensile stresses in the plank and restrain the extent and width of cracking in the concrete. The strain reversal from compressive to tensile strains after cracking is shown in Figure 6-16b, which shows the increasing tensile strains along the reinforcement. The location of the large tensile strains adjacent to one of the load points (~2600mm from internal support, 1000mm from external support) indicates that the cracking in the concrete plank is most extensive at this location. Also, it is noticeable that the order of magnitude of the tensile strains in the reinforcement after cracking are significantly greater than the compressive strains in the reinforcement prior to cracking. The observed cracking of the soffit of plank during the load test confirms that the extent and width of cracks were greatest adjacent to the load point closest to the external load point. The crack pattern on the plank soffit adjacent to the external load point after the load test is shown in Figure 6-17. The cracks generally run in the transverse direction along the plank soffit and the crack widths were greatest in the region adjacent to the external load point.

The main findings from analysis of the strain data from the ER gauges in the various load tests are:

- Top chord – Increasing compressive strains until buckling occurs.
- Diagonals – Inconsistent strain data which suggests that manufacturing imperfections and geometric layout of the girders can influence the load transfer mechanism in the lattice girders.
- Top surface of concrete plank – Increasing compressive strains.
- Bottom chord – Increasing compressive strains whilst plank is linear elastic. After cracking of concrete plank, increasing tensile strains.
- Longitudinal reinforcement – Increasing compressive strains whilst plank is linear elastic. After cracking of concrete plank, increasing tensile strains.

Chapter 6. Experimental Study of Hybrid Precast Concrete Lattice Girder Floor at Construction Stage

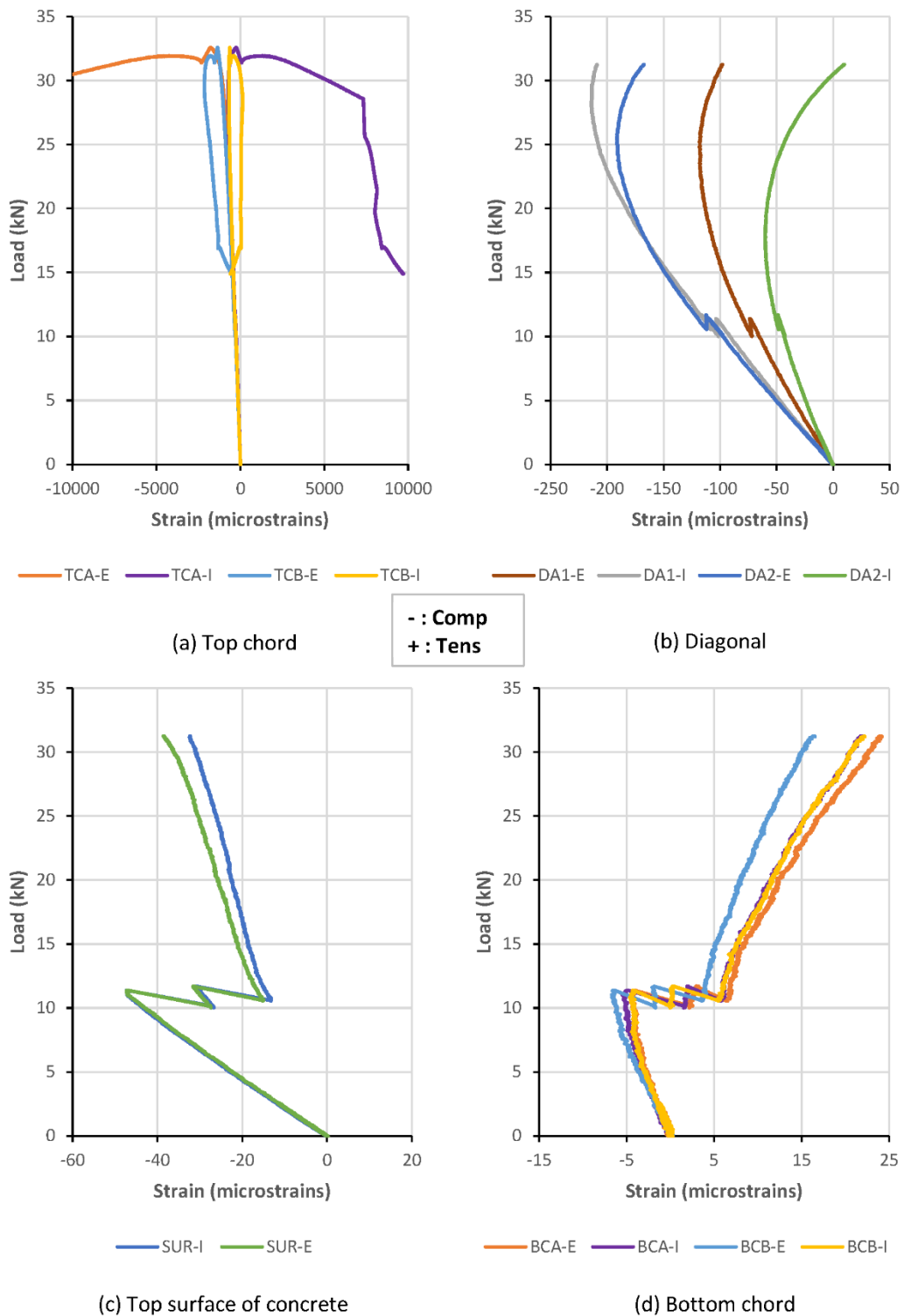


Figure 6-13 Measured strains of specimen S29-14/07/06-2018

(Refer to Figure 6-8 and Table 6-2 for nomenclature used for instrumentation)

Chapter 6. Experimental Study of Hybrid Precast Concrete Lattice Girder Floor at Construction Stage

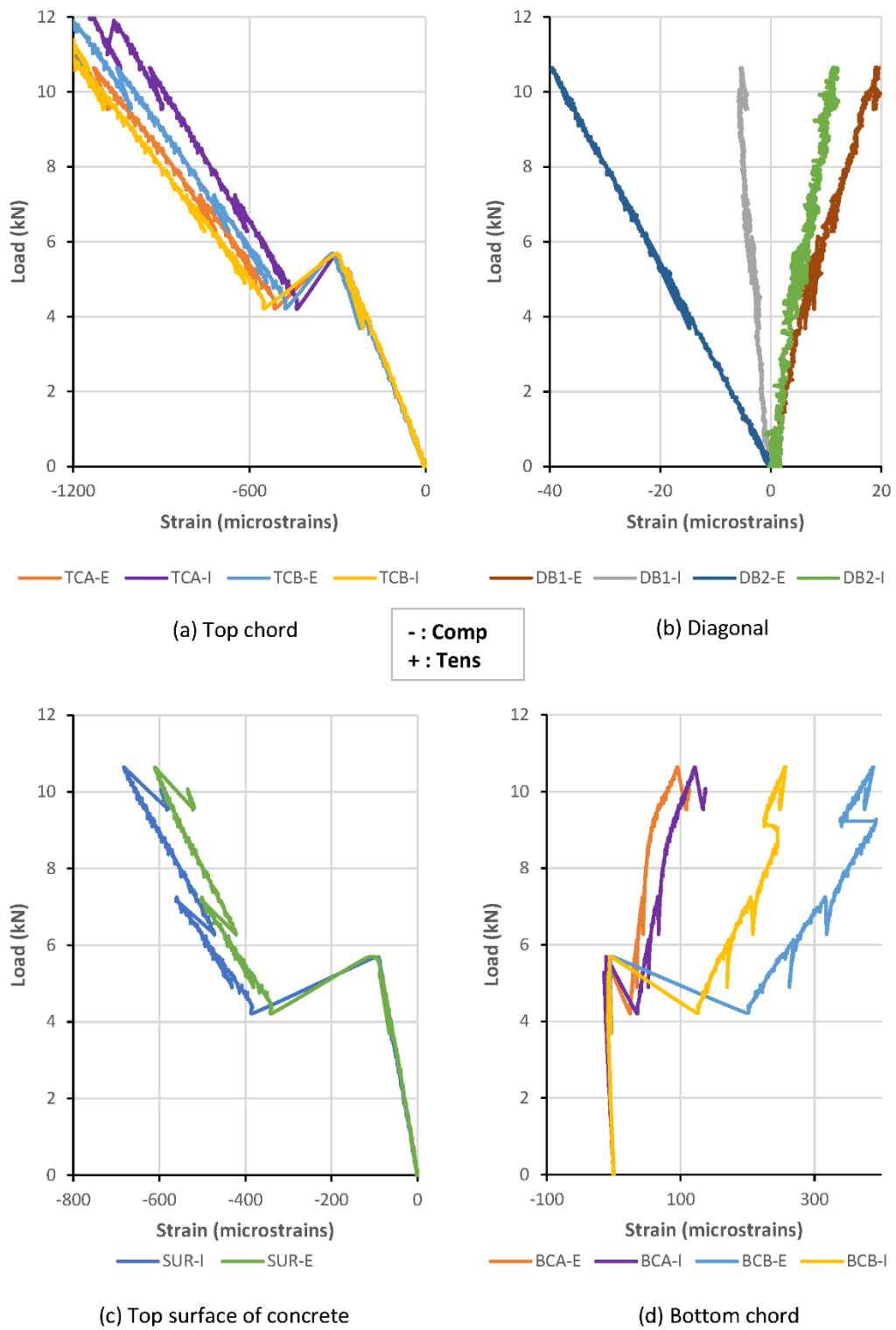


Figure 6-14 Measured strains of specimen S10-14/07/06-2018

(Refer to Figure 6-8 and Table 6-2 for nomenclature used for instrumentation)

Chapter 6. Experimental Study of Hybrid Precast Concrete Lattice Girder Floor at Construction Stage

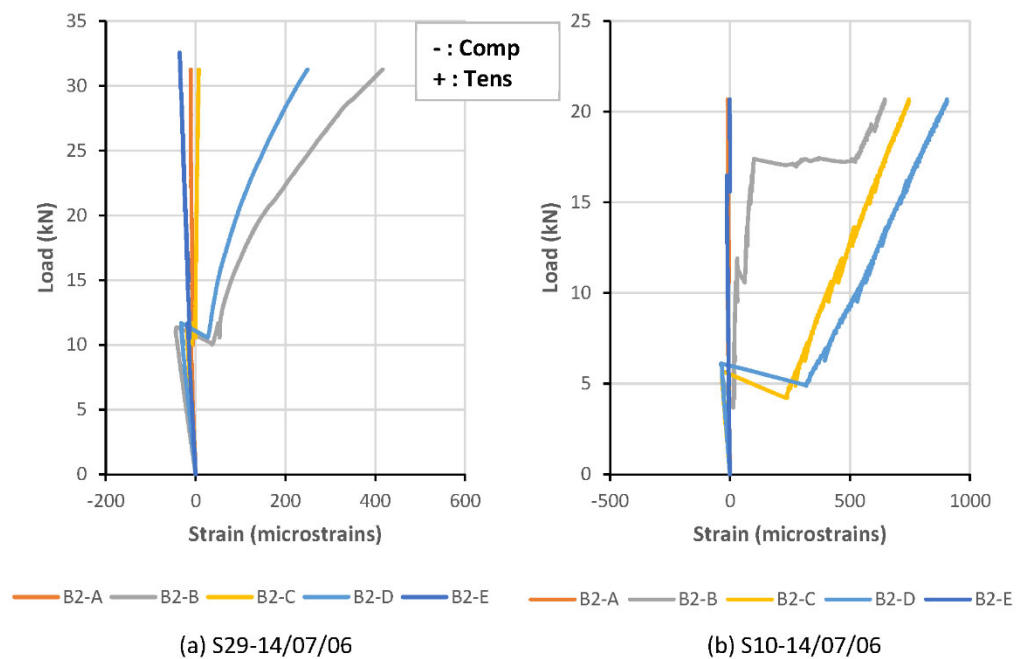


Figure 6-15 Strains in longitudinal reinforcement of concrete planks (a) S29-14/07/06 and (b) S10-14/07/06

The average strains in the top chord (4No.), top surface of concrete plank (2No.) and the bottom chords (4No.) for plank S29-14/07/06 and S10-14/07/06 are shown in Figure 6-18. Similar to strain profile generated for the concrete plank in Figure 6-12, the measured strains can be used to analyse the strain distribution through the overall section of the lattice girder plank. When the concrete is uncracked, the lattice girder plank is linear elastic. After the initiation of cracking of the concrete plank due to the tensile stresses, the stiffness of lattice girder plank reduces and the majority of the stiffness is provided by the lattice girder and the tensile reinforcement in the concrete plank. The measured strains illustrate the increasing tensile strains in the bottom chords and increasing compressive strains in the top chord as the load increases. The strain profile for the S10-14/07/06 plank (Figure 6-18b) clearly shows the linear elastic phase of the load test (up to ~5kN load) and the non-elastic phase after cracking of the concrete is initiated.

Chapter 6. Experimental Study of Hybrid Precast Concrete Lattice Girder Floor at Construction Stage

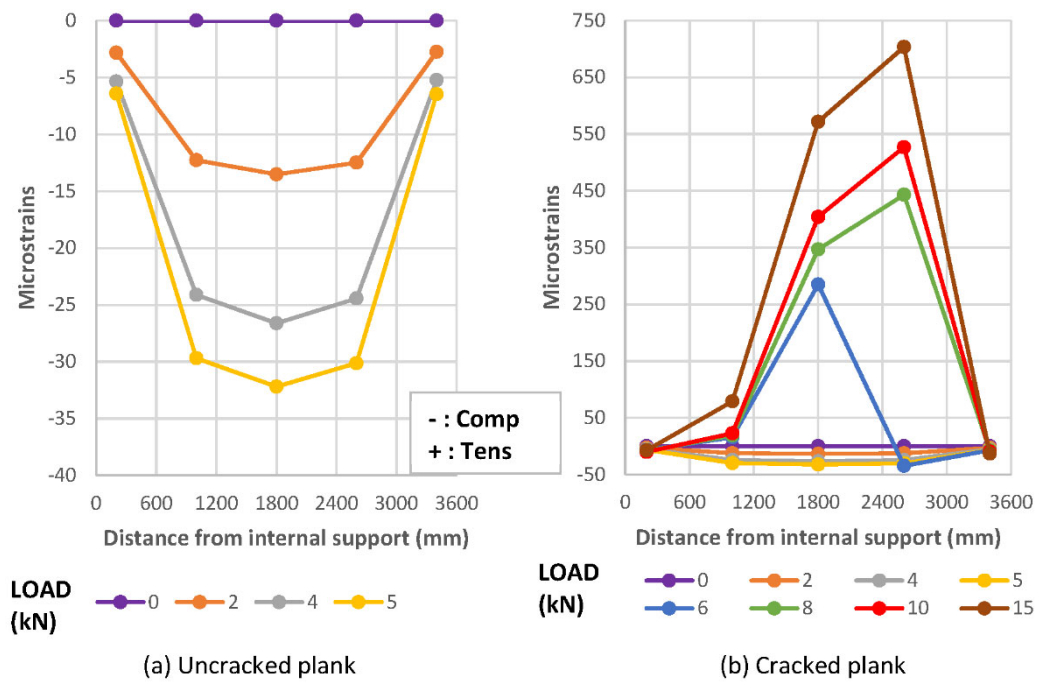


Figure 6-16 Strains profile along longitudinal reinforcement of plank (S10-14/07/06)

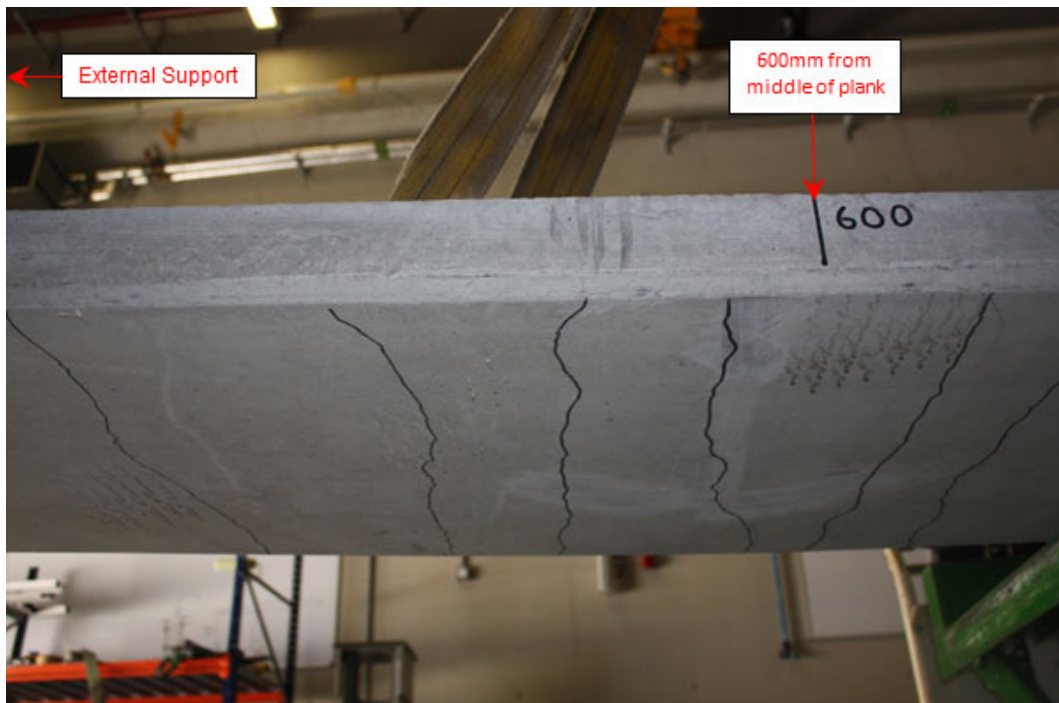


Figure 6-17 Crack pattern on plank soffit (S10-14/07/06)

Chapter 6. Experimental Study of Hybrid Precast Concrete Lattice Girder Floor at Construction Stage

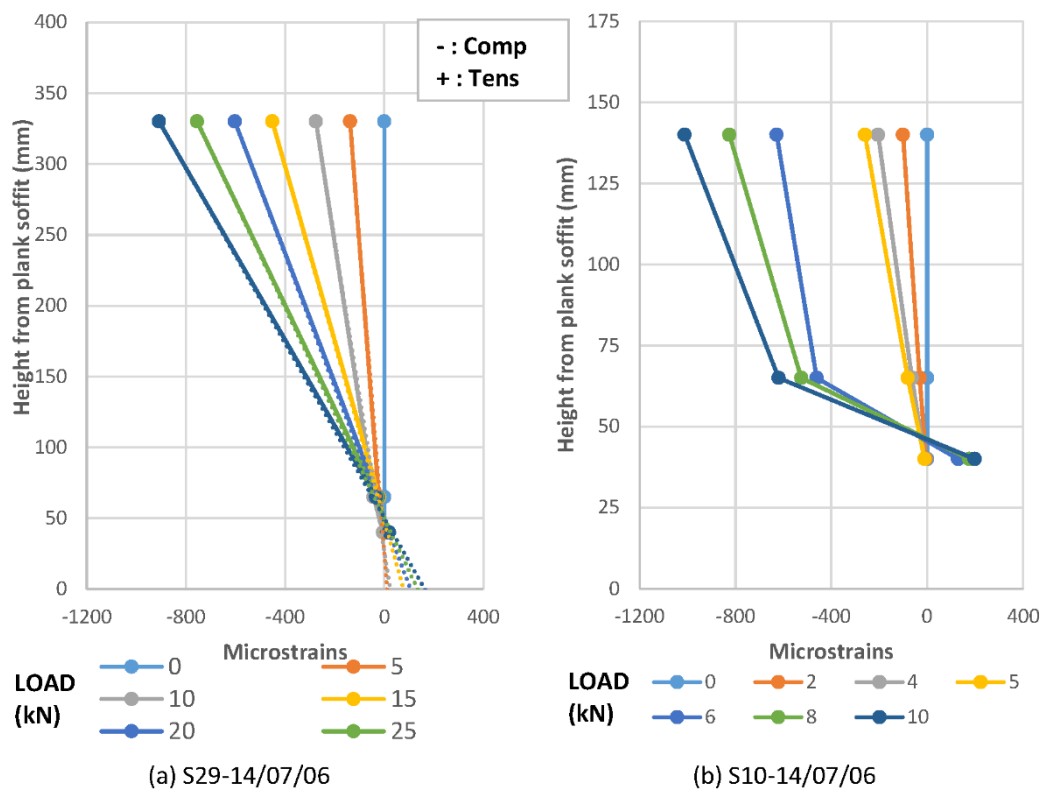


Figure 6-18 Strain profile for lattice girder plank

6.3.6 Ultimate limit state

Failure of the lattice girder planks is typically due to buckling of the top chord or diagonals in compression. Buckling of the diagonals is only critical for tall lattice girders (i.e. deep concrete slabs) in which the buckling length of the diagonals can be critical. In all cases, the deflection of the plank at failure (peak load) exceeded 10mm, which means that the serviceability limit state of deflection and cracking of concrete were the critical design checks rather than the ultimate limit state. In tests conducted for this study, three failure modes were observed (Figure 6-19); buckling of the diagonal (1No.), buckling of the top chord between diagonals (3No.) and lateral buckling of the top chord with lateral deformation (2No.). A summary of the failure modes and peak loads for the tests conducted is shown in Table 6-6. When failure was due to buckling of the diagonals, initial buckling occurred in diagonals close to the support and as the load increased, buckling of other diagonals followed. When the failure mode was buckling of the top chord, initial buckling was observed

Chapter 6. Experimental Study of Hybrid Precast Concrete Lattice Girder Floor at Construction Stage

close to the load point at one-third span which is the location of combined maximum moment and maximum shear acting on the plank.



(a) buckling of diagonals (S29-14/07/06_2015)



(b) lateral buckling of top chord (S29-14/07/06_2018)



(c) buckling of top chord between diagonals (W22.5-08/05/05)

Figure 6-19 Failure mode of planks

Although the test data is limited to six tests, the buckling failure mode of the top chord with tall girders (greater than 200mm) is more likely due to lateral buckling of the entire top chord rather than localised buckling between the diagonals. In contrast, buckling of the top chord with shallow girders is due to buckling of the top chord between the diagonals. As the length of diagonals increases for tall girders, the lateral restraint provided by the diagonals to the top chord is reduced and consequently lateral buckling of the top chord is more likely than buckling between the top chords. This suggests the buckling resistance of the top chord for tall girders is a function of the lateral restraint provided by the diagonals in addition to the diameter of the top chord. The other interesting observation from the tests conducted was the different failure mode for the same plank (S29-14/07/06) tested in 2015 and 2018. Although the initial stiffness of both planks were very broadly similar (1.53kN/mm and 1.54kN/mm), the plank tested in 2015 failed due to

Chapter 6. Experimental Study of Hybrid Precast Concrete Lattice Girder Floor at Construction Stage

buckling of the diagonals and the plank in 2018 failed due to the buckling of the top chord. There are several factors which could explain the different failure of two planks with the same lattice girder configuration such as initial imperfections that can result from the manufacturing process or handling of the lattice girder, material properties and restraint by diagonals. Based on the tensile tests conducted, the average yield stress for the top chord of the plank tested in 2015 was 20% higher than the yield stress of the top chord of the plank tested in 2018. The difference in material properties for the top chords of the two planks would mean that the compressive resistance of the top chords in the 2015 plank were significantly greater than the compressive resistance of the 2018 plank and may partially explain why the top chord buckled in the 2018 test and not in the 2015 tests even if the girder configuration and specification were similar. It is proposed to repeat this test for the next series of tests. The difference in failure modes for the same plank also highlights the difficulty in modelling the lattice girder plank and the importance of using accurate material properties in numerical modelling.

Table 6-6 Failure mode of planks

Plank Reference	Girder Height (mm)	Peak Load* (kN)	Failure Mode
S29-14/07/06 2015	290	19.98	Buckling of diagonals at support.
S29-14/07/06 2018	290	16.26	Lateral buckling of top chord.
S22-14/07/06 2018	220	20.36	Lateral buckling of top chord.
S10-14/07/06 2018	100	11.60	Peak load was not reached when midspan deflection was 50mm. Buckling of top chord between diagonals was observed when midspan deflection was manually increased to 66mm.
W22.5-08/05/05 2018	225	3.95	Buckling of top chord between diagonals.
W10-10/06/06 2018	100	4.66	Buckling of top chord between diagonals.

*Peak load per girder

Chapter 6. Experimental Study of Hybrid Precast Concrete Lattice Girder Floor at Construction Stage

The compression buckling resistance of the top chord and diagonal can be determined by using the provisions in Eurocode 3 (Design of steel structures) [21]. Similar to most structural codes of practice, the formulae for compression buckling provided in the Eurocodes are based on the elastic buckling load developed by the mathematician Euler and buckling curves to take account of imperfections which are based on empirical data and the Perry-Robertson formula. To accurately predict the buckling resistance of compression members one must also allow for geometric imperfections, non-homogenous material properties, residual stresses and end restraints conditions which may affect the actual behaviour of the top chord and diagonal. The assumed buckling length of the top chord and diagonal are two of the key parameters when predicting the compression buckling resistance. For the top chord, the assumed buckling length is typically assumed by designers to be 300mm which equates to 1.5 times the distance between the diagonals (200mm). However, the buckling behaviour of the top chord in the tests conducted suggest that the buckling length of the top chord is sensitive to imperfections and material properties and that the degree of lateral restraint provided by the diagonals may influence the buckling mode of the top chord. With regard to the buckling length of the diagonal, the actual length of the diagonal is easily defined but the degree of rotational restraint provided by the concrete at one end and the top chord at the other is difficult to determine. Using the formulae in Eurocode 3, the predicted peak load for the plank can be determined by calculating the load which will produce a compression force equivalent to the compression buckling resistance of the top chord and diagonal, respectively, and using the smaller load as this will be the critical failure load. A comparison of measured peak load and the predicted failure load for the lattice girder planks tested is shown in Table 6-7 based on the compression resistance of the top chord and diagonal determined in accordance with Eurocode 3. There is no guidance in the literature in relation to an appropriate buckling length of elements of a lattice girder composed of solid steel reinforcement. The assumed buckling length of the top chord was 300mm and the buckling length of the diagonal was assumed to 85% of the length of diagonal protruding from the concrete plank (based on assuming pinned-fixed end conditions and a buckling length = $0.85L$). In addition, the modulus of elasticity of the steel reinforcement was assumed to be 202GPa (mean modulus of elasticity of the top chords tested, refer to Section 6.2.3)

Chapter 6. Experimental Study of Hybrid Precast Concrete Lattice Girder Floor at Construction Stage

and a material partial safety factor of 1.0 (γ_s) was adopted for the strength of the steel reinforcement ($\gamma_s = 1.15$ defined in Eurocode 2 [18]).

It is clear from Table 6-7 that the current ultimate design check is conservative and the global factor of safety for the lattice girder plank when comparing the peak load and the predicted failure load (in accordance with Eurocode 3) ranges between 2.08 and 3.26. In addition, the predicted failure mode (top chord or diagonal buckling) is not always in agreement with the actual failure mode in tests. This suggests that further investigation is required to accurately predict the buckling length for top chords and diagonals in the lattice girder during construction stage so that better predictive models may be developed for the ultimate limit state behaviour of the lattice girder plank.

Table 6-7 Predicted failure of planks

Plank Reference	Predicted Failure Mode	Actual Failure Mode	Predicted based on Diagonal Resistance (kN)	Predicted based on Top Chord Resistance (kN)	Actual Failure Load (kN)*	Global Factor of Safety
S29-14/07/06 2015	Diagonal	Diagonal	6.43	14.05	19.98	3.11
S29-14/07/06 2018	Diagonal	Top Chord	6.43	14.05	16.26	2.53
S22-14/07/06 2018	Diagonal/ Top Chord	Top Chord	9.77	10.66	20.36	2.08
S10-14/07/06 2018	Top Chord	Top Chord	18.00	4.85	11.60	2.39
W22.5- 08/05/05 2018	Top Chord	Top Chord	2.69	1.39	3.95	2.85
W10-10/06/06 2018	Top Chord	Top Chord	11.19	1.43	4.66	3.26

*Failure load per girder

Chapter 6. Experimental Study of Hybrid Precast Concrete Lattice Girder Floor at Construction Stage

In all the tests conducted, failure of the bottom chords of the lattice girder was not recorded. The bottom chords of the lattice girder in conjunction with the longitudinal reinforcement resist the tensile forces during construction stage. To avoid tensile failure in the concrete plank, a minimum area of longitudinal reinforcement is specified in the plank to ensure that failure will occur due to the buckling of the top chord or diagonal.

Cracking was visually observed during the load tests and the cracking pattern on the plank soffit was recorded after each test. For all tests, initial cracking was noted on the side of the plank close to one of the load points and as the load increased the crack width would increase and propagate along the plank soffit (Figure 6-10). Cracks were typically running along the transverse direction of the plank (perpendicular with the span of the plank). The location of the first observed cracking typically coincided with the location of the initial buckling of the top chord and, at failure, the crack widths were largest at the same location of the buckled element (top chord or diagonal). At the end of the test, a series of transverse cracks were typically observed in the middle third of the plank between the load points (Figure 6-20). In some tests, in which peak load was reached relatively early during tests, additional transverse cracking developed in the outer third of the plank between the supports and the load point. The magnitude and extent of the largest transverse cracking was typically an indication of the location of a failed element in the lattice girder. When a component of the lattice girder buckles (top chord or diagonal), the tensile stresses and crack widths in the concrete plank at that location are increased as the bottom chords and longitudinal reinforcement must resist additional load.

Chapter 6. Experimental Study of Hybrid Precast Concrete Lattice Girder Floor at Construction Stage

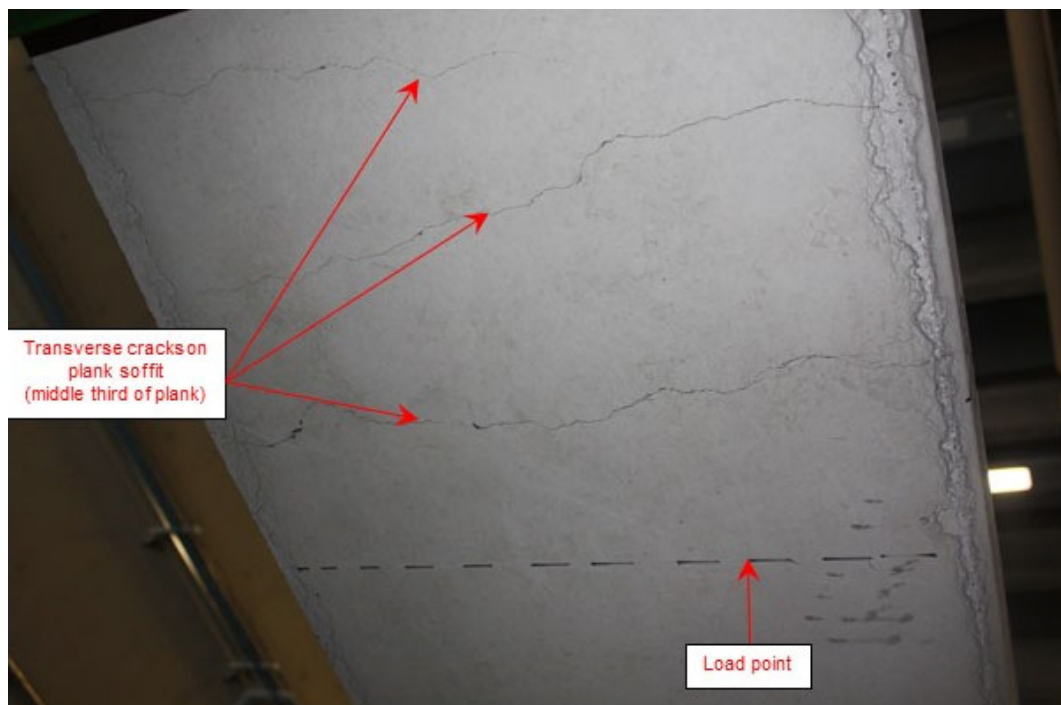


Figure 6-20 Transverse cracking on middle third of plank soffit

In addition to cracking on the plank soffit, some minor cracking was also observed on the top surface of the plank in some of the load tests (Figure 6-21). These typically occurred in latter part of the tests and none were observed on the top surface prior to cracking of the plank soffit. Most cracking was observed adjacent to the diagonals protruding from the plank and were not reflected on the plank soffit although cracking was observed between the lattice girders in one test (W22.5-08/05/05). Some of these cracks are thought to be due to concrete laitance (weak thin layer of fine aggregate and cement) and some of the cracking is in response to the deformation of the lattice girder components during the load test.



(a) Surface cracking between girders (W22.5-08/05/05)

(b) Surface cracking at diagonals (S22-14/07/06)

(c) Surface cracking at diagonals (S22-14/07/06)

Figure 6-21 Cracking on surface of plank

6.4 Conclusions

This paper describes six full-scale tests on precast concrete lattice girder planks which were undertaken at NUI Galway to investigate the behaviour of the hybrid concrete floor system during the construction stage. During the construction stage, the planks are temporarily propped until the in-situ concrete topping is poured and the props are removed when the in-situ topping has achieved a specified minimum strength. The concrete planks tested were similar except for the lattice girder configuration and the range of lattice girders (100-290mm) used were representative of the type of girders used in the construction industry. Material testing was undertaken to determine the properties of the concrete and steel in the lattice girder planks. It is envisaged that the greater understanding of this precast floor system at construction stage achieved through this experimental programme and previous research [9], [10] will make it possible to develop numerical models which can accurately predict the of the behaviour of the lattice girder plank floor during construction. The comprehensive range of instrumentation utilised in the tests allowed the behaviour of the various components in the lattice girder plank (top chord, bottom chord, diagonals, concrete, reinforcement) to be analysed. This rich data will contribute to the relatively little experimental data available and will assist with the development of accurate numerical modelling. The experimental results illustrate that there is potential for significant optimisation of the lattice girder precast floor system at construction stage which could reduce the cost and labour required for temporary propping. Several structural aspects can be concluded from the experimental tests conducted:

- The behaviour of the lattice girder plank has a number of distinct phases. The moment-deflection relationship is linear and elastic initially until the onset of cracking on the plank soffit. As load increases, the cracks widen and propagate, and the stiffness of the plank reduces until peak load/moment is reached.
- During the linear elastic phase, the neutral axis for the lattice girder plank for all tests was located below the longitudinal reinforcement in the concrete plank. The neutral axis was typically located in the middle of the concrete plank (65mm thick).

Chapter 6. Experimental Study of Hybrid Precast Concrete Lattice Girder Floor at Construction Stage

- The onset of cracking typically occurred at similar displacements for all tests and appeared to be related to the tensile strain capacity of the concrete. Using the measured strain profile on the lattice girder to extrapolate the strain on the plank soffit, it appeared that cracking was initiated when the strain exceeded the tensile strain capacity of the concrete. The tensile strain capacity was calculated using information from material testing of the concrete used in the plank.
- The initial stiffness and deflection of the lattice girder plank can be determined relatively accurately for tall girders (height $\geq 200\text{mm}$) using the transformed section method. The elastic deflection of the lattice girder plank with tall girders can be calculated to an accuracy of between +2 % and +53%.
- The transformed section method may be used as a lower bound estimate for the secondary stiffness of the lattice girder plank with tall girders.
- The transformed section method is not suitable for estimating the stiffness and deflection of the lattice girder plank with small height girders (height $\cong 100\text{mm}$).
- Experimental test data can be used to determine the deflection of the lattice girder planks with variable propping arrangements and variable construction loading. Taking account of the multi-span nature of lattice girder planks during construction can result in significant efficiencies for propping arrangements on site.
- Failure of the plank at construction stage is due to either buckling of the top chord (bending failure) or buckling of the diagonal (shear failure). In all cases, deflection of the plank at failure exceeded 10mm (maximum permitted deflection at construction stage).
- Imperfections due to the manufacturing and construction process of the lattice girders planks and differences in material properties can impact the behaviour of the lattice girder plank at the construction stage.
- The ultimate resistance of the lattice girder plank can be estimated using the compression buckling resistance provisions in Eurocode 3. This method is

Chapter 6. Experimental Study of Hybrid Precast Concrete Lattice Girder Floor at Construction Stage

sensitive to the buckling length assumed for the top chord and diagonal of the lattice girder and the material properties.

- An average global factor of safety of 2.7 was calculated when comparing the experimental failure load and the calculated failure load using Eurocode 3. This suggests that there is scope for more refinement to better predict the failure mode and load.

6.4.1 Recommendations for future research

Based on the experimental testing conducted and comparison of predicted and actual behaviour, it is recommended that further research should be undertaken in the following areas:

- Development of a general analytical model which can be used for the design of lattice girder planks at construction stage.
- Further experimental testing with different configurations of lattice girders (height, spacing, top chord diameter, diagonal diameter, reinforcement).
- Further experimental testing investigation on both single span and multi-span propping arrangements.
- Degree of restraint provided by the diagonals to the top chord of the lattice girder.
- Determine appropriate buckling lengths to be used for checking the buckling resistance of the top chord and diagonal of the lattice girder.
- Impact of reinforcement in the concrete plank on the stiffness, deflection and crack behaviour.
- Contribution of diagonals of the lattice girder to the overall stiffness of the lattice girder plank.
- Modelling of tension stiffening and residual stiffness of concrete plank after cracking.
- Parameter study to investigate optimisation of lattice girder configuration (top chord, diagonal, bottom chord, girder height, girder spacing).
- Design guide with more realistic temporary propping arrangements to control deflection and cracking.

Chapter 6. Experimental Study of Hybrid Precast Concrete Lattice Girder Floor at Construction Stage

- Appropriate factor of safety for lattice girder precast floor system at construction stage.

Acknowledgements

The authors would like to acknowledge the support of Oran Precast and in particular Dave Holleran (Engineering Manager) who manufactured all the precast elements which were tested for this project. The authors would like to thank Colm Walsh (Senior Technical Officer, NUI Galway) and Peter Fahy (Senior Technical Officer, NUI Galway) for their assistance with the laboratory testing and material testing respectively. The assistance of Gerard O’Kelly-Lynch (former masters student) with bonding of sensors during manufacture of the planks is also acknowledged. This project has received funding from the European Union’s Horizon 2020 research and innovation programme under grant agreement No. 637221 Built2Spec Project. The second author would also like to acknowledge the funding received from the Science Foundation Ireland through the Career Development Award programme (Grant No. 13/CDA/2200).

6.5 References

- [1] The Concrete Centre, “Hybrid Concrete Construction (TCC/03/53),” The Concrete Centre (UK), London, UK, 2005.
- [2] NSAI, “IS EN 13747: Precast concrete products - Floor plates for floor systems,” NSAI (National Standards Authority of Ireland), Dublin, Ireland, 2010.
- [3] J. Furche and Bauermeister U, “Load tests: Long erection spans with strengthened lattice girders,” *Betonwerk+ Fert.*, vol. 77, no. 8, pp. 4–17, 2011.
- [4] I. Löfgren, “Lattice Girder Elements in Four Point Bending – Pilot Experiment (Report No. 01:7),” Chalmers University, Sweden, Göteborg, 2001.
- [5] G. Bertram, J. Furche, J. Hegger, and U. Bauermeister, “Permissible Span of Semi-precast Slabs in Case of Erection (Zulässige Montagestützweiten von Elementdecken mit verstärkten Gitterträgern),” *Beton- und Stahlbetonbau*, vol. 106, no. 8, pp. 540–550, 2011.
- [6] Y. M. Cheng and Y. Fan, “Laboratory and numerical test on concrete plank composite with reinforcement truss,” *J. Struct. Eng.*, vol. 20, no. 4, pp. 207–216, 1994.
- [7] A. Torre, J. A. M. Martínez, A. R. Saiz, and V. O. Lopez, “Span in Construction of Concrete Precast Products: Bearing Beams and Reinforced Slabs,” *Int. J. Hous. Sci. Its Appl.*, vol. 35, no. 2, pp. 91–102, 2011.
- [8] S. Newell, M. Hajdukiewicz, and J. Goggins, “Real-time monitoring to investigate structural performance of hybrid precast concrete educational buildings,” *J. Struct. Integr. Maint.*, vol. 1, no. 4, pp. 147–155, 2016.
- [9] S. Newell and J. Goggins, “Real-time monitoring of concrete – lattice-girder slabs during construction,” *Proc. Inst. Civ. Eng. - Struct. Build.*, vol. 170, no. 12, pp. 885–900, 2017.

Chapter 6. Experimental Study of Hybrid Precast Concrete Lattice Girder Floor at
Construction Stage

- [10] S. Newell and J. Goggins, “Investigation of Thermal Behaviour of a Hybrid Precasted Concrete Floor using Embedded Sensors,” *Int. J. Concr. Struct. Mater.*, vol. 12, no. 1, p. 66, 2018.
- [11] D. Byrne and J. Goggins, “Evaluating the structural capacity of concrete elements through in-situ instrumentation,” *Key Eng. Mater.*, vol. 569–570, 2013.
- [12] J. Goggins, D. Byrne, and E. Cannon, “The creation of a living laboratory for structural engineering at the National University of Ireland, Galway,” *Struct. Eng.*, vol. 90, no. 4, pp. 12–19, 2012.
- [13] M. Hajdukiewicz, D. Byrne, M. M. Keane, and J. Goggins, “Real-time monitoring framework to investigate the environmental and structural performance of buildings,” *Build. Environ.*, vol. 86, pp. 1–16, 2015.
- [14] NSAI, “IS EN 12390-3: Testing hardened concrete – Part 3: Compressive strength of test specimens.,” NSAI (National Standards Authority of Ireland), Dublin, Ireland, 2009.
- [15] NSAI, “IS EN 12390-13: Testing hardened concrete - Part 13: Determination of secant modulus of elasticity in compression,” NSAI (National Standards Authority of Ireland), Dublin, Ireland, 2013.
- [16] NSAI, “IS EN 15630 Steel for the reinforcement and prestressing of concrete - Test methods - Part 1 : Reinforcing bars , wire rod and wire,” NSAI (National Standards Authority of Ireland), Dublin, Ireland, 2010.
- [17] FIB, “Externally bonded FRP reinforcement for RC structures (fib Bulletin No. 14),” FIB (The International Federation for Structural Concrete), Lausanne, Switzerland, 2001.
- [18] NSAI, “IS EN 1992-1-1: Eurocode 2: Design of concrete structures. Part 1-1: General rules and rules for buildings,” NSAI (National Standards Authority of Ireland), Dublin, Ireland, 2005.

Chapter 6. Experimental Study of Hybrid Precast Concrete Lattice Girder Floor at Construction Stage

- [19] The Concrete Society, “Deflections in concrete slabs and beams (TR No. 58),” The Concrete Society, Camberley, UK, 2005.
- [20] NSAI, “IS EN 1991-1-6: Eurocode 1 - Actions on structures - Part 1 -6 : General actions - Actions during execution (Including National Annex),” NSAI (National Standards Authority of Ireland), Dublin, Ireland, 2005.
- [21] NSAI, “IS EN 1993-1-1: Eurocode 3: Design of Steel Structures: Part 1-1: General Rules and Rules for Buildings,” NSAI (National Standards Authority of Ireland), Dublin, Ireland, 2005.

7 Conclusions

7.1 Chapter summary

This chapter summarises the main conclusions from the thesis following a programme of laboratory and field testing. **Section 7.2** describes the primary research findings and conclusions from each of the individual chapters and highlights the connections between the research components. Some brief reflections on the research presented in this thesis are outlined in **Section 7.2.1**. Elements of the research which the author considers original work and the contribution to knowledge are summarised in **Section 7.2.2**. Recommendations for future work are presented in **Section 7.3**.

7.2 Thesis conclusions

In comparison to other forms of structural floors, very little research has been published on the behaviour of hybrid concrete lattice girder flat slabs and this explains why much of the guidance in relation to its behaviour during construction is empirically based. Information on the critical parameters which impact on the behaviour of structural elements during construction can sometimes be difficult to determine. As engineers are typically conservative, if they do not fully understand how a structural element behaves, they will make conservative assumptions in relation to its behaviour to ensure that their design is safe. Unless information is available, engineers are likely to use overly conservative design principles which are uneconomical and unsustainable. This approach is not justifiable in the future as the construction industry, along with other industries, tries to make its practices more environmentally sustainable.

The research in this thesis focuses on a hybrid concrete floor product which is widely used to construct flat slabs in concrete frames throughout Europe and America. The hybrid concrete lattice girder flat slab is considered a Modern Method of Construction (MMC), as it offers many benefits in terms of economy, increased

speed, higher quality, better safety and reduced waste. Many governments are encouraging the greater use of MMC and off-site construction to improve the efficiency of the construction industry and ensure that it is competitive in the future. In this research, laboratory and field-based testing utilising structural health monitoring are employed to (i) improve the understanding of how hybrid concrete lattice girder flat slabs behave during construction, (ii) review current design practices in relation to the floor product and (iii) identify areas where further research might improve the efficiency and performance of the hybrid concrete flat slab.

The literature review in **Chapter 2** noted that despite the popularity of hybrid concrete lattice girder flat slabs, there is a lack of robust field data on their structural behaviour and performance. It was also noted that technological advances and the digital transformation of the industry (*'Industry 4.0'*) provides opportunities for structural health monitoring (SHM) to become standard practice and the development of 'smart structures' with embedded sensors which will provide real-time data in relation to the performance and/or health of the structure. Limited experimental data was available on the structural behaviour of lattice girder planks during construction and there was little information on the interaction between the various components of the lattice girder plank during construction when it must support its own self-weight, self-weight of the wet insitu concrete topping and construction loads. A number of researchers noted that erection spans (spacing between temporary props) are typically based on design methods which are overly conservative and that there is no model which predicts accurately the erection spans or deflection of the lattice girder planks during construction. Temporary propping of lattice girder planks is a significant cost element of the floor construction and any efficiencies achieved in the determination of erection spans would reduce formwork costs and labour resources on site.

The concept of SHM and its key benefits are introduced in **Chapter 3**. The service life of concrete structures is much longer than other commercial products and therefore, as engineers, we need to understand how they behave during their full life-cycle (construction, operation, maintenance, removal/recycle). The general SHM methodology which was implemented by the author is described and this

methodology can be easily adapted to other concrete structures. The SHM strategy allowed real-time monitoring of the behaviour of three concrete frame buildings constructed in NUI Galway in the last ten years. The sensors were installed prior to construction and were used to monitor the behaviour of hybrid concrete lattice girder flat slabs which was the primary form of floor construction in the three buildings. In **Chapter 3**, many of the potential applications of SHM data in a concrete slab are described:

- using the SHM data to evaluate structural capacity of the floor for potential retrofitting and strengthening of concrete slab.
- compare long-term predicted strains (using Eurocode 2) and measured strains in concrete floor and examine various magnitude of the various strain components.
- analyse early-age thermal effects in hybrid concrete slab.
- investigate construction stage behaviour of hybrid concrete slab.

The SHM of the three buildings in NUI Galway is on-going so that the long-term behaviour of the concrete floor can be investigated by students, professionals and researchers in the future. Since the construction of the Human Biology Building in 2016, the SHM system has also been used as a teaching tool for undergraduate civil engineering students (**Appendix D**). The students have taken part in load tests and were able to analyse the data from the sensors in the concrete floor. This approach is very beneficial for students as it allows them to develop greater understanding of structural behaviour and appreciate how structures respond to applied loads as specified in codes of practice. The application of the SHM strategy (outlined in **Chapter 3**) to the Human Biology Building (HBB) which was constructed in 2015-2016 in NUI Galway is described in **Chapter 4** and **Chapter 5**.

Chapter 4 reports on the practical applications of SHM data from the HBB to investigate the structural behaviour of the hybrid concrete lattice girder flat slab during the construction phase. Most design codes are developed following research conducted in a laboratory, in which it can be difficult to replicate the behaviour of real-life structures in the field. Data from the SHM system installed in the second floor of the HBB in conjunction with the material testing and weather monitoring

station provides rich data that can be used to study many aspects of the behaviour of the concrete slab and compare it with codes of practice and predictive models.

The temperature rise and temperature differentials in concrete are key parameters for early-age behaviour of concrete slabs and the potential for early-age thermal cracking but these can be very difficult to determine accurately at design stage. Much of the guidance about early-age thermal behaviour of concrete in literature relates to walls and there is very little field data on hybrid concrete slabs. The research in **Chapter 4** indicates that the predicted values (based on the design guides) for peak temperature rise and temperature differentials are conservative and suggest that for large volume pours, trial pours with the embedded sensors are required to accurately determine early-age thermal behaviour. Restraint factors, which represent the amount of restraint to movement, are required to predict the potential for early-age thermal cracking but are very difficult to determine at design stage. There is a scarcity of information provided in the literature in relation to restraint factors for suspended flat slabs (including slabs constructed using hybrid concrete construction). Choosing the incorrect value of restraint factor can lead to uneconomical over-design, or under-design leading to unacceptable cracking. Restraint factors were calculated throughout the hybrid concrete lattice girder slab in the HBB by determining the insitu restrained coefficient of thermal expansion during the cooling phase of the insitu concrete topping based on the data from the SHM sensors embedded in the concrete. It was found that the rotational restraint level measured at several locations throughout the depth of the insitu concrete topping varied between 0.16 and 0.37 (zero indicated no restraint, whereas one would indicate full restraint against rotation). This would equate to low-moderate rotational restraint and suggests that the supporting columns and wall provided limited rotational restraint to the slab during the early-age stages of the slab. There is no guidance in Eurocode 2 for determining restraint factors for suspended slabs but the superseded standard BS 8110 suggested a restraint factor of 0.2-0.4 for suspended slabs, which seems reasonable based on the data from this study.

During the construction stage of the four-storey over basement HBB, the lattice girder planks were temporarily propped until the insitu topping had reached the required compressive strength and the self-weight of successive floors were

Chapter 7. Conclusions

temporarily supported by the floors under. A temporary works engineer must determine the back-propping arrangements to ensure that the self-weight of load is transferred appropriately to the concrete floors below, without impacting on the structural integrity of the concrete slabs. It is rare that field data is available to determine the actual load transfer mechanisms throughout the floors and this is important to confirm that the temporary works design is fit for purpose. When designing back-propping, the critical parameter is the distribution of the loads between the levels of supporting slabs. The data from SHM indicated that the second floor supported approximately 70% of the self-weight of the third floor until the props were removed to the third floor. This demonstrates that the supporting floor below the falsework takes the majority of the load when backpropping and is in agreement with previous research conducted at the European Concrete Building Project (ECBP). Furthermore, the measured strain profile through the hybrid concrete flat slab show that the second-floor slab behaves as linear elastic during this construction phase and could be considered ‘uncracked’. It is very important during the construction phase that the structural integrity of the slabs are maintained as cracking of the concrete during construction can lead to durability and deflection issues.

The predicted bending moments using the linear elastic finite element model created by the designers was compared with the bending moments calculated using the measured strain from the embedded sensors in the hybrid concrete slab. Relatively good correlation was found between the predicted and ‘measured’ bending moments in the second floor of the HBB and possible reasons for differences are explored. Although rare, as engineers, it is very important that our design methods are validated using field data so that we can improve our predictive models and codes of practice and also better understand how our structures behave. SHM can also be used to provide confidence to engineers (and sometimes the public) in relation to the actual performance of structures.

Time dependent effects (TDE) in concrete are one of the most difficult phenomena to predict accurately. The large volume of literature devoted to the prediction of creep, shrinkage and deflection in concrete testifies to the complexity of this topic. The one consistent feature in the literature is the large degree of uncertainty for

Chapter 7. Conclusions

predicting long-term behaviour of concrete structures at serviceability limit states. Although the time period was only the first 6 months after the second floor was poured, the measured strains from the hybrid concrete floor in HBB were compared with the predicted strains using Eurocode 2. Predicted strains were based on the sum of the strains due to flexure, creep and shrinkage (thermal strain excluded) and relatively good correlation between the predicted and measured strains was observed for the six months analysed despite the large coefficient of variation for both creep and drying shrinkage. The dominant strain component was predicted to be shrinkage strain (60% of total strain).

Whereas **Chapter 4** focussed on structural aspects of a hybrid concrete flat slab, **Chapter 5** analysed the thermal behaviour of the same hybrid concrete lattice girder flat slab in the HBB using the data from SHM system. The period of focus is the first year after the second floor in the HBB is constructed. Data from the nearby weather station (less than 1km from HBB) provided valuable information in relation to ambient temperature, relative humidity, solar irradiance and wind speed so that the influence of environmental conditions on the thermal behaviour of the hybrid concrete floor could be studied. With increasing focus on exploiting the thermal mass of concrete floors in buildings, it is critically important that we understand the thermal behaviour of concrete floors and that we can predict their behaviour accurately. In order to develop and validate numerical models, robust field data is required which will allow designers simulate the real behaviour of concrete floors.

The thermal behaviour through the hybrid concrete slab at second floor in the HBB is studied in the horizontal and vertical direction. At most locations, there were four embedded sensors in the concrete floor (one in the precast lattice girder plank, three in the insitu topping) so that temperature profile through the slab and the effect of external environment conditions could be analysed. During the first 11 days after the insitu topping was poured, the top surface of the second floor was exposed to direct solar radiation. However, following erection of the third floor lattice girder planks overhead, the sector of second floor which was instrumented was largely shaded except for the perimeter of the slab. The ability of the concrete floor to act as a thermal mass to store and release heat is demonstrated by the time lag between the peak ambient temperature and the peak concrete temperature in the top of the

Chapter 7. Conclusions

slab (2-6 hours). As heating, cooling and lighting of buildings accounts for approximately 50% of UK CO₂ emissions, utilising the fabric energy storage characteristics of concrete has the potential to significantly reduce the environmental impact of buildings.

The temperature profile through the depth of the slab is studied for the first 24hrs after the insitu topping was poured, for a typical day in Winter in which there was a negative ambient temperature differential (-5°C) and a typical day in Summer in which there was a positive ambient temperature differential (+15°C). As expected, during the first 24 hrs, the highest temperatures are recorded in the middle of the insitu topping as it was insulated by the surrounding concrete and the precast lattice plank. Large temperature differentials through the depth of the slab can induce internal restraint but this was not the case for this 400mm thick hybrid concrete slab as it is relatively thin and temperature differential between sensors within the insitu topping never exceeded 3°C. The peak temperature in the insitu concrete topping was recorded 10 hrs after the concrete pour and because the concrete mix for the insitu topping had 30% GGBS (ground-granulated blast-furnace slag), the maximum difference between the concrete and ambient temperature never exceeded 13°C. The thermal profile through the depth of the slab was rarely linear and was continuously responding to the daily temperature changes. During the period in which there was a negative temperature differential, the temperature profile through the slab changed from convex to concave.

The influence of solar radiation on the thermal behaviour of the second floor in the HBB was also analysed. Temperature differentials of 3°C (0.37°C/m) were recorded horizontally across the width of the slab during the construction phase due to solar gain along the perimeter of the slab where the slab was not shaded by the concrete floors overhead. The relationship between daily total solar irradiance (measured from the nearby weather station) and the thermal behaviour of the precast lattice girder plank and hybrid concrete slab was analysed. It shows that solar irradiance is as important as ambient air temperature with respect to predicting the thermal behaviour of concrete slabs. The thermal data from the HBB suggest that orientation and exposure of concrete elements will influence the spatial temperature

Chapter 7. Conclusions

distribution and this could be important for exposed concrete slabs (car parks, reservoirs etc.) and in regions which are subject to high solar radiation.

As noted previously, estimating restraint factors for suspended slabs to estimate the potential for early-age thermal cracking is difficult. The restraint factors at different depths of the insitu topping were calculated and it was found that a method proposed by the American Concrete Institute (ACI) for determining restraint factors at a joint is potentially a useful tool for predicting restraint between the insitu topping and the precast lattice girder plank. Although there is a large variability in the calculated restraint factors, the average restraint factor of 0.25 at the bottom of the insitu topping compares favourably with the value of 0.24 calculated using the ACI method. The methodology described in this research can be applied to similar hybrid concrete slabs to build up a database of restraint factors from field data which could be used by designers.

A one-dimensional finite difference model (**Appendix C**) was developed to model the temperature profile in the 400mm thick hybrid concrete lattice girder slab and validated against the SHM data from the HBB. The model takes account of the heat of hydration from the cement and four modes of heat transfer: conduction, convection, solar radiation and thermal irradiation. In addition, environmental conditions such as ambient temperature, wind speed and solar irradiation measured from the weather station are used as input parameters in the model. The numerical model which had a spatial resolution of 20mm, was shown to have good correlation with the measured concrete temperatures from the embedded sensors and could potentially be used to predict the thermal behaviour of hybrid concrete slabs during construction and operation phase. In the future, numerical models which are validated using field data will be critical for the promotion and development of passive design strategies in buildings.

The thermal strains induced in buildings can sometimes be larger than those due to service loads, particularly in regions in which there are large temperature ranges. If movement due to thermal effects is not considered at design stage, it can cause cracking, curvature and affect the long-term serviceability of concrete structures. Although the climate in Ireland is temperate oceanic and it does not suffer extremes of temperature, the frequency of days with extremes of temperatures is likely to

Chapter 7. Conclusions

increase in the future with climate change and thermal strains during construction and operation may become a more significant issue.

The rich field data reported in **Chapter 4** and **Chapter 5** from the hybrid concrete flat slab in HBB should be a valuable resource for researchers, concrete technologists and engineering practitioners in the future as it provides information which can be used to improve our understanding of the lattice girder flat slab, develop numerical models and design guides. As the SHM system is continuously monitoring the behaviour of the second floor in the HBB since July 2015, there are future opportunities to investigate TDE in the hybrid concrete slab.

Chapter 6 describes the experimental investigation conducted to study the behaviour of lattice girder planks during construction. Currently, there is a lack of comprehensive experimental data on the behaviour of the lattice girder plank when it must support its own self-weight, self-weight of wet concrete from the insitu topping and construction loads. The experimental results reported conclude that there is potential optimisation of the arrangement of temporary propping possible for lattice girder planks during construction and this would reduce costs, labour and congestion on site which will improve the construction process for flat slabs.

The behaviour of lattice girder plank is described and the interaction between the various components of the lattice girder plank (top chord, bottom chord and diagonals of the lattice girder, concrete, reinforcement) was analysed. The dominant design parameters for controlling stiffness and the deflection of the plank during construction stage are the diameter of the top chord of the lattice girder and the spacing of the lattice girders. Initial cracking of the plank can be expected when the tensile strain on the bottom of the plank is at least half of the tensile strain capacity of the concrete (calculated using Eurocode 2). A numerical model using the transformed area method was found to give reasonable predictions for the initial stiffness and deflection of lattice girder plank for girders at least 200mm tall but not capable of predicting the behaviour of planks with shallower girders (~100mm tall). The experimental data was also used to produce design tables for erection spans which take account of the multi-span nature of lattice girder planks when temporarily propped.

Failure of lattice girder planks was due to buckling of the top chord or buckling of the diagonal but imperfections due to the manufacturing or construction process can impact on the behaviour and failure mode of the plank. Failure can be predicted by determining the compression buckling resistance of the top chord or diagonal, but the appropriate buckling length to use in calculations was not established. An average global factor of safety of 2.7 was calculated when comparing the ultimate experimental load of the six tests undertaken and ultimate load calculated using Eurocode 3. The experimental data will contribute to better understanding of how this popular precast concrete floor product behaves during construction and will allow numerical models to be developed which predict its behaviour accurately.

7.2.1 Reflection

The research on hybrid concrete lattice girder planks described in this thesis is not intended to finish with the completion of this work. It is envisaged that further experimental testing will be conducted in NUI Galway and that further analysis of the field data from HBB will be undertaken. Furthermore, it is likely that implementation of a SHM strategy for a new building in the college campus will be considered. Therefore, I have outlined some reflections in relation to my research which may be of assistance to future researchers in this area:

- With any proposed SHM scheme, pre-planning is critical to successful implementation; as once construction commences on site, the contractor will have a tight construction programme and will have little time to delay tasks to accommodate installation of sensors. Where possible, prefabricate cages to support sensors which will be embedded in concrete to simplify installation on site. Complete any operations which can be carried out off-site to minimise duties required on site as there will be many contractors and constraints which may impact the installation. Do not underestimate the time and labour required to install sensors. If possible, it can be useful to undertake a trial installation to check the feasibility of proposed scheme.
- Getting buy-in from site personnel is key to ensure that the sensors are not damaged during construction and therefore, building up a good rapport with them is important. Similarly, close monitoring of the quality of work is also very important during the installation of the sensors, but also during the

Chapter 7. Conclusions

placing of any subsequent reinforcement and concrete adjacent to the sensors to ensure that they remain orientated correctly and are not damaged.

- At the start of the SHM system design, clarify what is the purpose of the scheme and what you wish to measure. Select location of sensors carefully and if possible, try to locate some sensors in which some validation of the data is possible.
- Try to install as many sensors subject to available resources and the construction programme. Do not neglect the importance of sensors to record environmental data (ambient temperature, relative humidity, solar radiation, wind speed and direction, etc.) as many models require environmental input data to predict behaviour of concrete structures. Different environmental sensors may be required during a project as it progresses from manufacture, to site, to construction and to operation.
- Where possible, data acquisition should be tested as soon as they are installed to check that sensors are operational. Sometimes, it is possible to resolve the issue so that they function correctly relatively simply. On most SHM projects, it is expected that a small proportion of sensors will not function for a variety of reasons, particularly if they are embedded in concrete and can get damaged during the concreting process.
- Quantifying the stress-independent strains (thermal strain and shrinkage strain) when analysing the data from vibrating-wire strain gauges is essential if the strain data from the gauges are to be analysed correctly. In hindsight, it would have been useful if two additional vibrating-wire ‘no stress’ strain gauges were installed on the HBB project. The two gauges would be cast inside a pre-fabricated cylinder and then cast with the hybrid concrete slab at agreed locations. The cylinder would be lined with a flexible porous filter to prevent restraint between the cylinder and concrete. The function of the cylinder would be to isolate the concrete in the cylinder from the surrounding concrete and prevent stress transfer from the surrounding concrete to the concrete in the cylinder. This would ensure that the strain gauge in the cylinder would only measure stress-independent strain. This would allow measurement of both stress-independent strain and stress-dependent strain (flexure and creep) in the concrete slab.

Chapter 7. Conclusions

- With respect to the SHM and experimental testing, it would be advisable to conduct material testing to determine the modulus of elasticity and tensile strength of the concrete for samples cured in water in accordance with codes of practice and cured in same environmental conditions as the concrete slab and lattice girder plank. Because of difficulties with the testing machine in NUIG, some of the proposed concrete testing was not undertaken. As noted previously in the thesis, having accurate material properties are invaluable when using predictive models and investigating the sensitivity of the model with respect to input material properties. Similarly, material testing of all components of the lattice girder plank (top chord, diagonal, bottom chord) would be preferable for future experimental testing.
- During the experimental testing, it was noted buckling of the top chord was typically initiated in the middle third close to the loading points. In the tests conducted for this research, electrical resistance strain gauges were bonded to the top chord at midspan in the plank. It might be advisable for future testing to also have additional strain gauges bonded near the load point in the middle third so that the buckling behaviour of the top chord can be analysed in greater detail.
- Initial cracking in the lattice girder plank was difficult to observe and track, particularly on the soffit, during the experimental testing. If possible, it would be useful to have high definition recording of the plank soffit during the load tests so that the crack formation could be tracked. Recording of the plank soffit was attempted during this experimental programme but was not very successful due to the camera used and the low height of the plank in relation to the laboratory floor.
- Finally, a general point in relation to literature reviews. I found it invaluable to have concise notes from my literature review which was many years old in some instances when it came to write this thesis. Writing concise notes for specific topics related to your literature review also helps to clarify your understanding and the important aspects of the literature.

A comprehensive description of the design and installation phase of the SHM system implemented for the HBB is described in **Appendix F**.

7.2.2 Original work and contributions to knowledge

The contribution of the research work reported in this thesis may be distilled to the improvement in the understanding of the behaviour of hybrid concrete lattice girder flat slabs. The author considers the following as his original work and contribution to knowledge:

- The successful design and implementation of a SHM system for a hybrid concrete suspended slab. Although implementation of a SHM scheme is not new, the real-time monitoring of a hybrid concrete lattice girder flat slab is novel and the methodology described could be applied to other hybrid concrete slabs.
- Obtaining and interpreting robust field data on the structural and thermal behaviour of the hybrid concrete lattice girder flat slab.
- Comparison of field data with guidelines from codes of practice, structural design software and industry publications.
- Development of one-dimensional finite difference numerical model for modelling temperature profile in hybrid concrete suspended slab.
- Comprehensive experimental testing to investigate the behaviour of the lattice girder plank at construction stage.
- Analysis of the key components in the behaviour of lattice girder plank at construction stage and identification of potential optimisation with respect to erection spans.

The potential impacts of the research described herein are a more economical floor product (hybrid concrete lattice girder slab), improved understanding of how the floor behaves and the development of new numerical models and design guidelines. The experimental research can be used to develop better design tools or numerical models to predict the behaviour of lattice girder planks during the construction stage leading to more economical arrangement of temporary propping of the planks on site. The cost of temporary propping can range from €20-50/m² and consequently, a reduction in temporary propping will deliver significant benefits. This will result in cost savings, reduction in labour requirements on site and less congestion on site. All of this will lead to a more efficient and economical precast concrete floor product for the construction of flat slabs.

As an example of the potential economic benefits of using more accurate prediction of erection spans for lattice girder planks, the Human Biology Building can be used as a case study. The building had a construction cost of €34 million and had 6600m² of hybrid concrete lattice girder flat slabs. If we use an average cost of propping of €35/m² (typical range = €20-50/m²) and assume that the contractor profit was 1.5% of the construction cost (i.e. €550,000), it is possible to relate the cost of propping to the contractor profit. The experimental testing conducted in this research project confirms that the temporary prop spacing could have been increased from 2.4m (max allowed for HBB) to 3.6m (refer to Table 6-5). This would have reduced the cost of temporary propping by 33% and this equates to €77,000 which would increase the contractor profit by 15%.

The field data published in this research will provide a valuable feedback loop to the design process and can be used as a research tool for better understanding of the behaviour of the floor in real structures and better knowledge of the structural and environmental actions to which they are subjected. Without comprehensive field data, the validation of predictive models for the structural and thermal mass performance of concrete floors is difficult. Although the development of ‘smart structures’ is still in its infancy, the SHM methodology and application of the field data described in this thesis may inform the future development in this area. In addition to dissemination of case studies demonstrating the real benefits of monitoring of structures, the advancement of ‘smart structures’ will also require further development in sensor technology and life prediction models.

7.3 Recommendations for future work

This research has used SHM and experimental testing to gather information on the behaviour of hybrid concrete lattice girder slabs during construction. This research has also highlighted the need for further investigation in the following areas:

- The construction industry is traditionally conservative and slow to change. In order for SHM to become more widespread in buildings, more case studies need to be published which highlight good practice, demonstrate the benefits of intelligent monitoring of concrete structures and the ‘value of information’ (VoI) to the various stakeholders in the industry.

Chapter 7. Conclusions

- Advances in wireless sensor technology which are smaller, easier to install, durable and can be self-powering will be necessary to ensure increased utilisation of SHM strategies. In conjunction with technological advances, more research is required to develop life prediction models for concrete structures which can use the monitoring data to detect deterioration in concrete structures.
- The scope of this research was limited to the insitu monitoring of the concrete slab during the construction phase only. Consequently, there are opportunities to study time dependent effects (TDE) in the hybrid concrete flat slabs using the data from the SHM and compare the field data with the various predictive models in the literature.
- Further experimental testing of lattice girder planks at construction stage is required to study the broad range of configurations which are utilised in the construction industry.
- Development of a general analytical model which can predict the behaviour of lattice girder planks at construction stage and allow more economical propping arrangements to be specified.

Appendix A. Photographs of SHM implementation in HBB

Appendix A. Photographs of SHM implementation in HBB



Fig. A1 - VW Gauges in lattice girder planks prior to manufacture

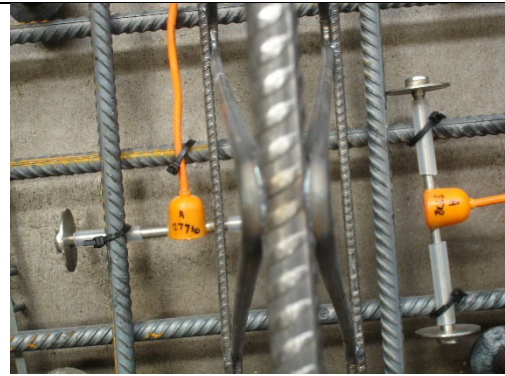


Fig. A2 - VW Gauges in lattice girder planks prior to manufacture



Fig. A3 - VW Gauges in lattice girder planks prior to manufacture



Fig. A4 - VW Gauges in lattice girder planks prior to manufacture



Fig. A5 - VW Gauges in lattice girder planks prior to manufacture



Fig. A6 - VW Gauges in lattice girder planks prior to manufacture

Appendix A. Photographs of SHM implementation in HBB



Fig. A7 – DAQ Unit recording data from sensors after manufacture of plank



Fig. A8 – DAQ Unit recording data from sensors after manufacture of plank



Fig. A9 – Erection of temporary props prior to erection of lattice girder planks



Fig. A10 – Erection of temporary props prior to erection of lattice girder planks



Fig. A11 – DAQ Unit connected to sensors prior to erection of lattice girder plank



Fig. A12 – VW Gauges mounted on U-bar prior to installation



Fig. A13 – VW Gauges mounted on U-bar prior to installation

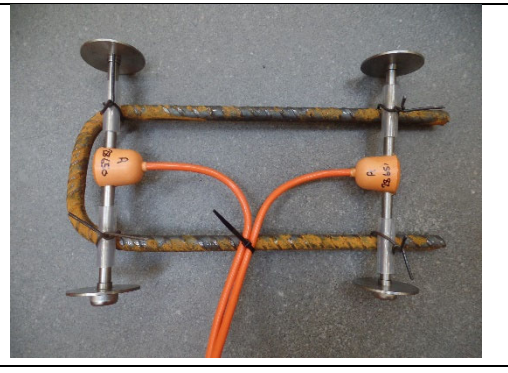


Fig. A14 – VW Gauges mounted on U-bar prior to installation

Appendix A. Photographs of SHM implementation in HBB



Fig. A15 – VW Gauges positioned in situ topping prior to pour



Fig. A16 – VW Gauges positioned in situ topping prior to pour



Fig. A17 – VW Gauges positioned in situ topping prior to pour

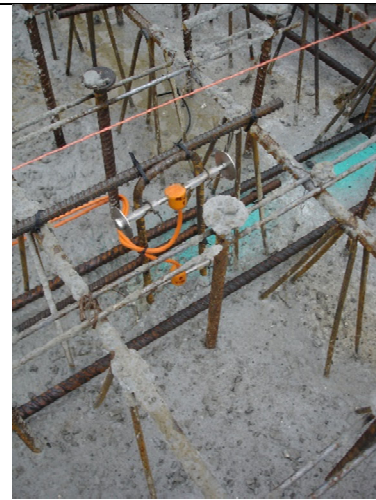


Fig. A18 – VW Gauges positioned in situ topping prior to pour

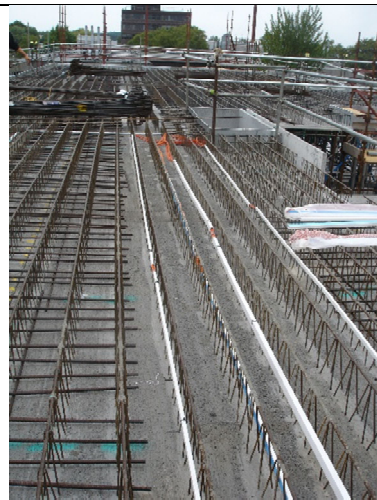


Fig. A19 – Trunking for cables from VW gauges to DAQ unit



Fig. A20 – VW Gauges positioned in situ topping prior to pour

Appendix A. Photographs of SHM implementation in HBB



Fig. A21 – VW Gauges positioned in situ topping prior to pour



Fig. A22 – VW Gauges positioned in situ topping for walkway plank prior to pour



Fig. A23 – Two cables for VW gauges broken prior to pour of insitu topping



Fig. A24 – VW Gauges positioned in situ topping for walkway plank prior to pour



Fig. A25 – Pour of insitu topping for 2nd floor of HBB



Fig. A26 – VW Gauges positioned in situ topping for walkway plank prior to pour

Appendix A. Photographs of SHM implementation in HBB

	
<p><i>Fig. A27 – Pour of insitu topping for 2nd floor of HBB</i></p>	<p><i>Fig. A28 – VW Gauges positioned in insitu topping prior to pour</i></p>
	
<p><i>Fig. A29 – DAQ unit on site during pour of 2nd floor of HBB</i></p>	<p><i>Fig. A30 – DAQ unit on site during pour of 2nd floor of HBB</i></p>
	
<p><i>Fig. A31 – Cables connected to DAQ unit</i></p>	<p><i>Fig. A32 – Downloading data from DAQ unit to laptop on site</i></p>
	
<p><i>Fig. A33 – Temporary props dropped and planks re-propped to 2nd floor soffit of HBB</i></p>	<p><i>Fig. A34 – Props removed from soffit of 2nd floor of HBB</i></p>

Appendix A. Photographs of SHM implementation in HBB



Fig. A35 – Final position of DAQ unit in service riser connected to local intranet



Fig. A36 – Final position of DAQ unit in service riser connected to local intranet



Fig. A37 – HBB (March 2017)



Fig. A38 – HBB (March 2017)



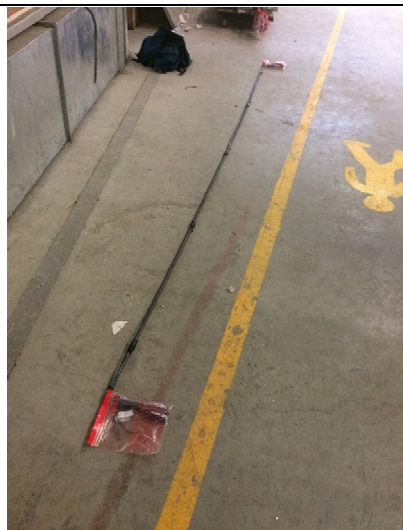
Fig. A39 – HBB (March 2017)



Fig. A40 – HBB (March 2017)

Appendix B. Photographs of experimental testing

Appendix B. Photographs of experimental testing

	
<p><i>Fig. B1 – Preparation of longitudinal reinforcement prior to bonding of ER gauge</i></p>	<p><i>Fig. B2 – ER gauge bonded to longitudinal reinforcement</i></p>
	
<p><i>Fig. B3 – Wax on bonded ER gauge for water-proofing</i></p>	<p><i>Fig. B4 – SB tape on bonded ER gauge for water-proofing and moisture protection</i></p>
	
<p><i>Fig. B5 – VM tape on bonded ER gauge for water-proofing and moisture protection</i></p>	<p><i>Fig. B6 – 5No. ER gauges bonded to longitudinal reinforcement</i></p>

Appendix B. Photographs of experimental testing



Fig. B7 – ER gauges bonded to bottom chord of lattice girder



Fig. B8 – ER gauges bonded to bottom chord of lattice girder



Fig. B9 – Reinforcement positioned in test plank shutter during manufacture

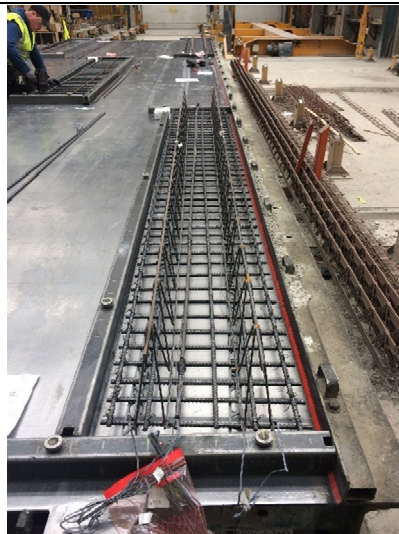


Fig. B10 – Test plank prior to concreting

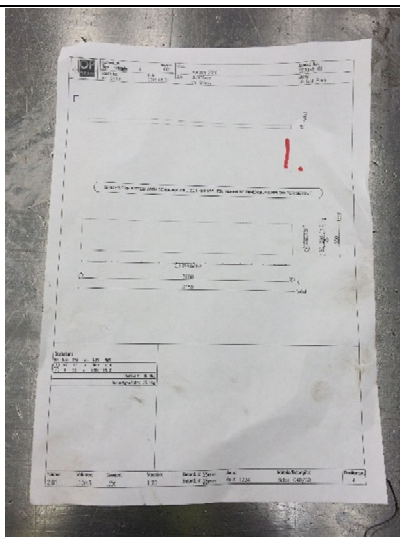


Fig. B11 – Manufacturing data sheet for test plank



Fig. B12 – ER gauges on bottom chord and longitudinal reinforcement prior to concreting

Appendix B. Photographs of experimental testing



Fig. B13 – Concreting of test plank in precast factory



Fig. B14 – Concreting of test plank in precast factory

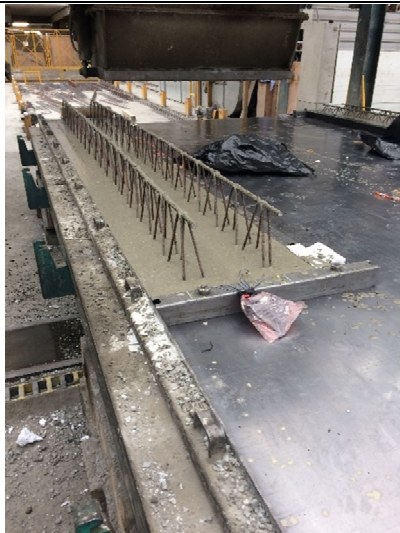


Fig. B15 – Test plank after concreting

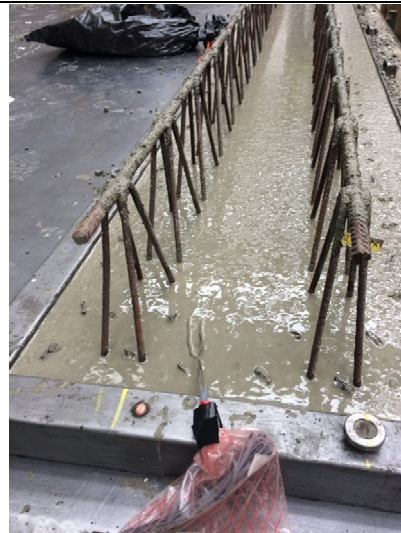


Fig. B16 – Test plank after concreting

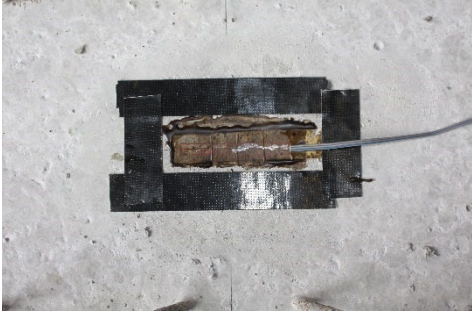


Fig. B17 – ER gauges bonded to diagonal of lattice girder



Fig. B18 – ER gauge bonded to top chord of lattice girder

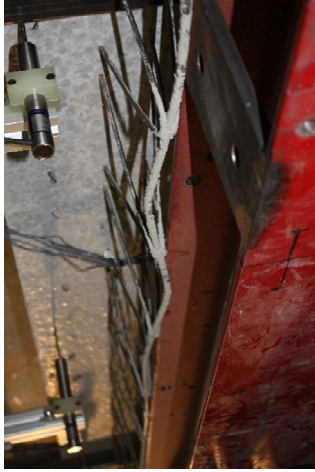
Appendix B. Photographs of experimental testing

	
<p><i>Fig. B19 – ER gauge bonded to top surface of lattice girder plank</i></p>	<p><i>Fig. B20 – 2No. ER gauges bonded to top surface of lattice girder at midspan</i></p>
	
<p><i>Fig. B21 – Test plank prior to load test</i></p>	<p><i>Fig. B22 – Test plank bearing on slip membrane at support</i></p>
	
<p><i>Fig. B23 – Actuator and spreader beam over test plank prior to testing</i></p>	<p><i>Fig. B24 – Spreader beam between lattice girders prior to testing</i></p>
	
<p><i>Fig. B25 – Test plank prior to load test</i></p>	<p><i>Fig. B26 – LVDT at load point on test plank</i></p>

Appendix B. Photographs of experimental testing

	
<p><i>Fig. B27 – LVDT at midspan on test plank</i></p>	<p><i>Fig. B28 – LVDT at support on test plank</i></p>
	
<p><i>Fig. B29 – Spreader beam at load point on test plank</i></p>	<p><i>Fig. B30 – LVDTs on test plank prior to test</i></p>
	
<p><i>Fig. B31 – Initial cracking on test plank at load point</i></p>	<p><i>Fig. B32 – Surface cracking on test plank at support</i></p>
	
<p><i>Fig. B33 – Buckling of top chord during load test</i></p>	<p><i>Fig. B34 – Buckling of top chord during load test</i></p>

Appendix B. Photographs of experimental testing

	
<p><i>Fig. B35 – Buckling of top chord during load test</i></p>	<p><i>Fig. B36 – Buckling of top chord during load test</i></p>
	
<p><i>Fig. B37 – Surface cracking on test plank at support</i></p>	<p><i>Fig. B38 – Transverse cracking on plank soffit at load point</i></p>
	
<p><i>Fig. B39 – Transverse cracking on plank soffit after load test</i></p>	<p><i>Fig. B40 – Spalling of concrete on top surface of plank adjacent to load point</i></p>
	
<p><i>Fig. B41 – Buckling of diagonals after load test</i></p>	<p><i>Fig. B42 – Buckling of diagonals after load test</i></p>

Appendix B. Photographs of experimental testing



Fig. B43 – Transverse cracking on plank soffit after load test



Fig. B44 – Test plank after load test



Fig. B45 – Buckled shape of top chord after load test



Fig. B46 – Buckled shape of top chord after load test



Fig. B47 – Buckled shape of top chord after load test



Fig. B48 – Buckled shape of top chord after load test

**Appendix C. One-dimensional numerical thermal model
for hybrid concrete slab**

C.1 Numerical thermal model for hybrid concrete slab

One-dimensional finite difference model was developed by Ross and Bray [1] and uses heat diffusion theory described by Crank [2]. The model is similar to the model described in CIRIA Report C660 [3] and uses a two component model developed by Dhir *et al.* [4] to predict the heat of hydration.

The finite difference remains numerically stable, if the following is valid for the time increment:

$$\Delta t \leq (C \rho / 2k) \cdot \Delta x^2 \quad (\text{Eqn. C1})$$

where:

Δt = time increment

Δx = space increment

C = specific heat of the concrete

ρ = density of the concrete

k = thermal conductivity of the concrete

Hybrid concrete slab consists of 335mm thick insitu topping on 65mm thick lattice girder precast plank.

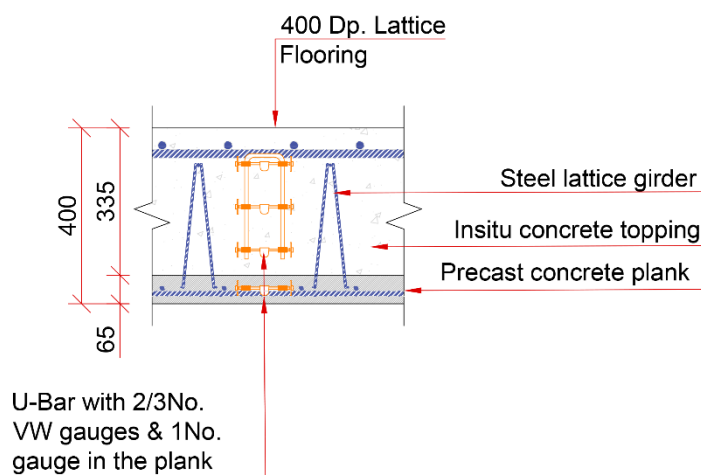


Fig C.1 Section of hybrid concrete slab

C.2 Thermal properties of concrete

The thermal properties of concrete change with time but in this model, the properties of concrete were assumed to be constant. However, the properties of the concrete inputted in the numerical model may be changed without difficulty.

(a) Density (ρ)

The mix design for the insitu topping (C30/37) was:

Aggregate (Limestone)	1140 kg/m ³
Aggregate (Limestone)	760 kg/m ³
Cement content (30% GGBS)	330 kg/m ³
Water	<u>150 kg/m³</u>
Wet density of concrete =	2380 kg/m ³

(b) Thermal conductivity (k)

Thermal conductivity of concrete is a measure of the rate at which heat passes through it. The principal properties which influence the thermal conductivity of concrete are the aggregate type, aggregate volume and moisture content. Thermal conductivity is not dealt with in the Eurocode 2 [5]. Published values of thermal conductivity vary considerably but are typically in the range of 1.0-2.5 W/m°C. The thermal conductivity can also be determined using a series model and a parallel model and they represent lower and upper bounds respectively [3]. Using these models, the thermal conductivity of the concrete was estimated to be between 1.0 and 3.2 W/m°C.

The thermal conductivity used in the model was 2.34 W/m°C which is based on the thermal conductivity of the concrete obtained from Clauser and Huenges [6] for concrete with limestone aggregates and percentage reinforcement used in the concrete slab.

(c) Specific heat (C)

The specific heat of the concrete is determined by the specific heat of the individual components. The range of values for concrete may vary from 0.75 to 1.17 kJ/kg°C [7] and a value of 1.0 kJ/kg°C can be used if no reliable data is available. Specific heat is not dealt with in the Eurocode 2 [5]. The two properties which significantly influence the specific heat of concrete are the aggregate type and the water content. The relative amounts of free and bound water must be known to calculate the specific heat of concrete. A method is described in CIRIA C660 to determine the degree of hydration and consequently the amounts of free and bound water in the concrete mix. The specific heat for concrete based on the mix constituents and that one third of the water was bound in the concrete (degree of hydration) was calculated to be 0.97 kJ/kg°C. The specific heat used in the model was 1.0 kJ/kg°C.

(d) Thermal diffusivity (D)

Diffusivity represents the rate at which the temperature changes within a mass. The range of typical values of diffusivity of concrete is between 0.002 and 0.006 m²/hr [8]. The thermal diffusivity is calculated using the equation:

$$D = k/C_p \quad (\text{Eqn. C2})$$

The thermal diffusivity of the concrete used in the model was 0.00354 m²/hr. This value also dictates the time increments (Δt) used in the numerical model for a specific spatial increment (Δx) so that the model remains stable (Eqn. C.1).

(e) Convection coefficient (h)

Convection coefficient (also known as thermal conductance) measures the rate at which heat is lost from the surface by convection. The value of the convection coefficient is determined by the nature of the formwork (if any) and the wind speed. Where no formwork applies, the convection coefficient for the concrete surface can be determined using the relationship proposed by Bentz [9]:

Appendix C. One-dimensional numerical thermal model for hybrid concrete slab

$$h = 5.6 + 4.0 v_{\text{wind}} \quad \text{for } v_{\text{wind}} \leq 5\text{m/s} \quad (\text{Eqn. C3})$$

$$h = 7.2 v_{\text{wind}}^{0.78} \quad \text{for } v_{\text{wind}} > 5\text{m/s} \quad (\text{Eqn. C4})$$

Wind speed will have less impact where the formwork has good insulating properties. Values proposed by Harrison [10] were used to determine the convection coefficient of the precast lattice girder plank which is located under the insitu topping. The convection coefficient for the 65mm precast plank used in the model was 12.4 W/m²°C. The wind speed on site was determined from the weather station [11] which was located less than 1km from the site. When the external cladding was installed it was assumed that the wind speed was zero. The average wind speed during the day of the pour of the insitu topping was 3.91m/s and the convection coefficient of the concrete surface was calculated as 21.2 W/m²°C.

C.3 Heat of hydration of concrete

The heat of hydration is modelled using a two-component curve which was developed by Dhir *et al.* [4] following a significant test programme conducted in the University of Dundee which measured the heat generation of a variety of combinations of CEM I cements with fly ash and ggbs (ground granulated blastfurnace slag).

The two part equation for heat generation (kJ/kg) is of the form:

$$Q(t) = Q_1 + Q_2 = \frac{Q_{\text{ult}}}{2} (1 - \exp(-B \cdot t^c)) + \frac{Q_{\text{ult}}}{2} \cdot \frac{t - t_2}{t - t_2 + D} \quad (\text{Eqn. C.5})$$

where

Q_{ult} = ultimate heat generation which is based on heat generation after 41 hours (Q_{41})

$$Q_{\text{ult}} = Q_{41} / (0.00003(\%ggbs)^2 - 0.0014(\%ggbs) + 0.925) \quad (\text{Eqn. C.6})$$

$Q_{41(\text{CEM I})}$ = Heat generation after 41 hours for CEM I = 338kJ/kg

$$\text{For ggbs, } Q_{41(\text{ggbs})} = Q_{41(\text{CEM I})} - 60 \left(\frac{(\%ggbs)}{100 - \%ggbs} \right)^{0.6} \quad (\text{Eqn. C.7})$$

B = coefficient = 0.011724, regardless of cement type

Appendix C. One-dimensional numerical thermal model for hybrid concrete slab

C = coefficient which depends on the type of addition and the amount used.

$$\text{For ggbs, } C = 1.6 - 0.0072(\% \text{ggbs}) - 0.00003(\% \text{ggbs})^2 \quad (\text{Eqn. C.8})$$

D = coefficient which depends on the type of addition and the amount used.

$$\text{For ggbs, } D = 6.2 - 0.0848(\% \text{ggbs}) - 0.0004(\% \text{ggbs})^2 \quad (\text{Eqn. C.9})$$

t_2 = activation time for component 2 of heat generation curve

$$\text{For ggbs, } t_2 = 3.5 + 0.0125(\% \text{ggbs}) \quad (\text{Eqn. C.10})$$

The data on heat generation were derived from semi-adiabatic temperature rise measurements by the University of Dundee. Values are based on a mean ambient temperature of 15 °C and a placing temperature of 20 °C. The difference of 5 °C is typical and has been derived from UK observations ([12], [13]). The ambient air temperature measured from the weather station at the time of the pour of the insitu topping (10.00, 20/07/2015) was 15.09°C and the mean ambient temperature on the day of the pour was 14.87°C (max = 16.77°C, min = 12.63°C). At the commencement of the pour, the precast plank is assumed to be the same temperature as the ambient temperature (15.09°C) and the placing temperature of the concrete is assumed to be 20°C (5°C difference is typical based on previous studies in the UK).

Using Eqn. C.5, the heat generation curve for the first 100 hrs after casting for the insitu topping in HBB is shown in Figure C.2.

Appendix C. One-dimensional numerical thermal model for hybrid concrete slab

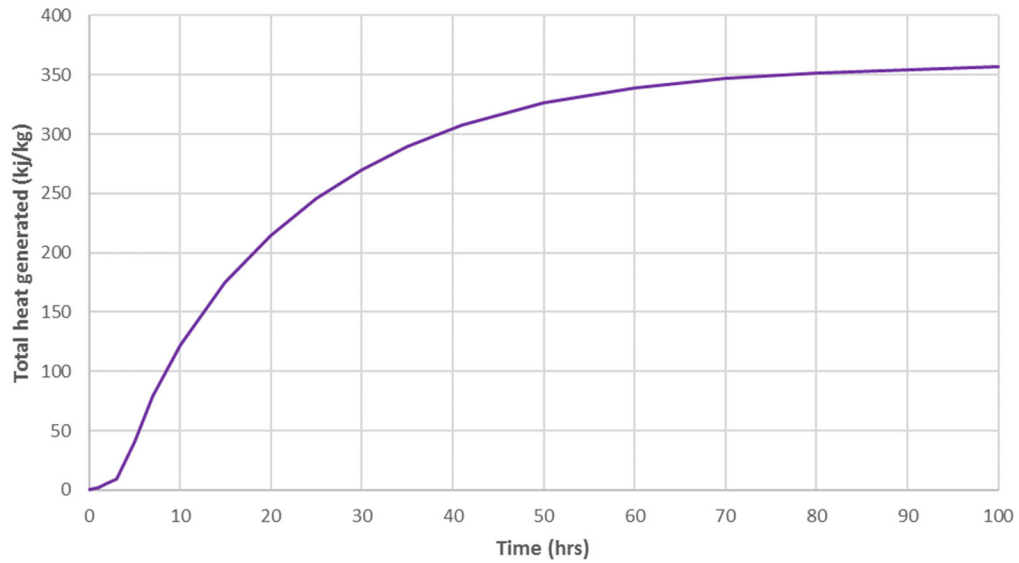


Fig C.2 Heat generation curve for concrete in insitu topping for HBB

The adiabatic heat generation curve is converted to an adiabatic temperature rise for the concrete using Equation C.11:

$$T_{\text{adt}}(t) = \frac{Q(t)}{\rho C} \quad (\text{Eqn. C.11})$$

The adiabatic temperature rise for the concrete in the insitu topping in HBB, based on a placing temperature of 20°C is shown in Figure C.3.

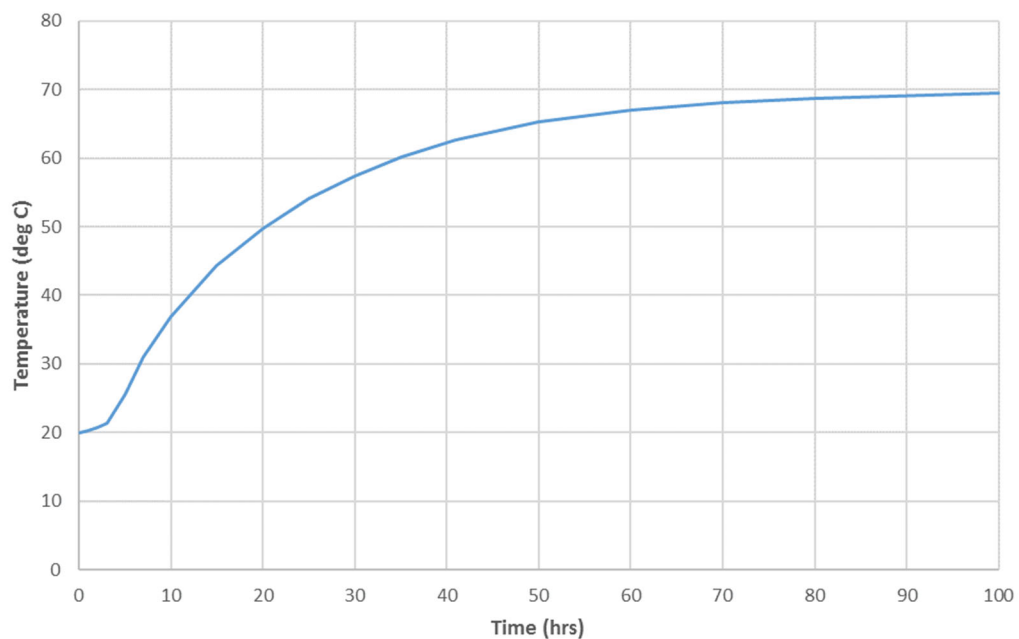


Fig C.3 Adiabatic temperature rise for concrete in insitu topping for HBB

Appendix C. One-dimensional numerical thermal model for hybrid concrete slab

The numerical model uses adiabatic hydration models (i.e. heat transfer is not lost or gained from the surrounding). The hydration models were validated against a number of published studies and shown to be able to predict the temperature rise in concrete with a reasonable degree of accuracy. Some studies [14] have shown that models based on adiabatic hydration models are more reliable when predicting rises in thick sections rather than thin sections.

C.4 Heat transfer model

The 400mm hybrid concrete slab (335mm insitu topping 65mm precast plank) is modelled as a one-dimensional slab and is divided into 20mm increments (Δx) in the vertical direction. The time increments for the finite difference model is based on ensuring that the model remains numerically stable ($\Delta t = 0.5 \Delta x^2/D$). At the top and bottom surface, four modes of heat transfer are considered: conduction into the concrete, convection, solar absorption and thermal irradiation. In addition, the temperature rise due to the heat of hydration is included in the model for the first seven days after the insitu topping is poured.

(a) Conduction

$$q_{\text{cond}} = k(T_0 - T_1)/ \Delta x \quad (\text{Eqn. C.12})$$

where k is the thermal conductivity of the concrete, T_0 and T_1 are the surface and internal temperature at the first internal node, respectively, and Δx is the node spacing.

(b) Convection

$$q_{\text{conv}} = h(T_0 - T_a) \quad (\text{Eqn. C.13})$$

where h is the convection coefficient of the concrete surface, T_0 is the concrete surface temperature and T_a is the ambient temperature.

(c) Solar radiation

$$q_{\text{sol}} = \gamma_{\text{abs}} Q_{\text{inc}} \quad (\text{Eqn. C.14})$$

Appendix C. One-dimensional numerical thermal model for hybrid concrete slab

where γ_{abs} is the solar absorptivity of the concrete and Q_{inc} is the incident solar radiation. The solar absorptivity of the concrete is a measure of how much of the solar radiation is absorbed on the surface. A value of 0.65 was used in the model for unfinished concrete surface ([15], [16]). The incident solar radiation was measured every minute from the nearby weather station.

(d) Thermal irradiation

$$q_{\text{irr}} = \sigma \varepsilon (T_{0k}^4 - T_{\text{sky}}^4) \quad (\text{Eqn. C.15})$$

where σ is the Stefan-Boltzmann constant ($5.669 \times 10^{-8} \text{ W}/(\text{m}^2 \text{ }^\circ\text{C}^4)$), ε is the emissivity of the concrete, T_{0k} is the concrete surface temperature (in Kelvin) and T_{sky} is the sky temperature (in Kelvin). Emissivity is a relative measure (0.0 to 1.0) of the ability of a surface to emit heat by radiation. The emissivity of concrete in the model was assumed to be 0.9 ([15], [17]). The sky temperature was calculated using the following equations presented by Walton [18]:

$$T_{\text{sky}} = \varepsilon_s^{0.25} \times T_a \quad (T \text{ in K}) \quad (\text{Eqn. C.16})$$

where the sky emissivity (ε_s) is given by:

$$\varepsilon_s = 0.787 + 0.764 \times \ln\left(\frac{T_{\text{dew}}}{273}\right) \times F_{\text{cloud}} \quad (\text{Eqn. C.17})$$

where T_{dew} is the dewpoint temperature (in Kelvin) and the cloud cover factor, F_{cloud} , as:

$$F_{\text{cloud}} = 1.0 + 0.024N - 0.0035N^2 + 0.00028N^3 \quad (\text{Eqn. C.18})$$

where N is the “tenths cloud cover”, taking values between 0.0 and 1.0

The dewpoint temperature and cloud cover data was taken from the nearest Met Eireann weather station [19].

The solar radiation only applied to the top surface of the concrete slab. When the external cladding was installed, it was assumed that the wind speed was zero for the purposes of determining the convection coefficient and there was no solar radiation or thermal irradiation.

Appendix C. One-dimensional numerical thermal model for hybrid concrete slab

The above equations are employed in a general finite difference solution to a one-dimensional heat transfer. The time step in the finite difference scheme is governed by the layer thickness ($\Delta x = 20\text{mm}$) and thermal properties of the concrete to ensure numerical convergence of the solution (Eqn. C1).

C.5 References

- [1] A. D. Ross and J. W. Bray, “The prediction of temperatures in mass concrete by numerical computation,” *Mag. Concr. Res.*, vol. 1, no. 1, pp. 9–20, Jan. 1949.
- [2] J. Crank, *The mathematics of diffusion*, 2nd Ed. London, UK: Oxford University Press, 1975.
- [3] P. B. Bamforth, “CIRIA Report C660: Early-age thermal crack control in concrete,” CIRIA, London, UK, 2007.
- [4] R. K. Dhir, L. Zheng, and K. a Paine, “Measurement of early-age temperature rises in concrete made with blended cements,” *Mag. Concr. Res.*, vol. 60, no. 2, pp. 109–118, 2008.
- [5] NSAI, “IS EN 1992-1-1: Eurocode 2: Design of concrete structures. Part 1-1: General rules and rules for buildings,” NSAI (National Standards Authority of Ireland), Dublin, Ireland, 2005.
- [6] C. Clauser and E. Huenges, “Thermal conductivity of rocks and minerals,” in *Rock physics and phase relations: a handbook of physical constants*, vol. 3, T. J. Ahrens, Ed. American Geophysical Union, 1995, pp. 105–126.
- [7] US Army Corps of Engineers, “Temperature control of mass concrete (Engineering Manual EM1110-2-2200),” USACE, Washington, US, 1995.
- [8] A. M. Neville, *Properties of concrete*, 5th Ed. Upper Saddle River, NJ, USA: Prentice Hall, 2011.
- [9] D. P. Bentz, “A computer model to predict the surface temperature and time-of-wetness of concrete pavements and bridge decks (NISTIR 6551),” National Institute of Standards and Technology (NIST), Maryland, USA, 2000.
- [10] T. Harrison, “CIRIA R67 - Tables of minimum striking times for soffit and vertical formwork,” CIRIA, London, UK, 1978.

Appendix C. One-dimensional numerical thermal model for hybrid concrete slab

- [11] IRUSE Weather, “IRUSE Weather,” *Informatics research unit for sustainable engineering NUI Galway weather website*. [Online]. Available: <http://weather.nuigalway.ie/>. [Accessed: 20-Jul-2019].
- [12] M. Anson and P. M. Rowlinson, “Early-age strain and temperature measurements in concrete tank walls,” *Mag. Concr. Res.*, vol. 40, no. 145, pp. 216–226, Dec. 1988.
- [13] The Concrete Society, “In situ concrete strength. An investigation into the relationship between core strength and standard cube strength (CS 126),” The Concrete Society, Camberley, UK, 2004.
- [14] K. Vitharana, N; Sakai, “Early-age behaviour of concrete sections under strain-induced loadings,” in *Proceedings of the 2nd International Conference on Concrete under Severe Conditions (CONSEC '95) Sapporro, Japan, 2-4 August 1995*, 1995, pp. 1571–1581.
- [15] E. Schlangen, “Online Help/Manual module HEAT of FEMMASSE (1999-2000),” FEMMASSE b.v., Netherlands, 2000.
- [16] A. A. Keste and S. R. Patil, “Investigation of concrete solar collector: a review,” *IOSR J. Mech. Civ. Eng.*, pp. 26–29, 2013.
- [17] J. R. Howell, M. P. Mengüç, and R. Siegel, *Thermal Radiation Heat Transfer*, 6th Ed. CRC Press, 2015.
- [18] G. N. Walton, “Thermal Analysis Research Program—Reference Manual—INBSIR 83–2655,” Department of Commerce, National Bureau of Standards, Building Physics Division, Washington, US, 1983.
- [19] Met Eireann (The Irish Meteorological Service), “Meteorological Data,” *Available Data*, 2019. [Online]. Available: <https://www.met.ie/climate/available-data/>. [Accessed: 21-Aug-2019].

Appendix D. SHM as a teaching tool

The following articles which were published in 2017 demonstrate the potential to use SHM as a teaching tool in civil engineering education.

S. Newell and J. Goggins, “Embedded instrumentation as a teaching tool for construction students.” *Engineers Journal*, 2017. [Online]. Available: <http://www.engineersjournal.ie/2017/04/11/embedded-instrumentation-teaching-tool-construction-engineering/> [Accessed: 31-Jul-2019].

S. Newell, “GMIT construction students weigh in for load test as part of their degree studies.” *Irish Building Magazine*, 2017. [Online]. Available: <https://www.irishbuildingmagazine.ie/2017/03/03/gmit-construction-students-weigh-in-for-load-test-as-part-of-degree-studies/> [Accessed: 31-Jul-2019].

Embedded instrumentation as a teaching tool for construction students

11 April 2017

Shane Newell writes that embedded instrumentation, which is used to monitor the performance of buildings, can also be used as a teaching tool for construction engineering students



Fig 1: The Human Biology Building in NUI Galway

 Tweet  Share  Like 18

Civil engineering and construction-management students from Galway-Mayo Institute of Technology (GMIT) visited the recently constructed Human Biology Building (HBB) in NUI Galway and took part in a load test on a concrete slab with embedded sensors.

The HBB is a four-storey building over basement and roof-level plant enclosure with a gross floor area of 8200m² (Figure 1) and was constructed by **BAM Ireland**. The HBB is primarily constructed using precast concrete elements, including the building frame, twinwall system, hybrid concrete lattice girder slabs and hollowcore slabs, which were designed, manufactured and installed by Oran Pre-Cast Ltd in Galway.

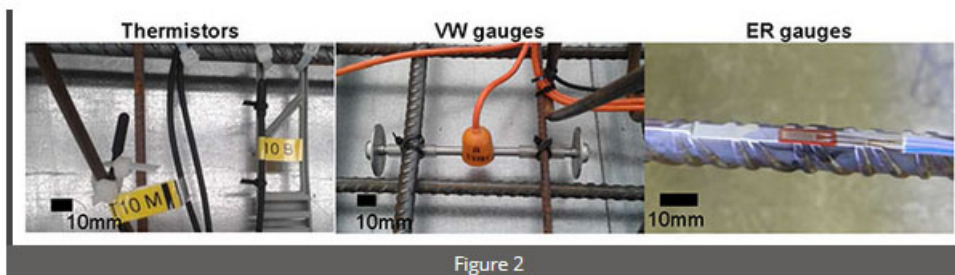
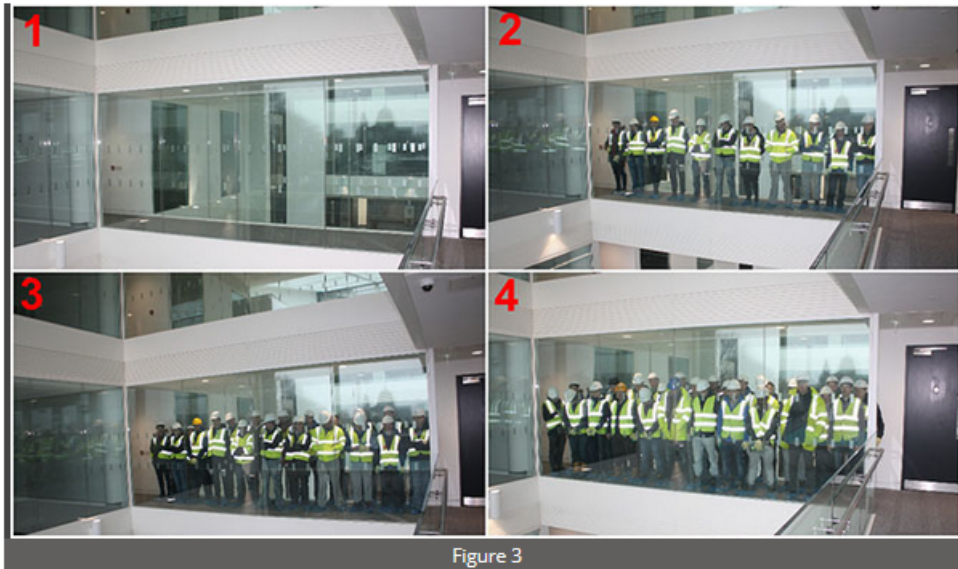


Figure 2

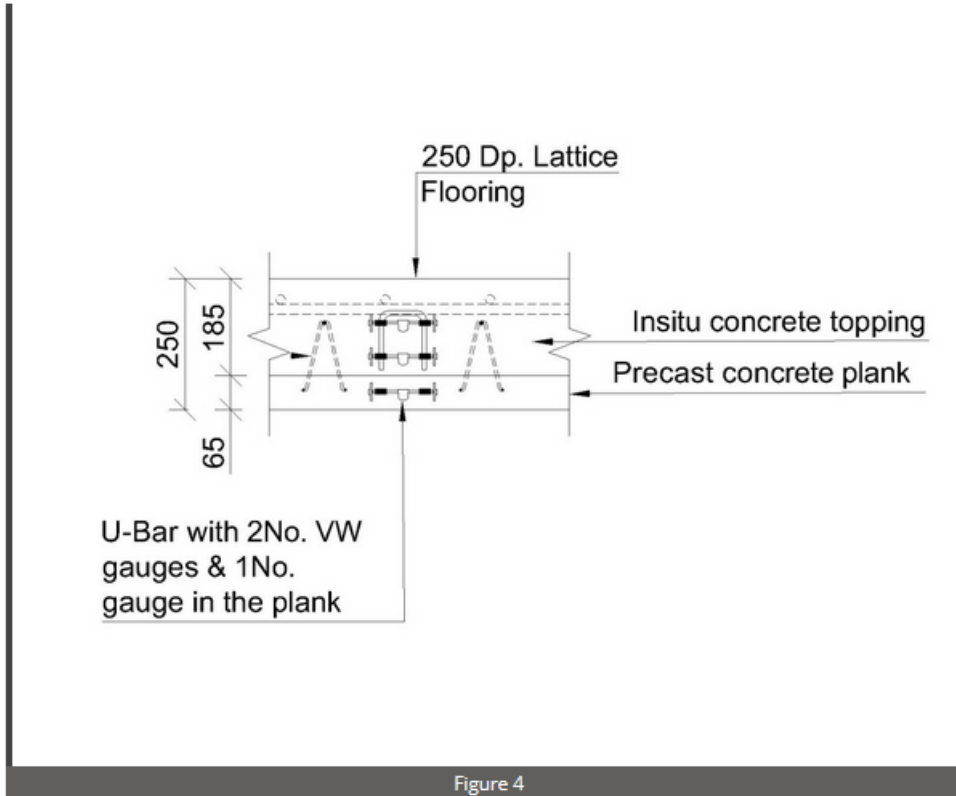
Appendix D. SHM as a teaching tool

During the construction phase, a variety of sensors (vibrating wire (VW) strain gauges, electrical resistance strain gauges, thermistors – Figure 2) were embedded in the floor structure (lattice girder flat slab) to allow real-time monitoring of the structural and environmental performance of the concrete floor during the construction and operational phase of the building.



The weight of students was used to apply a specified load to a concrete walkway in stages (Figure 3). The 250mm thick walkway slab is approximately 1.5m wide and spans 6m over the atrium in the HBB and consists of a 65mm thick precast lattice girder plank and 185mm insitu concrete topping.

The walkway has VW strain gauges embedded at approximately 1.5m centres along the walkway. At each location, there are three VW gauges positioned through the depth of the slab (one in the precast plank and two in the in-situ topping) so that the strain and temperature profile through the slab could be measured (Figure 4).



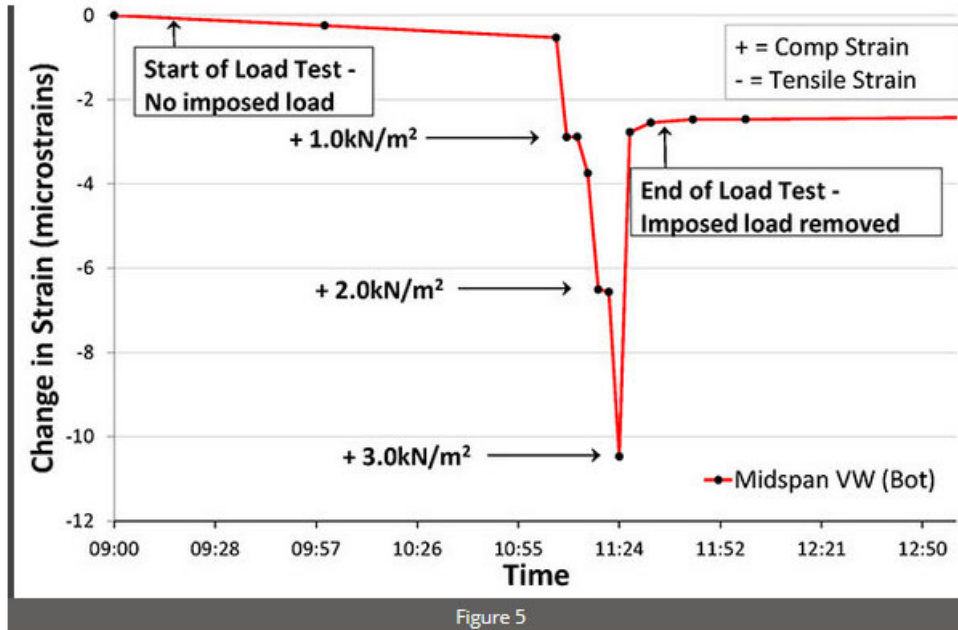
Built2Spec European project

The embedded sensors are part of a research project in which they are being used to study the behaviour of the floor during the manufacture, construction and operational phase of the building. This project is part of the **Built2Spec European project** in which the structural and environmental performance of buildings are continuously monitored using smart sensor-embedded construction elements (smart building components).

The HBB project is one of a number of projects which forms part of a measurement framework strategy developed at NUI Galway to continuously monitor the structural and environmental performance of buildings during construction and operation [1].

The load test is great way for students to develop a greater understanding of structural behaviour and an appreciation of the response of structures to load. Following the load test, the students are able to analyse the data and compare the actual behaviour of the floor with the predicted behaviour using design standards (such as **Eurocode 2**).

Appendix D. SHM as a teaching tool



The walkway was designed for an imposed load of 4.0kN/m^2 and the load test was designed to apply an imposed load of 3.0kN/m^2 in 1.0kN/m^2 increments. In Figure 5, an example of the measured strain data from one of the vibrating wire strain gauges located in the precast plank (bottom of the slab) at approximately midspan in the walkway is plotted during the load test.

The strain data, which was recorded every three minutes during the load test, clearly shows the incremental change in strain in response to the self-weight of the students. This strain data can then be converted to bending moments and used by students to study the response of the walkway to their own self-weight.

These moments derived from measured strains are compared by the students to the linear elastic finite element model developed by Oran-Precast, which is used to highlight differences between assumed and actual behaviour of the floor structure to students. It is very beneficial for students to explore the reasons for differences between actual and modelled behaviour of structures because of the increasing use of software in engineering.

'Living laboratories' used for teaching

This load test, undertaken by the students from GMIT, is similar to the approach adopted in NUI Galway in which a number of educational buildings are used as 'living laboratories' [2] through the use of embedded instrumentation as a teaching tool for students to investigate a wide variety of engineering concepts.

Dr Jamie Goggins, senior lecturer in **civil engineering at NUI Galway** and principal investigator responsible for the materials and structures research area in the **Centre for Marine and Renewable Energy (MaREI)**, noted: "It's envisaged that the rich data from the embedded sensors in the HBB and other demonstrator buildings in NUI Galway will be stored for many years and will be available to students and professionals for teaching and research applications.

"This is the third building on the NUI Galway campus that we've developed as a 'living laboratory' - the first two being the **Alice Perry** Engineering Building, completed in 2010, and the Institute for Lifecourse and Society Building, completed in 2014," he continued.

"Not only are they are fantastic resources to help our students better understand building physics and structural engineering, they're also being used in a number of European Commission Horizon 2020 and other collaborative research projects with industry and academic partners to develop and test technologies and approaches that drive design, construction and the performance of future buildings and retrofits," Goggins concluded.

In addition to the teaching applications of the embedded sensors, real-time monitoring offers potential benefits in relation to optimisation of structural components by understanding the actual behaviour of components in use and the possibility to develop and calibrate numerical models that predict structural performance.

The authors would like to acknowledge the assistance of Oran Pre-Cast and BAM contractors during the HBB project.

Authors:

Shane Newell, lecturer and chartered engineer, Galway-Mayo Institute of Technology (shane.newell@gmit.ie)

Dr Jamie Goggins, senior lecturer and chartered engineer, NUI Galway (jamie.goggins@nuigalway.ie)

References

[1] Newell, S., Goggins, J., & Hajdukiewicz, M. (2016). Real-time monitoring to investigate structural performance of hybrid precast concrete educational buildings. *Journal of Structural Integrity and Maintenance*, 1(4), 147-155.

[2] Goggins, J., Byrne, D., & Cannon, E. (2012). The creation of a living laboratory for structural engineering at the National University of Ireland, Galway. *The Structural Engineer*, 90(4), 12-19.

*The **Built2Spec** project has been funded through the European Commission Horizon 2020 programme (2015-2018) as part of the Built2Spec project **'Tools for the 21st century construction site'** (H2020 EeB2014 637221).*



GMIT construction students weigh in for load test as part of degree studies

📅 March 3, 2017 👁 958 Views

Civil Engineering and Construction Management students from GMIT visited the recently constructed Human Biology Building (HBB) in NUI Galway and took part in a load test on a concrete slab with embedded sensors, as part of their GMIT degree studies.

The weight of the students was used to apply a specified load to a concrete walkway, in stages. The concrete floor in HBB is embedded with a number of sensors which allow real-time monitoring of the structural and environmental performance of the concrete floor. The embedded sensors are part of a research project in which Shane Newell, GMIT Dept of Building & Civil Engineering, is using the embedded sensors to study the behaviour of the floor during the manufacture, construction and operational phase of the building.

“The load test is great way for students to develop a greater understanding of structural behaviour and an appreciation of the response of structure to load” noted Mr Newell. “Real-time monitoring offers potential benefits in relation to optimisation of structural components by understanding the actual behaviour of components in use and the possibility to develop and calibrate numerical models that predict structural performance,” he adds.

During the visit Dr Mark Kelly, GMIT Dept of Building & Civil Engineering, also gave students a summary of the research undertaken by GMIT and BAM (contractor for the HBB), which explored opportunities to reduce energy use, water use and waste production during the construction phase of the project.

For further information on Shane Newell’s research project: please email shane.newell@gmit.ie or tel. 091-742880

For information on courses in GMIT’s Dept of Building & Civil Engineering, see:

<http://www.gmit.ie/building-civil-engineering/department-building-and-civil-engineering>

[Pictured above](#)

Stages of load test by GMIT Civil Engineering and Construction Management students on the concrete walkway floor in new Human Biology Building at NUIG, as part of their GMIT degree studies.

**Appendix E. Data sheets for instrumentation used in
research**

Appendix E. Data sheets for instrumentation used in research

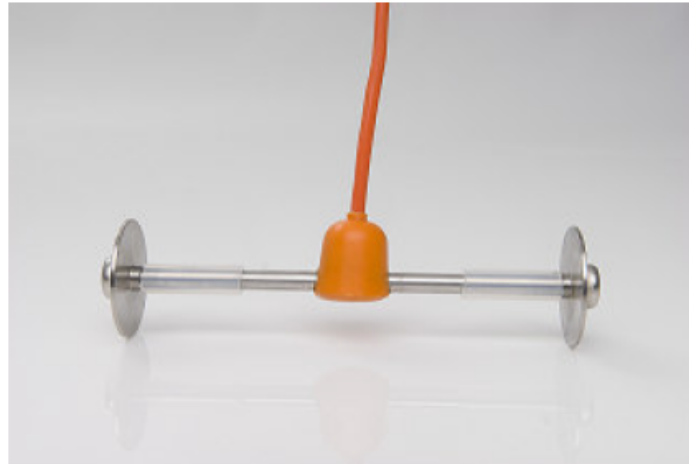


Gage Technique International Ltd.
 GEOTECHNICAL & STRUCTURAL INSTRUMENTATION

Unit 9, Spectrum West, St. Laurence Avenue, 20/20 Business Estate, Allington, Maidstone, KENT ME16 0LL.

Phone : (+44) 1622 68 56 20 Fax : (+44) 1622 60 99 50 E-Mail : info@gage-technique.com Web : http://www.gage-technique.com

VIBRATING WIRE EMBEDMENT STRAIN GAUGE.



TECHNICAL SPECIFICATION

Gauge Type :	TES/5.5/T embedment strain gauge.
Gauge Length :	5.5 inches.
Gauge factor :	3.025×10^{-4} microstrain per frequency squared.
Measurement range :	Greater than 3000 microstrain.
Resolution :	Better than 1 microstrain.
Coil Resistance :	Approximately 100 ohms.
Operating temperature range :	From -20°C to 80°C.
Thermal coefficient of vibrating wire :	11 ppm per 0C.
Thermistor temperature sensor :	Optional
Cable diameter :	4.5 millimetres.
Cable colour code – Brown :	Coil +ve.
Blue :	Coil -ve.
Yellow :	Thermistor (optional).
Green :	Thermistor (optional).

The type TES/5.5/T embedment vibrating wire strain gauge for concrete is based on a design by the Road Research Laboratory (now known as the Transport Research Laboratory), that was initially developed in 1969. Gauges of this type have been used successfully, worldwide, for the past 40 years, in major Civil Engineering projects such as the Channel Tunnel Rail Link in the UK & Storæbelt Crossing in Denmark.

Typical applications include pre-cast tunnel linings, concrete bridge sections, dams and concrete creep tests.

The gauges are suitable for long term use, the oldest working examples still in operation are over 30 years old and still providing reliable data!

THE VIBRATING WIRE EQUATION

DATASHEET - VW Embedment Strain Gauge.doc

Appendix E. Data sheets for instrumentation used in research



Gage Technique International Ltd.
GEOTECHNICAL & STRUCTURAL INSTRUMENTATION

Unit 9, Spectrum West, St. Laurence Avenue, 20/20 Business Estate, Allington, Maidstone, KENT ME16 0LL.

Phone : (+44) 1622 68 56 20 Fax : (+44) 1622 60 99 50 E-Mail : info@gage-technique.com Web : http://www.gage-technique.com

The change in engineering units, microstrain ($\mu\epsilon$), is given by the following expression :-

$$\mu\epsilon = (F_1^2 - F_2^2) \times GF$$

where: -

F_1 = the initial or Datum frequency reading

F_2 = a subsequent measured frequency

GF = the appropriate Gauge Factor for the gauge.

This equation may be expressed in terms of period reading (T), as displayed by the GT1174 Miniature Strain Meter:

$$\mu\epsilon = \left(\frac{10^{14}}{T_1^2} - \frac{10^{14}}{T_2^2} \right) \times GF$$

T_1 = the initial or Datum period reading

T_2 = a subsequent measured period reading.

Note: A positive change in microstrain indicates a compressive strain change.

MEASUREMENT RANGE AND RESOLUTION

The following table gives typical upper limit, lower limit, mid range values to 5 significant figures, and resolutions in microstrain, for all strain gauges of the same gauge length:

TES/5.5/T Gauge Length (GL), 5.5 inches Gauge Factor (GF), $3.025e^{-3}$ Microstrain per Frequency squared						
	T	F	Lin	Change $\mu\epsilon$	GT1174	GT1192
Upper Limit	08500	1176.5	1384.1	-1489.5	0.93	0.71
Mid Range	10590	944.29	891.68	0.0	0.51	0.06
Lower Limite	16000	625.00	390.63	1515.7	0.15	0.04

NOTES

- The Period (T) is the reading as displayed by the GT1174 Miniature Strain Meter in seconds $\times 10^7$.
- The Frequency (F) is the reading as displayed by the GT1192/615 Geologger in hertz and is equivalent to $10^7/T$.
- The Linear value (Lin.) is $F^2/1000$ and is equivalent to $10^{11}/T^2$.
- The microstrain Change ($\mu\epsilon$) is derived from the Vibrating Wire Equation.
- The Resolution is given in microstrain. It is the resulting change in microstrain for a least significant digit change in the reading as displayed by the GT1174 or GT1192. Resolution varies over the frequency range of the gauge, and is related to the parameter being measured by the readout unit (period, frequency or linear value).

DATASHEET - VW Embedment Strain Gauge.doc

ATC Semitec – IP68 Rated Thermistor Sensors

A range of double insulated, fully encapsulated over moulded temperature sensors offering IP68 waterproof protection. We have numerous NTC thermistor options to suit your specific application.

Applications:

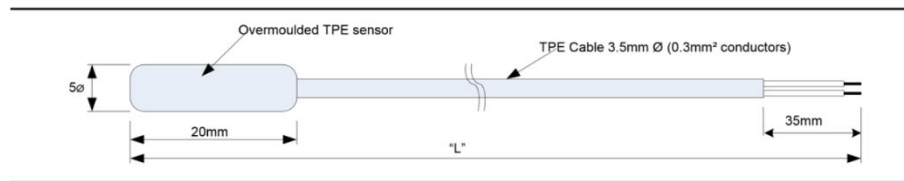
- Heat pumps
- Under-floor Heating
- Refrigeration
- HVAC
- Solar



These sensors ensure absolute integrity against moisture ingress.

Features:

- Temperature range -50 to 110°C (125°C intermittent)
- IP68 waterproof integrity
- Di-electric strength: 4kVAC
- Insulation: primary PP and secondary TPE
- Cable lengths: 200mm to 10metres (others available on request)
- IP65 version up to 150°C available



Thermistor options:

The IP68 Series probes can use the following thermistor series;

NTC Range	R25 values	R25 Tolerances	NTC Temp. Range
AP Series	2kΩ – 200kΩ	0.5%-1%	-60/+150°C
SP Series	1kΩ – 100kΩ	0.2%-0.5%	-60/+150°C
AT Series	1kΩ – 100Ω	1%	-50/+110°C
NT Series	5kΩ – 1MΩ	1%-3%	-60/+300°C
ET Series	2kΩ – 232kΩ	1%-3%	-60/+100°C

Mounting and other options:

A range of stainless-steel housings can be added to increase sensor robustness or provide various mounting options. Different colour versions are also available.

EL-USB-2+

High Accuracy Humidity, Temperature and Dew Point USB Data Logger

FEATURES

- Higher accuracy sensor when compared with the EL-USB-2
- 0 to 100%RH measurement range
- -35 to +80°C (-31 to +176°F) measurement range
- Dew point indication via Windows control software
- USB interface for set-up and data download
- User-programmable alarm thresholds for %RH & T
- Status indication via red and green LEDs
- Supplied with replaceable internal lithium battery and Windows control software
- Environmental protection to IP67

This standalone data logger measures and stores up to 16,382 relative humidity and 16,382 temperature readings over 0 to 100%RH and -35 to +80°C (-31 to +176°F) measurement ranges. The user can easily set up the logger and view downloaded data by plugging the data logger into a PC's USB port and running the purpose designed software under Windows 2000, XP, Vista & 7. Relative humidity, temperature and dew point (the temperature at which water vapour present in the air begins to condense) data can then be graphed, printed and exported to other applications. The data logger is supplied complete with a long-life lithium battery, which can typically allow logging for 1 year.



ORDERING INFORMATION

Standard Data Logger (Data Logger, Software on CD, Battery)	EL-USB-2+
Replacement Battery	BAT 3V6 1/2AA

Specifications		Minimum	Typical	Maximum	Unit
Relative Humidity	Measurement range	0		100	%RH
	Repeatability (short term)		±0.1		%RH
	Accuracy (overall error)		±2.0*	±4.0	%RH
	Internal resolution		0.5		%RH
	Long term stability		0.5		%RH/yr
Temperature	Measurement range	-35 (-31)		+80 (+176)	°C (°F)
	Repeatability		±0.1 (±0.2)		°C (°F)
	Accuracy (overall error)		±0.3 (±0.6)	±1.5 (±3)	°C (°F)
	Internal resolution		0.5 (1)		°C (°F)
Dew Point	Accuracy (overall error)		±1.1 (±2)**		°C (°F)
Logging rate		every 10s		every 12hr	-
Operating temperature range		-35 (-31)		+80 (+176)	°C (°F)
1/2AA 3.6V Lithium Battery Life			1***		Year

* This specifies the overall error in the logged readings for relative humidity measurements between 10 and 90%RH.

** This specifies the overall error in the calculated dew point for relative humidity measurements between 40 and 100%RH at 25°C.

*** Depending on sample rate and ambient temperature



www.lascarelectronics.com



Appendix E. Data sheets for instrumentation used in research

**Leadwire
-integrated**

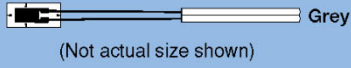
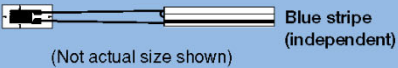
series "F"



Compatible adhesive & Operational temperature
 CN : -20~+80°C
 P-2 : -20~+80°C EB-2 : -20~+80°C

Operational temperature -20~+80°C
 Temperature compensation range +10~+80°C
 Quarter bridge with 3-wire system is usable to avoid an unexpected effect of resistance change with temperature.

GENERAL USE

Gauge pattern	Type	Gauge size		Backing		Resistance in Ω	
		L	W	L	W		
<p>This gauge has a pre-attached vinyl lead wire to F series strain gauge. Works for lead wire connection such as strain gauge terminal installation and lead wire soldering are not required. It saves much time and labor.</p> <p>●Single-element (G.F. 2.1 approx.)</p> <p>0.11mm² integral vinyl leadwire Total leadwire resistance per meter : 0.32Ω</p> <p>2-wire system</p>  <p>(Not actual size shown)</p> <p>3-wire system</p>  <p>(Not actual size shown)</p> <div style="border: 1px solid black; padding: 5px; margin-top: 10px;"> <p style="text-align: center;">FLA-1-11-3LT</p> <p>Length of integral leadwire (m) └──┘</p> <p>Code of integral leadwire └──┘</p> </div> <p>Minimum order is 10 gauges or more. Other gauge is also available for leadwire-integrated service, contact TML or your local representatives.</p>		L : length W : width (Unit : mm)					
	FLA-1-11 -17 -23		1	1.3	5.0	2.5	120
	FLA-2-11 -17 -23	-1L	2	1.5	6.5	3.0	120
	FLA-3-11 -17 -23	-3L	3	1.7	8.8	3.5	120
	FLA-5-11 -17 -23	-5L	5	1.5	10.0	3.0	120
	FLA-6-11 -17 -23		6	2.2	12.5	4.3	120
	FLA-1-11 -17 -23		1	1.3	5.0	2.5	120
	FLA-2-11 -17 -23		2	1.5	6.5	3.0	120
	FLA-3-11 -17 -23	-3LT	3	1.7	8.8	3.5	120
	FLA-5-11 -17 -23	-5LT	5	1.5	10.0	3.0	120
	FLA-6-11 -17 -23		6	2.2	12.5	4.3	120

FOIL STRAIN GAUGES series F

-196°C **Operating temperature range** +150°C
 Temperature compensation range
 +10°C **Temperature compensation range** +100°C

Suffix code for temperature compensation materials
 -11: Mild steel  -17: Stainless steel  -23: Aluminium 
 For ordering, the above suffix code should be added to the basic gauge type.

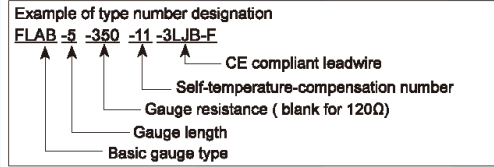
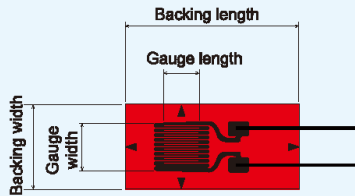
Applicable adhesives	CN	-196 ~ +120°C
	P-2	-30 ~ +150°C
	EB-2	-60 ~ +150°C

GENERAL USE

Strain gauges compliant to RoHS2 Directive 2011/65/EU are added to the lineup in F series. They are supplied with CE marking as standard specification. Our logo GOBLET, which is an abbreviation of "Gauges Of Brilliant Lifespan and Environmental Thoughtful", is marked on the package of these gauges.



Single element



Gauge pattern	Basic type	Gauge size		Backing		Resistance		
		L	W	L	W	Ω		
Single element		FLGB-02	0.2	1.4	3.5	2.5	120	
		FLGB-1	1	1.1	6	2.5	120	
		FLAB-03	0.3	1.4	3	2	120	
		FLAB-05	0.5	1.2	4.3	2.2	120	
		FLAB-1	1	1.3	5	2.5	120	
		FLAB-2	2	1.5	6.5	3	120	
		FLAB-3	3	1.7	7.7	3.5	120	
		FLAB-3-60	3	1.2	7.7	3	60	
		FLAB-5	5	1.5	10	3	120	
		FLAB-6	6	2.2	11	4.3	120	
		FLAB-10	10	2.5	15.4	5	120	
		FLAB-30	30	2	35	5	120	
	FLK pattern with narrow gauge width		FLKB-1	1	0.7	4.5	1.4	120
			FLKB-2	2	0.9	5.5	1.5	120
		FLKB-6	6	1	11	2.2	120	
		FLKB-10	10	1.6	15	3.8	120	
350Ω Single element		FLAB-1-350	1	1.6	4.5	3	350	
		FLAB-2-350	2	1.9	6	3.5	350	
		FLAB-3-350	3	1.6	7.2	3	350	
		FLAB-5-350	5	1.8	9.4	3.8	350	
		FLAB-6-350	6	2.6	10.8	4.5	350	
		FLAB-10-350	10	3	16	5	350	
		FLAB-6-1000	6	4.6	11	7	1000	

Each package contains 10 gauges.

Appendix E. Data sheets for instrumentation used in research

Developing Strain Gauges and Instruments

POLYESTER STRAIN GAUGES

series P/PF

Operating temperature range
 -20°C +80°C
 Temperature compensation range
 +10°C +80°C

Suffix code for temperature compensation materials
 -11: Mild steel
 For ordering, the above suffix code should be added to the basic gauge type.



Applicable adhesives	Operating temperature range
CN-E	-20 ~ +80°C
RP-2	-20 ~ +80°C
PS	-20 ~ +80°C

STEEL, CONCRETE, MORTAR MATERIAL USE

Gauge pattern	Basic type	Gauge size L W	Backing L W	Resistance Ω
series P				
<p>These are wire strain gauges utilizing a transparent plastic backing impregnated with polyester resin. The gauge length is available in 3 ranges of 60, 90 and 120mm, so it is suited to the measurement of concrete strain. Since the backing is transparent, the bonding position can easily be checked in the installation works.</p>				
Single element				
	PL-60			
	PL-60-11			
<p>Example of type number designation.</p> <p>PL-60 -11 -3LJC-F</p> <p>↑ ↑ ↑</p> <p>Basic strain gauge type CE compliant integral leadwire Self-temperature-compensation for Mild steel</p>				
Integral leadwire is available only for single element PL, but not for 2-element PLC and 3-element PLR.				
Single-element Each package contains 10 gauges.				
	PL-60-11	60 1	74 8	120
	PL-90-11	90 1	104 8	120
	PL-120-11	120 1	134 8	120
Each package contains 10 gauges.				
0°/90° 2-element stacked Rosette				
	PLC-60-11	60 1	74 74	120
0°/45°/90° 3-element stacked Rosette				
	PLR-60-11	60 1	74 74	120
series PF				
<p>These are foil strain gauges utilizing a polyester resin backing which is the same as the P series. The gauge length is available in 3 ranges of 10, 20 and 30mm, so it is suited mainly to strain measurement on concrete or mortar. The backing is transparent and the installation is easy.</p>				
Single element				
	PFL-10-11			
	PFL-20-11			
	PFL-30-11			
Each package contains 10 gauges.				
0°/90° 2-element stacked Rosette				
	PFLC-20-11	20 1.2	28 28	120
	PFLC-30-11	30 2.3	40 40	120
0°/45°/90° 3-element stacked Rosette				
	PFLR-20-11	20 1.2	28 28	120
	PFLR-30-11	30 2.3	40 40	120
<p>Recommendable integral leadwire for P/PF series with single element. No integral leadwire is available for rosette element PLC, PLR, PFLC and PFLR.</p>				
Application	Leadwires	Operating temperature (°C)	Leadwire code exemplified	
General use (temperature unchanged during measurement)	Paralleled vinyl -LJB-F/-LJC-F	-20~ +80	PL-60-11-3LJB-F PFL-10-11-3LJC-F	
General use	3-wire paralleled vinyl -LJBT-F/-LJCT-F	-20~ +80	PL-60-11-3LJBT-F PFL-10-11-3LJCT-F	
1-gauge 4-wire measurement	0.08mm ² polypropylene 4-wire paralleled -LQM-F	-20~ +100	PL-60-11-3LQM-F	

Appendix E. Data sheets for instrumentation used in research

Developing Strain Gauges and Instruments

STRAIN GAUGE ADHESIVES

TYPE		Contents	Component	Applicable specimen	Operational temperature	Curing temperature and time
CN	Single component Room-temperature-curing	Single 2g×5	Cyanoacrylate	Metal, Plastics, Composite	-196~+120°C	Room temperature 20sec. -1 min. (thumb pressure)
CN-E	Single component Room-temperature-curing	Single 2g×5	Cyanoacrylate	Porous, Concrete, Mortar, Wood	-30~+120°C	Room temperature 40sec. -2 min. (thumb pressure)
CN-R	Single component Room-temperature-curing	Single 2g×5	Cyanoacrylate	Metal, Plastics, Composite	-30~+120°C	Room temperature 10-30 sec. (thumb pressure)
CN-Y	Single component Room-temperature-curing	Single 2g×5	Cyanoacrylate	Metal, Plastics, Composite	-30~+80°C	Room temperature 20sec. -1 min. (thumb pressure)
P-2	Two component Room-temperature-curing (Mixing ratio: 1-3%)	A:100g B:10g	Polyester	Metal	-30~+180°C	Room temperature Pressure 50-300kPa 2~3 hrs.
RP-2	Two component Room-temperature-curing (Mixing ratio: 2-4%)	A:100g B:10g	Polyester	Concrete, Mortar	-30~+180°C	Room temperature Pressure 50-300kPa 2~3 hrs.
PS	Two component Room-temperature-curing (Mixing ratio: 2-4%)	A:200g B:20g	Polyester	Concrete, Mortar	-30~+100°C	Room temperature 2~3 hrs.
NP-50	Two component Room-temperature-curing (Mixing ratio: 2-4%)	A:50g B:10g	Polyester	Metal, Composite	-30~+300°C	Room temperature Pressure 50-300kPa 2~3 hrs.
C-1	Single component Heat-curing	Single 50g	Phenol	Metal	-269~+200°C	130°C 1hr. pressed 200°C 1hr.
EA-2A	Two component Room-temp.-or heat curing (Mixing ratio: 2:1)	A:50g B:25g	Epoxy	Metal, Concrete, Composite	-269~+50°C	Room temp. 1 day or heating 50°C 2hrs. Pressure 50~300kPa
EB-2	Two component Room-temperature-curing (Mixing ratio: 10:3)	A:10g×3 B:3g×3	Epoxy	Metal, Composite	-30~+150°C	Room temperature Pressure 50-300kPa 1 day
A-2	Two component Heat-curing (Mixing ratio: 10:1)	A:50g B:5g	Epoxy	Bolt	-30~+100°C	Room temperature 12 hrs. and 140°C 3 hrs.

N.B.:

Shelf life Effective storing duration while the adhesive is properly kept in a cool, dry and dark place such as a refrigerator (+5~+10°C, do not store in a freezer).

Thumb pressure 100~300kPa

● For two-component adhesive, use the supplied mixing vessels.

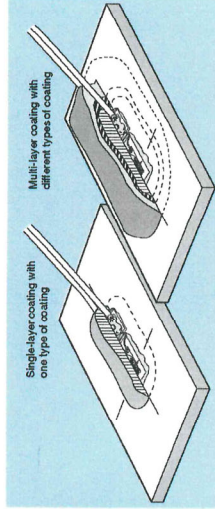
Mixing vessels: Polyethylene make
75mm-diameter, 10mm depth

Point

- In general, curing condition of room-temperature-curing type adhesives varies with an ambient temperature and humidity. Taking consideration of standard application described in operation manual, test curing should be recommended in site before measurement.
- CN Adhesive (Cyanoacrylate component) use minute quantities of moisture in the air or on the surface of the specimen to quickly polymerize and generate adhesive strength. A certain amount of moisture is required for the adhesive to harden.

COATING MATERIALS

TML coating materials are used for water- or moisture-proofing over bonded strain gauges. For long-term use or field measurement, the strain gauges and connecting terminals require protection from ambient moisture.



The type of coating required and the application method differ depending on the environment in which the strain gauge is to be used. In general, if one type of coating is not sufficient, multiple coatings can be combined to protect the strain gauges. At TML, the coating applied directly to the surface of the strain gauge is referred to as the first coating, with subsequent coating layers referred to sequentially as the second coating, third coating, etc. Multi-layer coatings are recommended for strain gauge protection.

TYPE	Materials	Content per unit	Operational temperature	Curing conditions	Purpose	Applications
W-1	Microcrystalline wax solid	Single 500g	0~+50°C	Hot melling 100~120°C, hardening in room temperature	Moisture and Water-proofing	General-purpose coating for laboratory and field requirements where mechanical protection is not needed, or as a prime-coat for duplex coating.
N-1	Neprene rubber	90g	-30~+80°C	Air-drying solvent-thinned a half day in room temperature	Moisture and Water-proofing	General-purpose coating for laboratory and less severe field requirements where a high degree of mechanical protection is not needed. Long term stability.
K-1	Special rubber	90g	-196~+60°C	Air-drying solvent-thinned a half day in room temperature	Cryogenic temperature-resistant	For laboratory requirements from cryogenic to room temperature. Does not provide a high degree of mechanical protection.
SB tape	Butyl	10mm×3mm 5m long/roll	-30~+80°C	Pressure sensitive	Moisture and Water-proofing	3-mm thick tape-form coating. Very convenient usage.
VM tape	Butyl	38mm×1mm 8m long/roll	-20~+80°C		Moisture and Water-proofing	1-mm thick tape-form coating.
Epoxy resin	Epoxy	AW106 canned 1.8kg	-60~+100°C	Two-component room-temperature - curing Mixing ratio 10 to 6	Physical protection	General purpose coating for mechanical protection
		Araldite standard tube 170g				
Epoxy resin AV138	Epoxy	Canned 1.4kg	-60~+180°C	Two-component room-temperature - curing Mixing ratio 10 to 4	Physical protection	Coating for mechanical protection in high-temperature usage
Three Bond 1521B	Chloroprene rubber	150g	-30~+100°C	Air-drying solvent-thinned a half day in room temperature	Moisture and Water-proofing	A finish coating for multi-layer applications.
KE-948	Silicon rubber	100g	-50~+200°C	Air-drying solvent-thinned a half day in room temperature	Heat-resistant	Suitable for laboratory requirements with harsh temperature conditions where a high degree of mechanical protection is not needed.
TSE9976-B	Silicon rubber	100g	-50~+300°C	Air-drying solvent-thinned a half day in room temperature	Heat-resistant	Suitable for laboratory requirements with harsh temperature conditions where a high degree of mechanical protection is not needed.

N.B.: MSDS (Material Safety Data Sheet)
TML supplies an MSDS for all its strain gauge adhesives and coatings. Contact your TML supplier for more information.
Coatings in special substances
For use in special substances such as acids, alkalis and alcohols, contact TML or local representatives.

Appendix E. Data sheets for instrumentation used in research

PFTE Slip Membrane

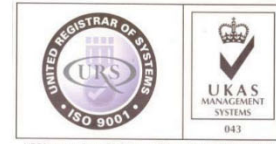


Alperton Engineering Ltd

Dublin Industrial Estate,
Glasnevin, Dublin11, Ireland

www.alperton.com info@alperton.ie

Phone +353 1 8306277



URS is a member of Registrar of Standards (Holdings) Ltd.

Product: 100% Virgin PTFE (Polytetrafluoroethylene)

Material Specification (Typical Properties)

Property	Method	Units	Specification
Specific Gravity	ISO 13000-2	g/cm ³	2,130 – 2,180
Tensile Strength	ISO13000-2	MPa	>20
Elongation	ISO13000-2	%	>200
Hardness	ISO13000-2	Shore D	>54
Ball Hardness	ISO13000-2	MPa	>23
Compression Strength @ 1% deformation		KG/cm ²	>70
Deformation under load (140kg/cm ² for 24hr. At 23°C)	ASTM D621	%	10 - 17
Permanent deformation (After 24hrs. Relaxation at 23°C)	ASTM D621	%	6 – 7,5
Coefficient of static friction	ASTM D621		0,08 – 0,10
Coefficient of dynamic friction	ASTM D621		0,06 – 0,08
Thermal Conductivity	ASTM D621	W / m.K	0,24
Dielectric Constant (ε) At 60Hz to 2Ghz	ASTM D621	/	2,1
Dielectric Strength	ASTM D621	KV/mm	20 – 70
Volume Resistivity	ASTM D621	Ohm-cm	10 ¹⁸
Flammability	UL 94		V-0
Water Absorption	ASTM D621	%	0,01

Service Temperature

Excellent resistance to continuous service temperatures up to 260 °C and, for limited periods, even to higher temperatures; the low temperature resistance of the product allows satisfactory performance at as low as -200 °C.

Chemical Resistance

PTFE Processes a high inertness towards nearly all known chemicals. It is only attacked by elemental alkali metals, chlorine trifluoride and elemental fluorine at high temperatures and pressure

Solvent Resistance

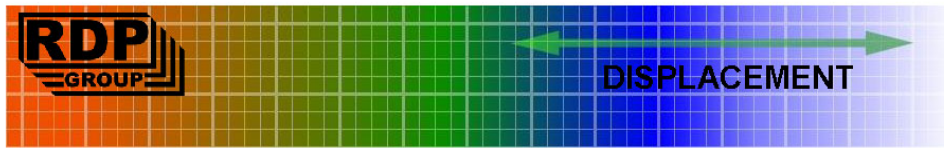
PTFE is insoluble in all solvents up to temperatures as high as 300 °C (572°F) Certain highly fluorinated oils only swell and dissolve PTFE at temperatures close to the crystalline melting point.

FDA Approved

(Code of federal regulation 21 CFR Ch.1 revised as of April 1st 1991 edition), Sections 175.105 – 175.300 – 176.170 – 176.180 – 177.1520 - 177.1550 - 177.2600 – 178.3570. “Perfluorocarbon Resins” of the Food and Drug Administration

Disclaimer. These figures are typical values for the material and do not represent a product specification. Properties will vary depending on source of raw material, method of processing, physical form of product, direction of measurement etc.
Updated 4/24/2015 2:37 PM

Page 1



ACT LVDT Displacement Transducer

- High accuracy
- High cycle life
- Infinite resolution
- Stainless steel

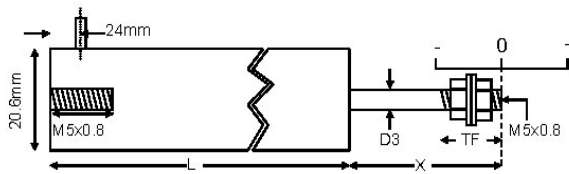


These transducers are for displacement / position measurement. They make an accurate position measurement of the movement of the armature (the sliding part) relative to the body of the displacement transducer.

This transducer uses the Linear Variable Differential Transformer (LVDT) principle which means that it is probably the most robust and reliable position sensor type available. The strength of the LVDT sensor's principle is that there is no electrical contact across the transducer position sensing element which for the user of the sensor means clean data, infinite resolution and a very long life.

This series of displacement transducer is available as either an unguided, captive or spring return version.

Captive guided version.

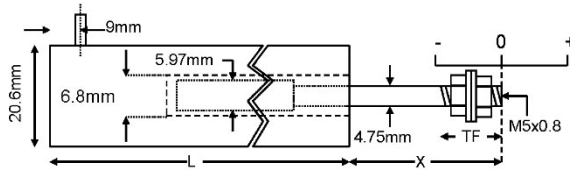


Our captive guided displacement transducer has bearings to guide the armature inside the measurement sensor. Captive LVDTs are for position measurement applications where guidance may be poor and end bearings may be required.

Type	Range	Linearity error (% F.S.)	L	X	D3	Total weight	TF	Inward over-travel	Outward over-travel	Sensitivity (nom)
ACT500C	±12.5mm	<±0.5/±0.25/±0.1	152mm	38mm	4.75mm	284g	15mm	10mm	12mm	0.7V/V
ACT1000C	±25mm	<±0.5/±0.25/±0.1	180mm	63mm	4.75mm	340g	15mm	13mm	10mm	0.9V/V
ACT2000C	±50mm	<±0.5/±0.25/±0.1	295mm	76mm	4.75mm	511g	15mm	10mm	14mm	1.5V/V
ACT3000C	±75mm	<±0.5/±0.25/±0.1	406mm	114mm	4.75mm	653g	15mm	24mm	15mm	1.5V/V
ACT4000C	±100mm	<±0.5/±0.25/±0.1	452mm	127mm	4.75mm	710g	15mm	8mm	14mm	3.2V/V
ACT6000C	±150mm	<±0.5/±0.25	643mm	178mm	4.75mm	1.0kg	15mm	12mm	17mm	2.4V/V
ACT8000C	±200mm	<±0.5/±0.25	833mm	254mm	4.75mm	1.4kg	32mm	22mm	25mm	1.5V/V
ACT10000C	±250mm	<±0.5/±0.25	1030mm	305mm	4.75mm	1.6kg	27mm	34mm	35mm	2.0V/V
ACT15000C	±375mm	<±0.5	1435mm	406mm	4.75mm	2.1kg	19mm	13mm	13mm	3.2V/V
ACT18500C	±470mm	<±0.5	1702mm	508mm	6.00mm	2.5kg	27mm	5mm	33mm	3.6V/V

Appendix E. Data sheets for instrumentation used in research

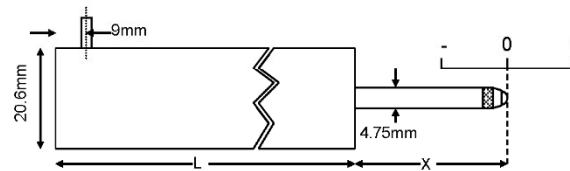
Unguided version.



On our unguided LVDTs the armature assembly is a separate component, to make a measurement the user must guide the armature inside the body without touching the sides. Unguided position measurement transducers are appropriate where external guidance is available and give truly non-contact operation

Type	Range	Linearity error (% F.S.)	L	X	Total weight	Armature weight	TF	Inward over-travel	Sensitivity (nom)
ACT500	±12.5mm	<±0.5/±0.25/±0.1	127mm	43mm	170g	17g	15mm	16mm	0.7V/V
ACT1000	±25mm	<±0.5/±0.25/±0.1	155mm	68mm	227g	23g	15mm	22mm	0.9V/V
ACT2000	±50mm	<±0.5/±0.25/±0.1	270mm	81mm	320g	37g	15mm	16mm	1.5V/V
ACT3000	±75mm	<±0.5/±0.25/±0.1	380mm	120mm	454g	55g	15mm	29mm	1.5V/V
ACT4000	±100mm	<±0.5/±0.25/±0.1	427mm	132mm	568g	71g	15mm	16mm	3.2V/V
ACT6000	±150mm	<±0.5/±0.25	617mm	183mm	824g	100g	15mm	16mm	2.4V/V
ACT8000	±200mm	<±0.5/±0.25	808mm	259mm	1.2kg	140g	29mm	27mm	1.5V/V

Spring return version.



Our spring displacement transducer has bearings to guide the armature inside the measurement sensor and a spring which pushes the armature to the fully out position. Spring return LVDTs are appropriate where it is not possible to connect the transducer armature to the moving component being measured.

Type	Range	Linearity error (% F.S.)	L	X	Total weight	Spring force at X	Spring rate	Inward over-travel	Outward over-travel	Sensitivity (nom)
ACT500A	±12.5mm	<±0.5/±0.25/±0.1	133mm	38mm	184g	1.3N	0.2N/cm	1mm	13mm	0.7V/V
ACT1000A	±25mm	<±0.5/±0.25/±0.1	161mm	63mm	227g	2.0N	0.3N/cm	3mm	10mm	0.9V/V
ACT2000A	±50mm	<±0.5/±0.25/±0.1	276mm	75mm	398g	1.8N	0.2N/cm	8mm	14mm	1.5V/V
ACT3000A	±75mm	<±0.5/±0.25/±0.1	387mm	114mm	483g	6.0N	0.4N/cm	15mm	15mm	1.5V/V

Specification	
Excitation/supply (acceptable)	0.5V to 7V rms, 2kHz to 10kHz (sinusoidal)
Excitation/supply (calibrated)	5V rms, 5kHz (sinusoidal)
Output load	100k Ohms
Temperature coefficient (zero)	±0.01% F.S. /°C (typical)
Temperature coefficient (span)	±0.01% F.S. /°C (typical)
Operating temperature range	-50°C to 125°C
Electrical termination	2m (integral cable) Longer available to order.

Appendix F. SHM strategy for HBB

F.1 Design phase for SHM

1) Determine what parameter(s) you wish to measure and how they will be measured. In the case of this project, strain and temperature in the concrete slab in HBB were the parameters which we wished to measure.

2) Select appropriate sensors which can measure the desired parameter and are sufficiently robust for the life-span of the project. Other considerations are accuracy, reliability, power requirements, sensor installation and cost. The Gage Technique embedment vibrating wire (VW) strain gauge (Type TES/5.5/T) was selected for HBB and it measured longitudinal strain and temperature in the concrete. Gauges of this type have been successfully used in many engineering projects and were found to be very robust and provide reliable data.

2) A copy of the engineering and architectural drawings of HBB were studied to determine the most appropriate locations of the VW strain gauges. Possible locations of the data acquisition (DAQ) unit was also a consideration as the VW strain gauges were wired sensors. Ideally, it is preferable if the DAQ unit can be positioned in its long-term location, or close as possible, during the installation phase so that wires do not need dis-connected and re-connected at a later date. In HBB, DAQ units were positioned in the service riser so that the DAQ unit would be accessible when the building became operational for maintenance and/or inspection.

3) The finite element model developed by the precast manufacturer for the floor slab was analysed and the location of sensors were chosen so that the changes in strain measured by the embedded sensors would be of significant magnitude. The VW gauges were positioned in two orthogonal directions in the floor slab and along the walkway so that bending behaviour of the hybrid concrete floor could be studied during the construction and operational phase.

4) A proposal documentation (Appendix F.3) was prepared and submitted to the contractor, structural engineer, precast manufacturer and client (NUI Galway in this case) to explain the proposed SHM scheme. Particularly for stakeholders who have not dealt with a SHM scheme previously, it is important to explain the proposal and get agreement for the location of the sensors and DAQ unit and address any

Appendix F. SHM strategy for HBB

concerns that may arise. Meetings were organised with the contractor (BAM) and precast manufacturer (Oran Precast) to discuss the proposed methodology and location of the sensors. The key concern from the contractor is that the proposed installation of the sensors would not impact site operations or the construction programme. This stakeholder engagement is a key part of the design phase and should happen as early as possible so that any queries or potential difficulties can be resolved before the installation phase.

5) A risk assessment and method statement was submitted to the contractor and the precast manufacturer for the installation of the sensors in both the precast factory and on site respectively.

6) The proposed cable routes of the wires were marked on drawings to check that the wires were long enough to connect to the DAQ unit. VW strain gauges were ordered with different wire lengths to suit the proposed installation.

7) During much of the construction phase, provision of power will typically not be possible. Therefore, re-chargeable batteries must be used and changed at regular intervals. The batteries selected should be such that they have long-life so that it minimises the number of site visits.

8) The data interval for the sensors depends on the parameter being measured and how quickly its magnitude changes. The other consideration is data management. Most DAQ units have built-in data logging and data transmission facilities. In HBB, the data interval was 10 seconds during the construction phase and 1 hour during the operational phase. The DAQ system consisted of CR1000 data loggers, AM16/32B multiplexers and AVW200 vibrating wire interface from Campbell Scientific. During the construction phase, the data was manually collected each month from the DAQ unit and transferred to a laptop. When the HBB was networked, the data was transferred over the local college network using Campbell Scientific's NL116 Ethernet interface and compact flash module.

9) Environmental conditions are likely to have an influence on the behaviour of structural elements and therefore, it is important to consider if additional sensors are required to record environmental parameters such as ambient temperature, relative humidity, wind speed and solar radiance. In HBB, the nearby weather

station was invaluable as it monitored the environmental conditions near the site. In addition, when external cladding was erected in HBB, a data logger which recorded ambient temperature and relative humidity inside the building during the construction phase.

F.2 Installation phase for SHM

1) The installation of sensors typically must be undertaken so that it does not affect the construction programme. Where possible try to complete as many tasks off-site as possible to minimise the site operations. In the case of sensors which are embedded in concrete, there is usually a short timeframe to install the sensors before concreting. In HBB, the VW strain gauges were tied to u-shaped reinforcement bars (**Appendix A**) so that they could be installed on site relatively quickly. In most cases, three VW strain gauges were positioned on the u-bar so that strain could be measured at different depths in the concrete slab. VW strain gauges in the precast planks were tied individually to the reinforcement in the plank and all the wires were routed to one location so that it would simplify erection of the plank on site.

2) Accurate record keeping is key to any SHM scheme. The reference number of all VW gauges on each u-bar was noted and photos taken of each u-bar prior to site installation. All VW gauges were tested to ensure that they were operational and that the output data was within operational ranges.

3) During the installation phase, it is important to get buy-in from site personnel to ensure that the sensors are not damaged during the construction. Regular contact with relevant site personnel is maintained to ensure that installation of the sensors does not impact on site operations.

4) When approval was provided by the contractor, the top layer of reinforcement was positioned. Temporary string lines were erected and the u-bars with VW strain gauges were positioned at designated positions in the slab. It is important to check that the u-bars are tied sufficiently to the main reinforcement in the slab and that the gauges are tied to the u-bar. It is critical that the gauges and/or u-bar will not move during concreting operation. The height, orientation (direction and horizontality), position and reference number of all sensors was recorded, and photos taken of each sensor.

Appendix F. SHM strategy for HBB

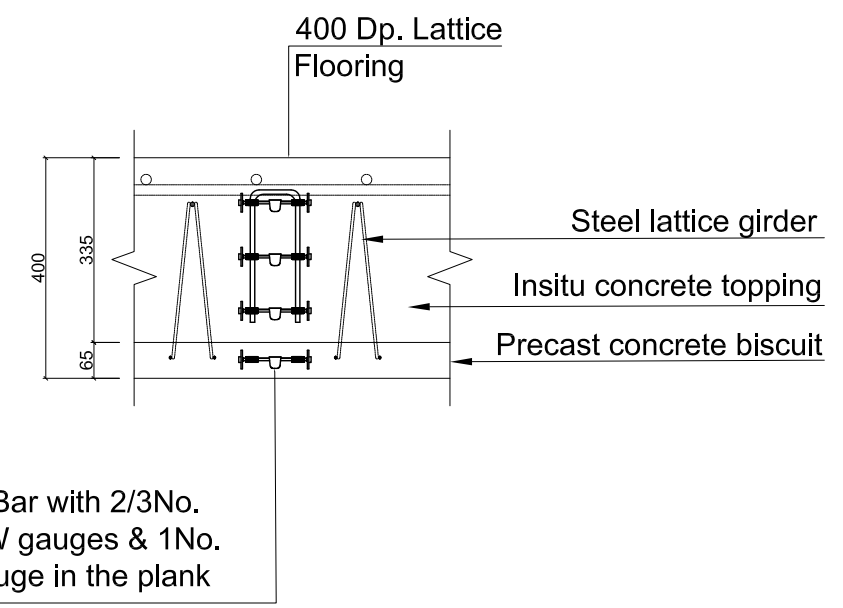
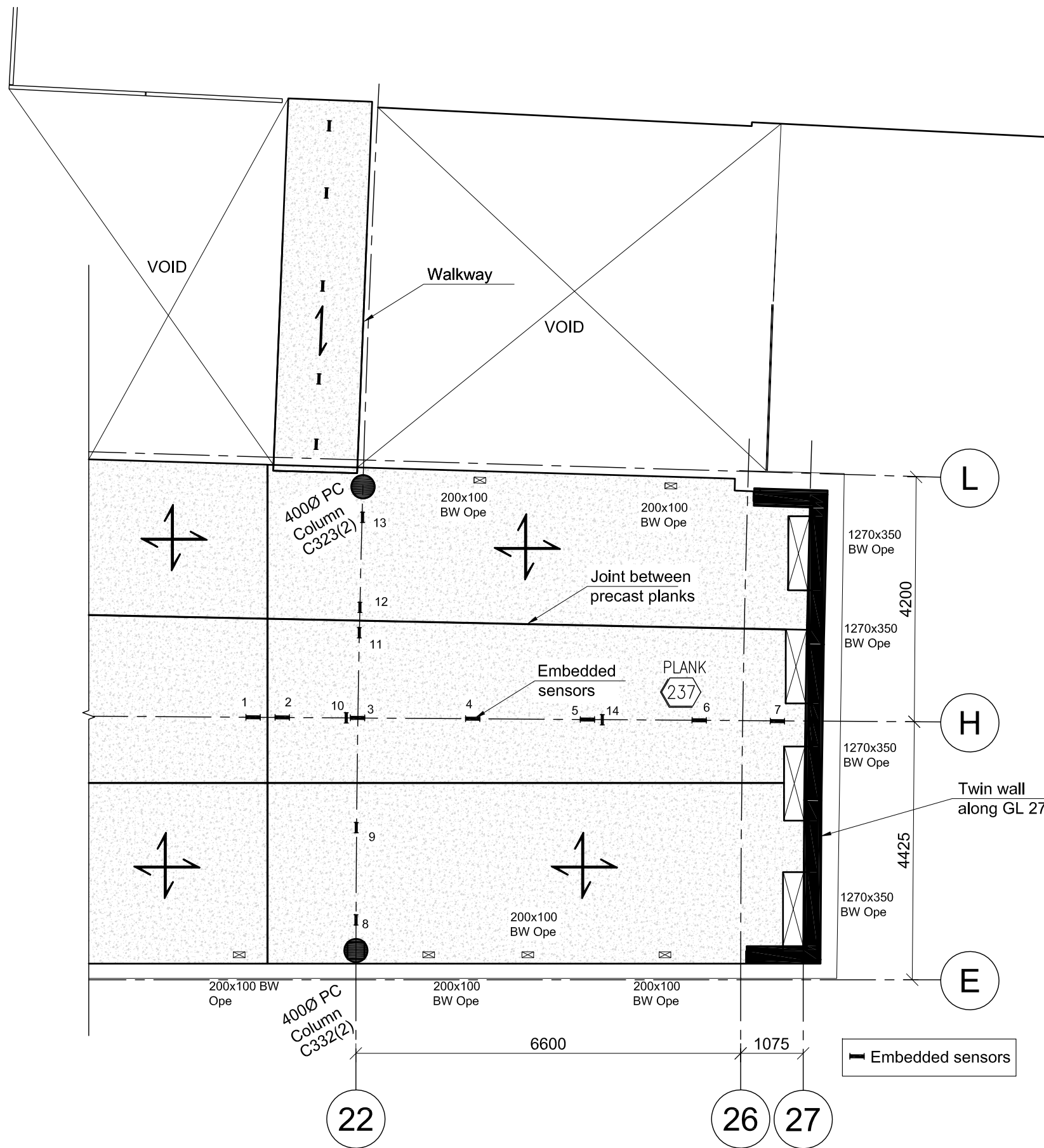
5) The cables from the VW strain gauges run parallel with the reinforcement and where possible run in long straight runs. Some slack should be left in cables near the VW strain gauge to allow for any movement. In HBB, the cables were grouped and housed in ducting and ran in long straight runs towards the service riser. Where cables change direction, they were tied to the reinforcement and never left unsupported.

6) The DAQ unit was positioned in the service riser and all cables from the sensors were connected to the DAQ unit in accordance with an agreed schedule. In HBB, four wires were connected to the DAQ unit for each sensor (2 for temperature, 2 for strain). The reference number for each VW strain gauge and the corresponding channel number in the DAQ unit was recorded. Any additional lengths of cables were coiled and tidied so that they would not impact any future site operations or get damaged.

7) Prior to concreting a set of readings was taken to check that all sensors are working. Sometimes, null readings can be caused by loose connections when connected to the DAQ unit.

8) During the concreting, it is important to be on site and highlight to the site operatives that embedded sensors can be damaged by the vibrator poker and request that they are careful when concreting near sensors.

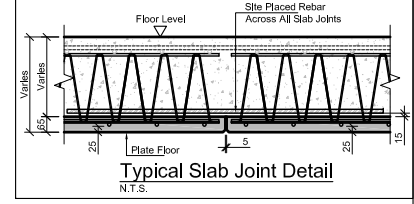
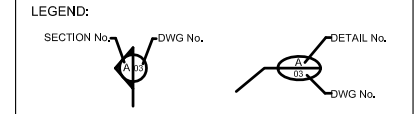
9) When using embedment VW strain gauges, it is also advisable to install two 'no-stress' strain gauges (**Sec. 7.2.1**) near the area of the instrumented slab. A 'no-stress' strain gauge is typically housed in a pre-fabricated cylinder and is used to measure stress-independent strain. This is very useful information when post-processing of the strain data is undertaken.



Typical section at location of embedded sensors

HBB - Instrumentation 2nd Floor

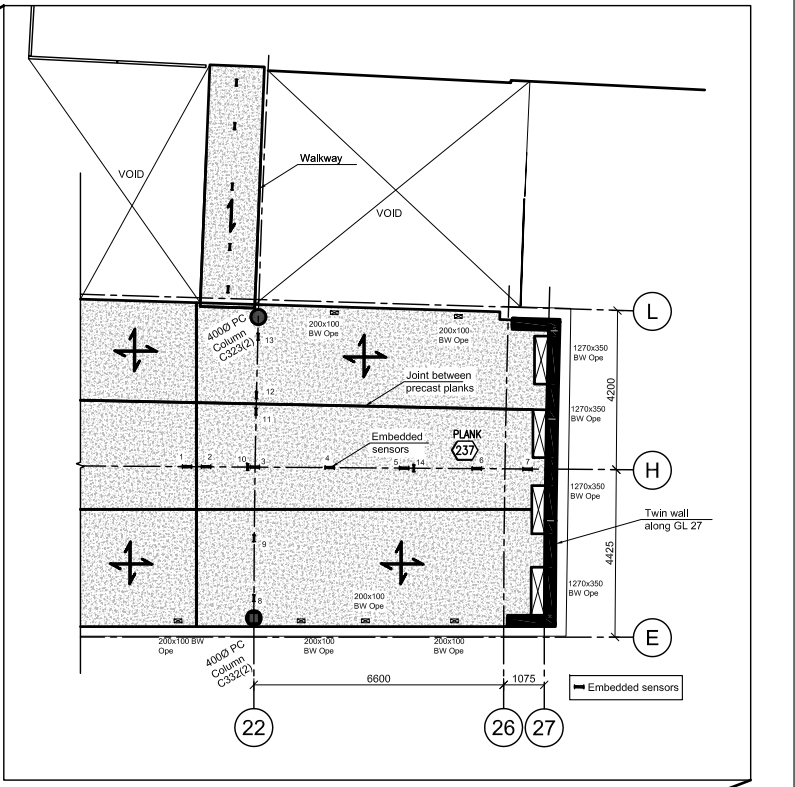
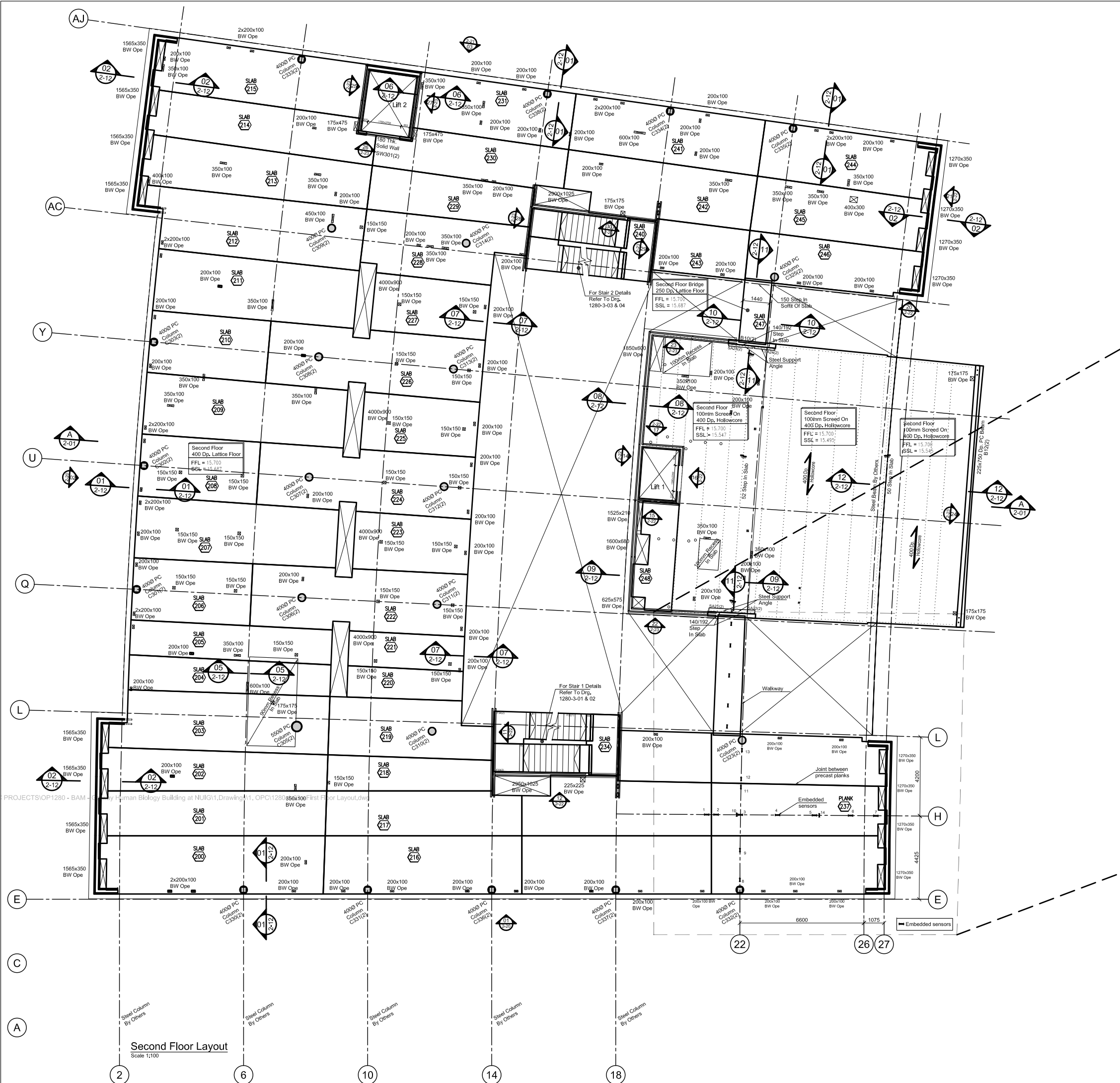
NOTES:
 This drawing must be checked by the client, his agent or the main contractor and approval given in writing.
 Manufacture can not commence until written approval is given and thereafter the client or main contractor will be liable for any additional expenses incurred by them.
 Do not scale from this drawing, use figured dimensions only.
 All dimensions in millimetres.
 All levels in meters.



For Section Refers To Second Floor Sections, Drawing 1280-2-12

Feasibility Of Builders Work Ope Locations Will Only Be Confirmed Upon Completion Detailed Slab Design

Any Builders Work Ope Locations Less Than 150 To Be Cored On Site



PROJECTS\OP1280 - BAM - Galway Human Biology Building at NUIG\1.Drawing\1.OPC1280\850x100 First Floor Layout.dwg

C1	General Revisions Issued For Construction	C.R.	06/07/15	M.R.	06/07/15
P2	General Revisions	C.R.	10/04/15	M.R.	10/04/15
REV.	DESCRIPTION	DRAWN	DATE	CHECKED	DATE

DRAWING STATUS: For Construction

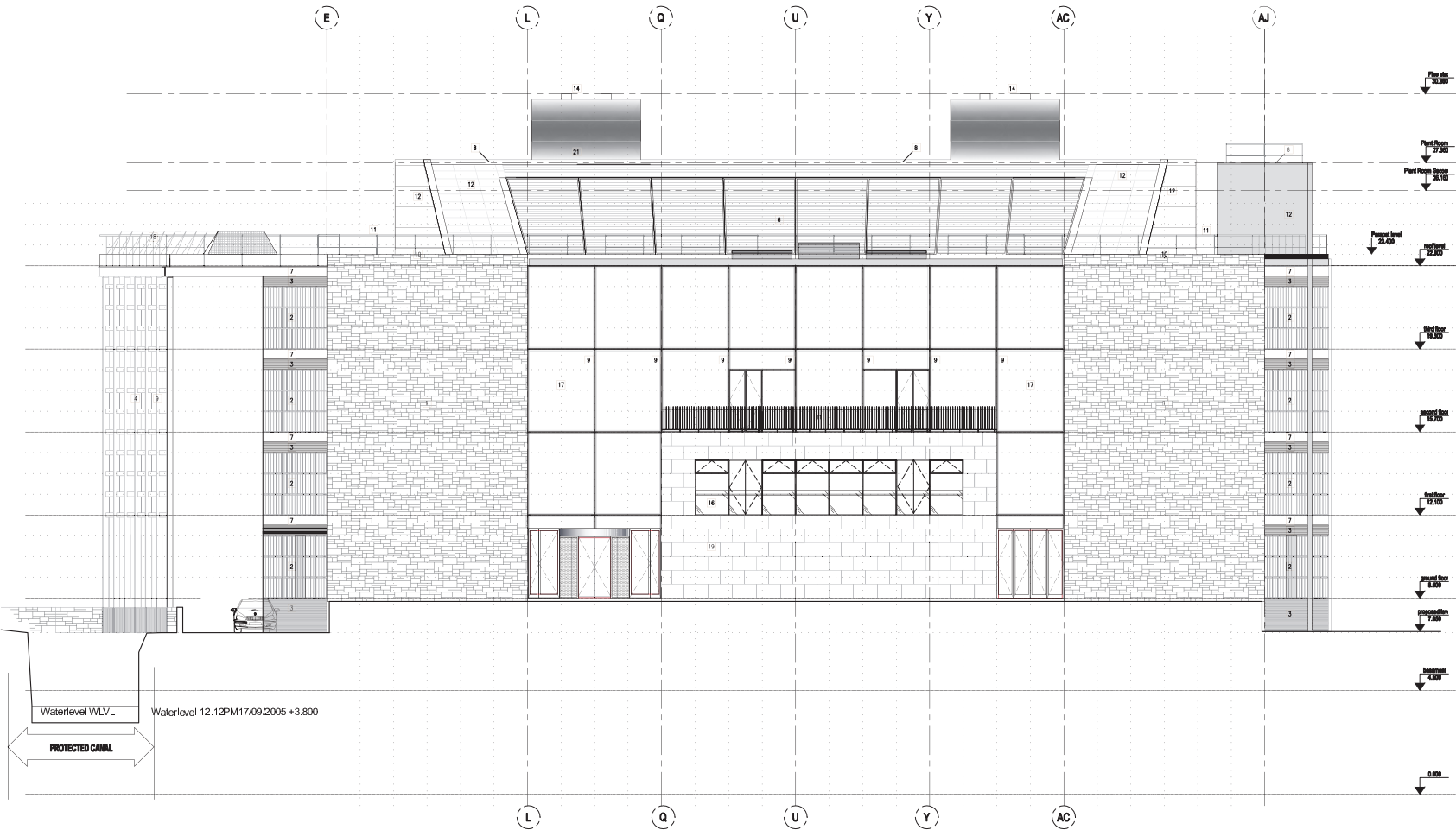


DEERPARK INDUSTRIAL ESTATE
 ORANMORE, Co. GALWAY.

TELEPHONE: (091) 794537
 FAX: (091) 794586
 E-MAIL: info@oranprecast.ie
 Web: www.oranprecast.ie

CLIENT:	BAM Contracting Ltd					
PROJECT:	Galway Human Biology Building, NUIG					
DRAWING:	Second Floor Layout					
DRAWN BY:	DATE:	CHECKED BY:	DATE:			
C.R.	04/03/15	M.R.	04/03/15			
PROJECT NO:	OP1280		SCALES:	1:100, :20		
DRAWING NO:	1280-1-04				REV.	C1

Second Floor Layout
Scale 1:100



- LEGEND**
- 1 ROUGH COURSED LIMESTONE CLADDING
 - 2 ALUMINIUM BI-MODULAR CURTAIN WALL SYSTEM WITH DOUBLE GLAZING, AOV AND MANUAL OPENING
 - 3 ALUMINIUM LOUVERS SPANDREL
 - 4 HORIZONTAL ALUMINIUM SUN SHADING / SCREEN
 - 5 ALUMINIUM BI-MODULAR CURTAIN WALL SYSTEM WITH ERITTED DOUBLE GLAZING, AOV AND MANUAL OPENING
 - 6 GLAZED ROOF WITH SUN SHADING
 - 7 ALUMINIUM CHANNEL 450MM
 - 8 ALUMINIUM CAPPING
 - 9 PAINTED STEEL COLUMN
 - 10 STONE CAPPING
 - 11 HANDRAIL AND INTERMEDIATE RAILS AT 450 CL
 - 12 INSULATED ALUMINIUM CLADDING PANEL
 - 13 PLANT ROOM WITH ALUMINIUM LOUVER PANELS
 - 14 FLUE STACK STRUCTURE CLAD IN PERFORATED STAINLESS STEEL
 - 15 ALUMINIUM CANOPY COVERED AREA
 - 16 GLAZED BALUSTRADE WITH STAINLESS STEEL HANDRAIL
 - 17 GLASS FACADE
 - 18 ROOF LIGHT
 - 19 CUT LIMESTONE CLADDING
 - 20 METAL LOUVRE DOORS / PANELS
 - 21 BITUMINOUS DOUBLE LAYER MEMBRANE ROOF
 - 22 ALUMINIUM CLADDING PANEL AND FIXING BY GLAZING & CLADDING SPECIALIST
 - 23 PLANT ROOM WITH ALUMINIUM LOUVERS
 - 24 PLANT ROOM MEMBRANE ROOF
 - 25 -
 - 26 TRANSLUCENT GLAZING

NOTE: TO BE READ IN CONJUNCTION WITH SPECIFICATION

SOUTH ELEVATION

Scott Tallon Walker Architects 10 Market Square Dublin 2 Ireland Tel: +353-1-6660000 Fax: +353-1-6619330

CLIENT NUI GALWAY	DRAWING SOUTH ELEVATION	CAD REF: K1212108TENDERGEN
PROJECT HUMAN BIOLOGY BUILDING	SCALE 1:100	PROJ. NO. TYPE DWG. NO. ISSUE 12108-GEN-020 TE2
SITE NUI	PROJECT ARCHITECT AT PD	E-mail: info@stwa.ie Web: www.stwa.ie

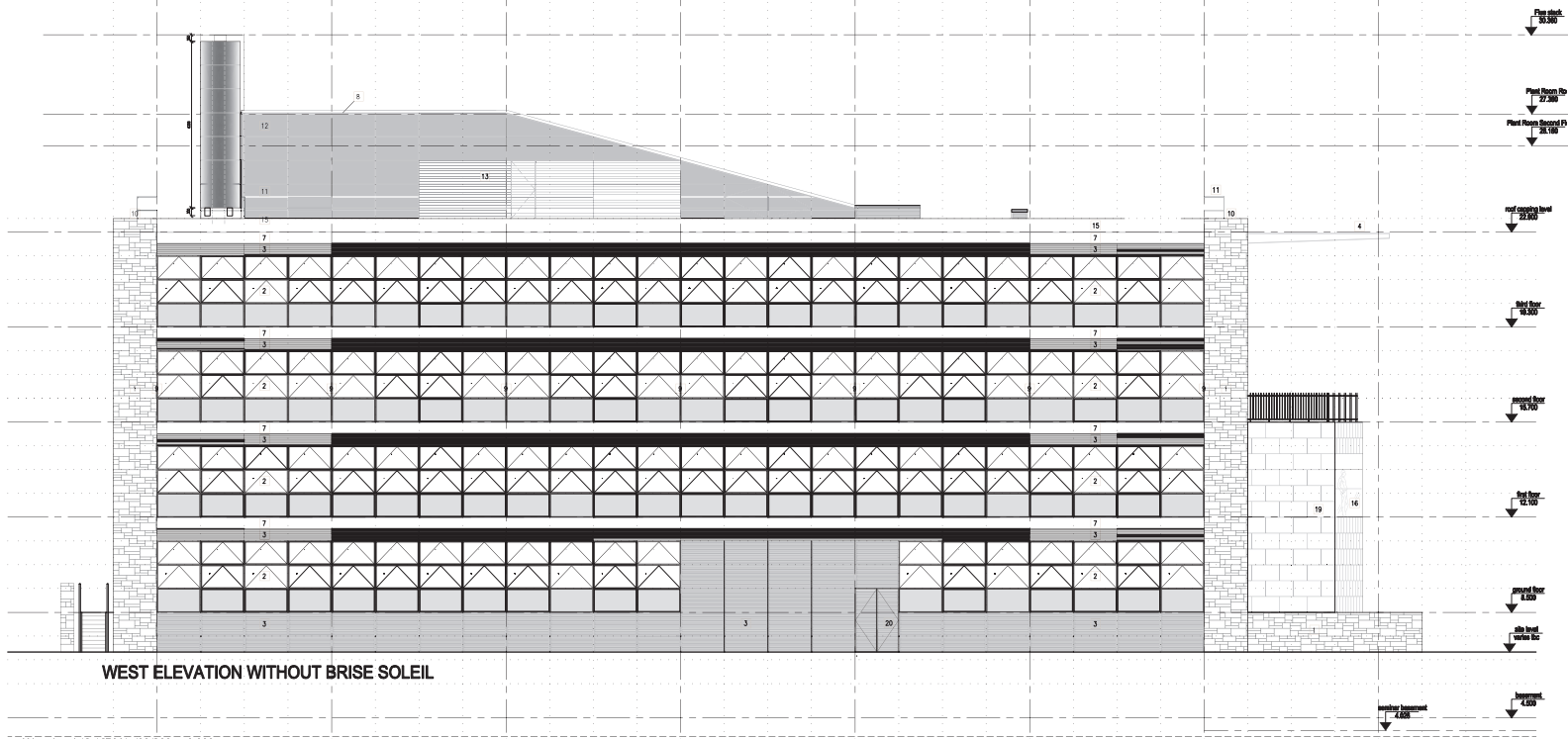
DO NOT SCALE FROM THIS DRAWING. WORK ONLY FROM FIGURED DIMENSIONS.
ALL ERRORS AND OMISSIONS TO BE REPORTED TO THE ARCHITECT.
THIS DRAWING TO BE READ IN CONJUNCTION WITH RELEVANT CONSULTANT'S DRAWINGS.

PAGE SETUP: ----- SHEET SET: ####
PLOT SCALE: 1:11 STYLE TABLE: _STW-General Arrangement.ctb
MOD. TIME: 11/25/2013 5:18:32 PLOT DEVICE: PDS-XChange-Not Secure-Batch.pc3
PLOT TIME: 11/25/2013 5:18:45 MOD. BY: Kamila Synak

ORIG.	CHK.	DATE	ISSUE

ISSUED FOR TENDER	FCS	PD	22.11.2013	TE2
FOR TENDER	ORIG.	CHK.	DATE	ISSUE

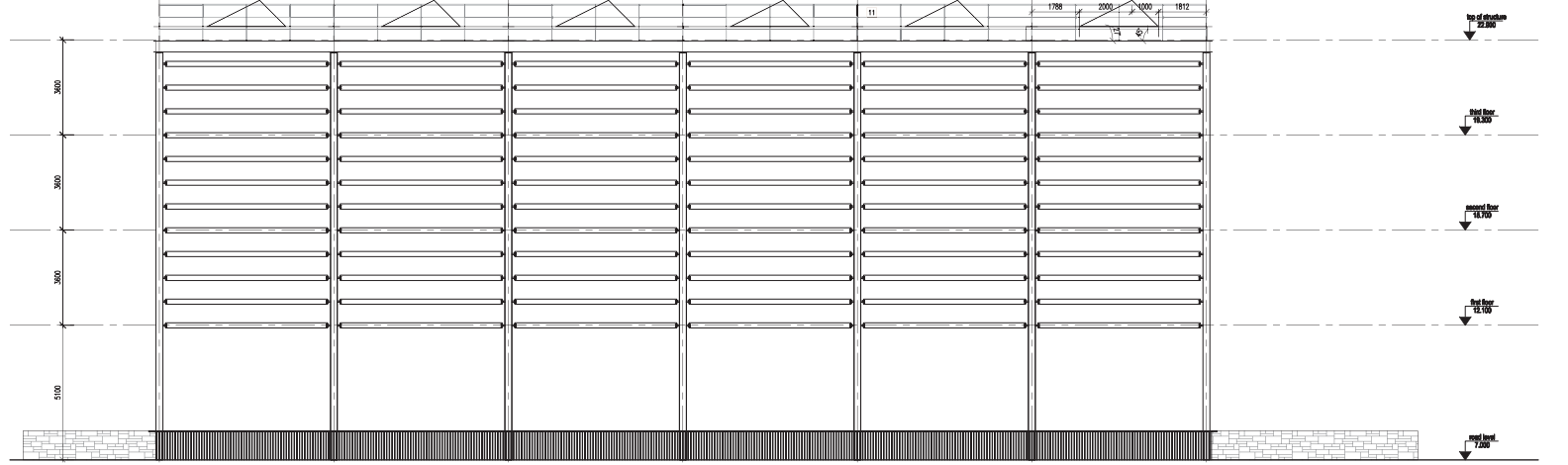
1 2 3 4 5 6 7 8 9 10 11 12 13 14 15 16 17 18 19 20 21 22 23 24 25 26 27 28 29 30 31 32



WEST ELEVATION WITHOUT BRISE SOLEIL

Waterlevel 12.12PM17/09/2005 +3.800

2 3300 3300 6 3300 3300 10 3300 3300 14 3300 3300 18 3300 3300 22 3300 3300 26 1788 2000 4000 1812



WEST ELEVATION BRIS SOLEIL

- LEGEND**
- 1 ROUGH COURSED LIMESTONE CLADDING
 - 2 ALUMINIUM BI-MODULAR CURTAIN WALL SYSTEM WITH DOUBLE GLAZING, AOV AND MANUAL OPENING
 - 3 ALUMINIUM LOUVERS SPANDREL
 - 4 HORIZONTAL ALUMINIUM SUN SHADING / SCREEN
 - 5 ALUMINIUM BI-MODULAR CURTAIN WALL SYSTEM WITH FRITTED DOUBLE GLAZING, AOV AND MANUAL OPENING
 - 6 GLAZED ROOF WITH SUN SHADING
 - 7 ALUMINIUM CHANNEL 450MM
 - 8 ALUMINIUM CAPPING
 - 9 PAINTED STEEL COLUMN
 - 10 STONE CAPPING
 - 11 HANDRAIL AND INTERMEDIATE RAILS AT 450 CL
 - 12 INSULATED ALUMINIUM CLADDING PANEL
 - 13 PLANT ROOM WITH ALUMINIUM LOUVER PANELS
 - 14 FLUE STACK STRUCTURE CLAD IN PERFORATED STAINLESS STEEL
 - 15 ALUMINIUM CANOPY COVERED AREA
 - 16 GLAZED BALUSTRADE WITH STAINLESS STEEL HANDRAIL
 - 17 GLASS FACADE
 - 18 ROOF LIGHT
 - 19 CUT LIMESTONE CLADDING
 - 20 METAL LOUVRE DOORS / PANELS
 - 21 BITUMINOUS DOUBLE LAYER MEMBRANE ROOF
 - 22 ALUMINIUM CLADDING PANEL AND FIXING BY GLAZING & CLADDING SPECIALIST
 - 23 PLANT ROOM WITH ALUMINIUM LOUVERS
 - 24 PLANT ROOM MEMBRANE ROOF
 - 25 -
 - 26 TRANSLUCENT GLAZING

NOTE: TO BE READ IN CONJUNCTION WITH SPECIFICATION

WEST ELEVATION

DO NOT SCALE FROM THIS DRAWING. WORK ONLY FROM FIGURED DIMENSIONS.
ALL ERRORS AND OMISSIONS TO BE REPORTED TO THE ARCHITECT.
THIS DRAWING TO BE READ IN CONJUNCTION WITH RELEVANT CONSULTANT'S DRAWINGS.

OFFICE USE:	
PAGE SETUP: PD	SHEET SET: ###
PLOT SCALE: 1:1	SHEET TABLE: _STW-General Arrangement.ctb
MOD. TIME: 11/25/2013 5:20:47	PLOT DEVICE: PDS-Xchange-Net Secure-Batch.pc3
PLOT TIME: 11/25/2013 5:22:19	MOD. BY: Kamila Synak

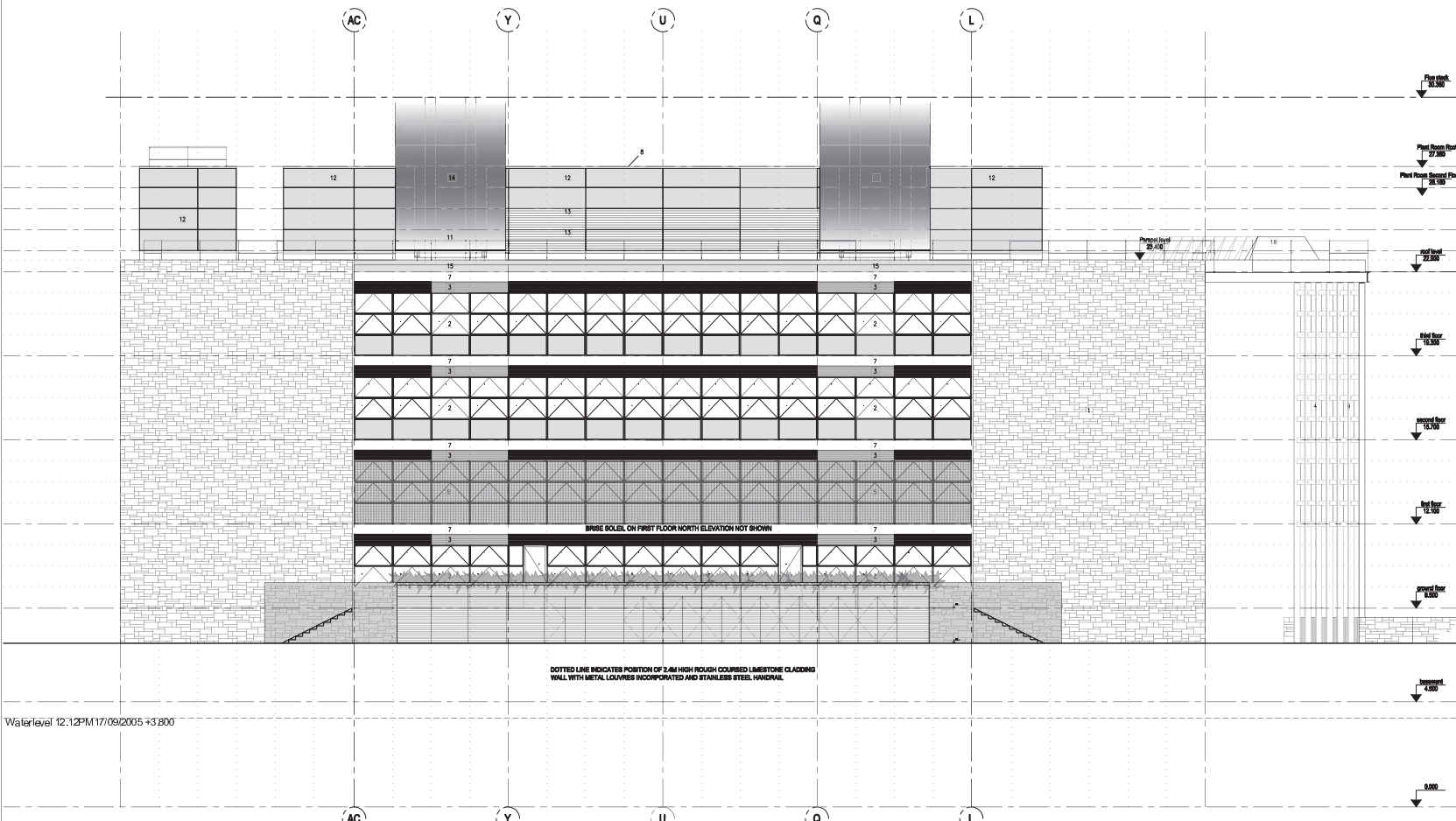
ORIG.	CHK.	DATE	ISSUE

ISSUED FOR TENDER	ORIG.	CHK.	DATE	ISSUE
BRIS SOLEIL AND ROOFLIGHTS REDUCED, 2ND FLOOR HANDRAILS TYPE CHANGED, CANOPY ROOF CHANGED	FCS	PD	22.11.2013	TE3
FOR TENDER	FCS	PD	28.05.2013	TE2
	FCS	PD	20.12.2012	TE1

Scott Tallon Walker Architects 10 Market Square, Suite 200, Auckland, New Zealand Tel: +61 9 314 6600 Fax: +61 9 314 6610

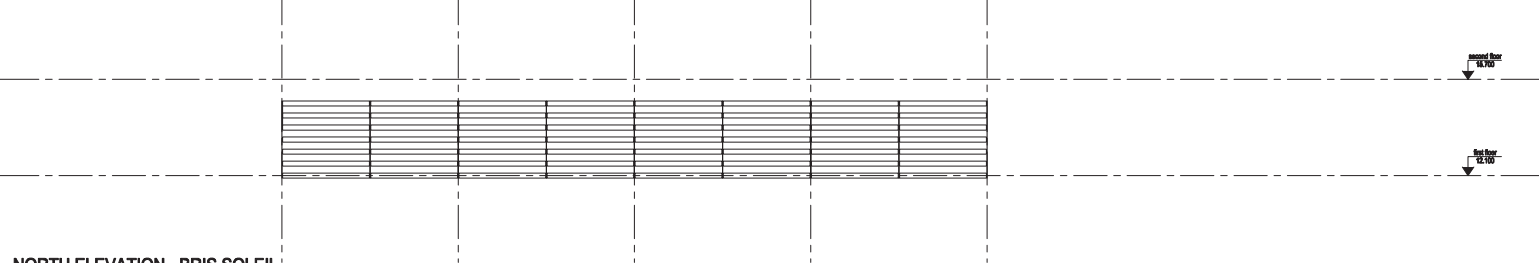
CLIENT NUI GALWAY	DRAWING WEST ELEVATION	CAD REF: K12108TENDER_GEN
PROJECT HUMAN BIOLOGY BUILDING	SCALE 1:100	PROJ. NO. TYPE DWG. NO. ISSUE 12108-GEN-021 TE3
SITE NUI	PROJECT ARCHITECT PD	E-mail: info@stwa.co.nz Web: www.stwa.co.nz

- LEGEND**
- 1 ROUGH COURSED LIMESTONE CLADDING
 - 2 ALUMINIUM BI-MODULAR CURTAIN WALL SYSTEM WITH DOUBLE GLAZING, AOV AND MANUAL OPENING
 - 3 ALUMINIUM LOUVERS SPANDREL
 - 4 HORIZONTAL ALUMINIUM SUN SHADING / SCREEN
 - 5 ALUMINIUM BI-MODULAR CURTAIN WALL SYSTEM WITH ERITTED DOUBLE GLAZING, AOV AND MANUAL OPENING
 - 6 GLAZED ROOF WITH SUN SHADING
 - 7 ALUMINIUM CHANNEL 450MM
 - 8 ALUMINIUM CAPPING
 - 9 PAINTED STEEL COLUMN
 - 10 STONE CAPPING
 - 11 HANDRAIL AND INTERMEDIATE RAILS AT 450 CL
 - 12 INSULATED ALUMINIUM CLADDING PANEL
 - 13 PLANT ROOM WITH ALUMINIUM LOUVER PANELS
 - 14 FLUE STACK STRUCTURE CLAD IN PERFORATED STAINLESS STEEL
 - 15 ALUMINIUM CANOPY COVERED AREA
 - 16 GLAZED BALUSTRADE WITH STAINLESS STEEL HANDRAIL
 - 17 GLASS FACADE
 - 18 ROOF LIGHT
 - 19 CUT LIMESTONE CLADDING
 - 20 METAL LOUVRE DOORS / PANELS
 - 21 BITUMINOUS DOUBLE LAYER MEMBRANE ROOF
 - 22 ALUMINIUM CLADDING PANEL AND FIXING BY GLAZING & CLADDING SPECIALIST
 - 23 PLANT ROOM WITH ALUMINIUM LOUVERS
 - 24 PLANT ROOM MEMBRANE ROOF
 - 25 -
 - 26 TRANSLUCENT GLAZING



Waterlevel 12:12PM 17/09/2005 +3.800

NORTH ELEVATION - BRIS SOLEIL NOT SHOWN



NORTH ELEVATION - BRIS SOLEIL

NOTE: TO BE READ IN CONJUNCTION WITH SPECIFICATION

NORTH ELEVATION

DO NOT SCALE FROM THIS DRAWING. WORK ONLY FROM FIGURED DIMENSIONS.
 ALL ERRORS AND OMISSIONS TO BE REPORTED TO THE ARCHITECT.
 THIS DRAWING TO BE READ IN CONJUNCTION WITH RELEVANT CONSULTANT'S DRAWINGS.

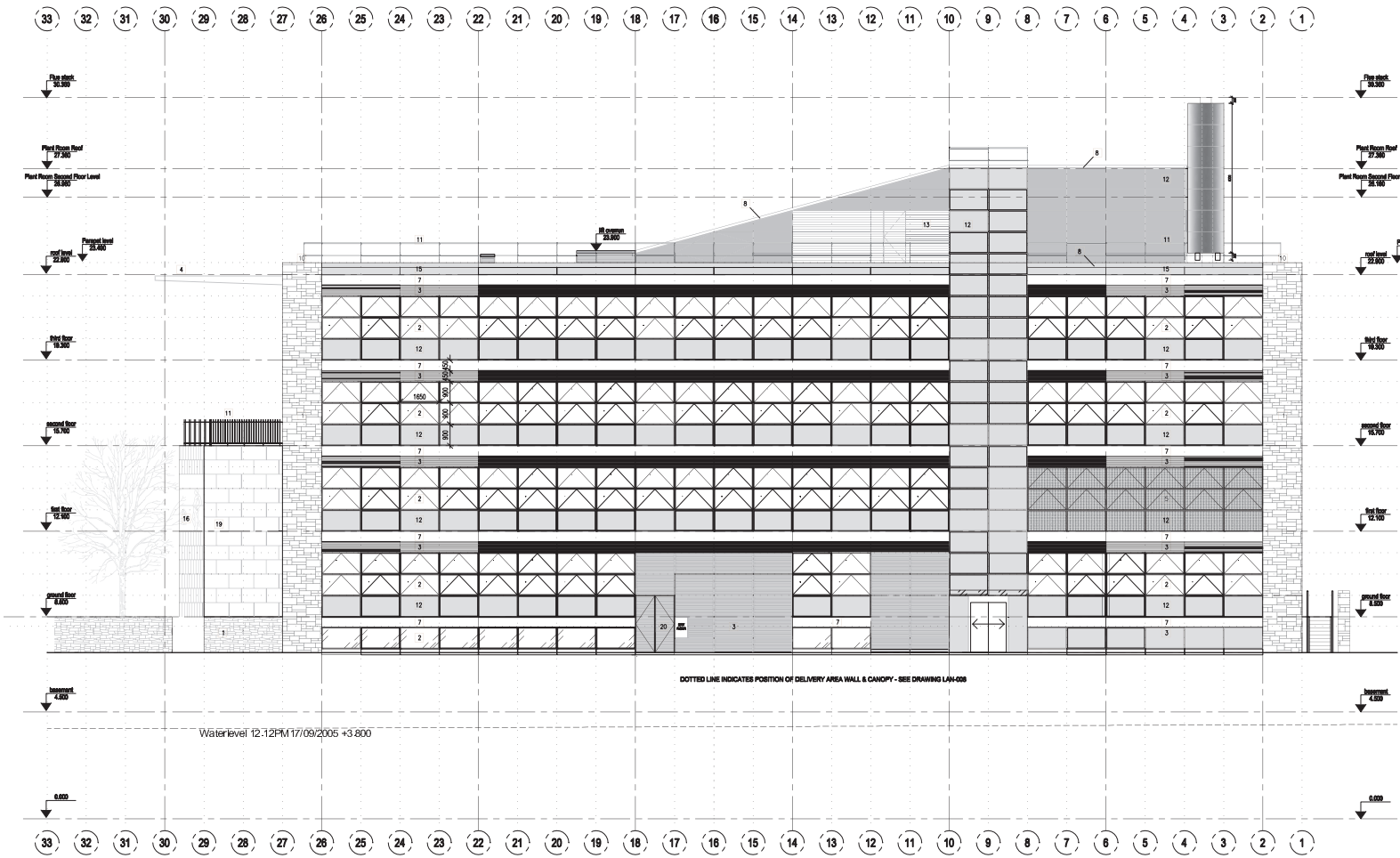
OFFICE USE:	
PAGE SETUP: ----	SHEET SET: ####
PLOT SCALE: 1:1	STYLE TABLE: _STW-General Arrangement.ctb
MOD. TIME: 11/26/2013 5:24:16	PLOT SOURCE: P:\P-Xchange-Net Secure-Batch\pc3
PLOT TIME: 11/26/2013 10:47:32	MOD. BY: Kamila Synak

ORIG.	CHK.	DATE	ISSUE

ISSUED FOR TENDER	FCS	PD	22.11.2013	TE3
OMIT BRIS SOLEIL, CHANGE WEST CANOPY, ADD RAILS TO LIFT ROOF	FCS	JH	28.06.2013	TE2
FOR TENDER	FS	PD	20.12.2012	TE1
	ORIG.	CHK.	DATE	ISSUE

Scott Tallon Walker Architects 10 Market Square, Suite 2, Hobart, Tas. 7000, Australia Tel: +61 3 616 6000 Fax: +61 3 616 6133

CLIENT NUI GALWAY	DRAWING NORTH ELEVATION	CAD REF: K12_12108_TENDER_GEN
PROJECT HUMAN BIOLOGY BUILDING	SCALE 1:100	PROJ. NO. TYPE DWG. NO. ISSUE 12108-GEN-022 TE3
SITE NUI	PROJECT ARCHITECT @A1 PD	E-mail: info@stwa.com.au Web: www.stwa.com.au



- LEGEND**
- 1 ROUGH COURSED LIMESTONE CLADDING
 - 2 ALUMINIUM BI-MODULAR CURTAIN WALL SYSTEM WITH DOUBLE GLAZING, AOV AND MANUAL OPENING
 - 3 ALUMINIUM LOUVERS SPANDREL
 - 4 HORIZONTAL ALUMINIUM SUN SHADING / SCREEN
 - 5 ALUMINIUM BI-MODULAR CURTAIN WALL SYSTEM WITH FRITTED DOUBLE GLAZING, AOV AND MANUAL OPENING
 - 6 GLAZED ROOF WITH SUN SHADING
 - 7 ALUMINIUM CHANNEL 450MM
 - 8 ALUMINIUM CAPPING
 - 9 PAINTED STEEL COLUMN
 - 10 STONE CAPPING
 - 11 HANDRAIL AND INTERMEDIATE RAILS AT 450 CL
 - 12 INSULATED ALUMINIUM CLADDING PANEL
 - 13 PLANT ROOM WITH ALUMINIUM LOUVER PANELS
 - 14 FLUE STACK STRUCTURE CLAD IN PERFORATED STAINLESS STEEL
 - 15 ALUMINIUM CANOPY COVERED AREA
 - 16 GLAZED BALUSTRADE WITH STAINLESS STEEL HANDRAIL
 - 17 GLASS FACADE
 - 18 ROOF LIGHT
 - 19 CUT LIMESTONE CLADDING
 - 20 METAL LOUVRE DOORS / PANELS
 - 21 BITUMINOUS DOUBLE LAYER MEMBRANE ROOF
 - 22 ALUMINIUM CLADDING PANEL AND FIXING BY GLAZING & CLADDING SPECIALIST
 - 23 PLANT ROOM WITH ALUMINIUM LOUVERS
 - 24 PLANT ROOM MEMBRANE ROOF
 - 25 -
 - 26 TRANSLUCENT GLAZING

NOTE: TO BE READ IN CONJUNCTION WITH SPECIFICATION

EAST ELEVATION

DO NOT SCALE FROM THIS DRAWING. WORK ONLY FROM FIGURED DIMENSIONS.
 ALL ERRORS AND OMISSIONS TO BE REPORTED TO THE ARCHITECT.
 THIS DRAWING TO BE READ IN CONJUNCTION WITH RELEVANT CONSULTANT'S DRAWINGS.

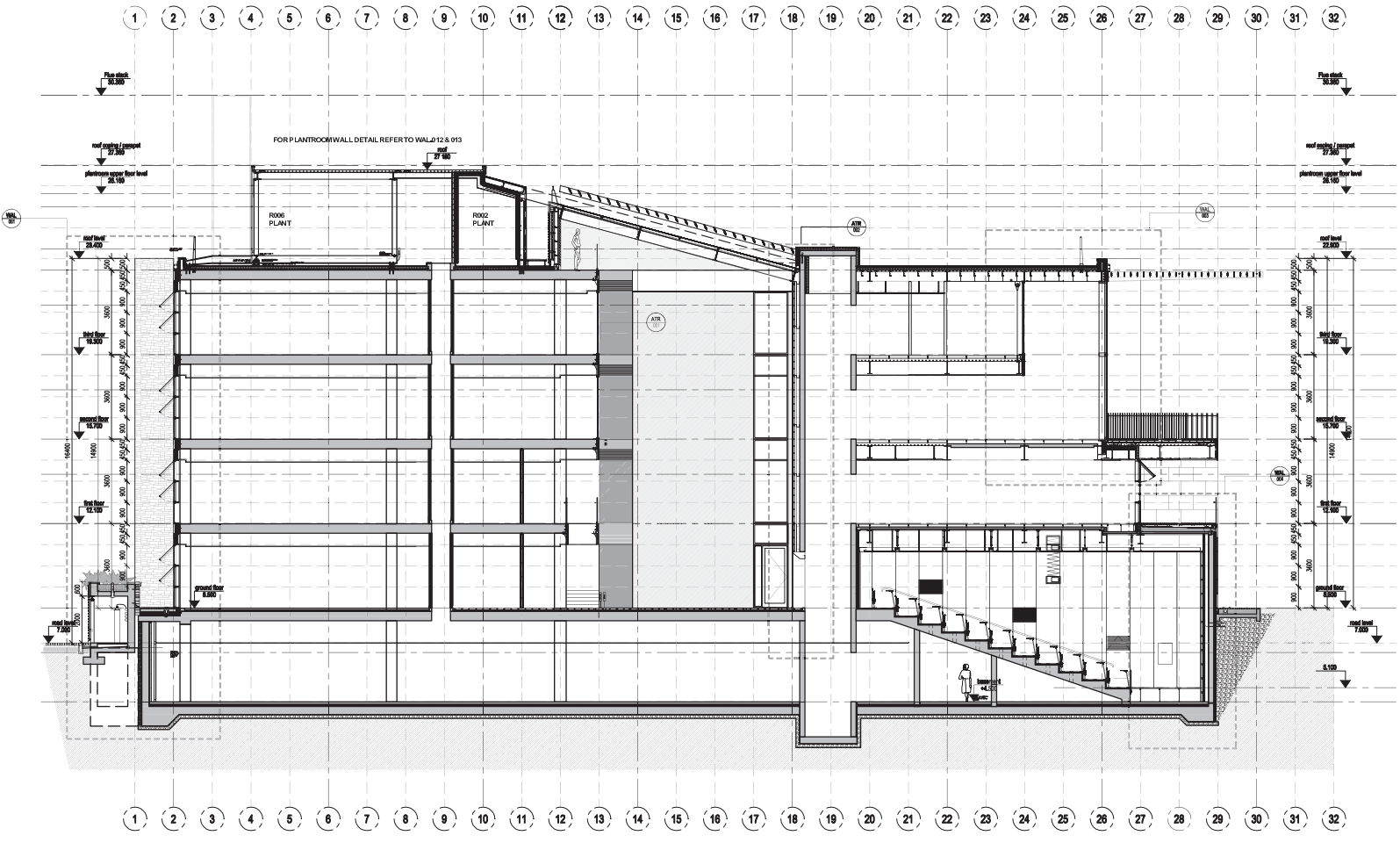
OFFICE USE:

PAGE SETUP: ----	SHEET SET: ###
PLOT SCALE: 1:1	STYLE TABLE: _STW-General Arrangement.ctb
MOD. TIME: 11/26/2013 10:51:27	PLOT SOURCE: P:\P-Xchange-Net Secure-Batch.pcs
PLOT TIME: 11/26/2013 10:52:34	MOD. BY: Kamila Synak

ORIG.	CHK.	DATE	ISSUE

ISSUED FOR TENDER	FCS	PD	DATE	TE
GLASS CANOPY ADDED TO LIFT DOOR, HANDRAIL ADDED TO LIFT ROOF, HANDRAIL TO FLOOR 2 CHANGED			22.11.2013	TE3
FOR TENDER			28.05.2013	TE2
			20.12.2012	TE1

Scott Tallon Walker Architects		10 Market Square, Dunedin		Tel: +91-3-4660000 Fax: +91-3-4619330	
CLIENT	NUI GALWAY	DRAWING	EAST ELEVATION	CAD REF:	R:\12108\TENDER\GEN
PROJECT	HUMAN BIOLOGY BUILDING	PROJ. NO.	12108-GEN-023	TYPE	DWG. NO.
SITE	NUI	SCALE	1:100	PROJECT ARCHITECT	TE3
				E-mail: info@stwa.ie	Web: www.stwa.ie



NOTE: TO BE READ IN CONJUNCTION WITH SPECIFICATION

SECTION B-B

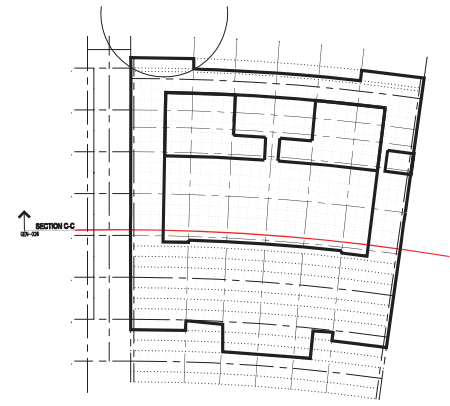
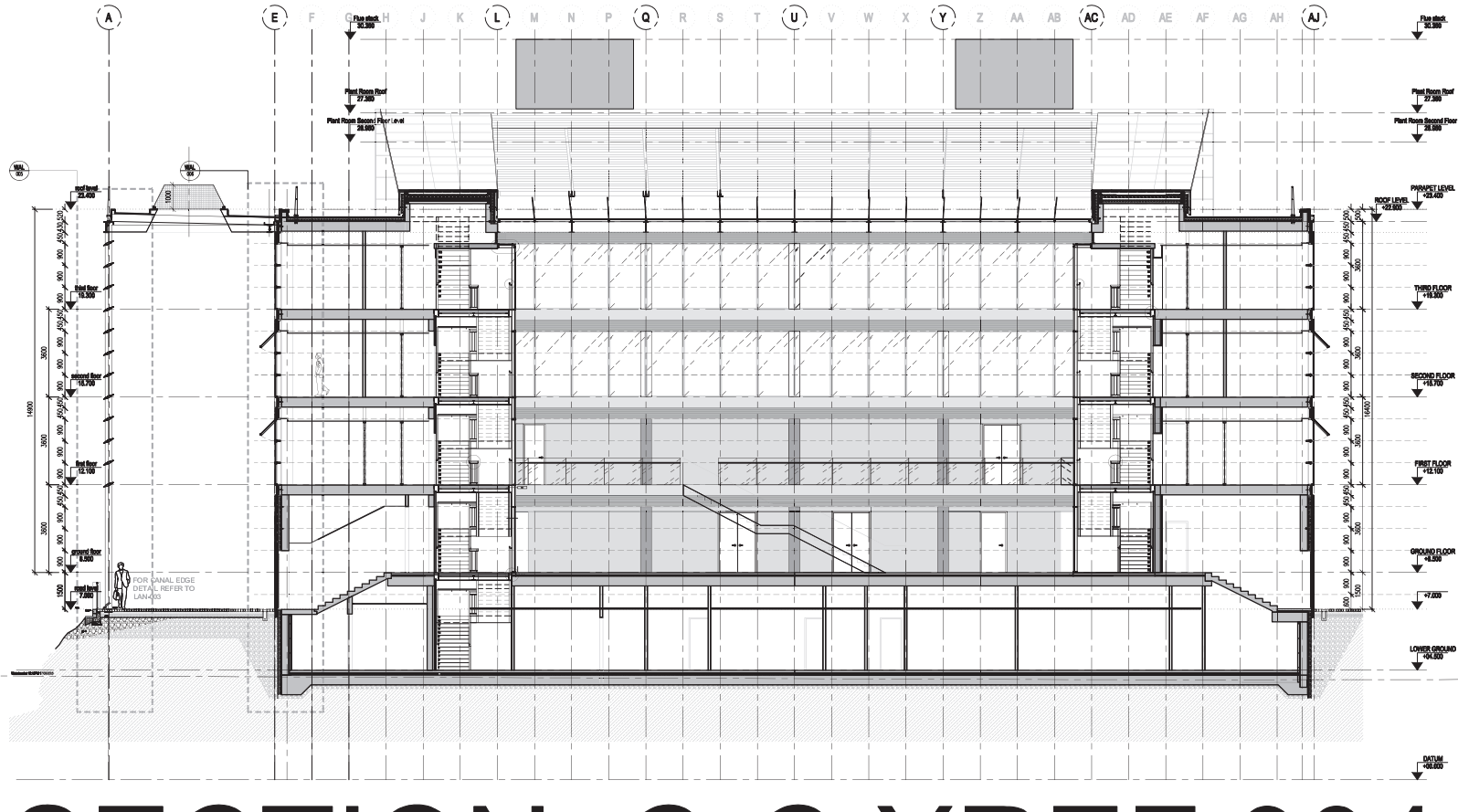
Scott Tallon Walker Architects 10 Market Square, Dublin 2, Ireland Tel: +353-1-6690000 Fax: +353-1-6693300

DO NOT SCALE FROM THIS DRAWING. WORK ONLY FROM FIGURED DIMENSIONS.	
ALL ERRORS AND OMISSIONS TO BE REPORTED TO THE ARCHITECT.	
THIS DRAWING TO BE READ IN CONJUNCTION WITH RELEVANT CONSULTANT'S DRAWINGS.	
OFFICE USE:	
PAGE SETUP: -----	SHEET SET: ####
PLOT SCALE: 1:1	STYLE TABLE: _STW-General Arrangement.ctb
MOD. TIME: 11/26/2013 10:57:42	PLOT DEVICE: PLOT-Xchange-Not Secure-Batch.pc3
PLOT TIME: 11/26/2013 10:58:01	MCD. BY: Kamila Syrak

ORIG.	CHK.	DATE	ISSUE

ISSUED FOR TENDER	FCS	PD	22.11.2013	TE3
STAR GLASS AND LECTURE THEATRE WALLS CHANGED TO PLASTERBOARD. PLANTS ON LEFT WALL OMITTED	FS	JH	28.06.2013	TE2
FOR TENDER	ORIG.	CHK.	DATE	ISSUE

CLIENT NUI GALWAY	DRAWING SECTION B-B	CAD REF: R:\12\12108\TENDER\GEN
PROJECT HUMAN BIOLOGY BUILDING	SCALE 1:100	PROJECT ARCHITECT PT
SITE NUIG CAMPUS	SCALE 1:100	PROJECT ARCHITECT PT
PROJ. NO. 12108-GEN-025	DWG. NO. 12108-GEN-025	ISSUE TE3
E-mail: info@stwa.ie		Web: www.stwa.ie



NOTE: TO BE READ IN CONJUNCTION WITH SPECIFICATION

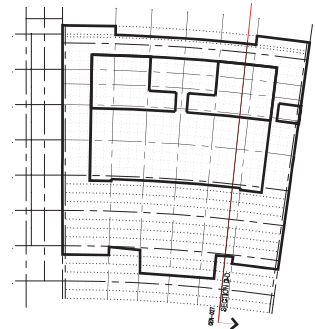
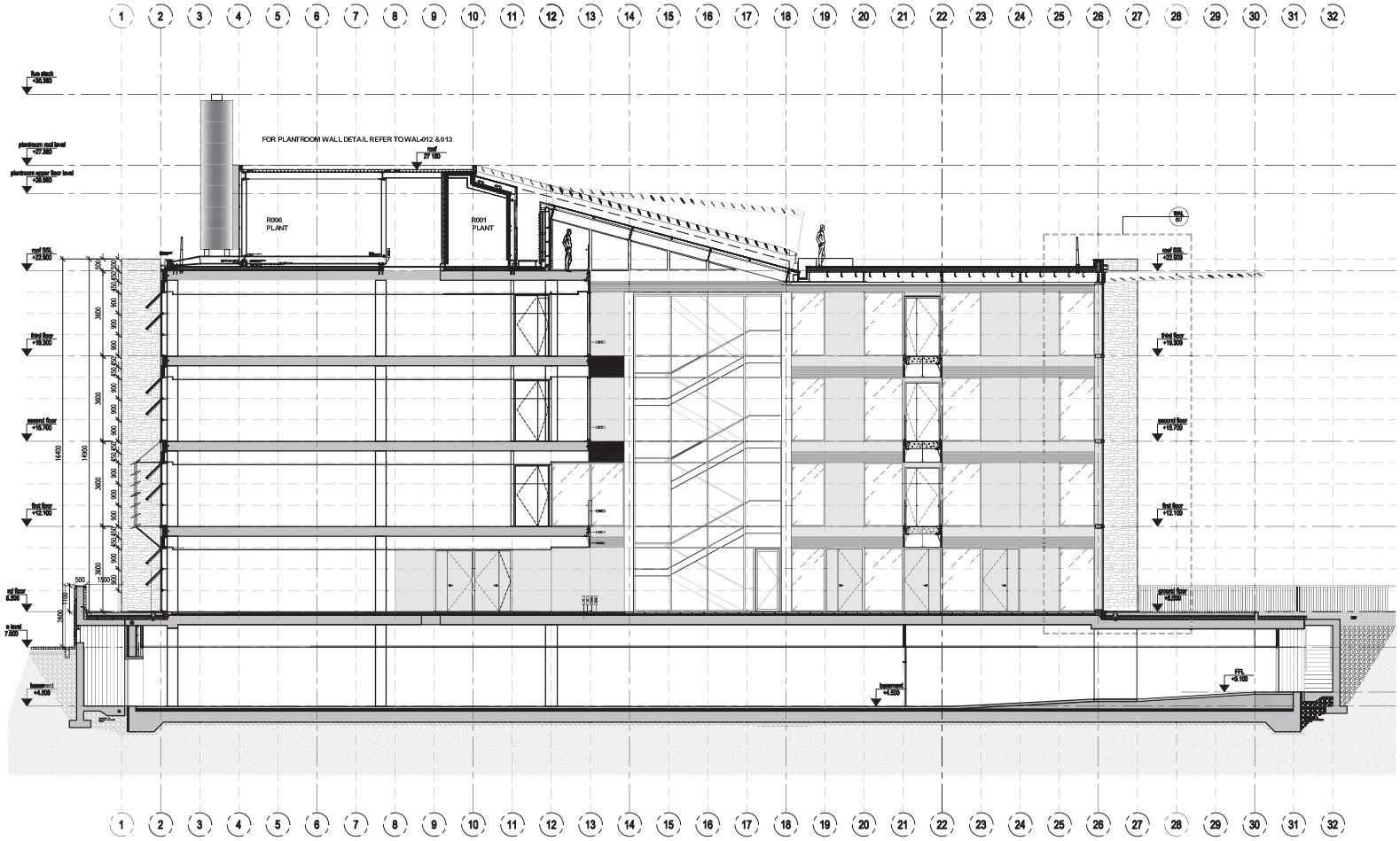
SECTION C-C

DO NOT SCALE FROM THIS DRAWING. WORK ONLY FROM FIGURED DIMENSIONS.	
ALL ERRORS AND OMISSIONS TO BE REPORTED TO THE ARCHITECT.	
THIS DRAWING TO BE READ IN CONJUNCTION WITH RELEVANT CONSULTANT'S DRAWINGS.	
OFFICE USE:	
PAGE SETUP: ----	SHEET SET: ####
PLOT SCALE: 1:1	STYLE TABLE: _STW-General Arrangement.ctb
MOD. TIME: 11/26/2013 11:00:34	PLOT SOURCE: P:\P-XChange-Net Secure-Batch.p3
PLOT TIME: 11/26/2013 11:01:54	MOD. BY: Kamila Syrak

ORIG.	CHK.	DATE	ISSUE

ISSUED FOR TENDER	FCS	PD	DATE	TE
WEST CANOPY CHANGED, GLASS AREA TO ATRIUM REDUCED, STAIR GLASS REPLACED WITH PLASTERBOARD	FCS	JH	28.06.2013	TE2
FOR TENDER	FS	PD	20.12.2012	TE1

Scott Tallon Walker Architects		10 Market Square, Deakin 2 Hobart, Tas. Tel: +61 3 64660000 Fax: +61 3 64613100	
CLIENT: NUI GALWAY	DRAWING: SECTION C-C	CAD REF: R:\12\12108\TENDER\GEN	PROJ. NO. TYPE DWG. NO. ISSUE
PROJECT: HUMAN BIOLOGY BUILDING	SCALE: 1:100	PROJECT ARCHITECT: @A1 PD	12108-GEN-026 TE3
SITE: NUIG CAMPUS	DATE: 11/26/2013	DATE: 11/26/2013	DATE: 11/26/2013



NOTE: TO BE READ IN CONJUNCTION WITH SPECIFICATION

SECTION D-D

DO NOT SCALE FROM THIS DRAWING. WORK ONLY FROM FIGURED DIMENSIONS.	
ALL ERRORS AND OMISSIONS TO BE REPORTED TO THE ARCHITECT.	
THIS DRAWING TO BE READ IN CONJUNCTION WITH RELEVANT CONSULTANT'S DRAWINGS.	
OFFICE USE:	
PAGE SETUP: -----	SHEET SET: ####
PLOT SCALE: 1:1	STYLE TABLE: _sTW-General Arrangement.ctb
MOD. TIME: 11/26/2013 11:03:41	PLOT DEVICE: PDS-Xchange-Net Secure-Batch.pc3
PLOT TIME: 11/26/2013 11:04:31	MOD. BY: Kamila Synak

ORIG.	CHK.	DATE	ISSUE

ISSUED FOR TENDER	FCS	PD	22.11.2013	TE3
GLAZING REDUCED	FCS	JH	20/09/2013	TE2
FOR TENDER	FS	PD	20.12.2012	TE1
	ORIG.	CHK.	DATE	ISSUE

Scott Tallon Walker Architects		10 Market Square, Deakin 2, Hobart, Tas. 7000		Tel: +61 3 546 69000 Fax: +61 3 546 69330	
CLIENT	NUI GALWAY	DRAWING	SECTION D-D	CAD REF:	K:\12\12108\TENDER\GEN
PROJECT	HUMAN BIOLOGY BUILDING	PROJ. NO.	12108-GEN-027	TYPE	DWG. NO.
SITE	NUIG CAMPUS	SCALE	1:100	PROJECT ARCHITECT	TE3
				E-mail: info@stwa.com.au	Web: www.stwa.com.au